FLAME SPREAD INTO SOLID ROCKET PROPELLANT CRACKS

Jerald L. Cunningham

Air Force Institute of Technology
Wright-Patterson Air Force Base, Ohio

December 1974

KEEP UP TO DATE

Between the time you ordered this report—which is only one of the hundreds of thousands in the NTIS information collection available to you—and the time you are reading this message, several *new* reports relevant to your interests probably have entered the collection.

Subscribe to the **Weekly Government Abstracts** series that will bring you summaries of new reports *as soon as they are received by NTIS* from the originators of the research. The WGA's are an NTIS weekly newsletter service covering the most recent research findings in 25 areas of industrial, technological, and sociological interest—invaluable information for executives and professionals who must keep up to date.

The executive and professional information service provided by NTIS in the **Weekly Government Abstracts** newsletters will give you thorough and comprehensive coverage of government-conducted or sponsored research activities. And you'll get this important information within two weeks of the time it's released by originating agencies.

WGA newsletters are computer produced and electronically photocomposed to slash the time gap between the release of a report and its availability. You can learn about technical innovations immediately—and use them in the most meaningful and productive ways possible for your organization. Please request NTIS-PR-205/PCW for more information.

The weekly newsletter series will keep you current. But *learn what you have missed in the past* by ordering a computer **NTISearch** of all the research reports in your area of interest, dating as far back as 1964, if you wish. Please request NTIS-PR-186/PCN for more information.

WRITE: Managing Editor
5285 Port Royal Road
Springfield, VA 22161

Keep Up To Date With SRIM

SRIM (Selected Research in Microfiche) provides you with regular, automatic distribution of the complete texts of NTIS research reports *only* in the subject areas you select. SRIM covers almost all Government research reports by subject area and/or the originating Federal or local government agency. You may subscribe by any category or subcategory of our WGA **(Weekly Government Abstracts)** or **Government Reports Announcements and Index** categories, or to the reports issued by a particular agency such as the Department of Defense, Federal Energy Administration, or Environmental Protection Agency. Other options that will give you greater selectivity are available on request.

The cost of SRIM service is only 45¢ domestic (60¢ foreign) for each complete microfiched report. Your SRIM service begins as soon as your order is received and processed and you will receive biweekly shipments thereafter. If you wish, your service will be backdated to furnish you microfiche of reports issued earlier.

Because of contractual arrangements with several Special Technology Groups, not all NTIS reports are distributed in the SRIM program. You will receive a notice in your microfiche shipments identifying the exceptionally priced reports not available through SRIM.

A deposit account with NTIS is required before this service can be initiated. If you have specific questions concerning this service, please call (703) 451-1558, or write NTIS, attention SRIM Product Manager.

This information product distributed by

NTIS U.S. DEPARTMENT OF COMMERCE
National Technical Information Service
5285 Port Royal Road
Springfield, Virginia 22161

UNCLASSIFIED

SECURITY CLASSIFICATION OF THIS PAGE (When Data Entered)

REPORT DOCUMENTATION PAGE	READ INSTRUCTIONS BEFORE COMPLETING FORM
1. REPORT NUMBER: GAE/AE/74D-14	2. GOVT ACCESSION NO.
	3. RECIPIENT'S CATALOG NUMBER: AD A023346
4. TITLE (and Subtitle): FLAME SPREAD INTO SOLID PROPELLANT CRACKS	5. TYPE OF REPORT & PERIOD COVERED: AFIT THESIS 1973-1974
	6. PERFORMING ORG. REPORT NUMBER: GAE/AE/74D-14
7. AUTHOR(s): JERALD L. CUNNINGHAM	8. CONTRACT OR GRANT NUMBER(s)
9. PERFORMING ORGANIZATION NAME AND ADDRESS: AIR FORCE INSTITUTE OF TECHNOLOGY WRIGHT PATTERSON AFB, OHIO 45433	10. PROGRAM ELEMENT, PROJECT, TASK AREA & WORK UNIT NUMBERS
11. CONTROLLING OFFICE NAME AND ADDRESS: Air Force Rocket Propulsion Laboratory/XTC Edwards Air Force Base, California	12. REPORT DATE: DECEMBER 1974
	13. NUMBER OF PAGES: 162
14. MONITORING AGENCY NAME & ADDRESS(if different from Controlling Office)	15. SECURITY CLASS. (of this report): UNCLASSIFIED
	15a. DECLASSIFICATION DOWNGRADING SCHEDULE

16. DISTRIBUTION STATEMENT (of this Report)

APPROVED FOR PUBLIC RELEASE; DISTRIBUTION UNLIMITED.

ES SUBJECT TO Change

17. DISTRIBUTION STATEMENT (of the abstract entered in Block 20, if different from Report)

18. SUPPLEMENTARY NOTES

APPROVED FOR PUBLIC RELEASE;
IAW AFR 190-17.

Jerry C. Hix

JERRY C. HIX, Capt, USAF
Director of Information

19. KEY WORDS (Continue on reverse side if necessary and identify by block number)

FLAME SPREAD
SOLID PROPELLANT CRACKS
FLASH
FLAME PROPAGATION

20. ABSTRACT (Continue on reverse side if necessary and identify by block number)

An experimental study was conducted to investigate the spread of combustion flames into solid rocket propellant cracks. Experiments were performed using a combustion vessel with a free flowing nitrogen atmosphere under pressures of 300, 500, and 750 psig. Samples of three different propellants having crack widths varying from 0.022 in to 0.044 in were used. The ignition of the samples and the flame spread were recorded with a high-speed motion camera. Tests showed that the flame velocity inside the crack channels

DD FORM 1 JAN 73 1473 EDITION OF 1 NOV 65 IS OBSOLETE

UNCLASSIFIED

SECURITY CLASSIFICATION OF THIS PAGE (When Data Entered)

increased as the crack width decreased, and an entrance delay time usually exists prior to the flame entering the crack channel. For the range of crack widths investigated, no crack width was found for which flame penetration did not occur. Crack width demonstrated a greater effect on flame spread velocity in the crack than combustion pressure. The flame velocity flow inside a crack as a function of pressure and crack size is unique for each propellant tested.

FLAME SPREAD INTO SOLID ROCKET PROPELLANT CRACKS

Thesis

GAE/AE/74D-14 Jerald L. Cunningham
Captain USAF

Approved for public release; distribution unlimited.

1-b

GAE/AE/74D-14

FLAME SPREAD INTO SOLID ROCKET PROPELLANT CRACKS

THESIS

Presented to the Faculty of the School of Engineering
of the Air Force Institute of Technology
Air University
in Partial Fulfillment of the
Requirements for the Degree of
Master of Science

by

Jerald L. Cunningham, B.S.A.E.
Captain USAF
Graduate Aeronautical Engineering

December 1974

Preface

This study represents a preliminary effort to gain an understanding of the spread of combustion flames into solid rocket propellant cracks. The results presented serve to substantiate and expand on previous findings. This work has also given me invaluable experience in experimental investigations and the satisfaction of individually attacking a problem and seeing it through to a conclusion.

My sincere thanks go to the following people for their much needed help in this effort: Major Robert Bestgen for suggesting this topic, contributing his well versed insight into this area and giving a lot of encouragement, Dr. William Elrod and Dr. Ernest Dorko for their availability and willingness to give of their time and knowledge, and Mr. John Parks for his assistance in solving the ever present "nuts" and "bolts" problems.

My deepest appreciation must go to Dave, Scott, Mark and my wife, Ginny, the four most important people in my life, who are very much involved in this as well as all my efforts.

Jerald L. Cunningham

Contents

List of Figures

List of Tables

List of Symbols

Symbol	Definition
A_b	Propellant burning surface area
A_c	Crack area
r_b	Linear burn rate of the solid propellant
V_e	Entrance flame velocity or crack threshold velocity
V_c	Flame velocity in the crack channel
V_{tot}	Overall flame velocity (includes the total time of the flame spread over the crack height)
W_c	Crack width
ρ_g	Gas density
ρ_s	Solid propellant density

Abstract

An experimental study was conducted to investigate the spread of combustion flames into solid rocket propellant cracks. Experiments were performed using a combustion vessel with a free flowing nitrogen atmosphere under pressures of 300, 500, and 750 psia. Samples of three different propellants having crack widths varying from 0.002 in to 0.044 in were used. The ignition of samples and the flame spread were recorded with a high-speed motion camera. Tests showed that the flame velocity inside the crack channels increased as the crack width decreased, and an entrance delay time usually exists prior to the flame entering the crack channel. For the range of crack widths investigated no crack width was found for which flame penetration into the crack did not occur. Crack width demonstrated a greater effect on flame spread velocity in the crack than combustion pressure. The flame velocity flow inside a crack as a function of pressure and crack size is unique for each propellant tested.

FLAME SPREAD INTO SOLID ROCKET PROPELLANT CRACKS

I. Introduction

Background

Considerable emphasis has been placed on studying steady and unsteady combustion mechanisms and on measuring burn rates of solid rocket propellants. Motor control problems can occur because of unsteady conditions produced by burning instabilities. Such instabilities can result in motor over-pressure conditions or overheating of the rocket's motor casing wall (Ref 1:79). One possible source of propellant burning instability, which has not received a great deal of attention, is flame encroachment into cracks which occurs in solid rocket propellants (Ref 2:3).

Although this subject has been looked at previously, very little detailed work has been carried out. The Air Force Space and Missile Systems Organization (SAMSO) expressed an interest in flame propagation into solid propellant cracks in the early 1960's. In response, the Air Force Rocket Propulsion Laboratory (AFRPL) generated preliminary experimental data in-house on flame spread into propellant cracks, and commenced to contract out for further research work. An independent study conducted by the Japanese closely paralleled the in-house effort by the AFRPL. The U.S. Navy also did some preliminary research

related to this area at their China Lake station. Much of the research performed confirmed that cracks did effect the operation of rocket motors and, in some cases, complete destruction of the motors occurred (Ref 1:55).

C. E. Payne found that the speed of flame propagation into cracks increased as the crack width decreased (Ref 3:4). T. Godai recorded similar observations, but noted a critical crack entrance width, or threshold width, for which the flame would not enter the crack (Ref 4:8). His conclusion supported previous research performed by J. L. Prentice (Ref 5:32).

Total rocket motor performance is affected when combustion gases and flames propagate down into fissures or cracks, igniting the cracks' wall surface areas to cause large increases in the total propellant burning area. This increased burning area allows consumption of more propellant which drives the rocket combustion chamber pressure higher, thus creating a greater driving pressure to propagate the flames into other cracks as well as increasing the linear burn rate of the propellant (Refs 1:36 and 2:5). This can lead to undesired burning instabilities and even motor failure.

The most critical crack defect occurs when the propellant debonds from the motor casing. Flames propagate into these areas denying the adjacent motor casing wall the insulating effect of the solid rocket propellant. A localized

hotspot develops which can destroy the motor by the rupture of the casing wall (Ref 6:3).

Cracks predominantly develop in solid propellant grains as the propellant ages in a rocket motor, although some are produced in the processing and curing stages of propellant production. Many of the cracks formed during production can be easily found through X-ray or microwave scanning techniques prior to release (Ref 2:59). Those cracks occurring during storage or operational readiness are more difficult to detect.

Objectives

This study provides an indepth look at the flame spread into a solid propellant crack and its penetration down the crack channel. The objectives of this research were to experimentally investigate:

(1) the effect of crack width on flame penetration into the crack channel,

(2) the effect of pressure on flame spread for a given crack width,

(3) the effect of combustion pressure and crack size on flame spread for different propellants.

Scope

An experimental investigation was made of the flame spread velocity into cracks fashioned by cubes (approximately 0.22 inches on a side) of solid rocket propellant set side-by-side. Three types of propellants were tested

at 300, 500, and 750 psig. The crack widths for each combination of propellant and pressure varied from 0.002 inches to 0.044 inches.

II. Experimental Apparatus and Procedures

Apparatus

A small combustion vessel, fitted with glass windows, was used to study the flame spread rates into solid propellant cracks. The ignition of propellant samples and the subsequent burning process were recorded on 16 mm high speed motion picture film. The combustion vessel and Fastax camera setup is shown in Fig. 1A. This was the same vessel used by Payne at the AFRPL in his preliminary investigation of flame propagation into solid propellant cracks (Ref 3). Figure 1B shows the disassembled view of the vessel. The inside dimensions are 2 inches in diameter by 4 inches in length. The windows are of 1/2 inch thick optical glass. The vessel itself is constructed of steel and can withstand working pressures up to 2000 psia.

The propellant holders (Fig. 1B(b)) were fashioned from nonconductive phenolic material with brass electrical plugs to fit into the semi-circular steel bracket (Fig. 1B(c)). Propellant samples are fastened onto the holder by steel pins fixed into the top surface of the holder. A length of nichrome wire, placed across the electrical posts of the holder, is in contact with the top surface of the propellant samples as shown in Fig. 1B. The propel lant holder plugs into the steel bracket that is installed inside the vessel chamber with set screws.

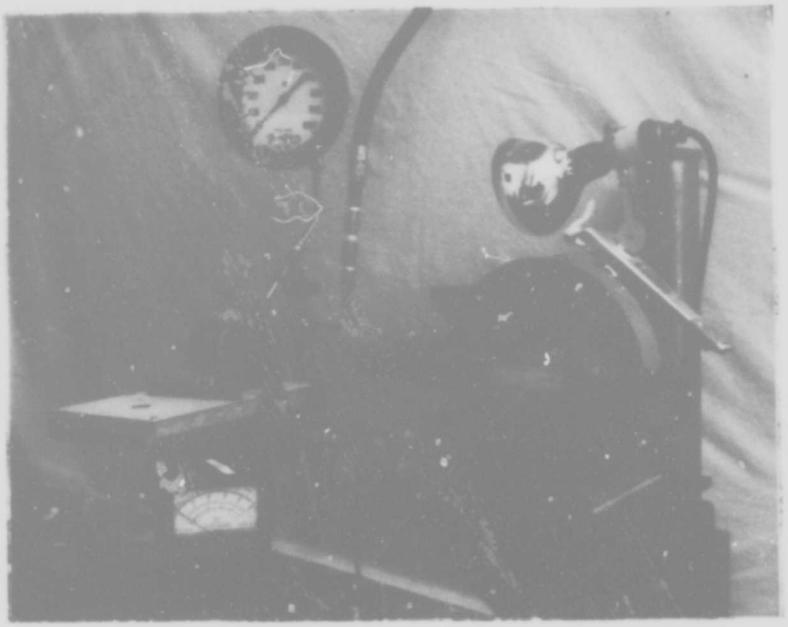

Fig. 1A. Experimental Apparatus.

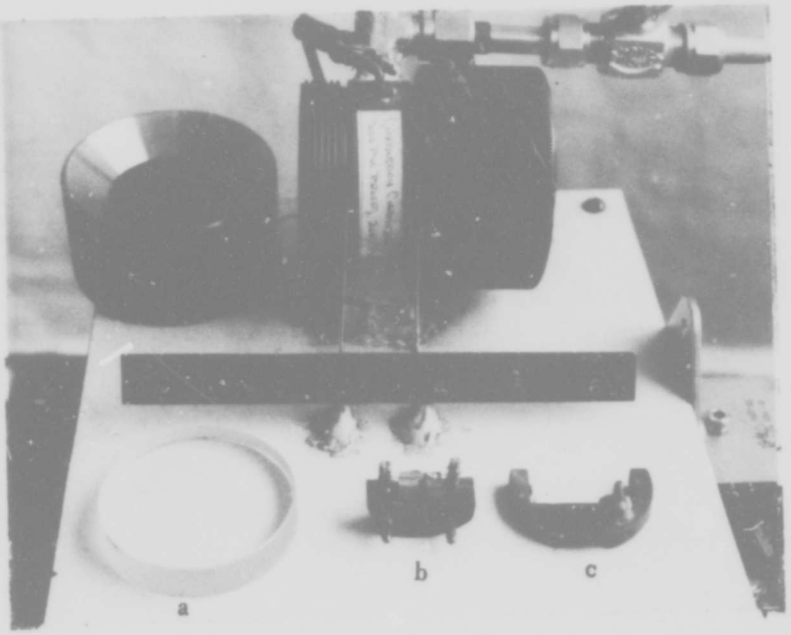

Fig. 1B. Combustion Bomb Assembly: (a) Optical Glass Window, (b) Propellant Holder, (c) Steel Mounting Bracket.

An electrical lead connects the top of the vessel to an insulated post through the steel bracket. With the propellant holder plugged into the steel bracket inside the vessel, insulated passage is provided for current to flow to the holder posts for the hot wire ignition system. The circuit was completed from the other holder post through the vessel itself. When current is applied, the nichrome wire is heated, igniting the propellant surface. The wire then is burned through and falls out of camera view. The current is controlled with a variable resistor (variac) placed in series with the vessel.

A pressurized dry nitrogen atmosphere is supplied to the vessel through the 1/2 inch diameter entrance hole in its bottom. The gas containing the nitrogen and combustion products is vented out a similar hole at the top of the vessel. A flow valve, attached to the vent tube, permits a free flow of nitrogen gas while mai taining a preset pressure within the vessel. This flow inhibits the accumulation of smoke inside the vessel and allows the recording of the event photographically.

A Fastax 16 mm high speed motion picture camera was focused on the propellant surfaces. The camera speed (2000 to 6000 frames/sec) is adjustable through a sequencer which is equipped with a variable time delay that allows the camera to come up to speed before initiating the combustion event. An average filming rate of 4000 frames/sec was used in this investigation. Time marks for data

reduction were placed on the film at 1 millisecond intervals by a sign wave generator which pulses exposure lights built into the camera. This apparatus setup is illustrated in Fig. 2.

Control pressure to the vessel is provided with bottled nitrogen piped into a domed control valve which regulated the high pressure nitrogen flow from a mobile trailer located outside the laboratory. The pressure was set using a calibrated pressure gage attached to the vessel as shown in Figs. 1A and 2. The increase in pressure caused by the burning of the propellant samples was monitored with a pressure transducer. The pressure increase was recorded on light sensitive oscillograph recording paper. All experimental apparatus was located in a test cell and controlled remotely from inside a control room for safety purposes.

The raw data were taken from the film using a light table for picking off the time marks and a Triad film reader for crack and flame spread measurements. The film reader has a variable speed capability which enables the viewer to review the burn in slow motion or in single frames at a magnification up to 60 times. It is equipped with a cross-hair referencing and measuring system which is tied in series with a digital read-out system and an IBM 029 keypunch. The data measured from the film were referenced, displayed and punched on computer cards automatically.

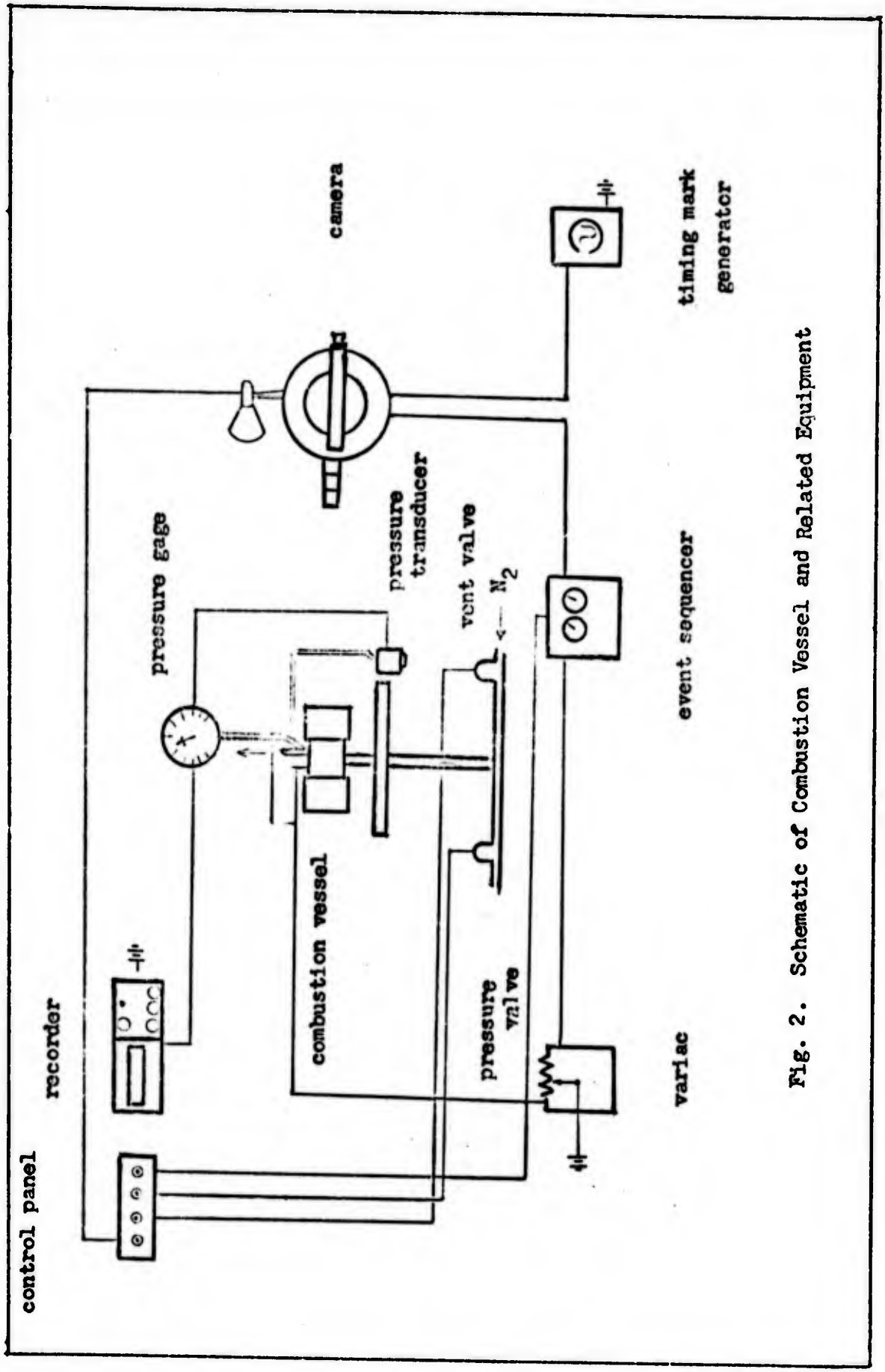

Fig. 2. Schematic of Combustion Vessel and Related Equipment

These data cards were incorporated into a computer program for use in a CDC 6600 computer for further reduction and display.

Procedures

The data from the study were taken from 16 mm motion picture film exposed during the time lapse from sample ignition until the flame spread to the bottom of the crack. Samples of each propellant were mounted on the holder at a measured distance apart to simulate a crack. A small segment of nichrome wire (0.0125 inches in diameter) was attached to the surface of the propellant samples facing the camera to serve as a known dimensional reference. This wire also provided a focal reference for the camera.

The three types of propellants selected for this study were supplied by the AFRPL, Edwards AFB, California. The propellants used are representative of operational propellants. Propellant A (see Table I) is a propellant which had aged in storage for approximately seven years before being selected for this study. Propellants B and C (Table I) are of more recent manufacture, perhaps two to four years old. Burn rates for each of the propellants, at the chamber pressure considered, were measured from film. Data for the burn rates are shown graphically in Fig. 7.

The crack geometry consisted of the rectangular area between the two propellant cubes. The widths between the two samples were first set with an automotive gap gage,

Table I

Propellant Composition

Propellant A	Propellant B	Propellant C
Double based binder (55% nitroglycerin, nitrocelluose and additives)	HTPB binder	CTPB binder
30% Ammonium perchlorate	67% Ammonium perchlorate	Ammonium perchlorate (90μ, 180μ)
15% Aluminum	21% Aluminum	Aluminum (35μ)

then remeasured from the film. Once mounted on the holder at the desired crack width, a Slastic RTV flame retardant sealer was placed on the sides of the propellant samples and at their bases. This assured that the sample would burn down in a uniform cigarette fashion and allow the flame to propagate into the fabricated crack. The front and back surfaces were protected from flame encroachment by the flow of nitrogen parallel to that surface.

Data Reduction Method

Once the exposed film was placed on the film reader, the diameter of the reference wire was measured on the screen, giving the magnification of the projected image. The crack width was then measured and the sample heights were taken.

The time base was set at a reference frame with the flame at the crack edge. The frame number from this reference was automatically counted and recorded at each measurement taken as the flame moved down the crack channel. Knowing the film speed at any point from the timing marks produced by the timing mark generator and the frame number at all measured points, the average time was calculated from the ratio of the frame number to the average camera speed in frames per second.

With the crack height measured and the time base known, the raw data were given to the CDC 6600 computer to produce a flame-into-crack height vs. time graph. This graph provides an accurate representation of the flame as it makes its way into the crack.

III. Results and Discussion

The data curves resulting from this study on flame spread into propellant cracks of various widths are compiled for the three propellants in Appendix B. These curves generally show an initial flame spread delay at the crack edge or threshold, then a rapid burn down to the crack bottom. This flame spread delay appeared in 93 of the 100 tests performed. Accordingly, flame propagation into a propellant crack is considered to undergo an initial pause before burning to the base of the crack. Figure 3 illustrates the typical case of flame propagation delay and subsequent flame spread in the propellant crack.

The initial entrance delay period occurs as the flame penetrates a short distance into the mouth of the crack and essentially "hovers". The slope of the delay period of Fig. 3 gives the averaged entrance velocity for the flame V_e. This velocity is very small compared to the flame velocity inside the crack channel V_c (given by the slope of the flame spread time portion of Fig. 3) or even the overall velocity V_{tot}, which accounts for the entire crack height and the total time of the burn from crack edge to the crack bottom.

The peaks and valleys shown on the data curves represent the unsteady penetration of the flame into the crack. The flame moves in and out of the crack mouth for finite lengths of time until prevailing combustion mechanisms

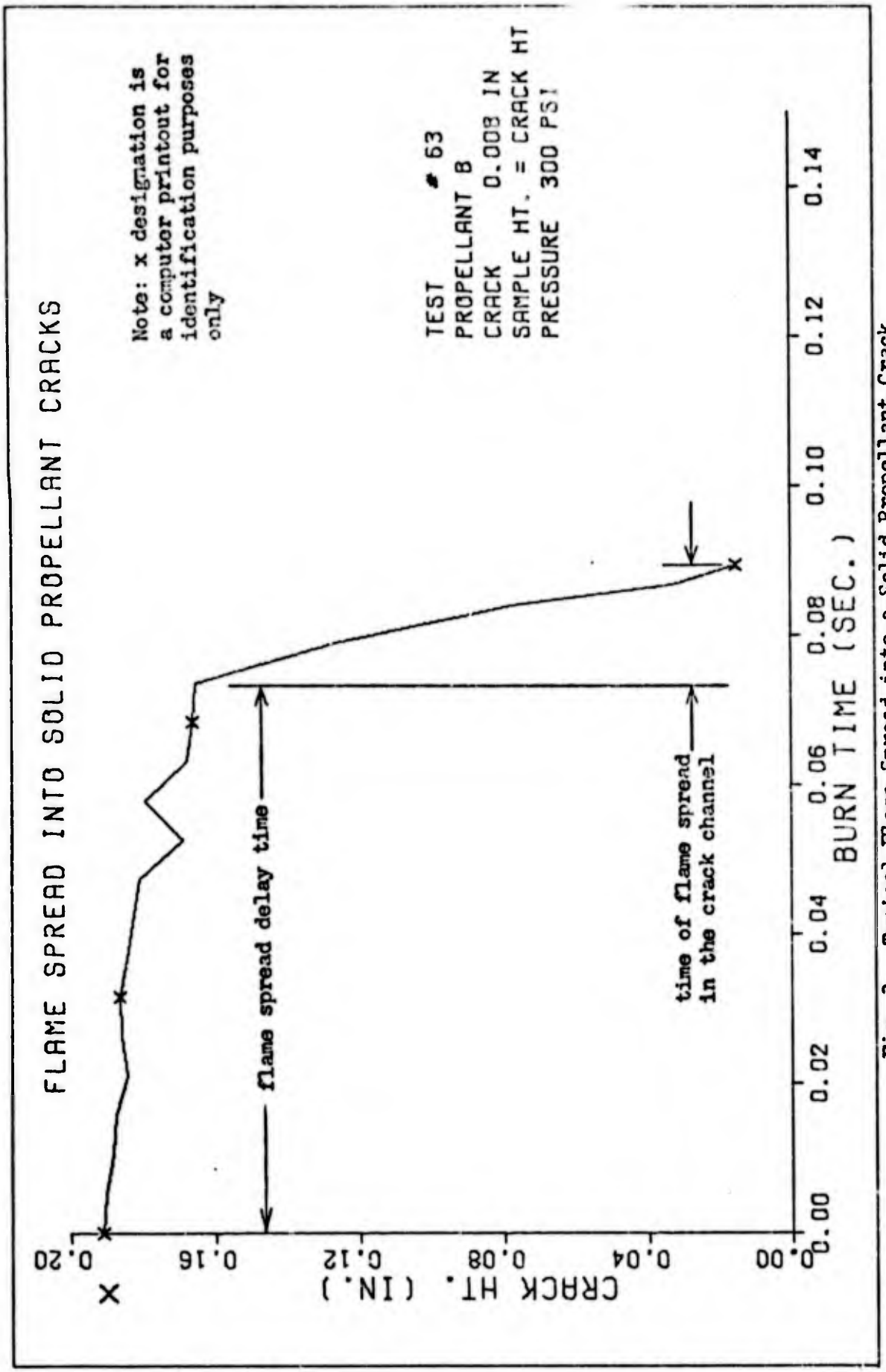

Fig. 3. Typical Flame Spread into a Solid Propellant Crack

allow the flame to penetrate further into the crack. This unsteady probing motion can continue as the flame moves to the bottom in the wider cracks (c.f., Fig. 16D). However, little unsteady motion is noticed for the narrower crack widths.

Allowing for the considerable data scatter, Fig. 4 plots the crack entrance velocity V_e against crack width. This data trend is represented as a nonlinear curve resulting from a data point averaging curve fit. Thus, the averaged entrance velocity of flame spread into a propellant crack decreases as crack width increases. This trend exists for all propellants used during this study for all pressures tested. The ratio of entrance velocity to the overall velocity V_e/V_{tot} as a function of crack width is plotted in Fig. 5 for a given propellant and vessel pressure. Here, the trend is for increased V_e/V_{tot} ratios as crack width increases.

As noted in Fig. 3, rapid flame penetration into the propellant crack is represented by the steep slope of the data curve (also see data of Appendix B). This is similar to the runaway flame spread velocity described by Prentice (Ref 5). When the crack width is plotted against this flame penetration velocity in the crack channel, the flame front velocity increases drastically as the crack width decreases (Fig. 6). This result is consistent for all tests.

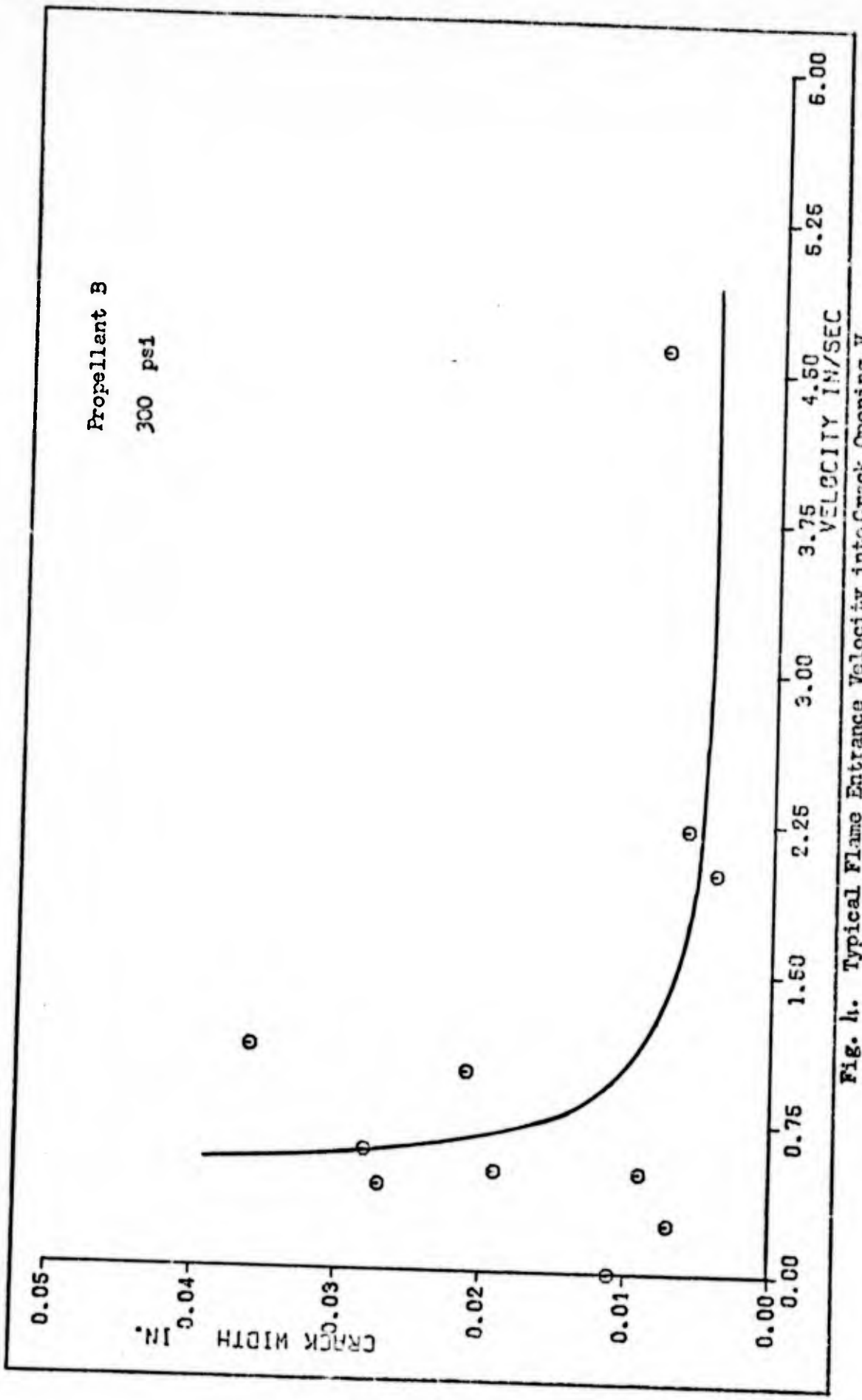

Fig. 4. Typical Flame Entrance Velocity into Crack Opening V_o

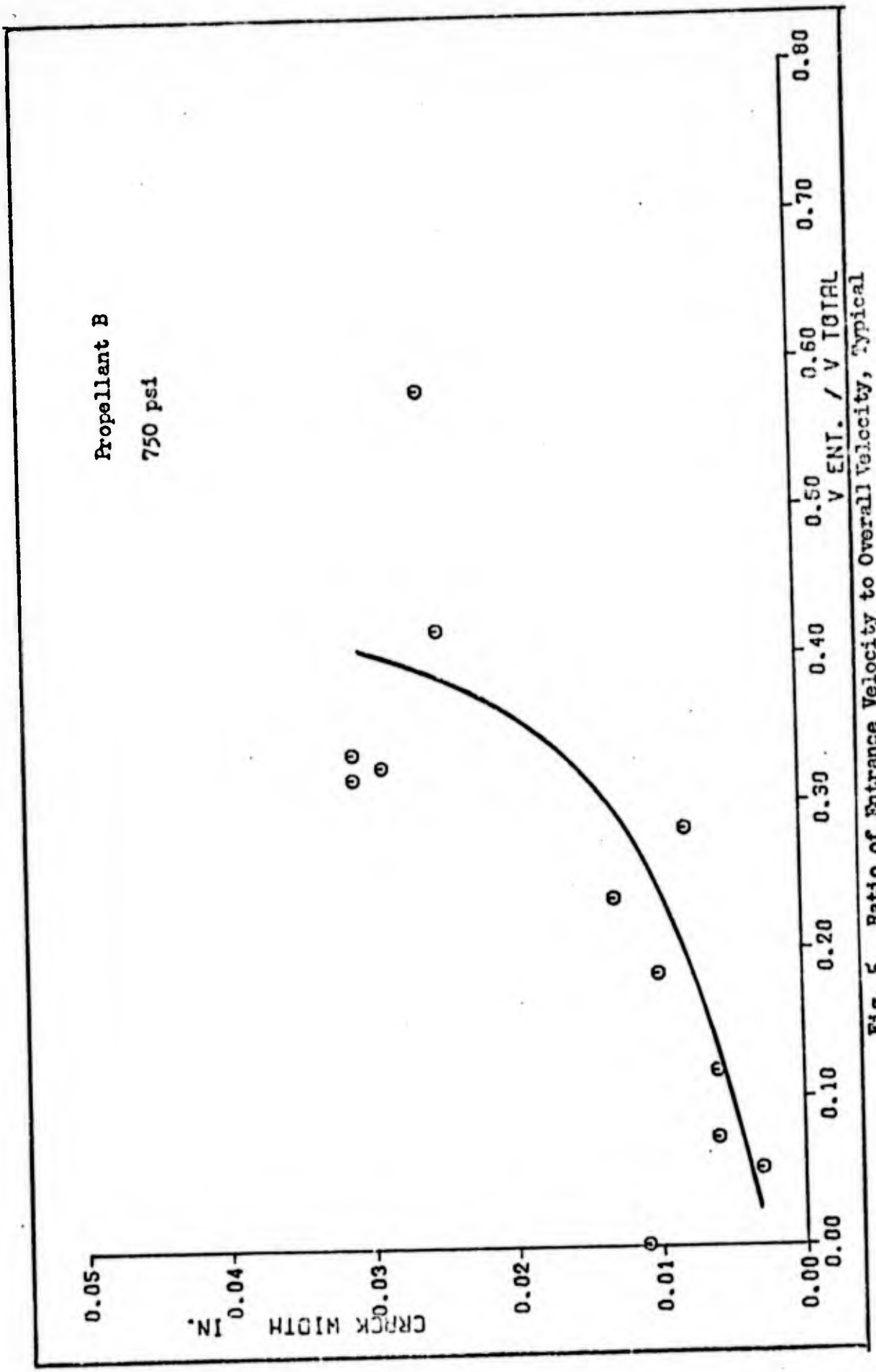

Fig. 5. Ratio of Entrance Velocity to Overall Velocity, Typical

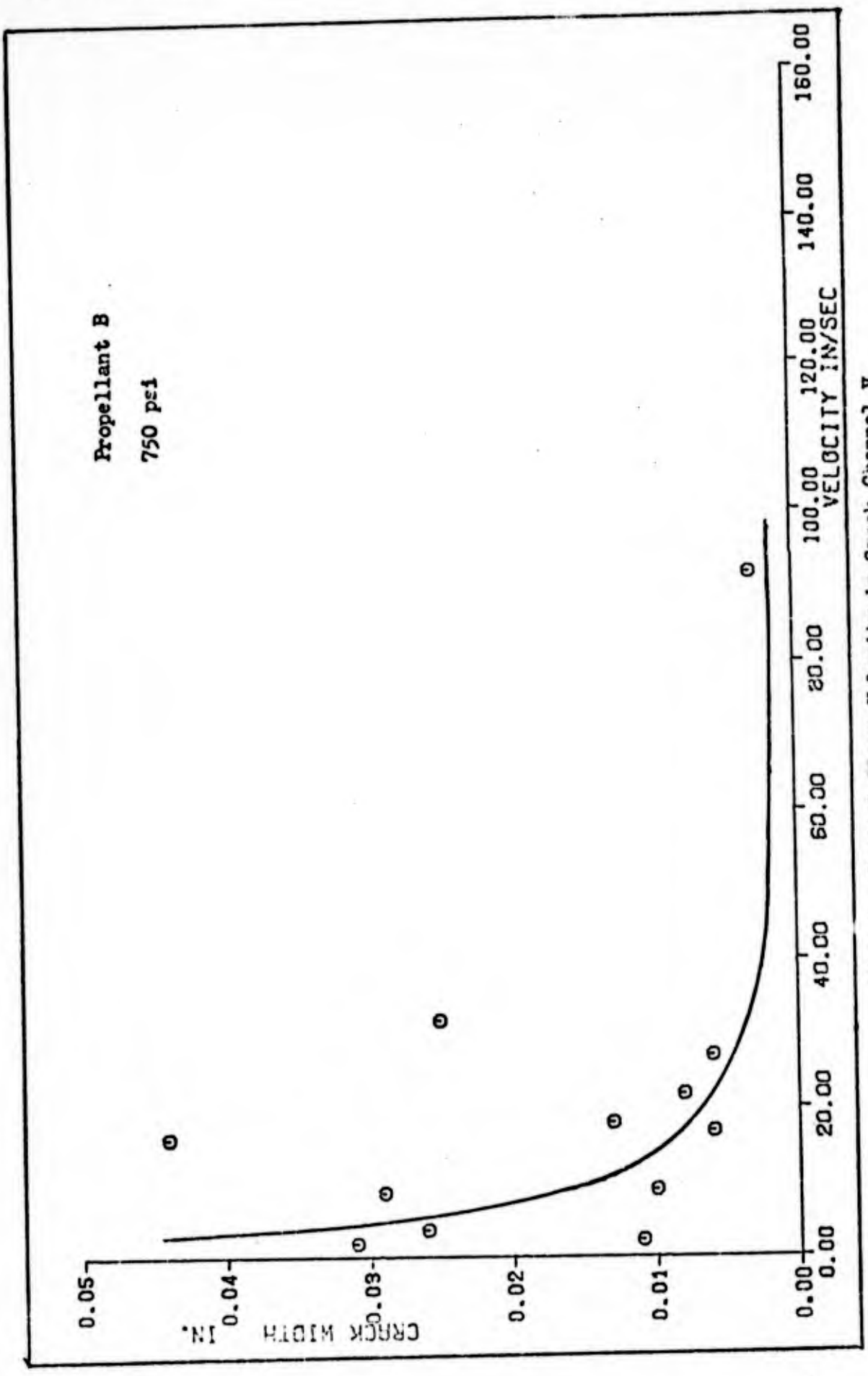

Fig. 6. Typical Flame Velocity in Crack Channel V_c

In the works of T. Godai (Ref 4) and J. L. Prentice (Ref 5), a critical crack width was reported for which the combustion flame would not penetrate into the propellant crack. For the range of crack widths tested in this study, there was no case in which the flame did not penetrate into the crack. However, the wider cracks did experience a much slower penetration velocity. If the crack was wide enough, it is conceivable that the two propellant samples could burn down with no flame interaction between them. It is possible, also, that the crack height-to-depth ratio and the geometric shape of a crack may affect its flame spread characteristics. In this experiment, as with that of Payne (Ref 3), rectangular crack geometries with heights of 1/4 inch were studied at relatively small crack widths. Payne reports results similar to those obtained here. Williams, at the University of Utah used triangular shaped cracks several inches long in pressure distribution studies and reported no instance in which the flame did not spread into the crack (Ref 1:4-26). Both Godai and Prentice used cylindrical shaped crack geometries of greater length than those used in this report. This might account for the critical crack diameter they encountered.

The threshold delay and the rapid flame spread into the crack channels can be explained through heat transfer and channel pressure considerations (Refs 3:5 and 7:36). According to O. C. de C. Ellis and W. A. Kirby, a flame

front will move into regions of lower pressure at a velocity which will increase as the driving pressure increases. The driving pressure is the pressure produced at the surface area where the pressure rise is proportional to the burning area of the flame (Ref 7:38). The build-up of pressure above the crack threshold due to the burning of the top surface will create a pressure differential between the burning surface and the crack region. This will provide an impetus for the flame to move into the crack. Although this supplies a driving force for movement of the flame into the crack and could contribute to the flame threshold delay, it does not offer an adequate explanation for the probing characteristic of the flame and the sudden rapid flame spread into the channel. For a flame to penetrate into a crack, conditions must exist inside the crack region to advance the flame. Therefore, the flame entrance into the crack threshold depends upon the increase in crack surface temperature and the amount of combustible gases inside the crack region as well as the existing pressure gradient between the top burning surface and the crack region.

In several of the test film strips, gas is shown flowing into the crack area upon the initial heating of the top surface. This was observed to occur before the top surface ignition was under way. The hot nichrome wire must heat the top surface to well over 400°C before the

propellant surface can sustain its own combustion (Refs 8:6, 9:16, and 11). This convection is similar to that described by Ellis and Kirby (Ref 7:16). The hot gases flow immediately into the crack filling it with combustible gases. The temperature of the crack walls is raised by heat convected through the gas film covering them. This heat is then conducted into the propellant surface raising the wall temperature to gas generation levels. This can provide a continued source of combustible gases inside the crack region.

The gas velocity in the propellant crack can be related to the reciprocal of the crack width as described by Payne (Ref 3:5).

$$V_g = \frac{A_b \rho_s r_b}{\rho_g} (1/W_c) \qquad (1)$$

Accordingly, the gas velocity inside the crack will increase linearly as the crack width decreases. For convective heat transfer, Summerfields' heat transfer coefficient for a gas film adjacent to a solid surface is related to the 0.8 power of the gas velocity (Ref 10:89). This related the heat transfer coefficient to the reciprocal of the crack width also but not linearly. Thus, a higher heat transfer coefficient is realized with the smaller crack widths. It is reasoned that the faster flame front propagation in a narrower crack results from higher gas velocities inside

the crack, a higher heat transfer coefficient, and less area to fill with combustible gas to fuel the flame. With combined factors of pressure, generated gas velocity and convective heat transfer as mechanisms for flame propagation, a linear relationship between crack width and flame spread velocity in the crack would not be expected. The curves plotted for crack width versus the flame spread velocity support this assertion (see Fig. 6).

Gas generation and convective heat transfer along with the pressure differential addressed above can offer an explanation of the entrance time delay also. For a flame entering a crack opening, a finite amount of time is needed for a pressure gradient to develop between the crack area and the burning propellant top surface. Some time is also required for heat transfer to the crack surfaces. The walls of the crack threshold are initially cool compared to the burning flame area. Any cooling contact provides the flame with an area of adhesion and energy is lost to the surface as opposed to the burning top surface area where energy is being liberated (Ref 7:38). The pressure build-up, the heating and filling of the crack by combustible gases, and flame energy absorption at the crack threshold may occur simultaneously to account for the time delay at the crack entrance and the unstable probing characteristics of the flame at that point.

The entrance delay followed by the rapid flame propagation into the channel are essentially two chronological steps in a single process. This flame spread characteristic was common among the three propellants at the pressures tested. Based upon these observations, one can assert that this is a general characteristic for flame propagation into solid rocket propellant cracks and can be expected in most solid propellants.

The curves developed for V_c in Appendix A were used to display the effects of pressure on flame spread for constant crack widths. Curves for this velocity, as well as the linear burn rates, for each propellant versus pressure appear in Fig. 7. The velocity inside the crack channel is shown to reach several hundred times the linear burn rate as the crack widths decrease. The greater increase in V_c occurs at crack widths below 0.020 inches. This high flame velocity in the crack channel was consistent for all propellants and pressures tested.

The results displayed in Fig. 7 clearly indicates that the crack width has a much greater effect on flame spread than the combustion pressure for the pressure range tested. For Propellant A, the V_c increase with pressure is similar in slope to the linear burn rate for the larger crack widths (0.20 inches to 0.40 inches). For small crack widths (below 0.020 inches), V_c decreases to a minimum and then increases as combustion pressure increases. Propellant B shows a

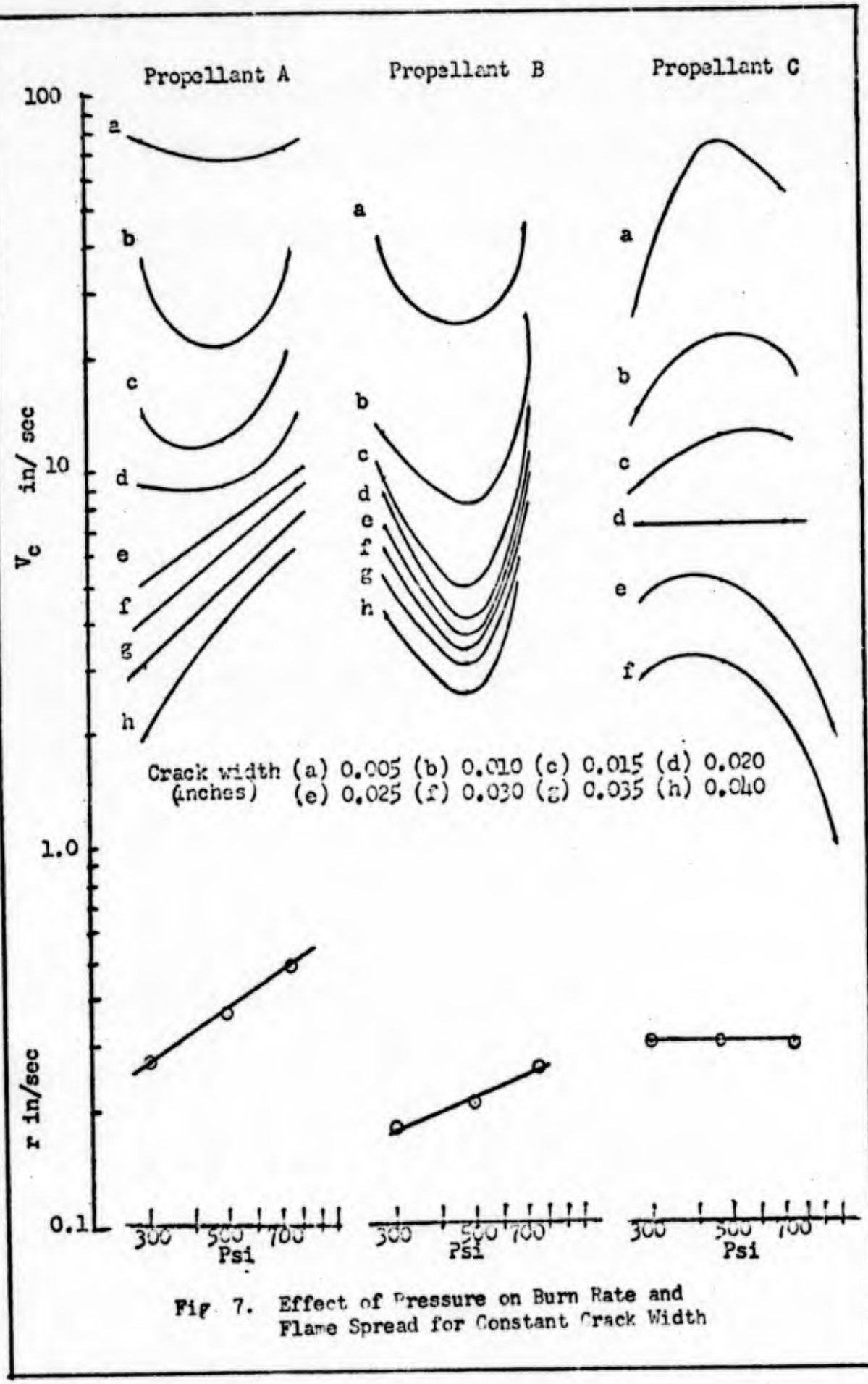

Fig 7. Effect of Pressure on Burn Rate and Flame Spread for Constant Crack Width

decreasing V_c at the lower pressure range to a minimum value, then increasing V_c as the pressure increases. This trend was consistent for all crack widths in Propellant B. The linear burn rate of Propellant C indicates that it is a plateau burner for the pressure range tested. For constant crack widths, it generally exhibits an increasing V_c to a maximum which then decreases as pressure increases (see Fig. 7). From the trends of Fig. 7, it appears that the effects of pressure on the flame spread inside a crack channel is different for each propellant.

IV. Conclusions

This study was conducted to experimentally investigate the effect of propellant crack width on the flame spread into cracks which appear in solid rocket propellants. Cracks were fabricated in three types of solid propellants and tested under pressures of 300, 500, and 750 psi for crack widths which varied from 0.002 inches to 0.044 inches in width.

The following conclusions on the influence of propellant crack width on flame spread were drawn from the results of this study:

(1) The flame experiences a delay time at the entrance to the crack. The associated entrance velocity increases, in proportion to the overall flame spread velocity, as the crack width increases.

(2) The flame spread velocity inside the crack channel increases as the crack width decreased (c.f. Fig. 4).

(3) The crack width has a much greater effect on flame velocity inside a crack than combustion pressure.

(4) Flame velocity inside a crack channel can be several hundred times the linear burn rate for small cracks (see Fig. 7).

(5) The flame velocity exhibits greater increases in crack widths below 0.020 inches.

(6) The specific flame velocity inside cracks as a function of pressure is unique for each propellant.

Based on the results of this study, it is probable that a large number of very small cracks in a rocket propellant could cause an adverse effect on a rocket motor's performance. The large increase in burning area and the associated pressure rise, along with the unsteady probing of the flame into the propellant cracks could couple with certain acoustic phenomena to produce oscillatory burning or other similar burning instability within the rocket motor.

V. Recommendations

Further work should be conducted in the area of flame propagation into solid propellant cracks to gain more information on flame spread phenomena to add to the limited amount of data currently available. The following work is recommended to verify certain assumptions and conclusions resulting from this experiment as well as to investigate conditions not addressed in this study:

(1) A similar experiment should be performed with the same sample configuration but higher vessel pressures.

(2) Crack samples should have a more realistic height-to-depth ratio, since natural cracks in solid propellants can be several inches long.

(3) An experiment should be devised to test the effect of crack geometry upon the flame propagation into the cracks. Flame spread into rectangular, triangular, cylindrical and nonuniform cracks should be compared at various widths and realistic lengths to determine any geometric effects.

(4) This experiment addressed propellant cracks which were open at the edges. A future study should consider cracks with closed edges and address the effects of combustion gases and pressures inside the crack which may affect flame spread. The nitrogen flow here could have some effect on the flame spread.

(5) Accurate pressure measurements should be considered to gage the pressure increase in relation to the surface area resulting from a crack. An effort to maintain constant pressure during the propellant sample burn should be made.

(6) This study tested older propellants which had aged for a period of time. Propellants of a more recent manufacture and type should be tested to determine what affect age has on flame spread.

(7) An effort to determine if flame radiation effect on the initial time delay of flame propagation should also be considered.

Bibliography

1. Williams, M. L. The Study of Crack Critically in Solid Rocket Motors. UTC DO 71-041, The University of Utah, Salt Lake City, Utah, January 1971.

2. United Technology Center. Development of Nondestructive Testing Techniques for Large Solid-Propellant Rocket Motors. UTC 2015-FR, Sunnyvale, California, April 1963.

3. Payne, C. E. Flame Propagation in Propellant Cracks. AFRPL-TR-69-66, Edwards AFB, California: Air Force Rocket Propulsion Laboratory, April 1969.

4. Godai, T. Flame Propagation into the Gap of Solid Propellant. National Aerospace Laboratory, Tokyo, Japan: Report No. 91, pp. 1-12 (1965), Translated from the Japanese language by the Redstone Scientific Information Center, Redstone Arsenal, Alabama, 1967.

5. Prentice, Jack L. Flashdown in Solid Propellants. NAVWEPS Report 7964, China Lake, California: U.S. Naval Ordinance Test Station, December 1962.

6. Jacobs, H. R. An Experimental Study of the Pressure Distribution in Burning Flaws in Solid Propellant Grains. AD-756 912, Salt Lake City, Utah: Utah University, October 1972.

7. Ellis O. C. de C. Flame. London, England: Matheuw and Co. LTD, 1936.

8. Price, E. W. Solid Propellant Combustion: State of Knowledge 1967. NWC TP 4520, China Lake, California: Naval Weapons Center, April 1968.

9. Strittmater, R. C. Measurement of Temperature Profiles in Burning Solid Propellants. Report No. 1737, Aberdeen Proving Grounds, Maryland: U.S. Army Material Command Ballistic Research Laboratory, March 1966.

10. Sutton, George P. Rocket Propulsion Elements. New York, New York: John Wiley and Sons, 1964.

11. Cotton, D. J. Solid Propellant Burning Mechanism Study. NAVWEPS Report No. 8573, Indian Head, Maryland: U.S. Naval Propellant Plant, May 1964.

Appendix A

Tables and Plots of Reduced Data

The tables and plots of data reduced from the curves of Appendix B are listed here. Tables II, III, and IV shows the data used in the following plots of V_e, V_c, and V_e/V_{tot} for each of the propellants tested.

TABLE II

Propellant A Data

Temperature 72°F

Test (#)	Crack Width (Inches)	V_o (in/sec)	V_g (in/sec)	V_c (in/sec)	V_g/V_{tot}	Crack Depth (in)
			300 psi			
18	0.027	2.27	1.00	4.50	0.441	0.25
24	0.021	10.60	3.75	16.00	0.354	0.19
19	0.020	7.00	2.61	21.40	0.373	0.18
4	0.019	5.00	1.87	15.00	0.374	0.21
25	0.015	2.88	1.17	8.00	0.406	0.23
36	0.010	7.37	2.67	20.00	0.362	0.14
30	0.008	4.78	1.43	10.00	0.299	0.22
			500 psi			
6	0.032	6.21	3.00	10.00	0.483	0.28
11	0.029	5.48	1.88	9.33	0.343	0.34
7	0.025	14.66	14.00	15.00	0.955	0.22
1	0.024	1.67	0.67	2.00	0.401	0.25
14	0.023	2,60	0.85	6.00	0.327	0.26
17	0.017	7.50	2.85	14.00	0.380	0.18
23	0.016	1.70	0.00	1.70	0.000	0.17
32	0.012	11.76	3.33	21.25	0.283	0.20
26	0.013	10.00	4.44	13.84	0.444	0.22
35	0.008	12.22	2.50	20.00	0.204	0.22
29	0.006	8.18	1.67	16.00	0.204	0.18
100	0.005	21.00	10.00	32.00	0.476	0.21
			750 psi			
2	0.037	0.83	0.49	1.00	0.575	0.20
8	0.034	9.00	4.00	14.00	0.444	0.18
12	0.032	6.43	3.00	8.33	0.466	0.18
21	0.025	10.45	4.71	30.00	0.451	0.23
16	0.021	10.47	3.57	24.48	0.341	0.22
33	0.017	9.52	5.00	17.77	0.525	0.20
27	0.015	2.50	0.00	5.00	0.000	0.20
22	0.014	18.46	10.00	24.44	0.542	0.20
28	0.011	10.00	2.72	18.90	0.272	0.21
34	0.009	13.13	1.43	22.22	0.110	0.21
101	0.006	62.50	0.00	62.50	0.000	0.25

TABLE III

Propellant B Data

Temperature 78°F

Test (#)	Crack Width (in.)	V_o (in/sec)	V_e (in/sec)	V_c (in/sec)	V_e/V_{tot}	Crack Ht. (in.)
			300 psi			
39	0.026	4.42	1.11	6.19	0.251	0.23
43	0.028	3.71	0.60	11.50	0.162	0.26
40	0.027	2.19	0.43	6.56	0.195	0.23
48	0.021	2.44	1.00	3.60	0.410	0.22
46	0.019	1.92	0.50	7.60	0.260	0.24
54	0.011	9.09	0.00	9.09	0.000	0.20
55	0.009	3.14	0.50	6.67	0.159	0.22
58	0.008	18.18	4.61	37.70	0.235	0.20
63	0.007	2.00	0.25	11.33	0.135	0.19
67	0.006	7.50	2.21	17.00	0.296	0.21
97	0.004	10.43	2.00	67.00	0.192	0.24
			500 psi			
38	0.035	6.67	0.00	6.67	0.000	0.18
53	0.031	5.47	1.36	10.00	0.249	0.23
41	0.026	3.01	1.02	7.39	0.332	0.22
44	0.020	0.54	0.00	0.54	0.000	0.19
45	0.018	1.81	0.00	1.81	0.000	0.18
47	0.021	3.13	1.00	5.00	0.320	0.25
56	0.012	3.91	0.00	5.11	0.266	0.24
59	0.011	2.10	0.80	3.40	0.390	0.21
62	0.008	1.82	0.50	6.16	0.275	0.20
64	0.005	6.90	1.81	10.00	0.262	0.20
68	0.006	1.68	0.00	1.68	0.000	0.19
99	0.004	16.15	2.50	38.00	0.152	0.21
			750 psi			
37	0.044	5.00	1.33	16.00	0.266	0.20
49	0.032	1.19	0.36	1.89	0.317	0.20
37A	0.031	11.50	3.85	25.70	0.335	0.23
50	0.029	2.40	0.85	8.50	0.325	0.24
42	0.026	2.98	1.67	3.67	0.580	0.23
52	0.025	24.00	10.00	31.70	0.417	0.24
57	0.011	2.14	0.00	2.14	0.000	0.15
60	0.010	2.33	0.43	9.00	0.184	0.21
61	0.008	9.33	2.35	22.80	0.282	0.20
69	0.006	8.00	0.59	27.00	0.074	0.20
98	0.003	48.00	4.00	92.00	0.083	0.24

TABLE IV

Propellant C Data

Temperature 84° F

Test (#)	Crack Width (in.)	V_o (in/sec)	V_e (in/sec)	V_c (in/sec)	V_e/V_{tot}	Crack Ht. (in.)
			300 psi			
70	0.021	6.67	1.82	9.47	0.272	0.20
76	0.019	2.22	0.20	4.75	0.000	0.20
81	0.016	5.83	1.67	7.92	0.286	0.21
88	0.003	4.89	0.55	16.92	0.112	0.24
92	0.002	12.00	0.00	12.00	0.000	0.24
96	0.006	25.00	10.00	40.00	0.400	0.25
95	0.007	25.00	0.00	25.00	0.000	0.25
			500 psi			
71	0.028	5.27	1.00	6.92	0.190	0.19
74	0.023	2.71	0.00	2.71	0.000	0.19
77	0.015	6.67	1.25	12.85	0.190	0.20
80	0.017	3.48	0.26	7.85	0.007	0.23
82	0.009	5.22	1.11	20.00	0.210	0.24
85	0.007	26.25	2.5	50.00	0.010	0.21
91	0.003	23.33	3.33	63.30	0.140	0.21
94	0.006	40.00	3.33	100.00	0.080	0.21
			750 psi			
72	0.026	3.82	0.00	3.82	0.000	0.21
73	0.018	5.00	1.00	5.88	0.200	0.22
78	0.020	3.29	0.67	8.00	0.200	0.23
79	0.021	2.00	0.00	2.00	0.000	0.20
84	0.016	4.28	0.50	22.20	0.120	0.21
83	0.010	6.97	0.95	17.15	0.140	0.23
86	0.004	5.64	0.31	30.00	0.060	0.22
90	0.003	30.00	11.40	57.10	0.380	0.24
93	0.002	100.00	0.00	100.00	0.000	0.22

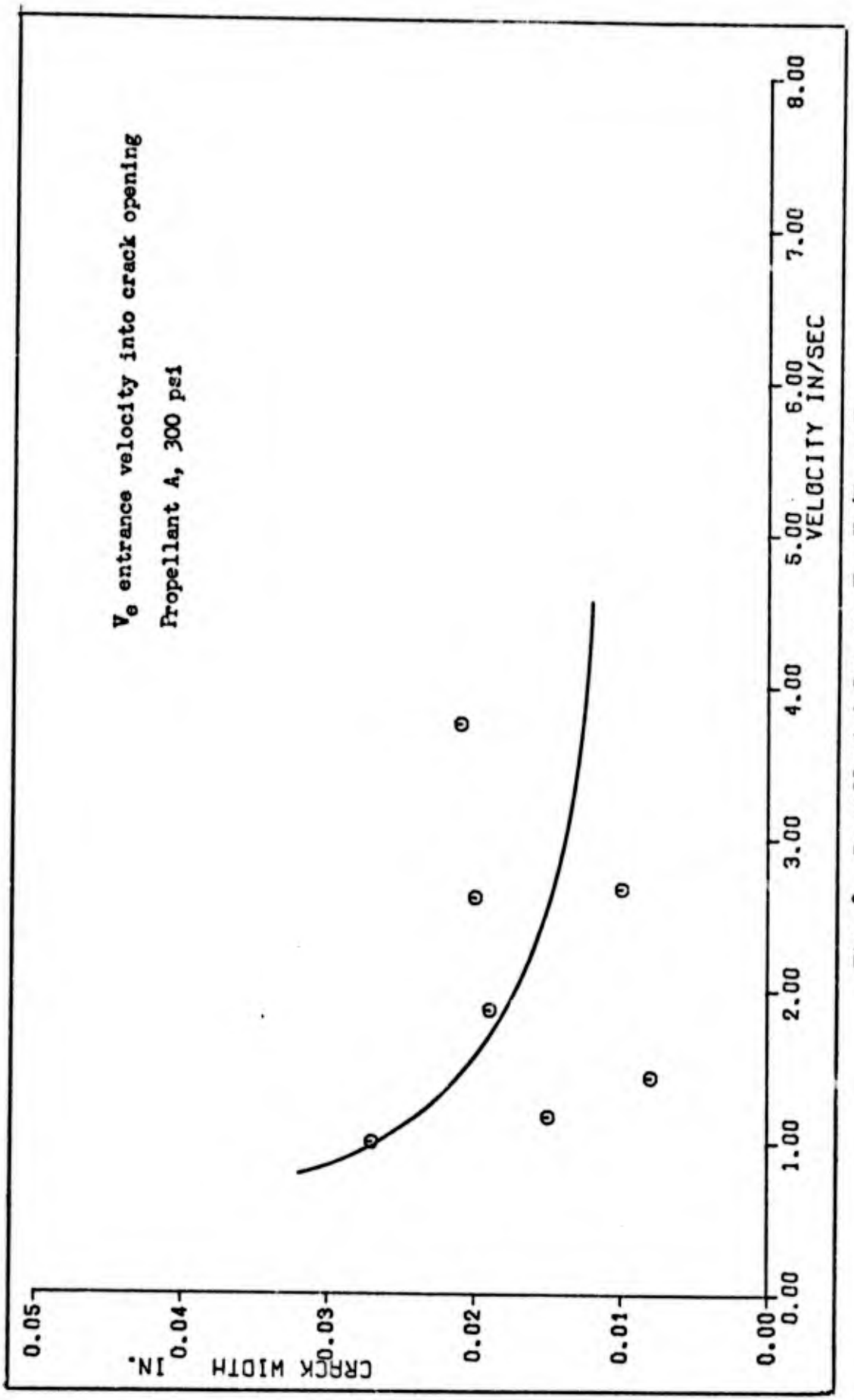

Fig. 8. Propellant A Curves: V_e, V_e/V_{tot}, V_c

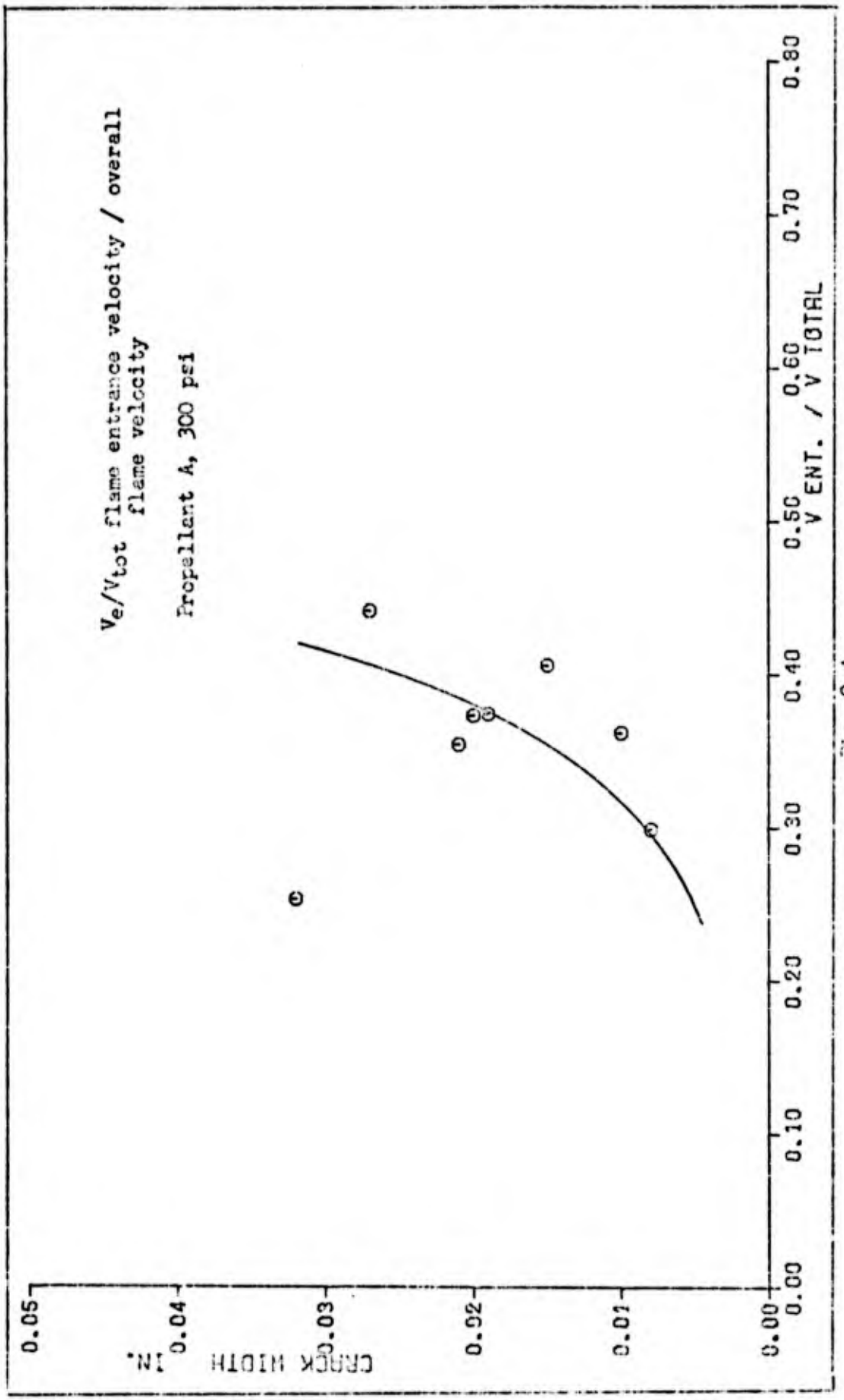
V_e/V_{tot} flame entrance velocity / overall flame velocity
Propellant A, 300 psi
CRACK WIDTH IN.
0.05
0.04
0.03
0.02
0.01
0.00
0.00
0.10
0.20
0.30
0.40
0.50
0.60
0.70
0.80
V ENT. / V TOTAL

Fig. 8 A.

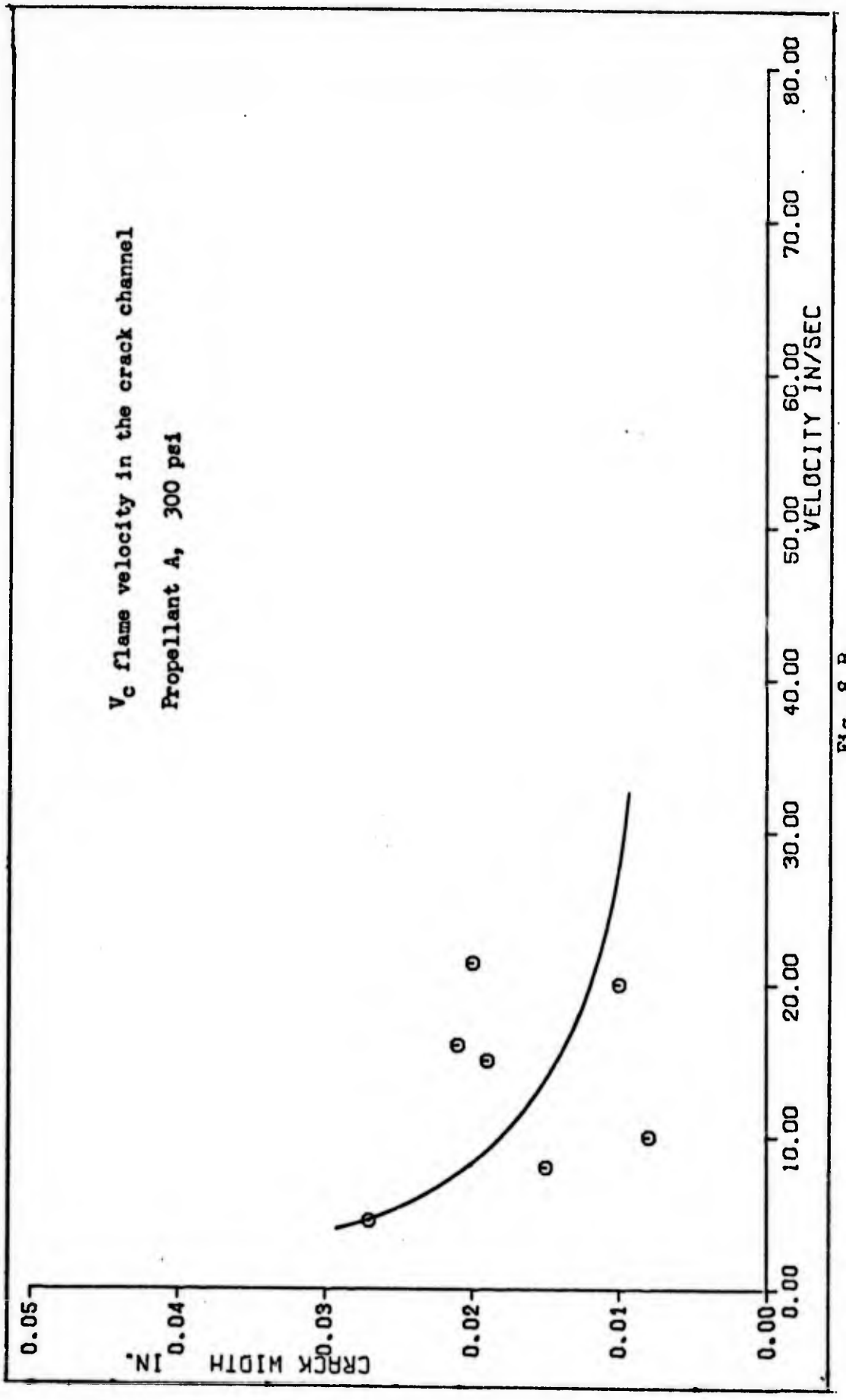
V_c flame velocity in the crack channel
Propellant A, 300 psi
CRACK WIDTH IN.
0.05
0.04
0.03
0.02
0.01
0.00
0.00
10.00
20.00
30.00
40.00
50.00
60.00
70.00
80.00
VELOCITY IN/SEC

Fig. 8 B.

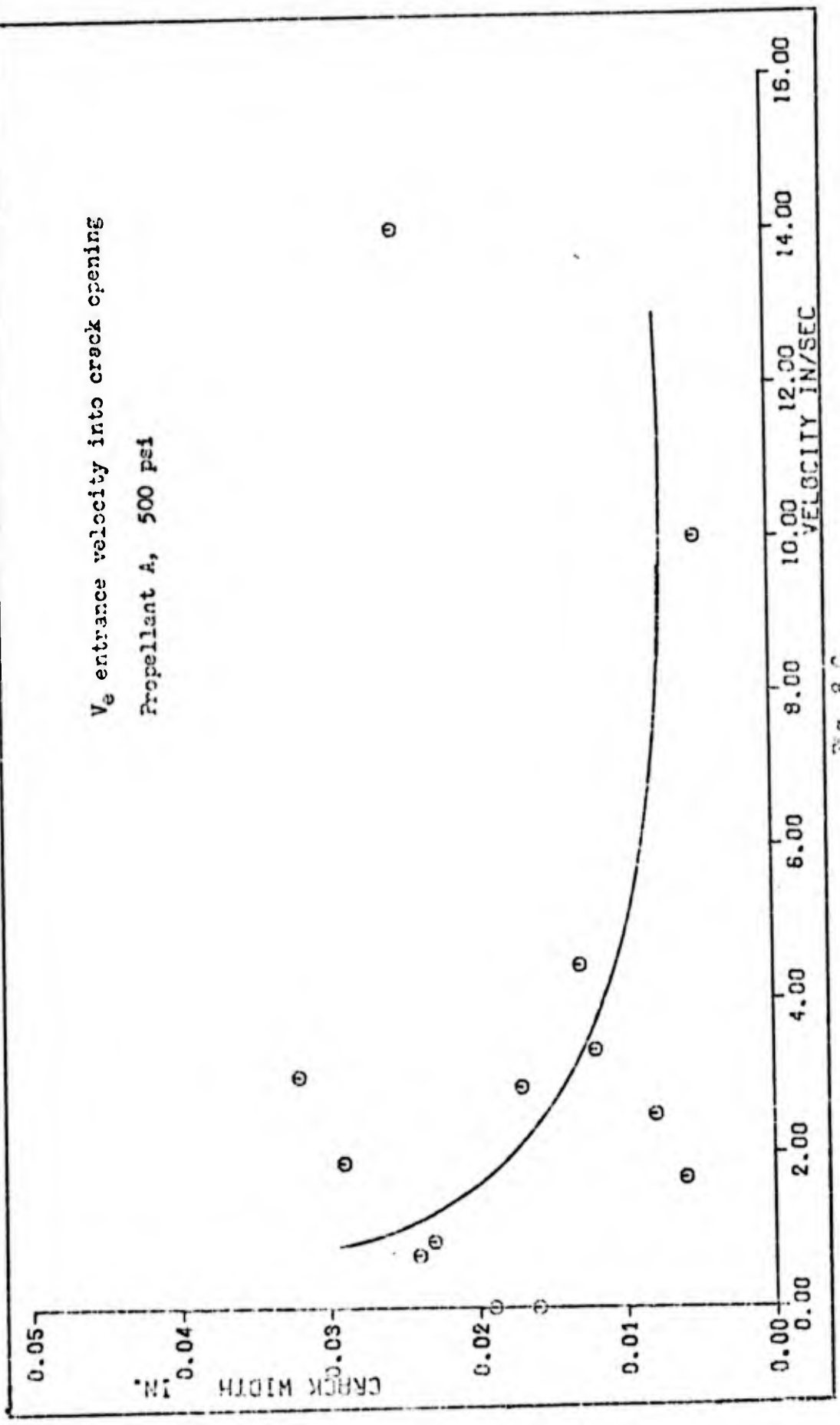
V_e entrance velocity into crack opening
Propellant A, 500 psi
CRACK WIDTH IN.
0.05
0.04
0.03
0.02
0.01
0.00
0.00
2.00
4.00
6.00
8.00
10.00
12.00
14.00
16.00
VELOCITY IN/SEC

Fig. 8 c.

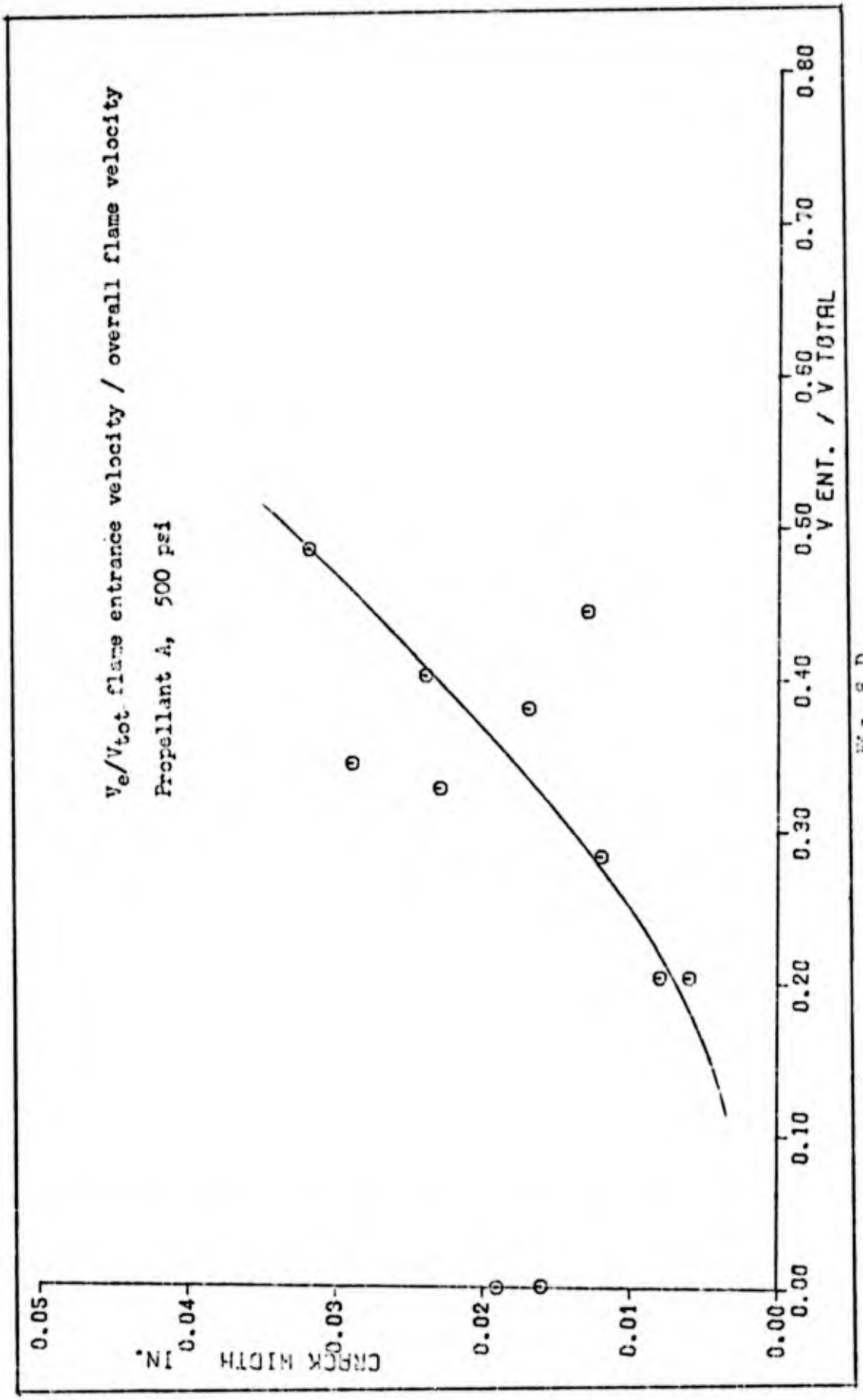
V_e/V_{tot} flame entrance velocity / overall flame velocity
Propellant A, 500 psi
CRACK WIDTH IN.
0.05
0.04
0.03
0.02
0.01
0.00
0.00
0.10
0.20
0.30
0.40
0.50
0.60
0.70
0.80
V ENT. / V TOTAL

Fig. 8 D.

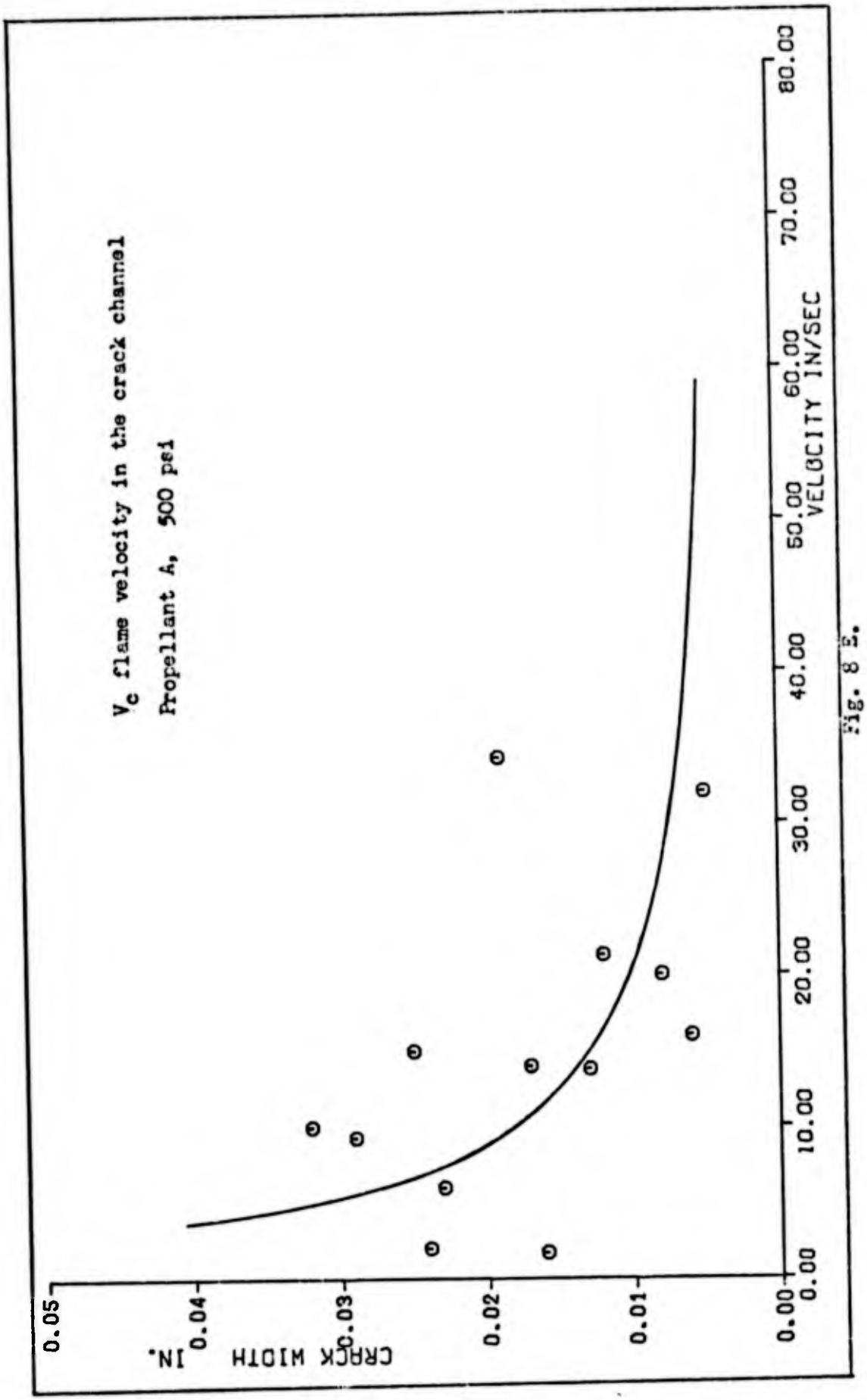
V_c flame velocity in the crack channel
Propellant A, 500 psi
CRACK WIDTH IN.
0.05
0.04
0.03
0.02
0.01
0.00
0.00
10.00
20.00
30.00
40.00
50.00
60.00
70.00
80.00
VELOCITY IN/SEC

Fig. 8 E.

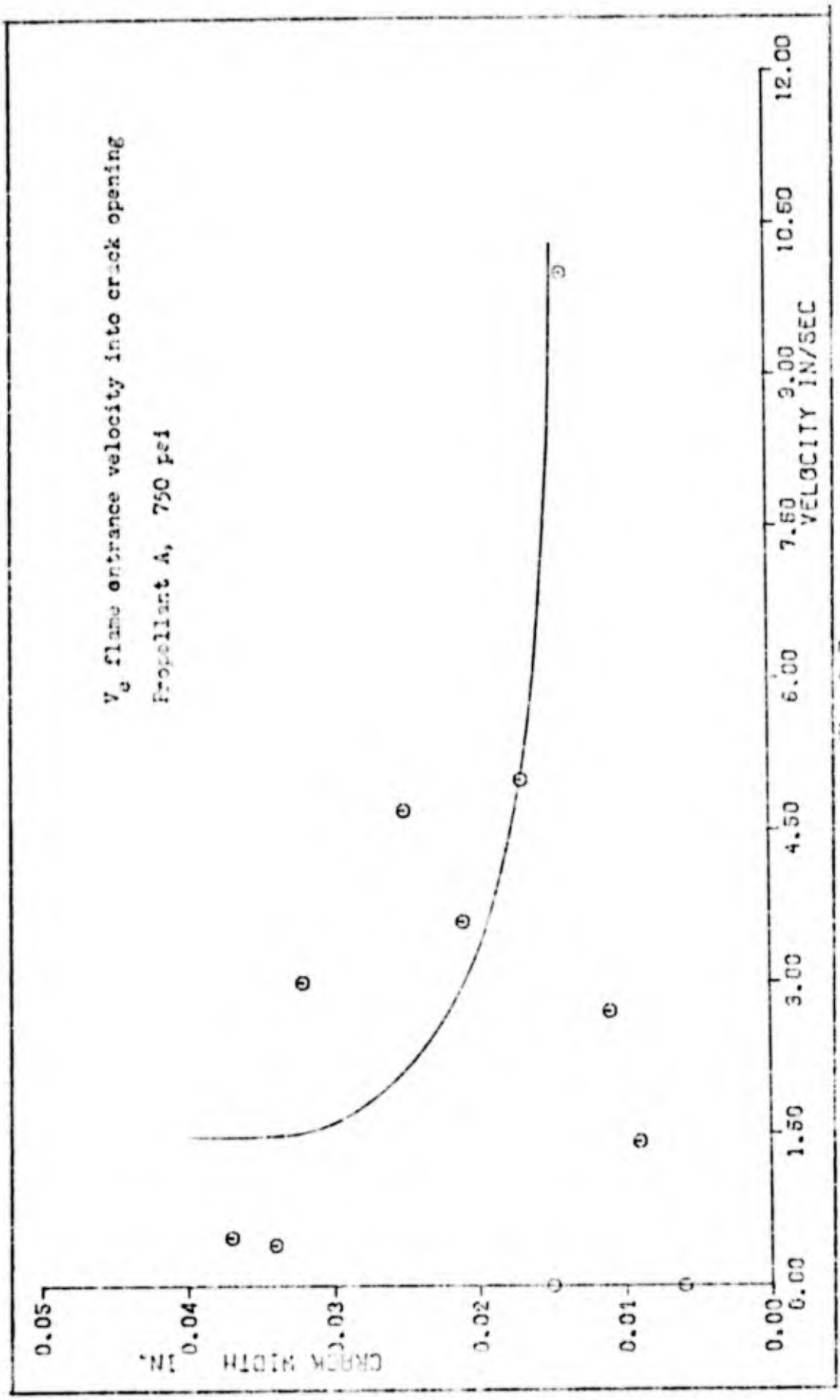
V_e flame entrance velocity into crack opening
Propellant A, 750 psi
CRACK WIDTH IN.
0.05
0.04
0.03
0.02
0.01
0.00
0.00
1.50
3.00
4.50
6.00
7.60
9.00
10.50
12.00
VELOCITY IN/SEC

FIG. 6 2.

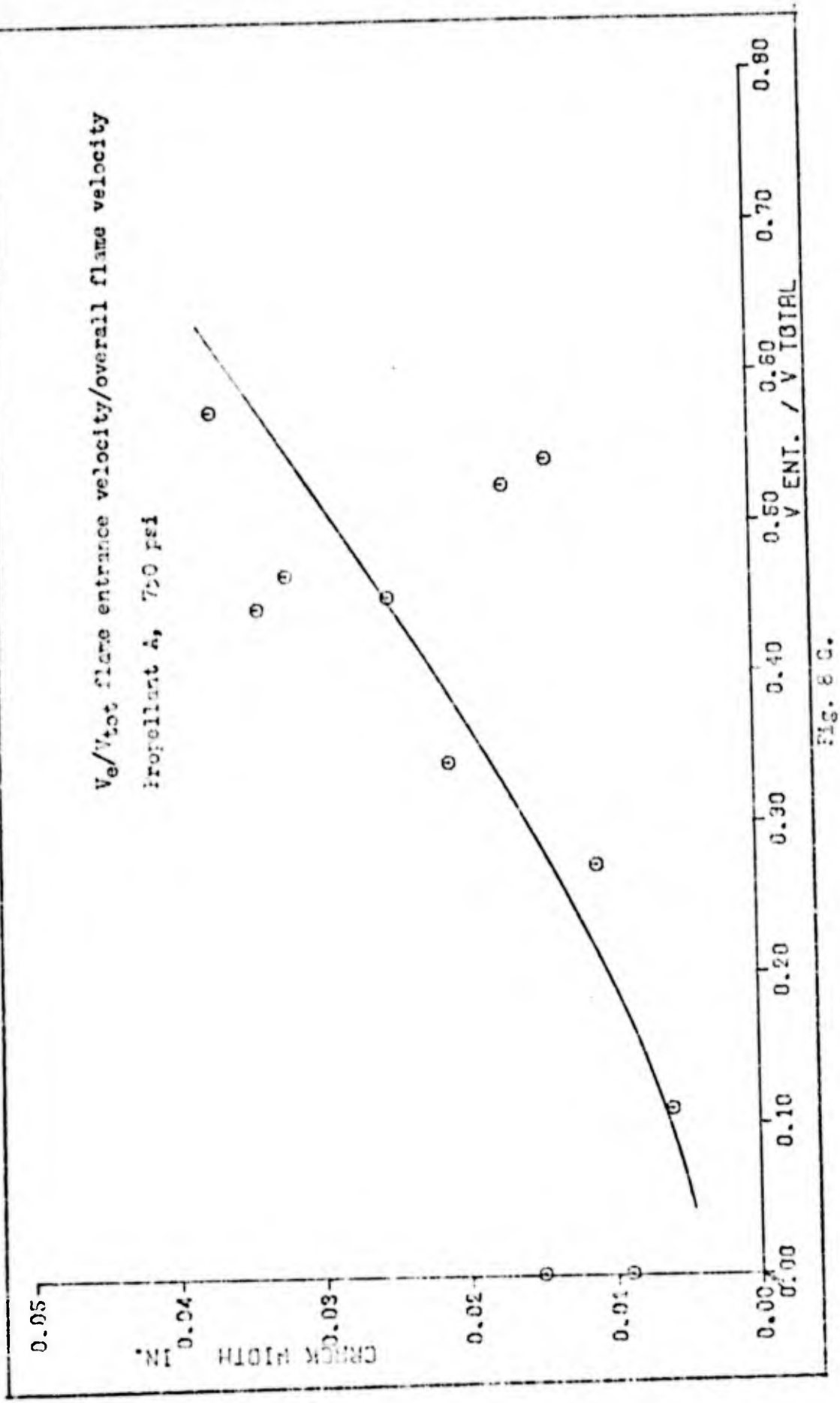
V_e/V_{tot} flame entrance velocity/overall flame velocity
Propellant A, 750 psi
CRACK WIDTH IN.
0.05
0.04
0.03
0.02
0.01
0.00
0.00
0.10
0.20
0.30
0.40
0.50
0.60
0.70
0.80
V ENT. / V TOTAL

Fig. 8 C.

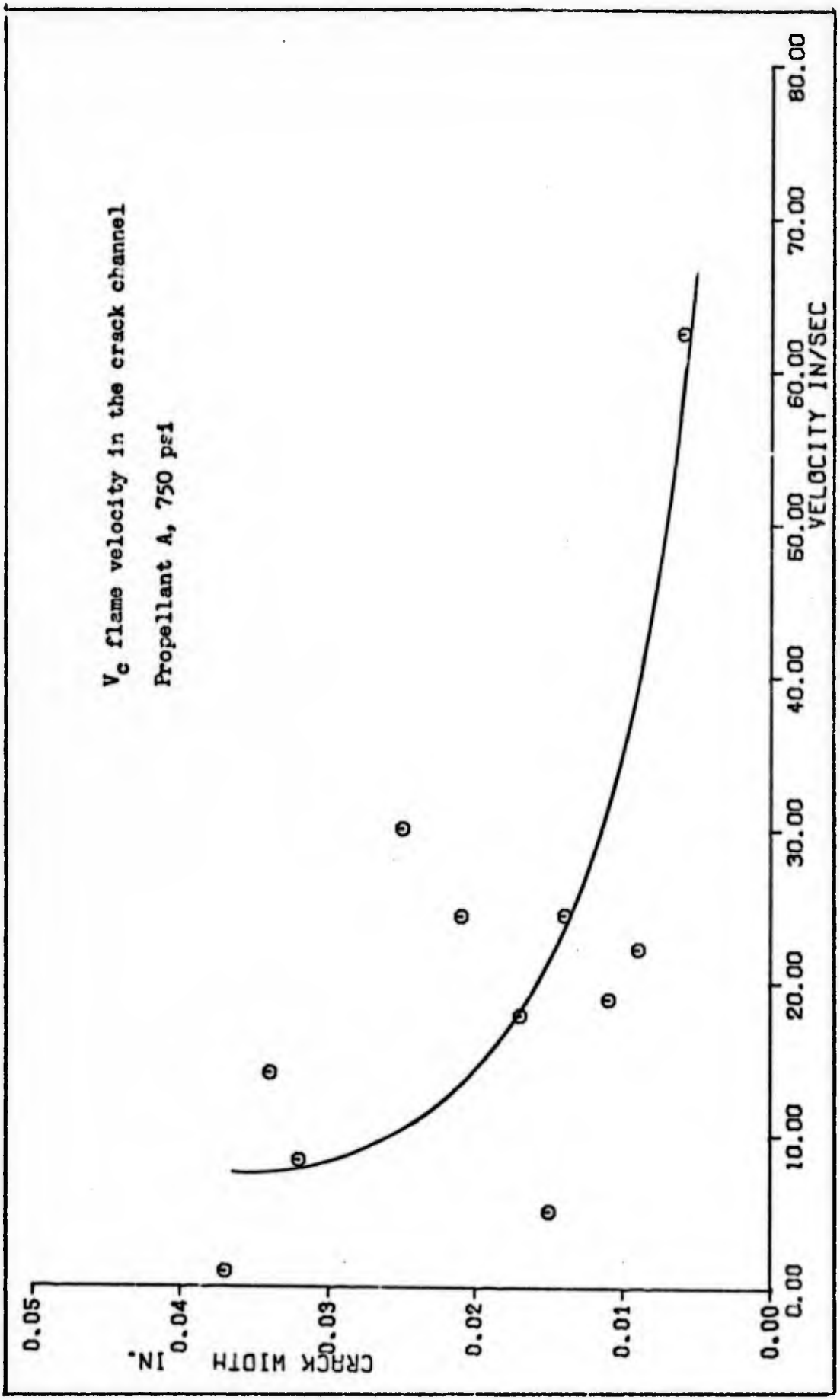
V_c flame velocity in the crack channel
Propellant A, 750 psi
CRACK WIDTH IN.
0.05
0.04
0.03
0.02
0.01
0.00
0.00
10.00
20.00
30.00
40.00
50.00
60.00
70.00
80.00
VELOCITY IN/SEC

Fig. 8 H.

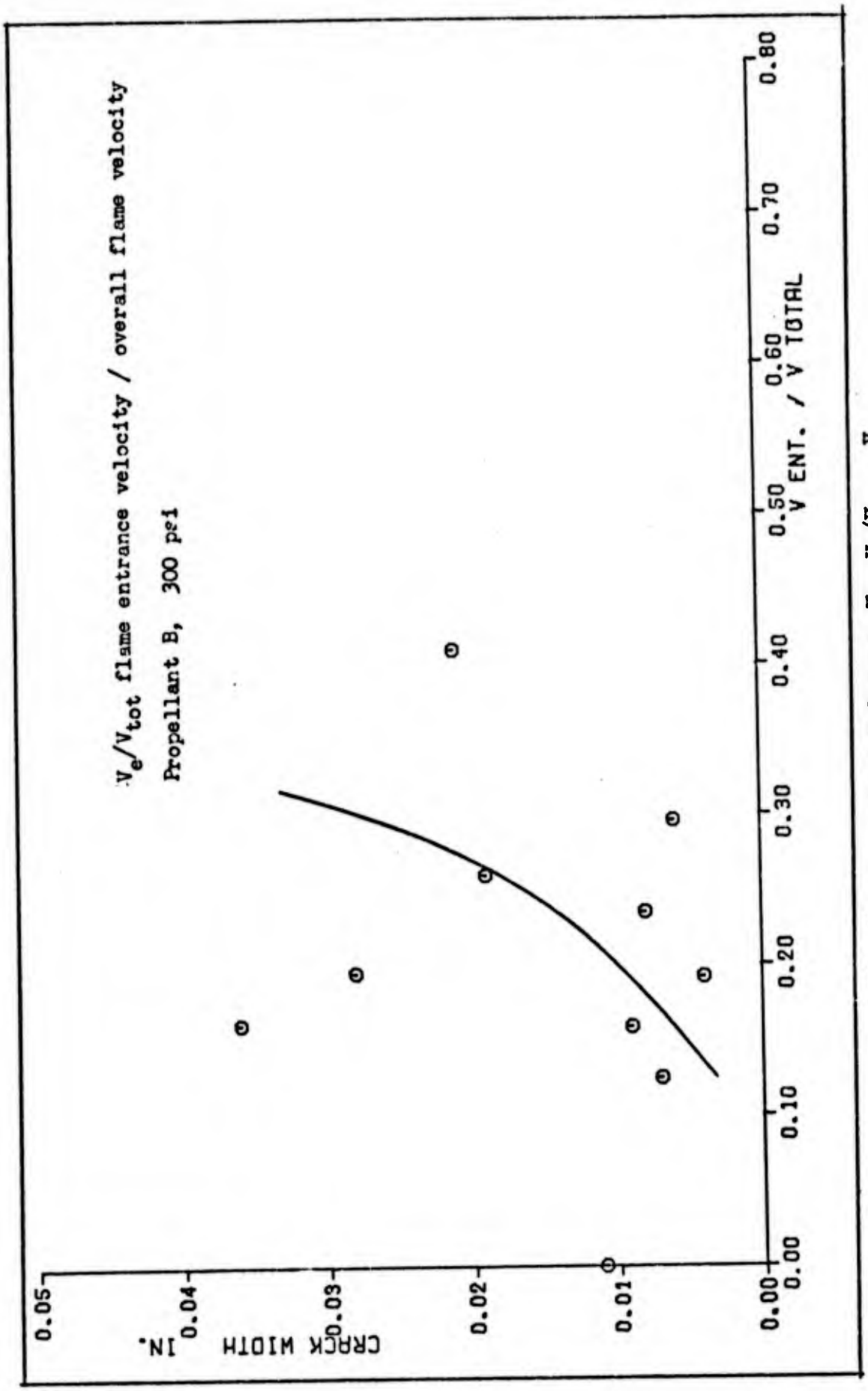

Fig. 9. Propellant B Curves: V_e, V_e/V_{tot}, V_c

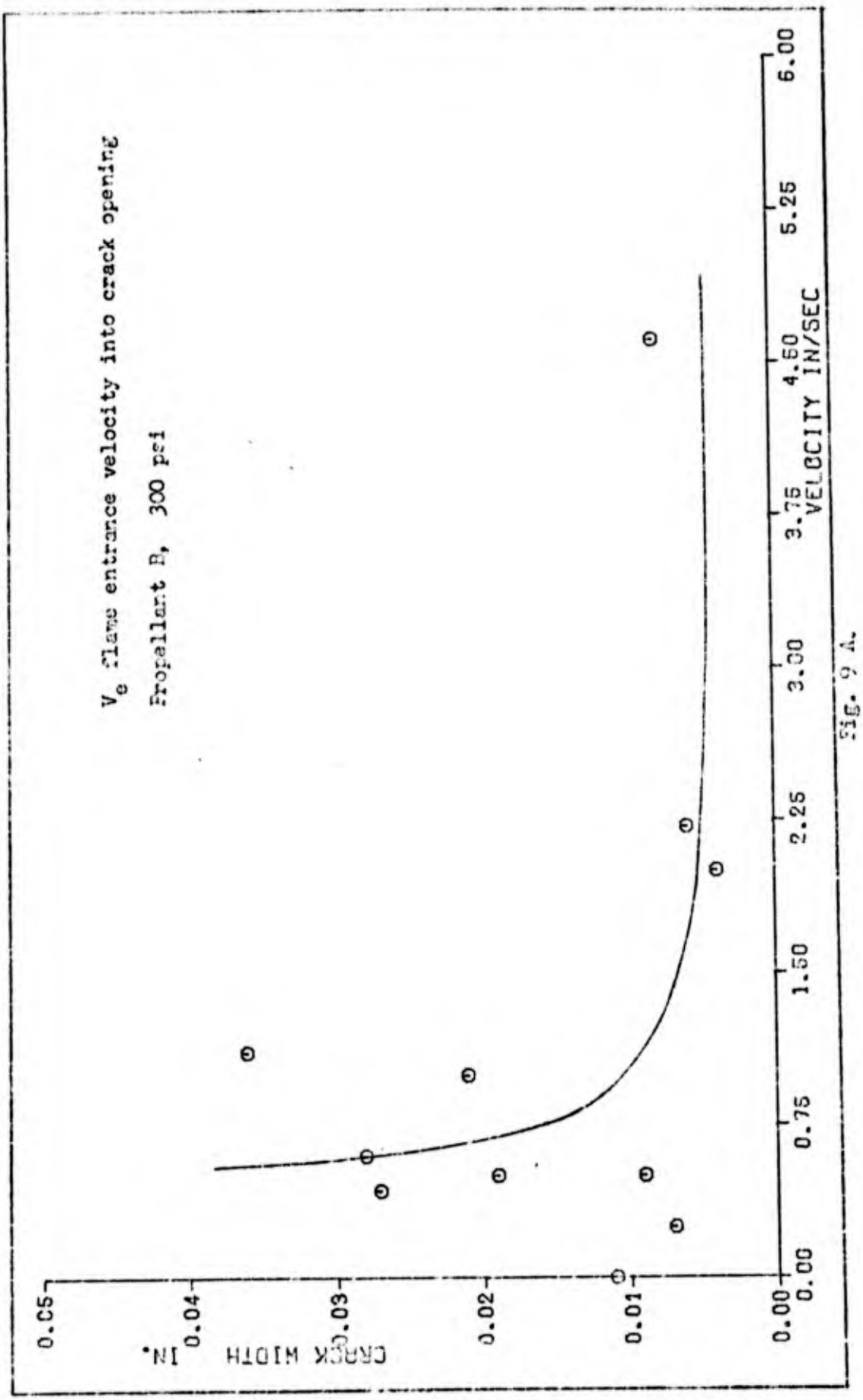
V_e Flame entrance velocity into crack opening
Propellant B, 300 psi
CRACK WIDTH IN.
0.05
0.04
0.03
0.02
0.01
0.00
0.00
0.75
1.50
2.25
3.00
3.75
4.50
5.25
6.00
VELOCITY IN/SEC

Fig. 9 A.

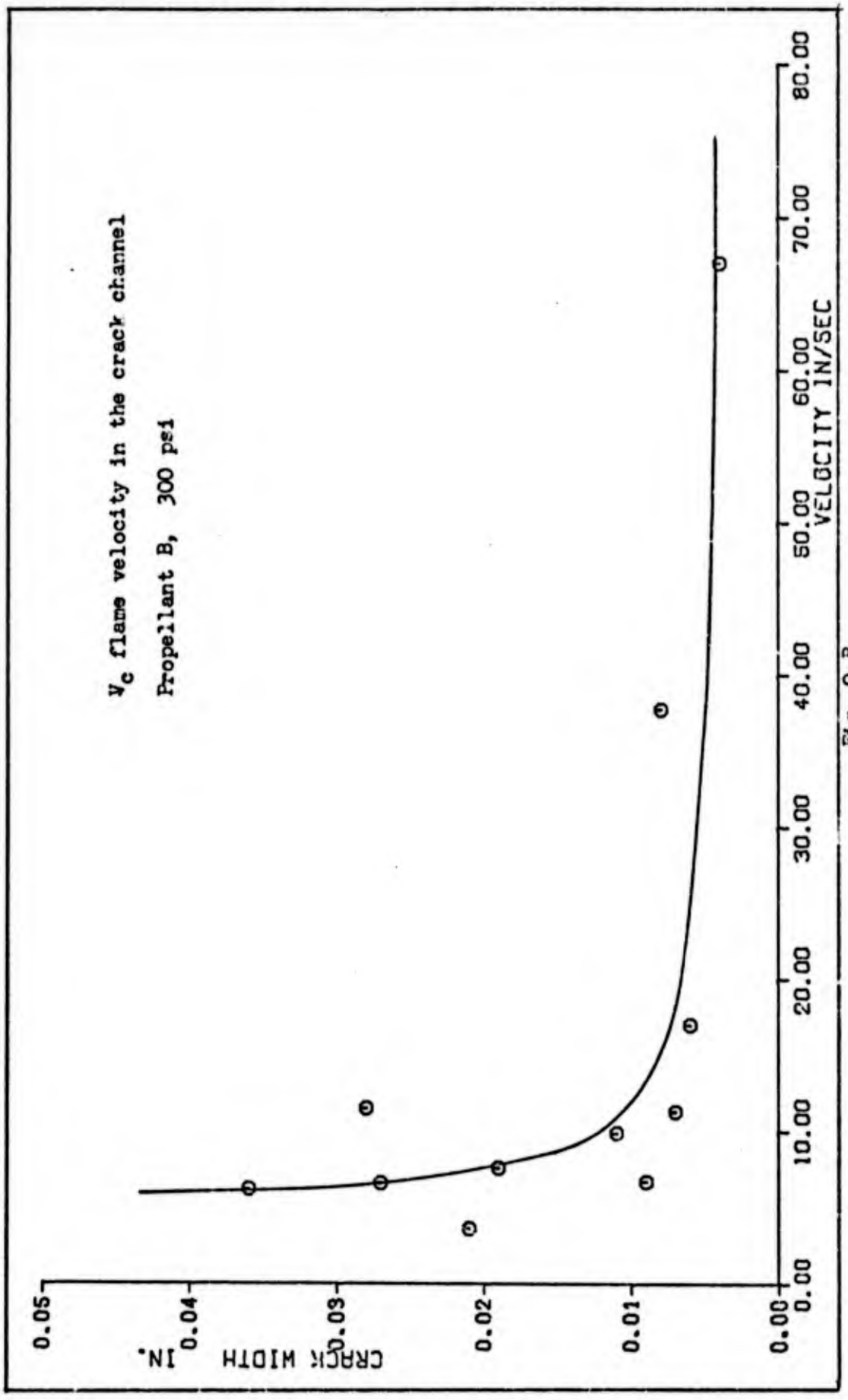
V_c flame velocity in the crack channel
Propellant B, 300 psi
CRACK WIDTH IN.
0.05
0.04
0.03
0.02
0.01
0.00
0.00
10.00
20.00
30.00
40.00
50.00
60.00
70.00
80.00
VELOCITY IN/SEC

Fig. 9 B.

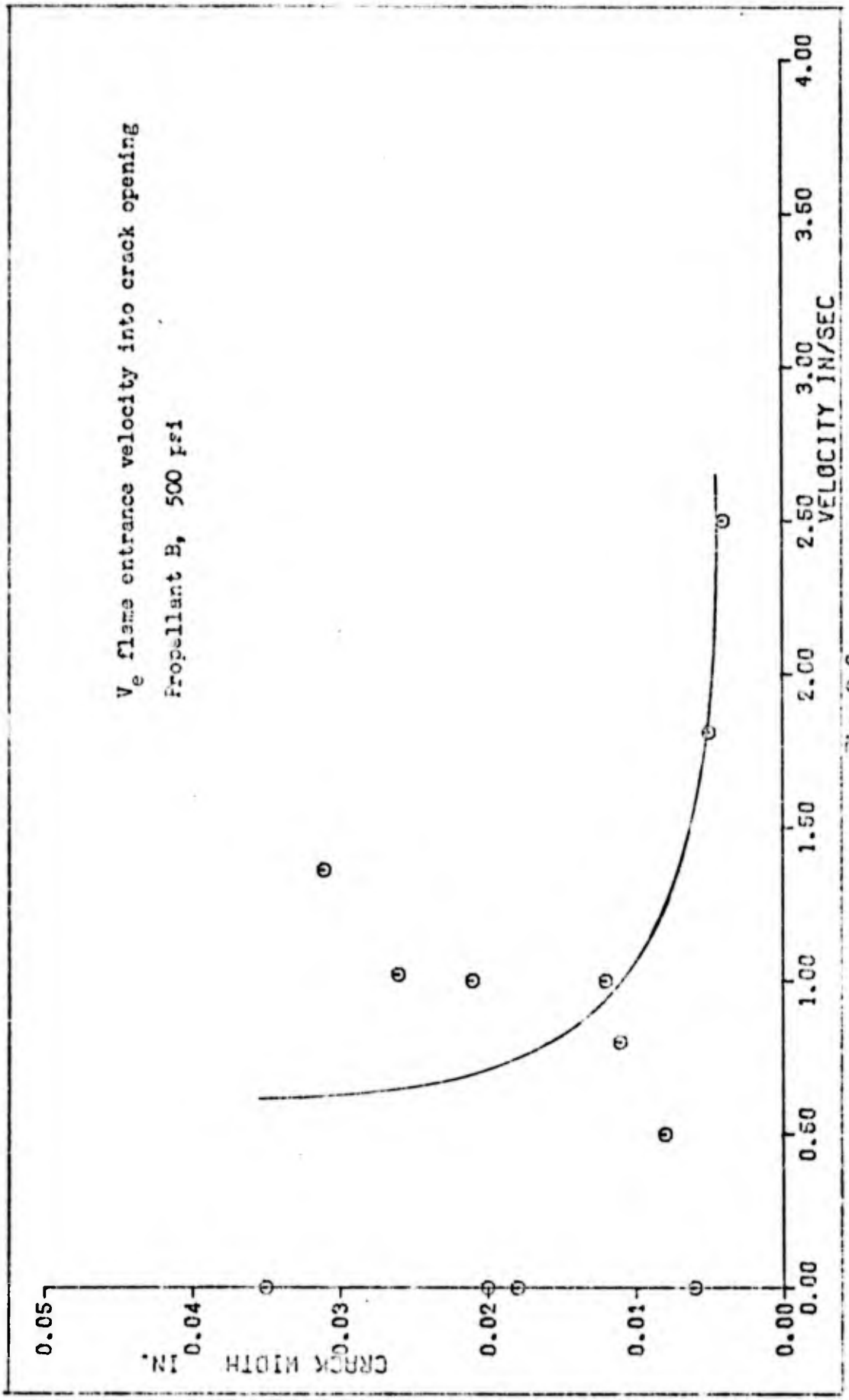
V_e flame entrance velocity into crack opening
Propellant B, 500 psi
CRACK WIDTH IN.
0.05
0.04
0.03
0.02
0.01
0.00
0.00
0.50
1.00
1.50
2.00
2.50
3.00
3.50
4.00
VELOCITY IN/SEC

Fig. 9 C.

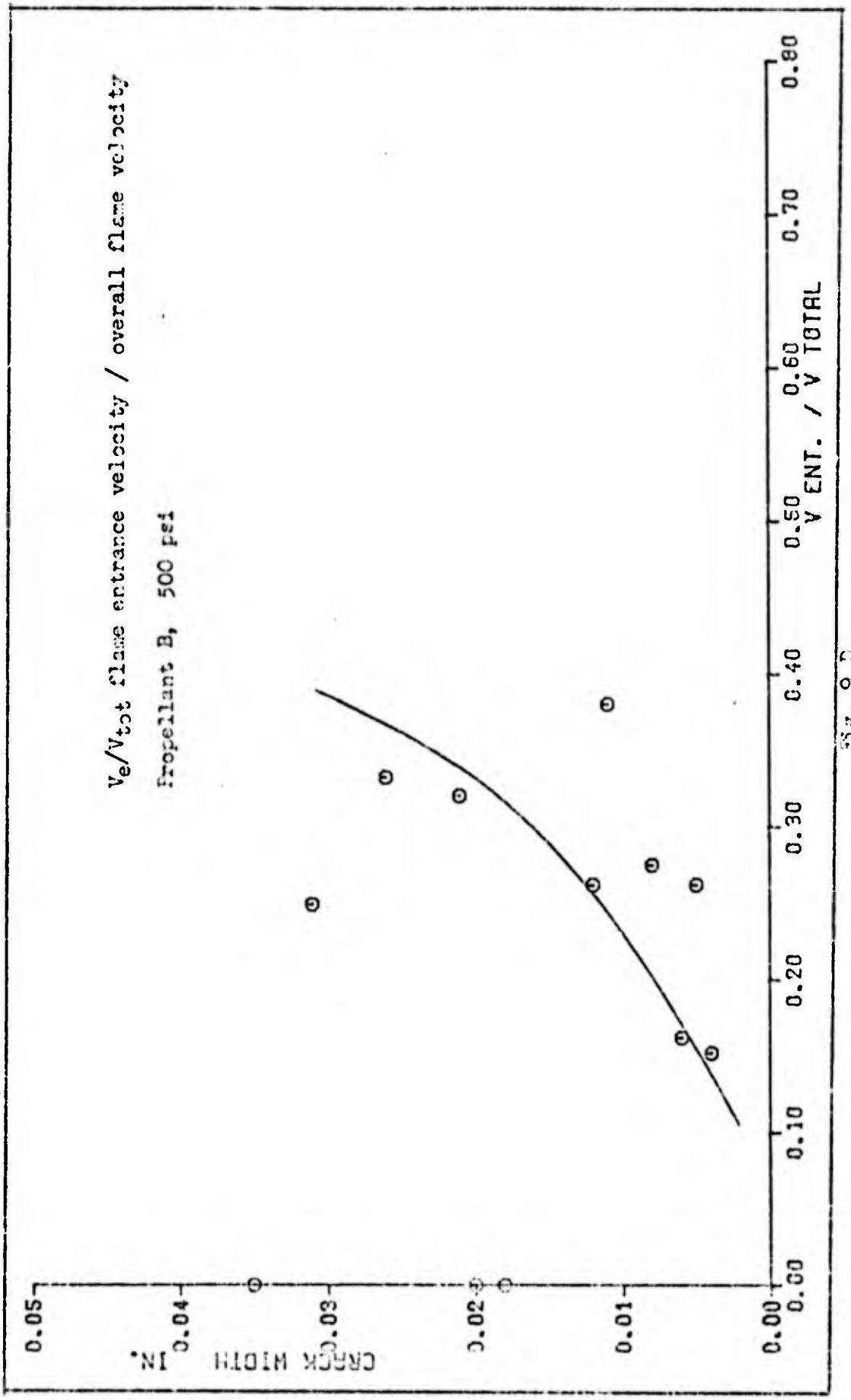
V_e/V_{tot} flame entrance velocity / overall flame velocity
Propellant B, 500 psi
CRACK WIDTH IN.
0.05
0.04
0.03
0.02
0.01
0.00
0.00
0.10
0.20
0.30
0.40
0.50
0.60
0.70
0.80
V ENT. / V TOTAL

Fig. 9 b.

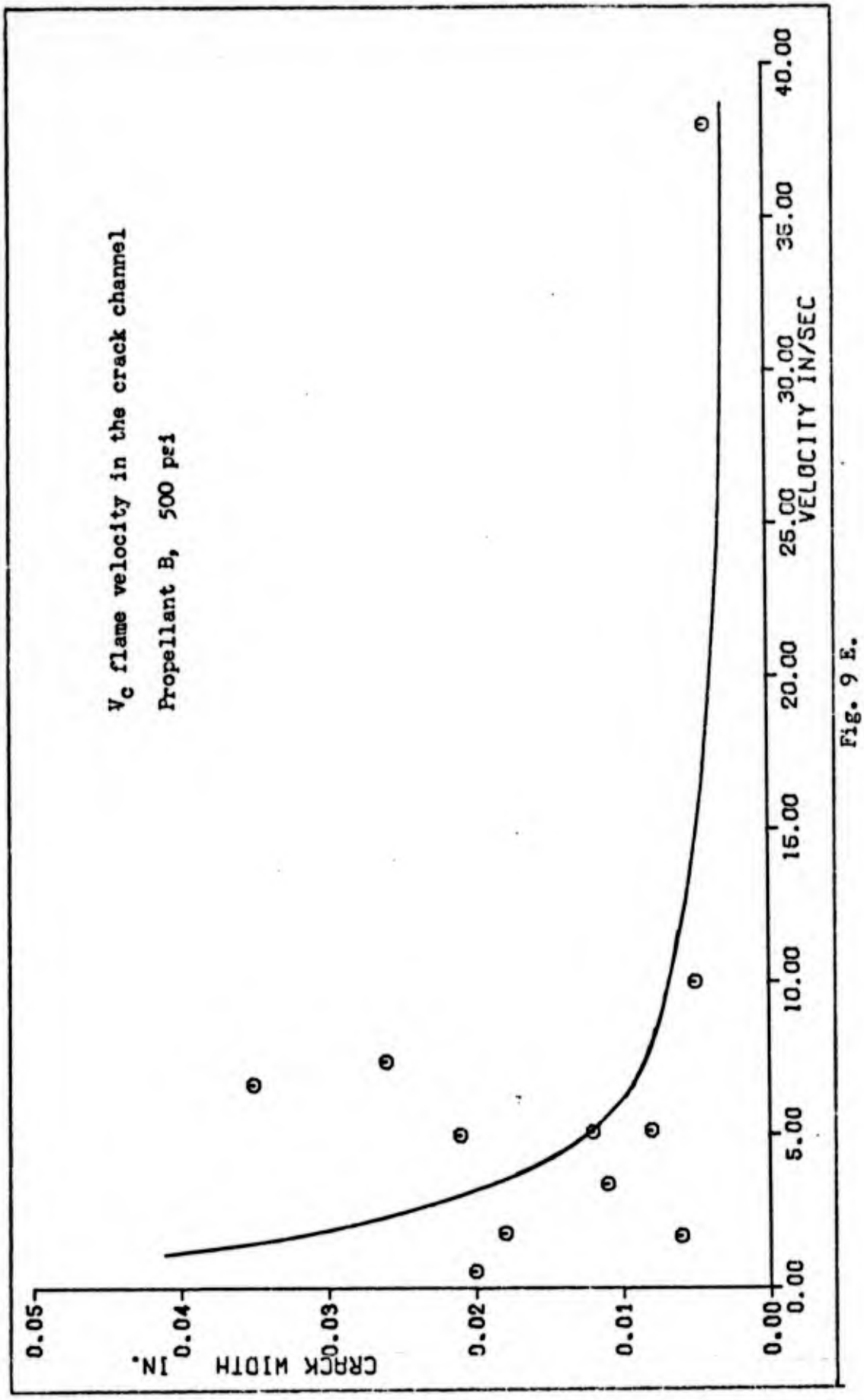
V_c flame velocity in the crack channel
Propellant B, 500 psi
CRACK WIDTH IN.
0.05
0.04
0.03
0.02
0.01
0.00
0.00
5.00
10.00
15.00
20.00
25.00
30.00
35.00
40.00
VELOCITY IN/SEC

Fig. 9 E.

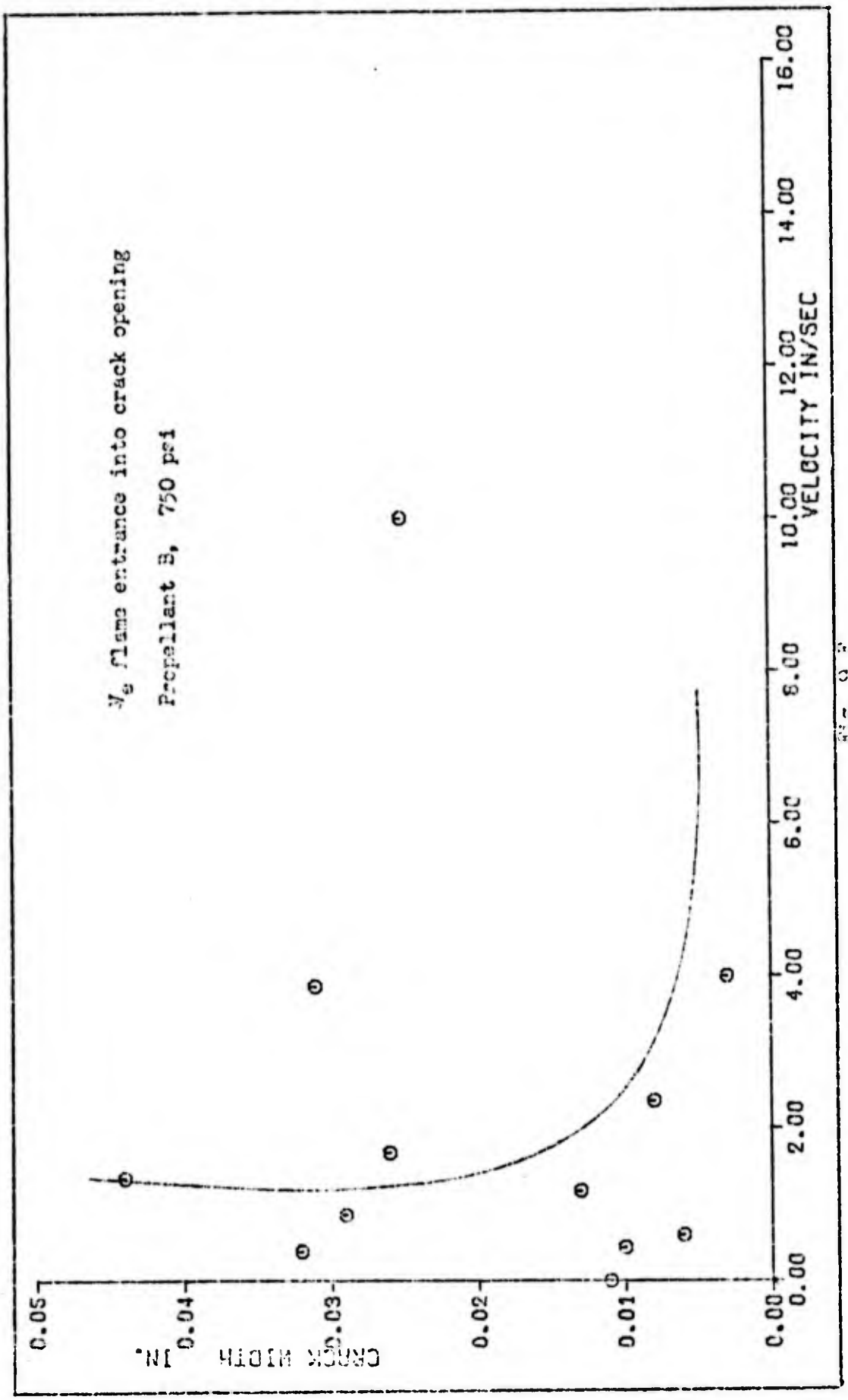
V_e flame entrance into crack opening
Propellant B, 750 psi
CRACK WIDTH IN.
0.00
0.01
0.02
0.03
0.04
0.05
0.00
2.00
4.00
6.00
8.00
10.00
12.00
14.00
16.00
VELOCITY IN/SEC

Fig. 9 2.

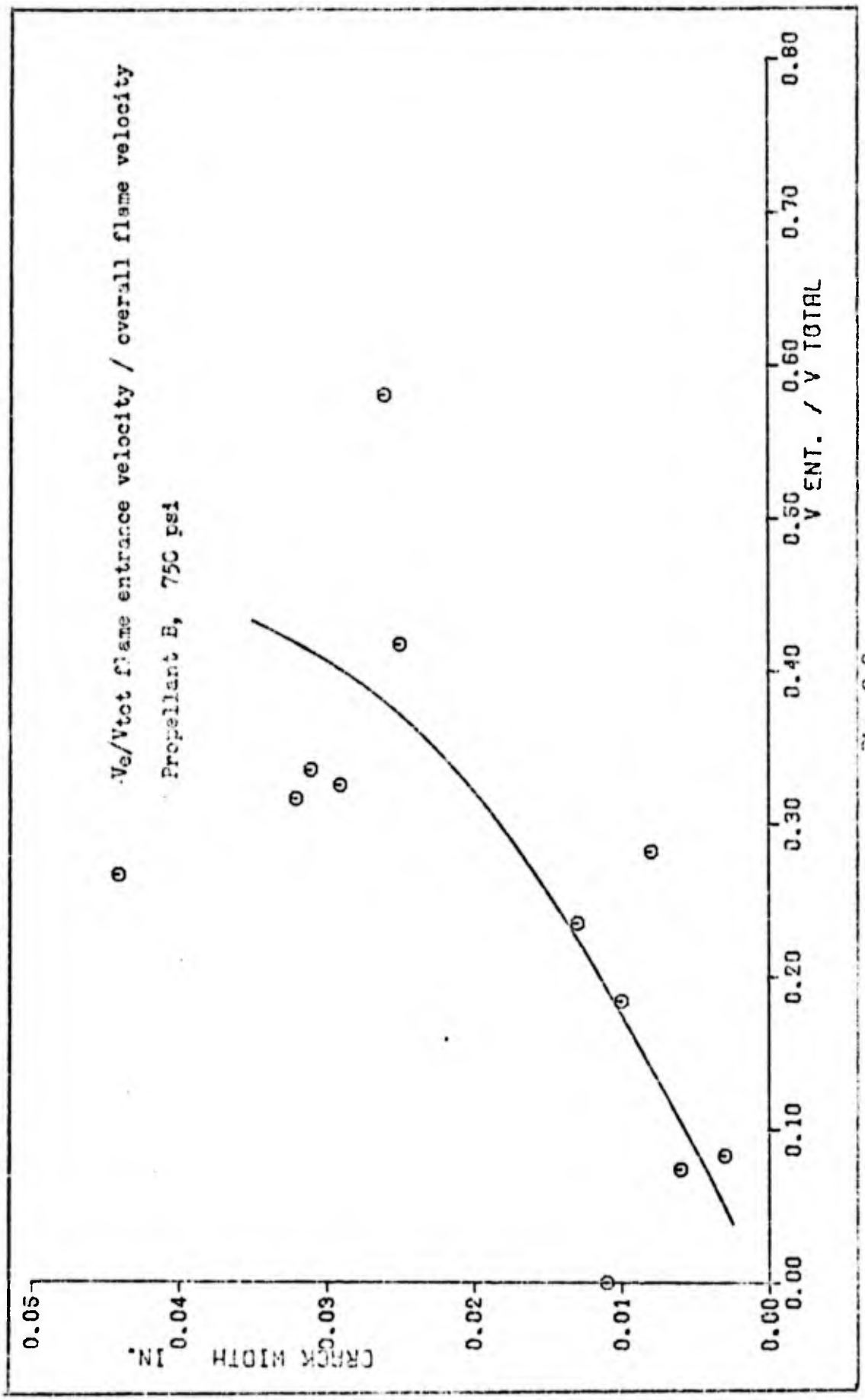
Ve/Vtot flame entrance velocity / overall flame velocity
Propellant B, 750 psi
CRACK WIDTH IN.
V ENT. / V TOTAL
0.05
0.04
0.03
0.02
0.01
0.00
0.00
0.10
0.20
0.30
0.40
0.50
0.60
0.70
0.80

Fig. 9 C.

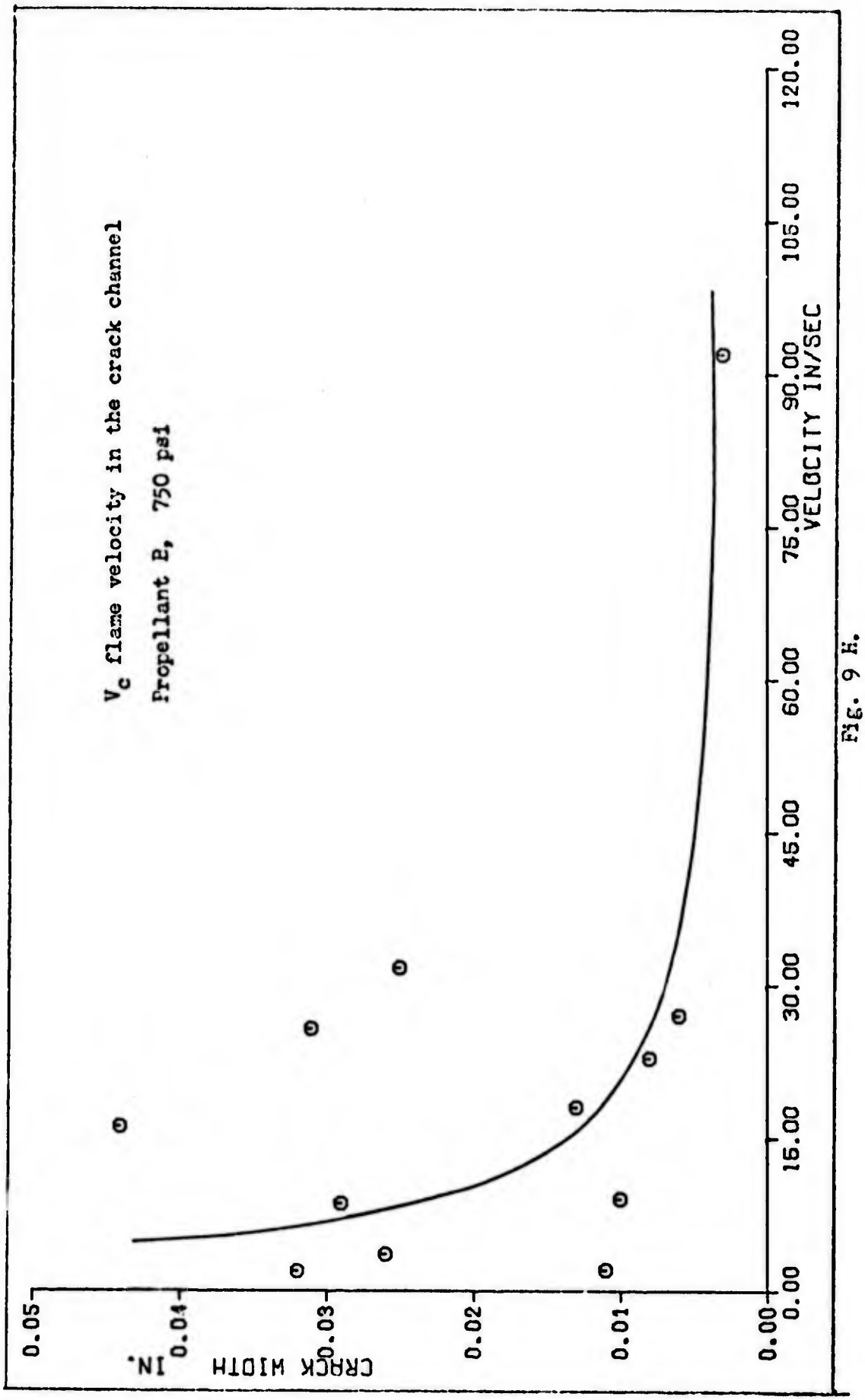
V_c flame velocity in the crack channel
Propellant E, 750 psi
CRACK WIDTH IN.
0.05
0.04
0.03
0.02
0.01
0.00
0.00
15.00
30.00
45.00
60.00
75.00
90.00
105.00
120.00
VELOCITY IN/SEC

Fig. 9 E.

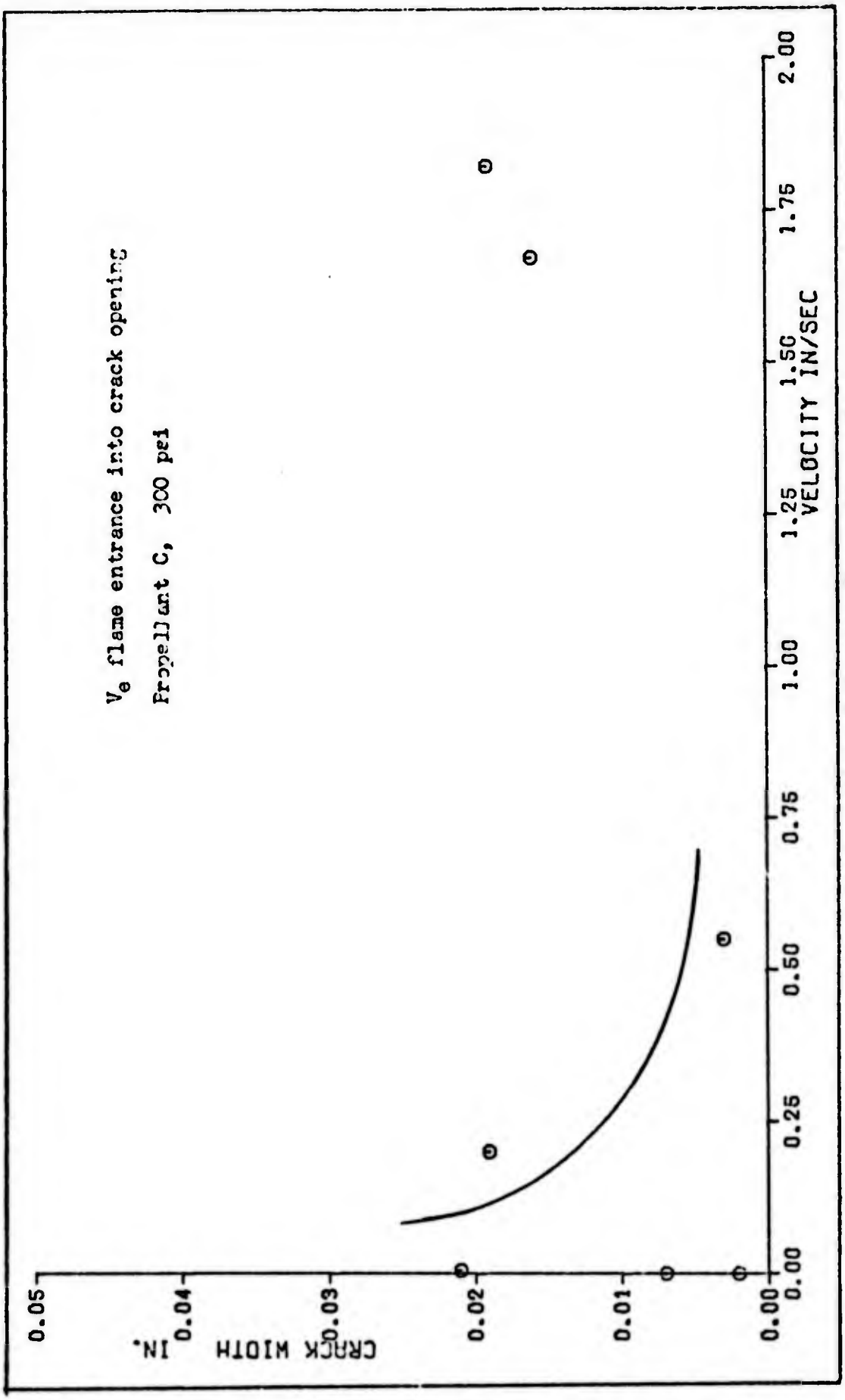

Fig. 10. Propellant C Curves: V_e, V_e/V_{tot}, V_c

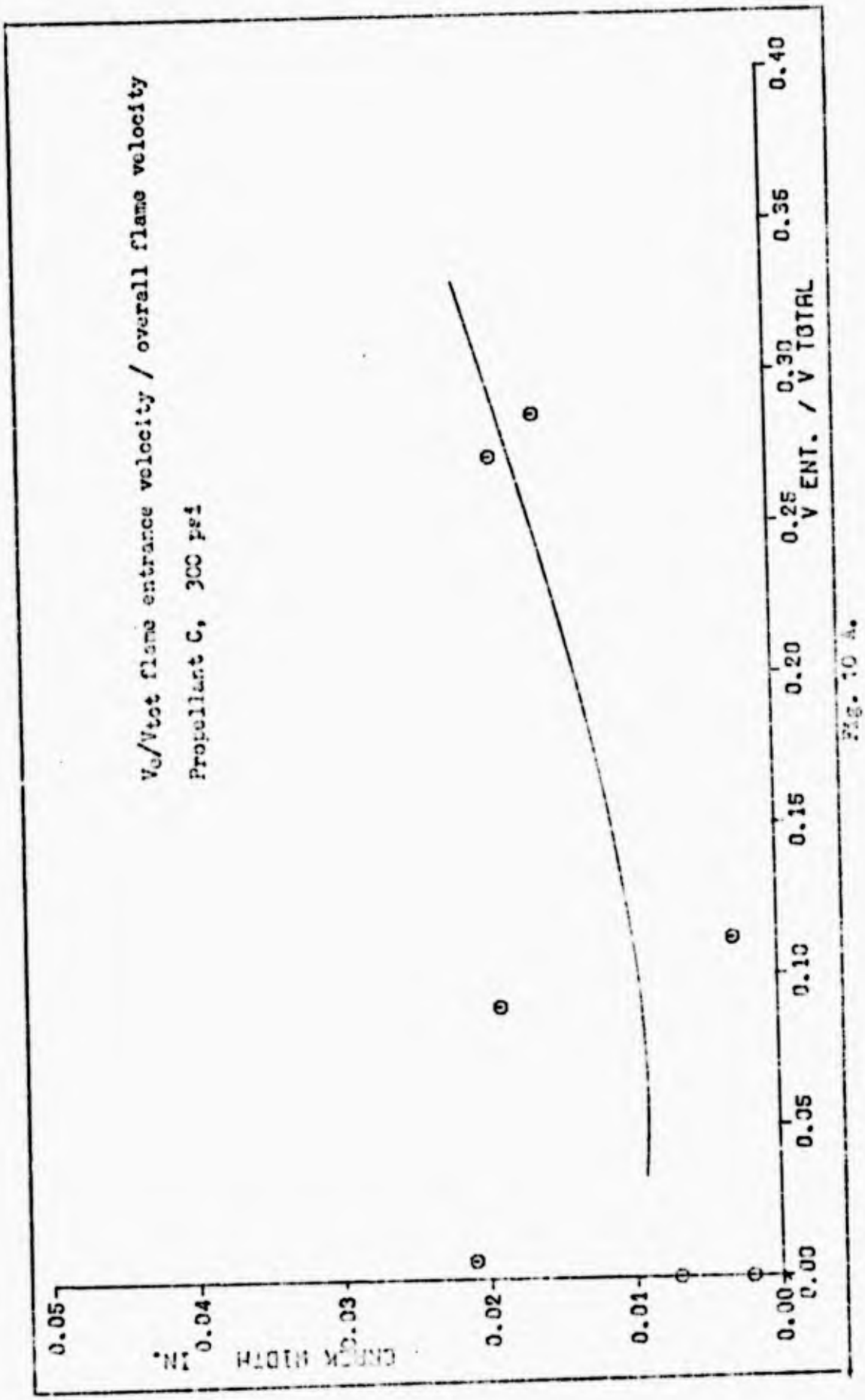
V_e/V_{tot} flame entrance velocity / overall flame velocity
Propellant C, 300 psi
CRACK WIDTH IN
0.05
0.04
0.03
0.02
0.01
0.00
0.00
0.05
0.10
0.15
0.20
0.25
0.30
0.35
0.40
V ENT. / V TOTAL

Fig. 10 A.

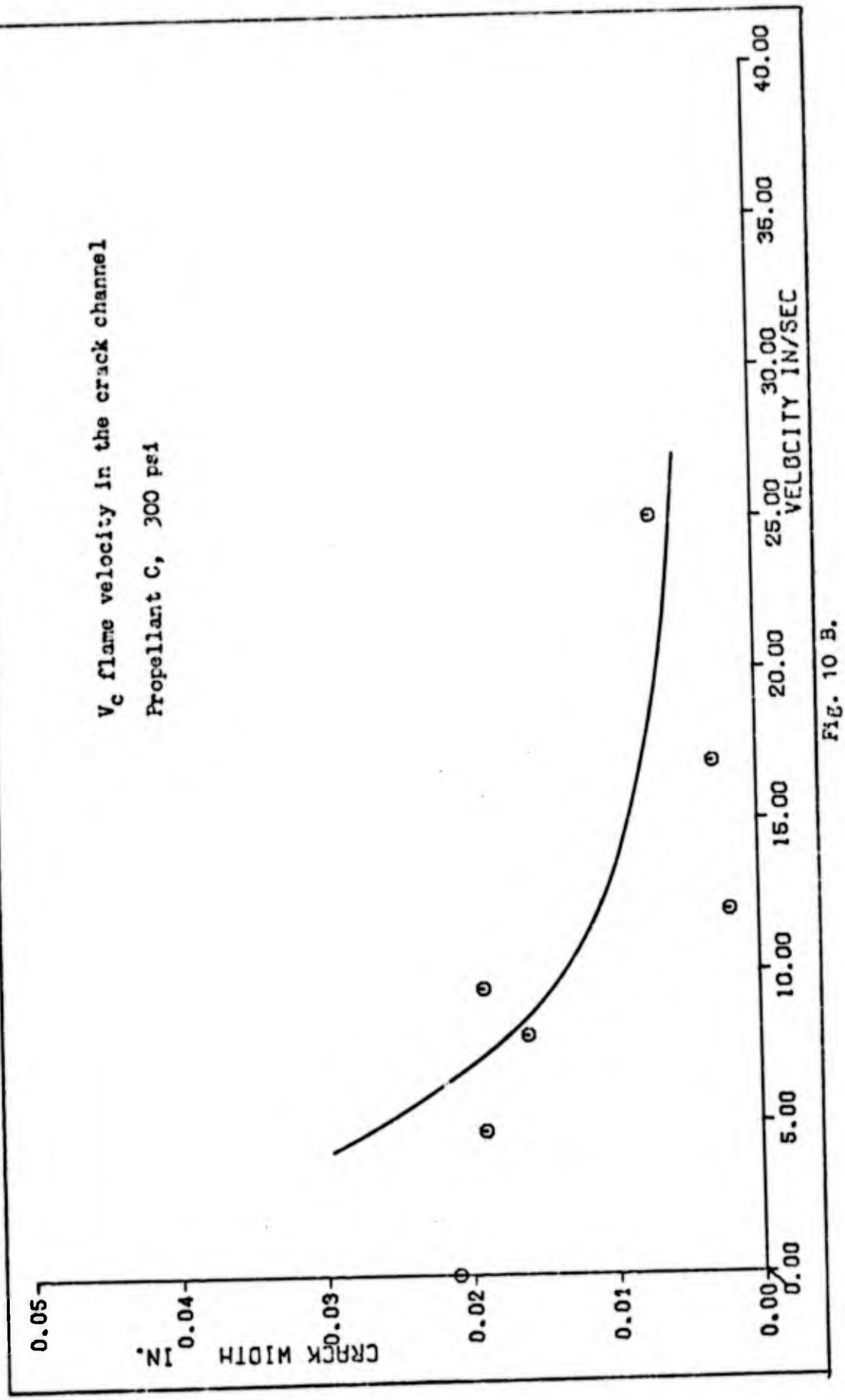
V_c flame velocity in the crack channel
Propellant C, 300 psi
CRACK WIDTH IN.
0.05
0.04
0.03
0.02
0.01
0.00
0.00
5.00
10.00
15.00
20.00
25.00
30.00
35.00
40.00
VELOCITY IN/SEC

Fig. 10 B.

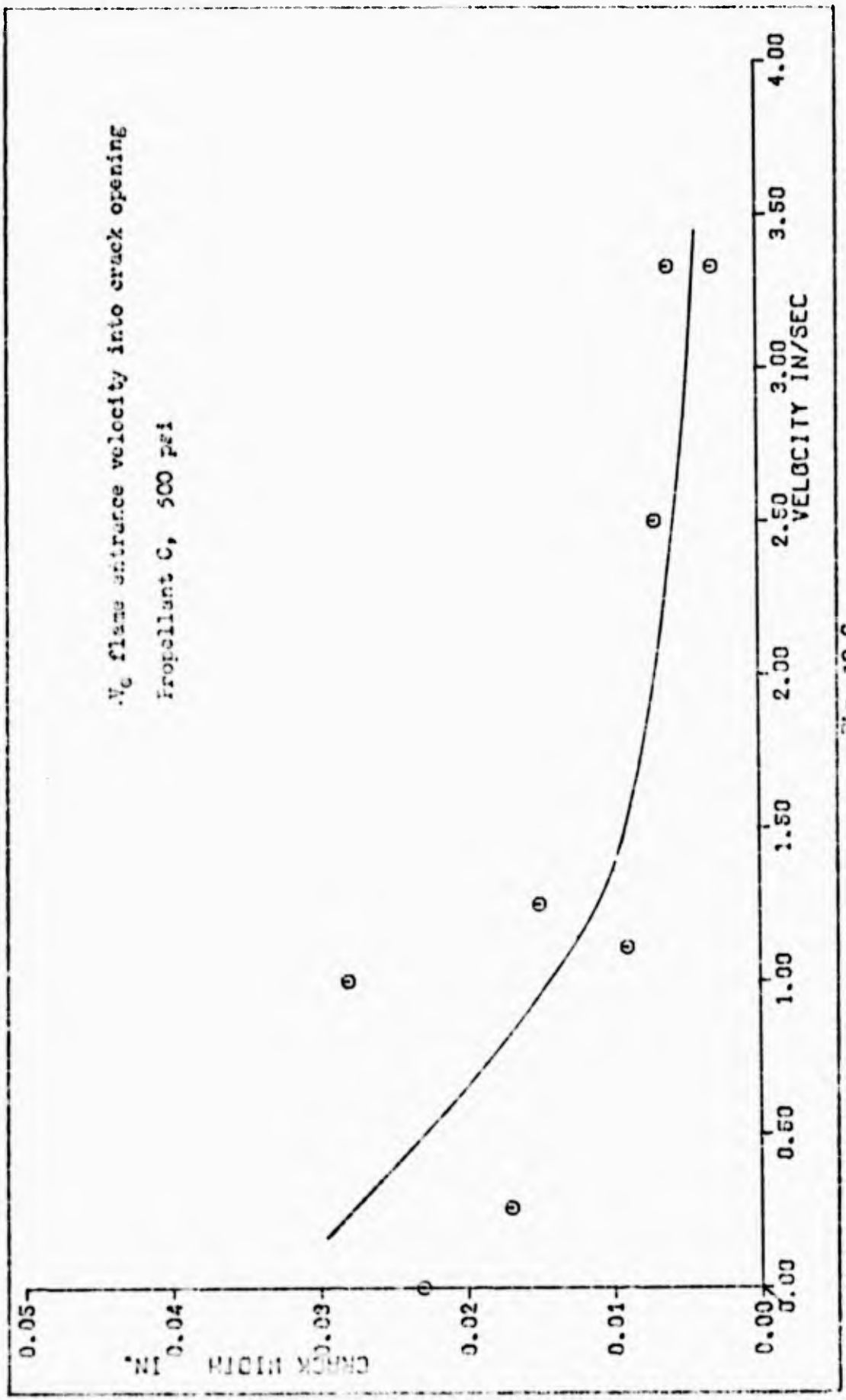
V_c flame entrance velocity into crack opening
Propellant C, 500 psi
CRACK WIDTH IN.
0.00
0.01
0.02
0.03
0.04
0.05
0.00
0.50
1.00
1.50
2.00
2.50
3.00
3.50
4.00
VELOCITY IN/SEC

Fig. 10 C.

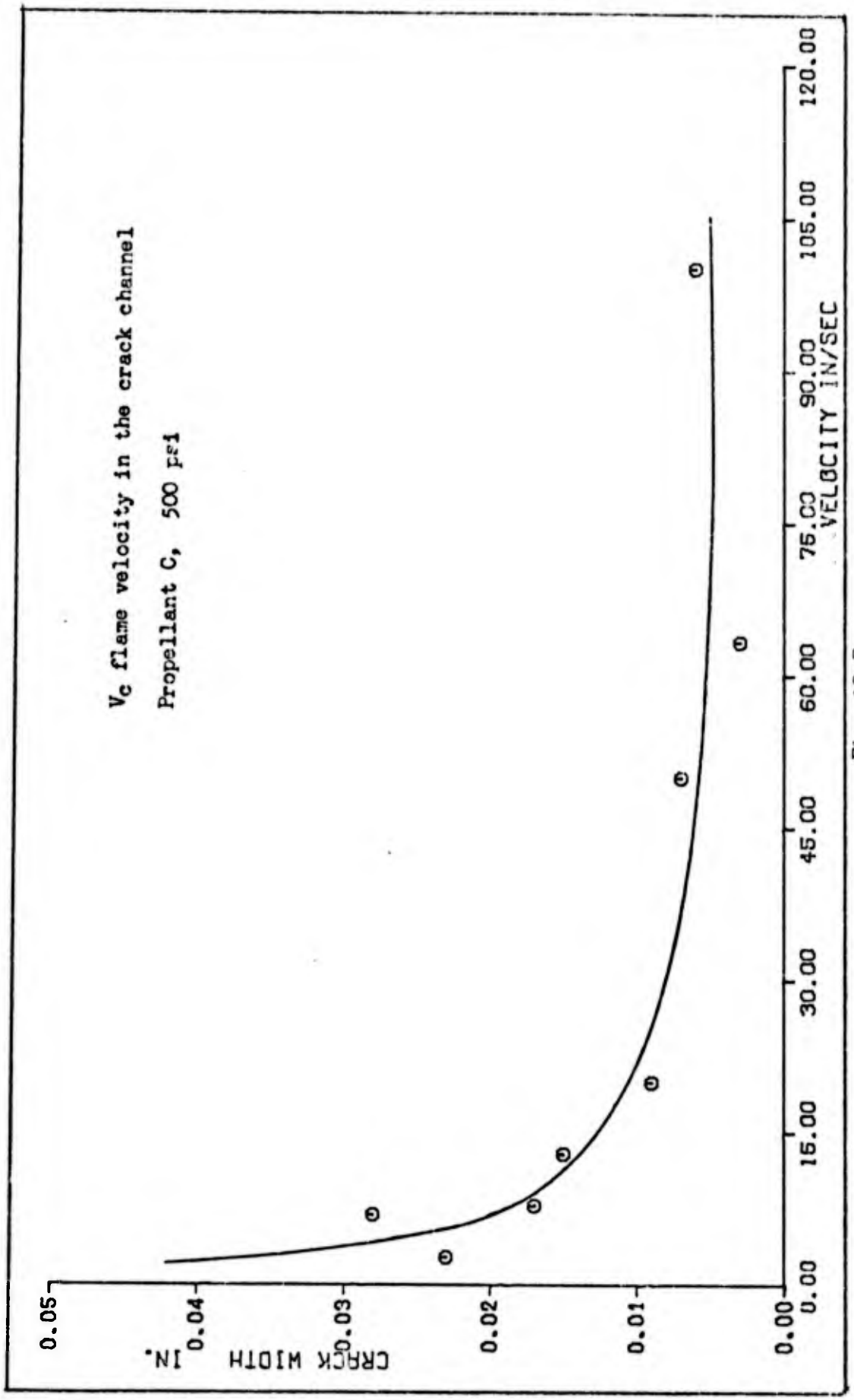
V_c flame velocity in the crack channel
Propellant C, 500 psi
CRACK WIDTH IN.
0.05
0.04
0.03
0.02
0.01
0.00
0.00
15.00
30.00
45.00
60.00
75.00
90.00
105.00
120.00
VELOCITY IN/SEC

Fig. 10 E.

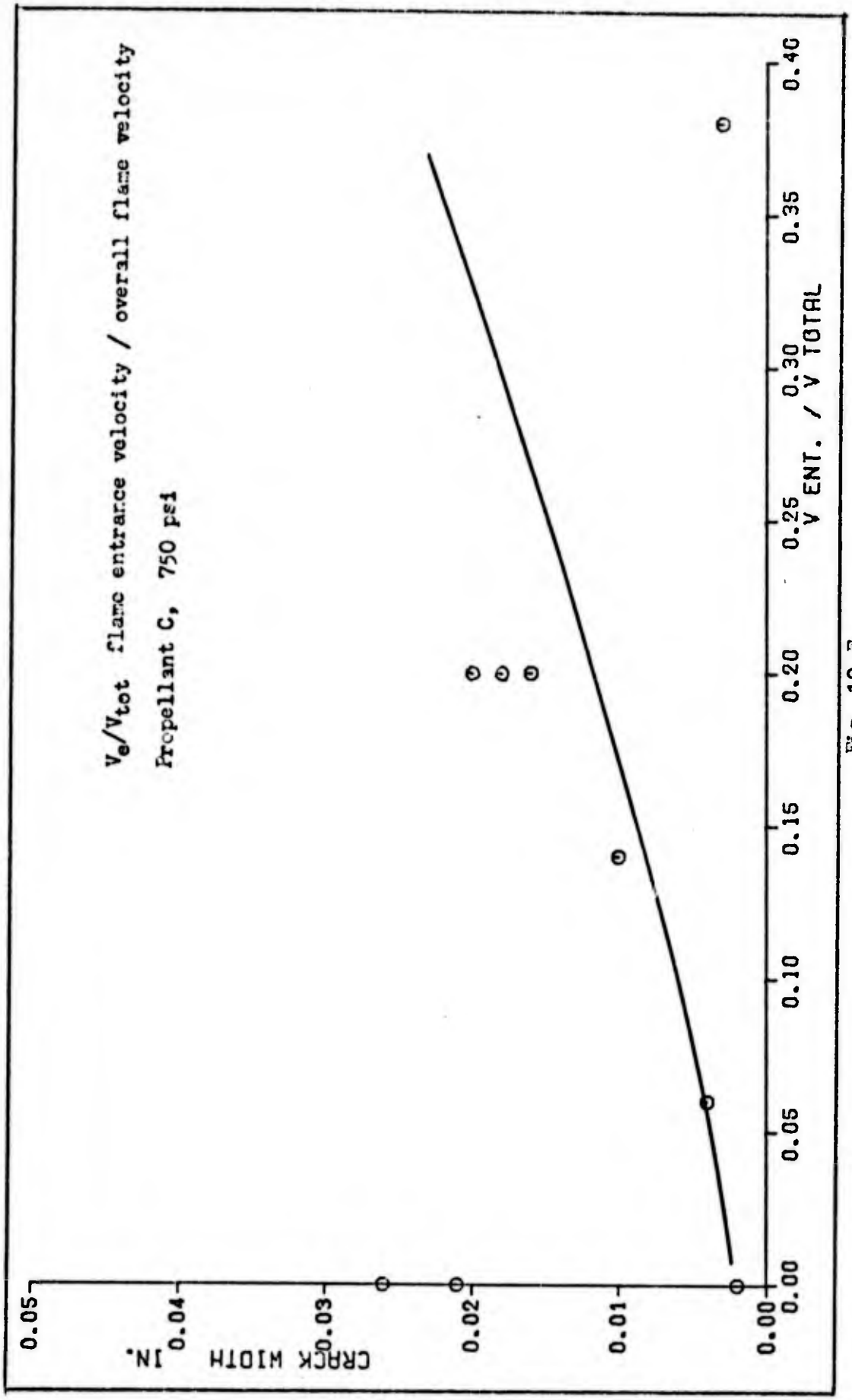
V_e/V_{tot} flame entrance velocity / overall flame velocity
Propellant C, 750 psi
CRACK WIDTH IN.
0.05
0.04
0.03
0.02
0.01
0.00
0.00
0.05
0.10
0.15
0.20
0.25
0.30
0.35
0.40
V ENT. / V TOTAL

Fig. 10 F.

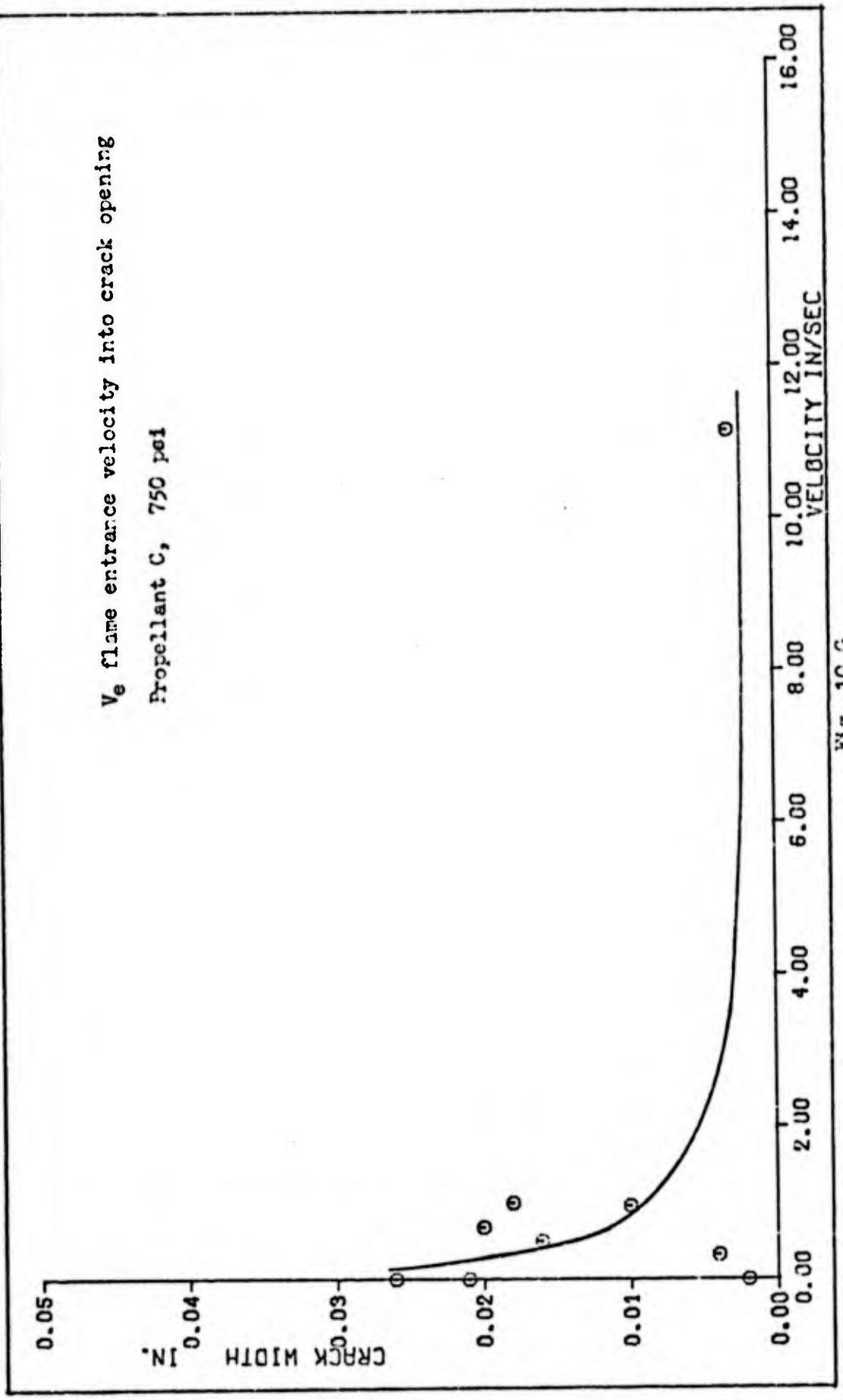
V_e flame entrance velocity into crack opening
Propellant C, 750 psi
CRACK WIDTH IN.
0.05
0.04
0.03
0.02
0.01
0.00
0.00
2.00
4.00
6.00
8.00
10.00
12.00
14.00
16.00
VELOCITY IN/SEC

Fig. 10 G.

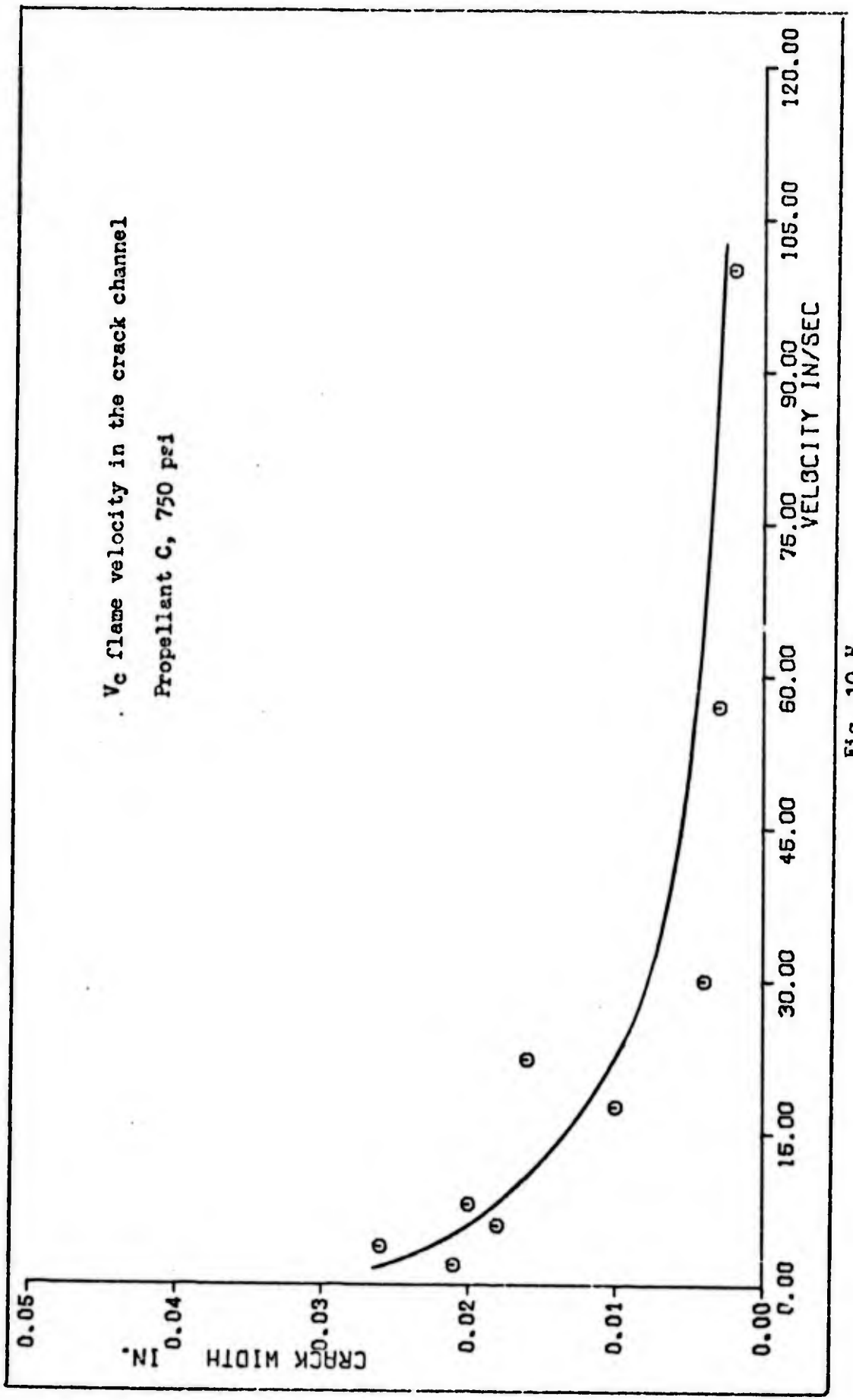
V_c flame velocity in the crack channel
Propellant C, 750 psi
CRACK WIDTH IN.
0.05
0.04
0.03
0.02
0.01
0.00
0.00
15.00
30.00
45.00
60.00
75.00
90.00
105.00
120.00
VELOCITY IN/SEC

Fig. 10 H.

Appendix B

Data Curves for Crack Widths versus Burn Time

Data curves for propellants A, B, and C tests appear in this appendix. The curves are grouped according to pressures of 300, 500, and 750 psi for each propellant. The curves for each pressure group are in decreasing crack widths. It is noted that the x designation printout on the data curves are computer program instructions for data identification purposes only.

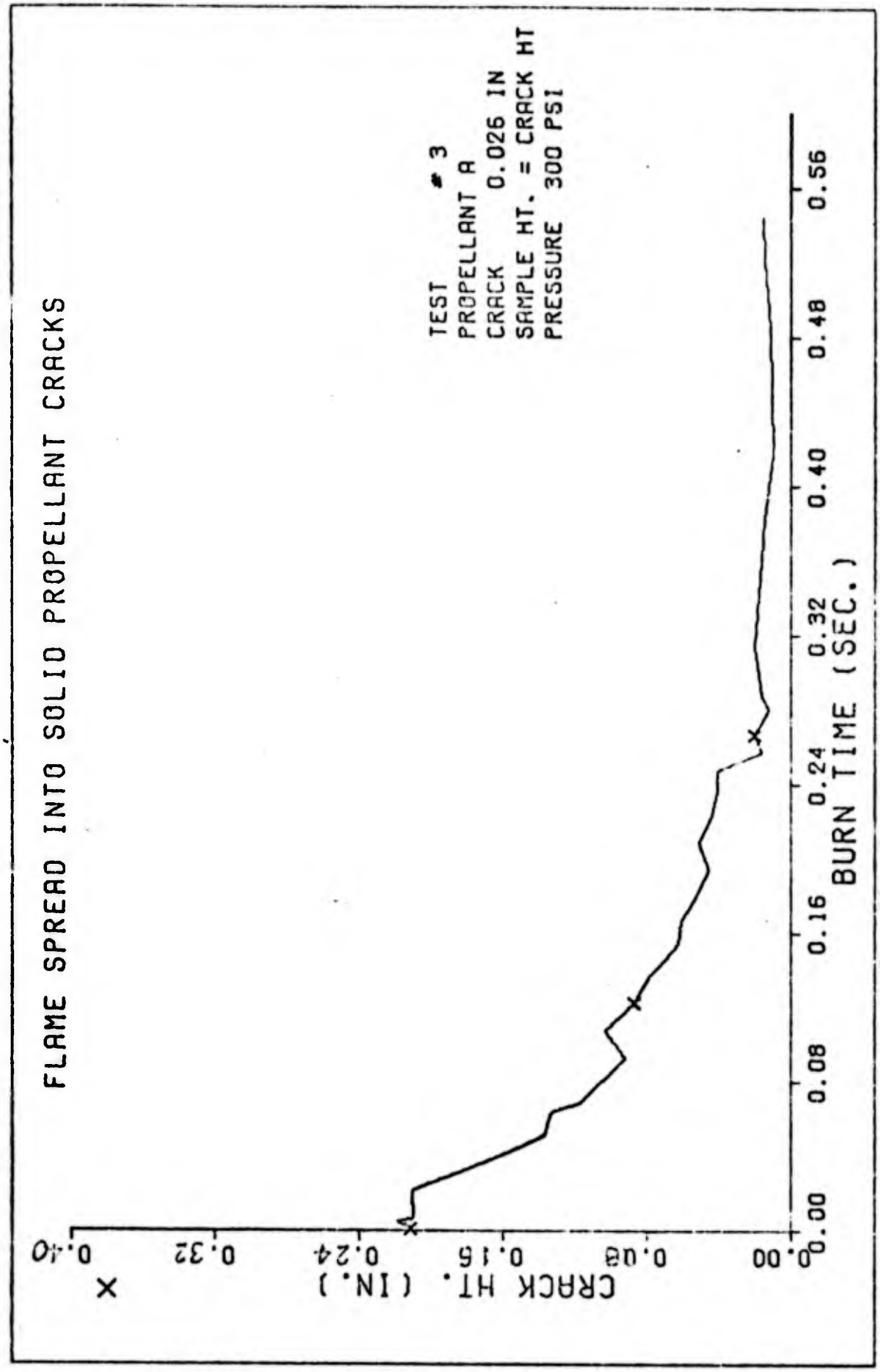

Fig. 11. Data Curves for Propellant A, 300 psi

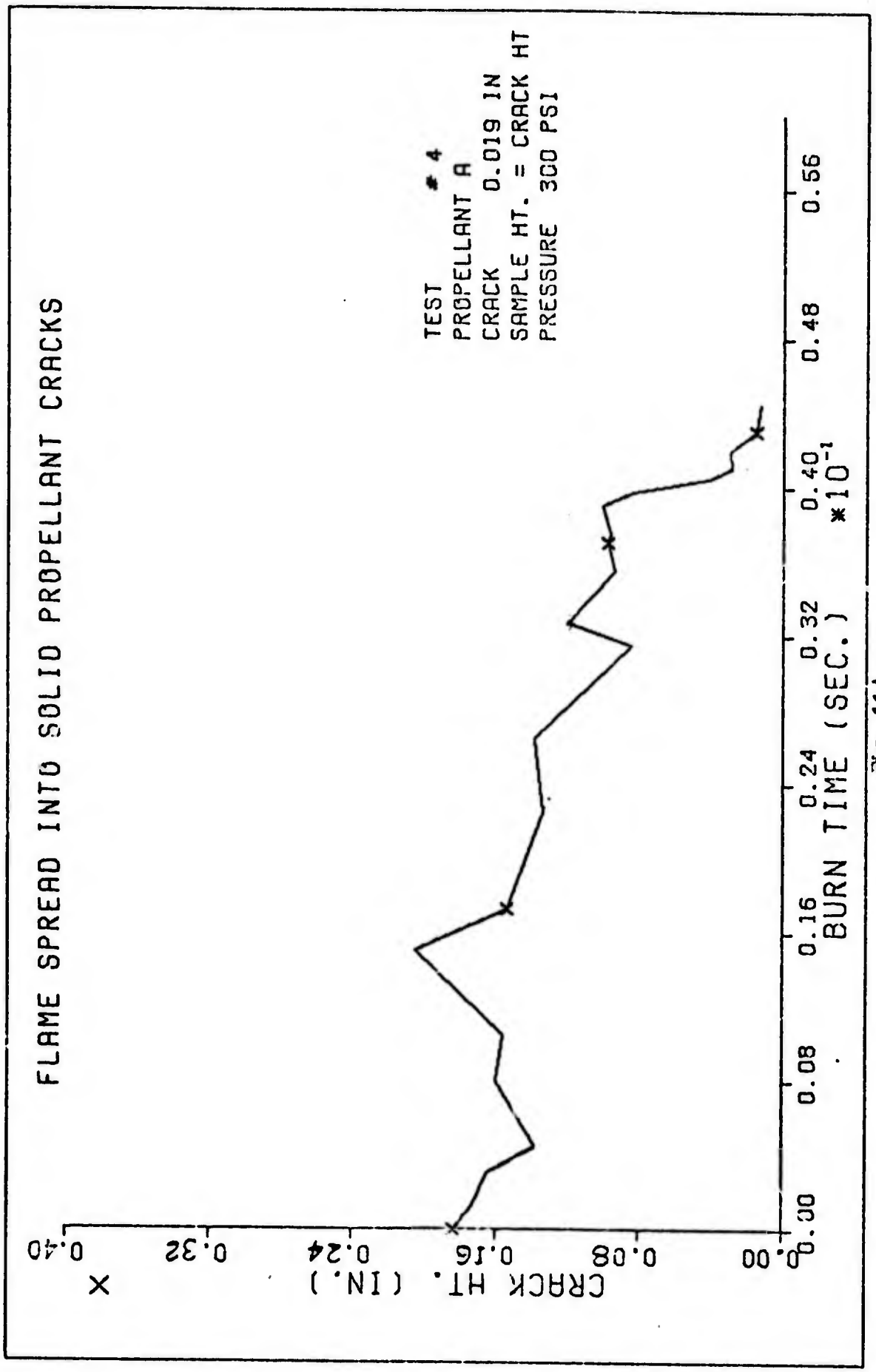
FLAME SPREAD INTO SOLID PROPELLANT CRACKS
TEST # 4
PROPELLANT A
CRACK 0.019 IN
SAMPLE HT. = CRACK HT
PRESSURE 300 PSI
CRACK HT. (IN.)
0.00
0.08
0.16
0.24
0.32
0.40
X
0.00
0.08
0.16
0.24
0.32
0.40
0.48
0.56
BURN TIME (SEC.)
*10⁻¹

Fig. 114.

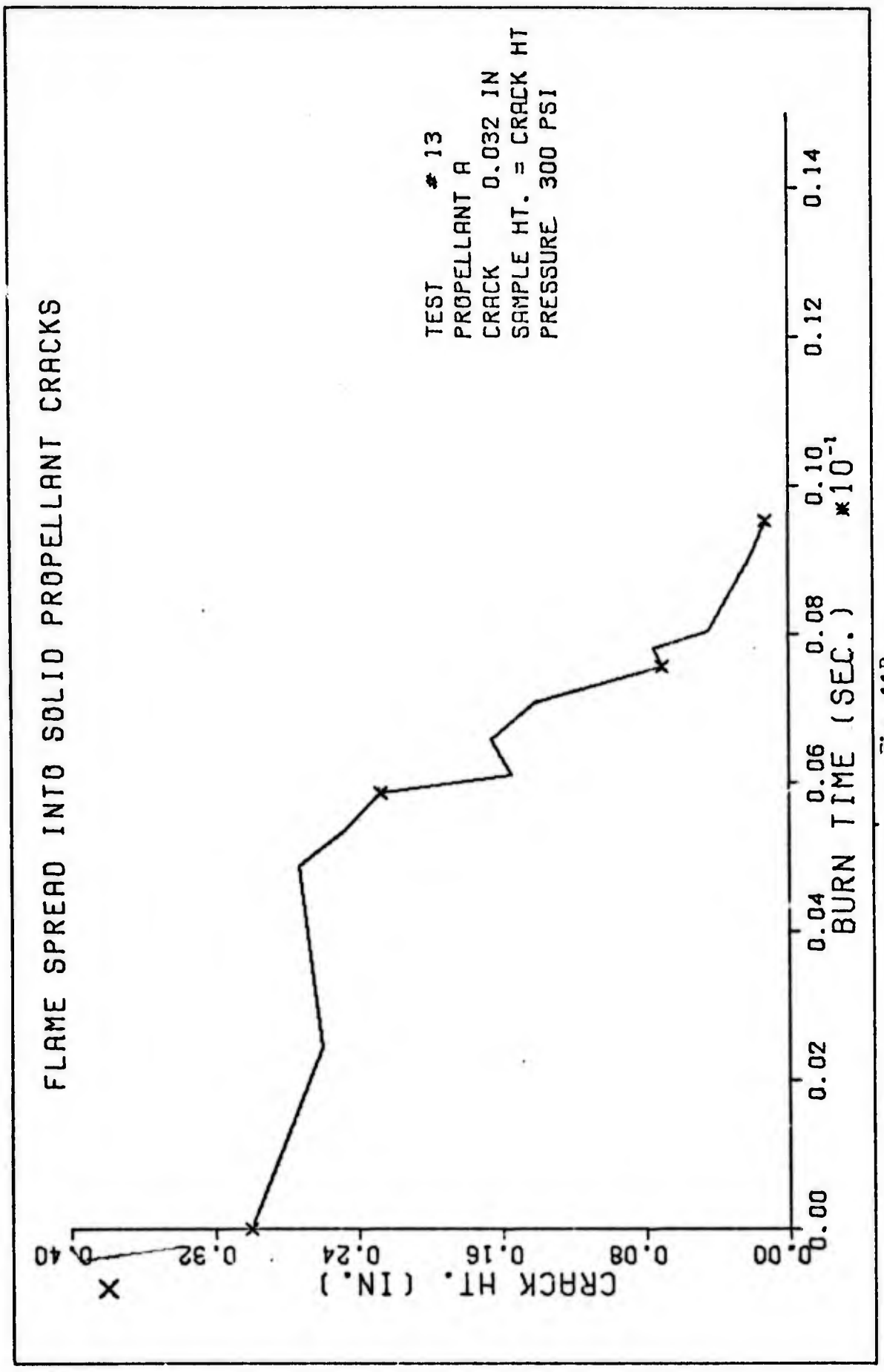
FLAME SPREAD INTO SOLID PROPELLANT CRACKS
TEST # 13
PROPELLANT A
CRACK 0.032 IN
SAMPLE HT. = CRACK HT
PRESSURE 300 PSI
CRACK HT. (IN.)
0.00
0.08
0.16
0.24
0.32
0.40
BURN TIME (SEC.)
0.00
0.02
0.04
0.06
0.08
0.10
0.12
0.14
*10⁻¹

Fig. 11B

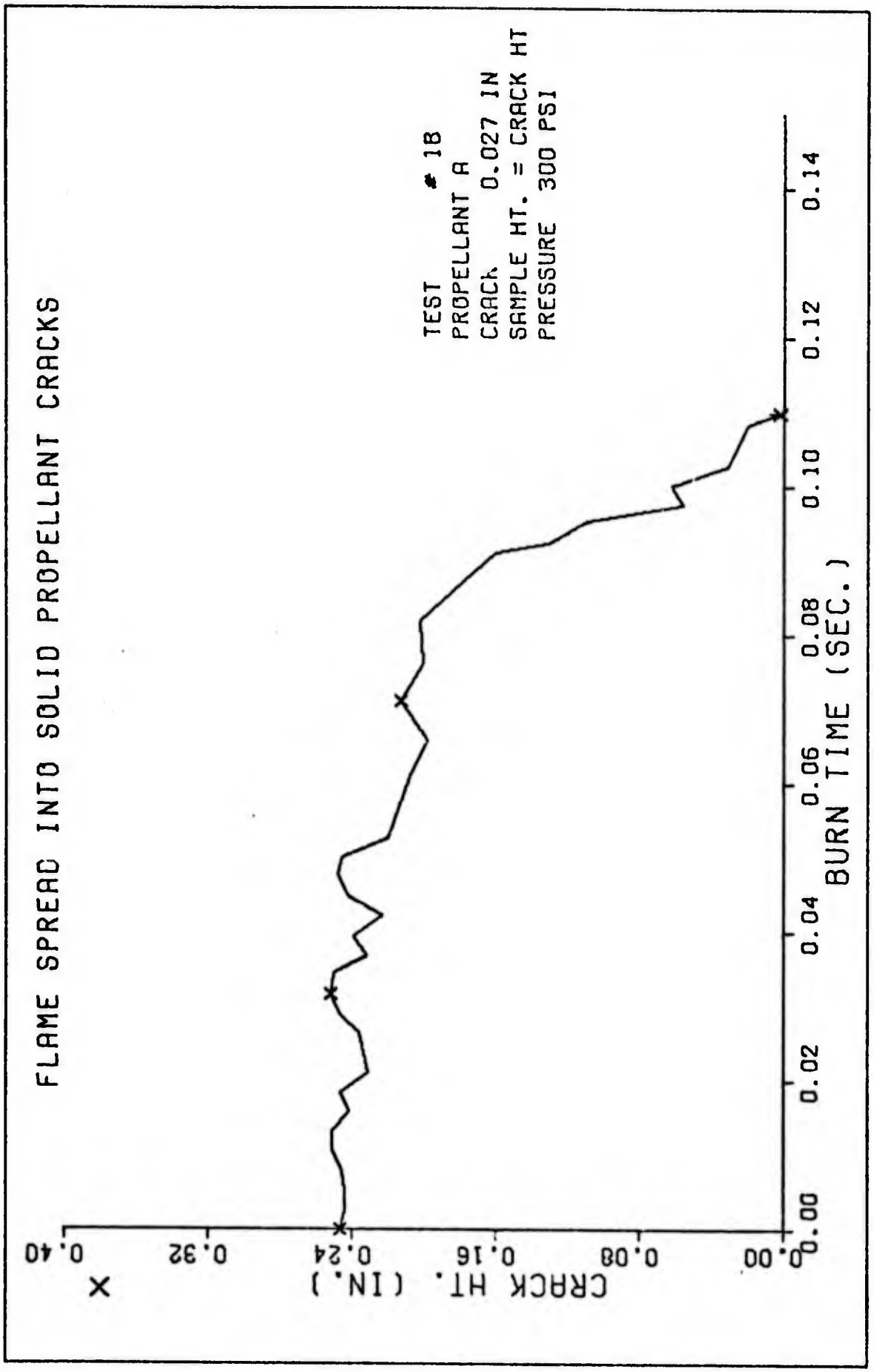
FLAME SPREAD INTO SOLID PROPELLANT CRACKS
TEST # 18
PROPELLANT A
CRACK 0.027 IN
SAMPLE HT. = CRACK HT
PRESSURE 300 PSI
CRACK HT. (IN.)
0.00
0.08
0.16
0.24
0.32
0.40
X
BURN TIME (SEC.)
0.00
0.02
0.04
0.06
0.08
0.10
0.12
0.14

Fig. 11c.

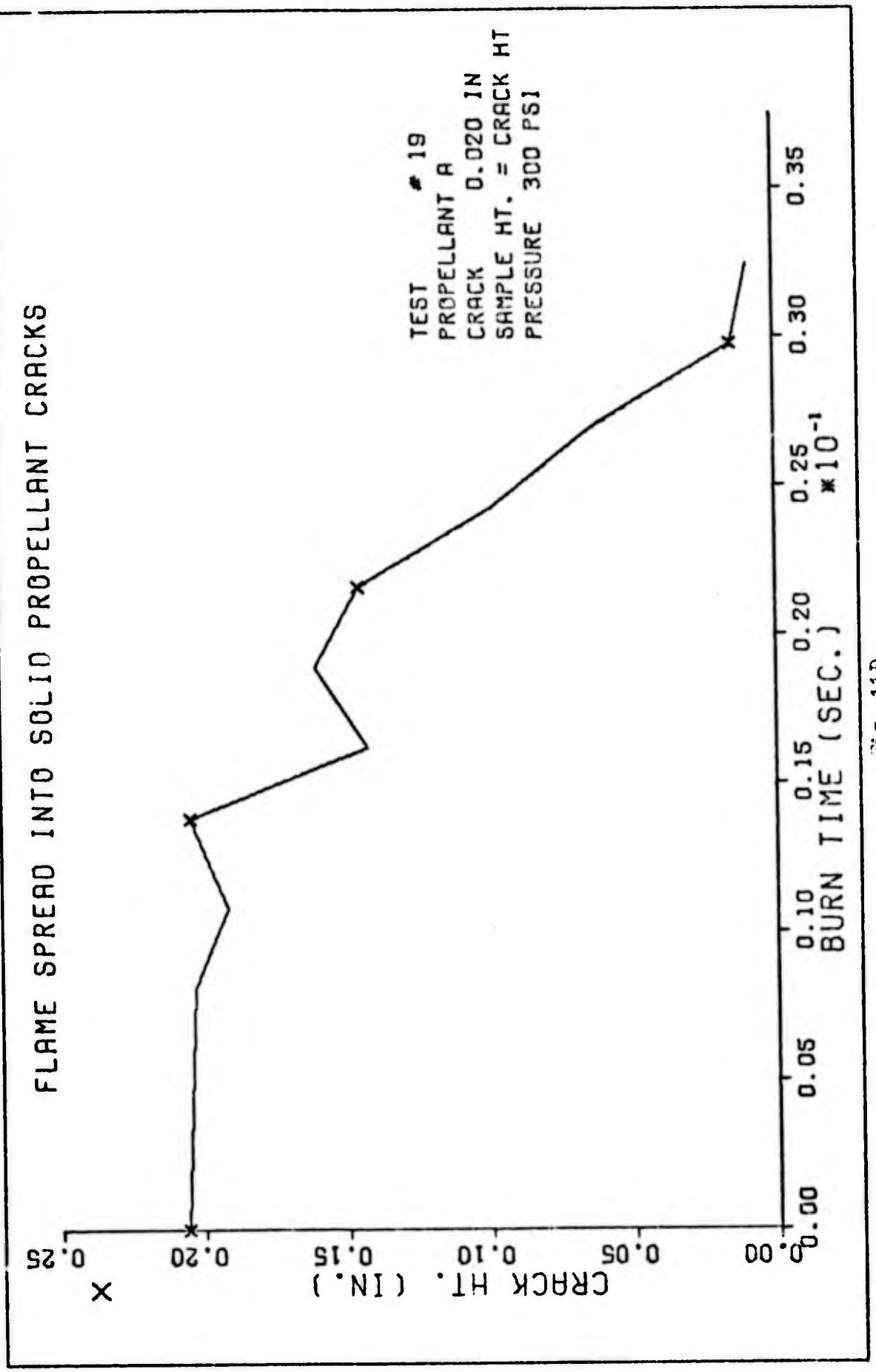
FLAME SPREAD INTO SOLID PROPELLANT CRACKS
TEST # 19
PROPELLANT A
CRACK 0.020 IN
SAMPLE HT. = CRACK HT
PRESSURE 300 PSI
CRACK HT. (IN.)
0.00
0.05
0.10
0.15
0.20
0.25
X
BURN TIME (SEC.)
0.00
0.05
0.10
0.15
0.20
0.25
0.30
0.35
*10⁻¹

Fig. 11D

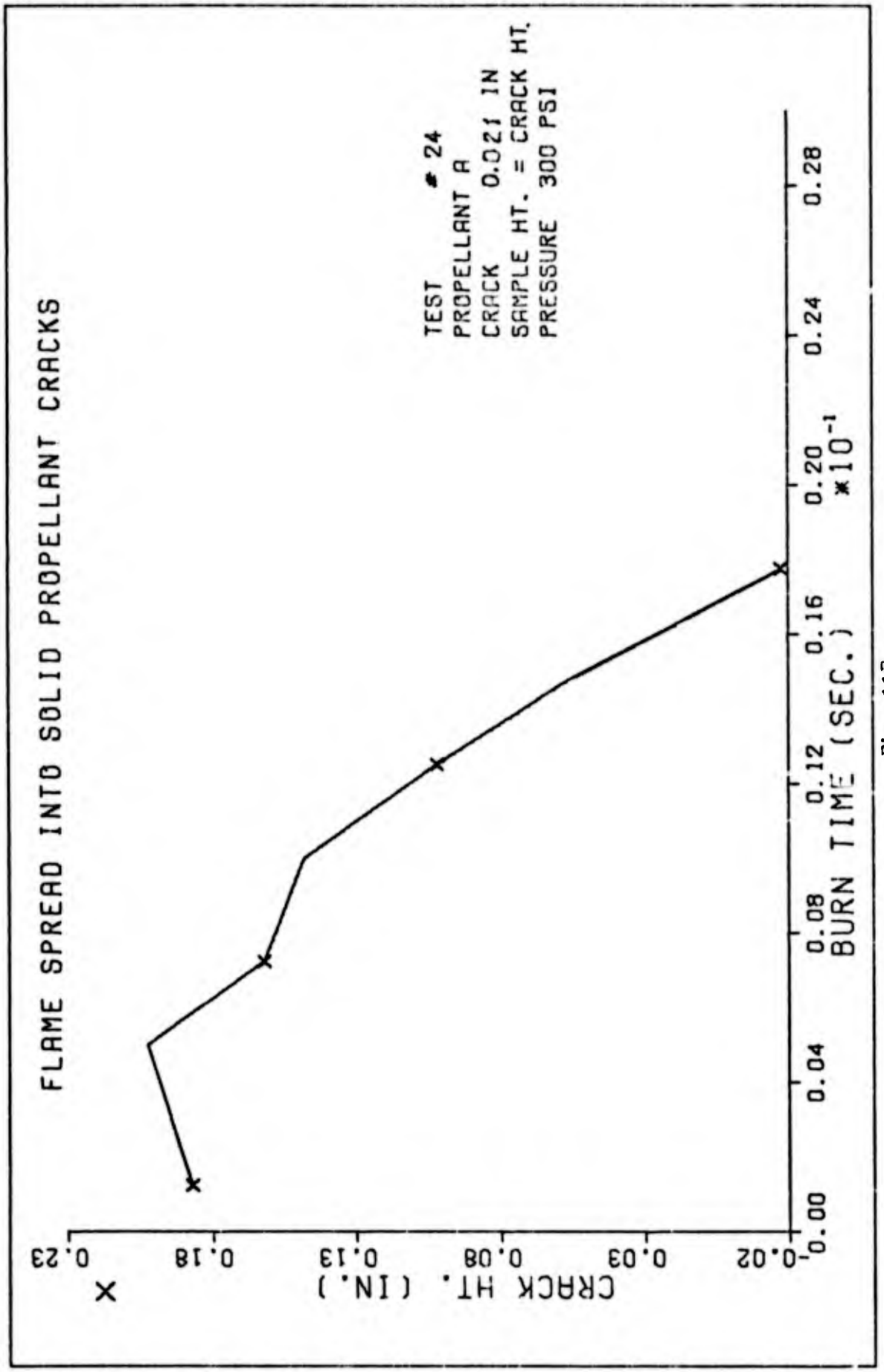
FLAME SPREAD INTO SOLID PROPELLANT CRACKS
TEST # 24
PROPELLANT A
CRACK 0.021 IN
SAMPLE HT. = CRACK HT.
PRESSURE 300 PSI
CRACK HT. (IN.)
0.00
0.02
0.03
0.08
0.13
0.18
0.23
0.04
0.08
0.12
0.16
0.20
0.24
0.28
BURN TIME (SEC.)
*10⁻¹

Fig. 113.

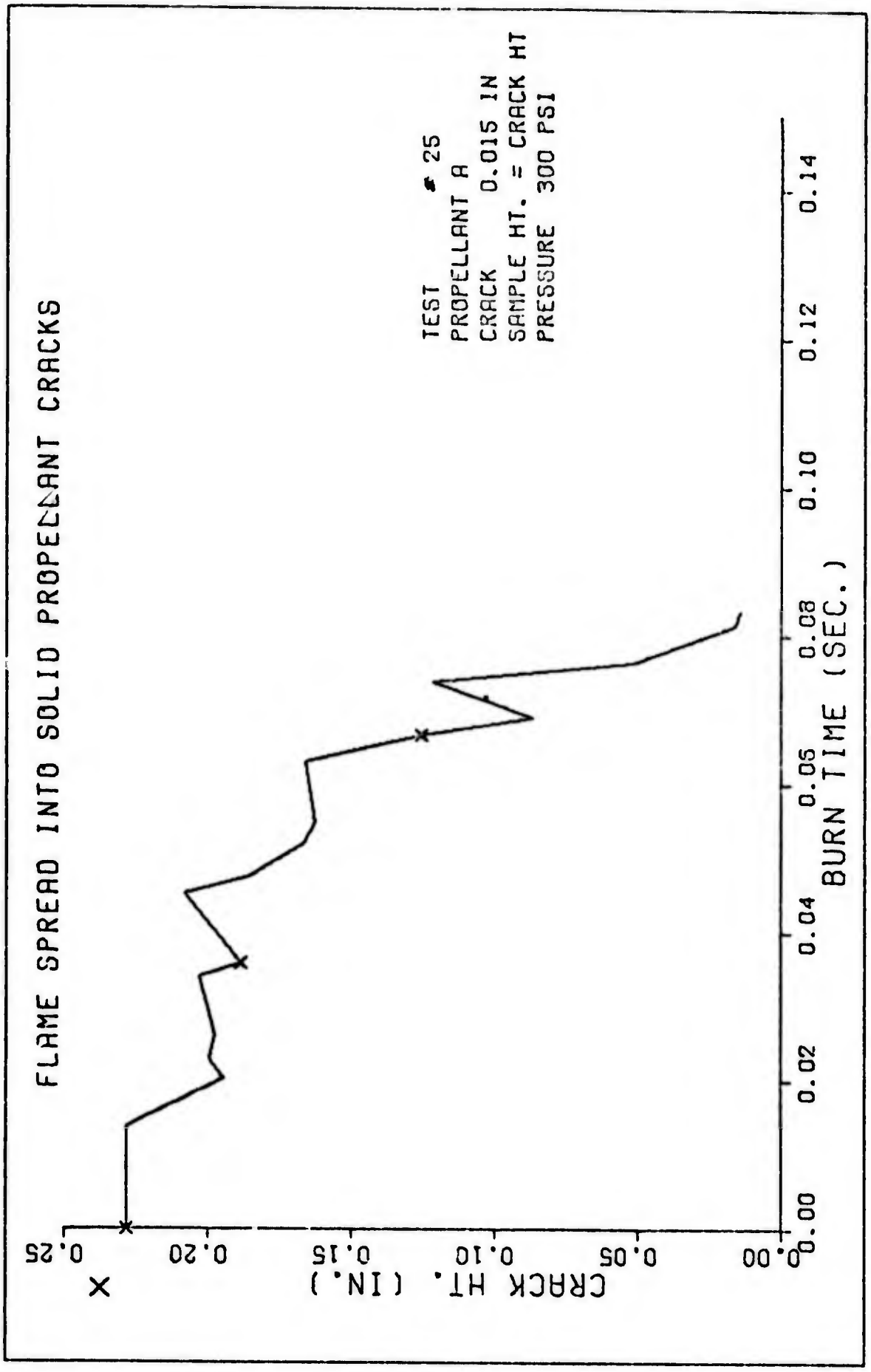
FLAME SPREAD INTO SOLID PROPELLANT CRACKS
TEST # 25
PROPELLANT A
CRACK 0.015 IN
SAMPLE HT. = CRACK HT
PRESSURE 300 PSI
CRACK HT. (IN.)
BURN TIME (SEC.)
0.00
0.05
0.10
0.15
0.20
0.25
0.00
0.02
0.04
0.05
0.08
0.10
0.12
0.14
X

Fig. 11F.

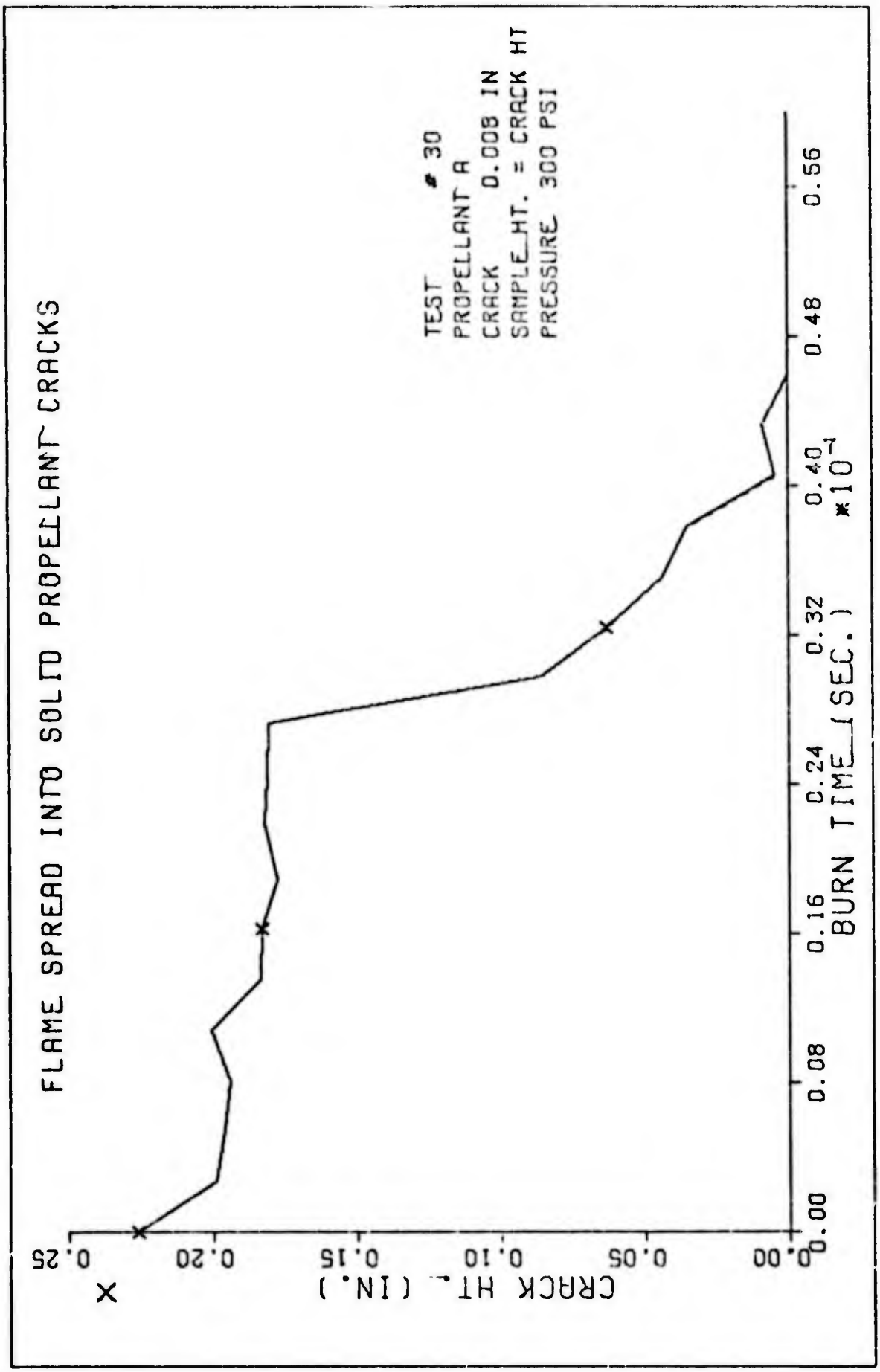
FLAME SPREAD INTO SOLID PROPELLANT CRACKS
TEST # 30
PROPELLANT A
CRACK 0.008 IN
SAMPLE HT. = CRACK HT
PRESSURE 300 PSI
CRACK HT. (IN.)
0.00
0.05
0.10
0.15
0.20
0.25
0.00
0.08
0.16
0.24
0.32
0.40
0.48
0.56
BURN TIME (SEC.)
*10⁻¹

Fig. 11b.

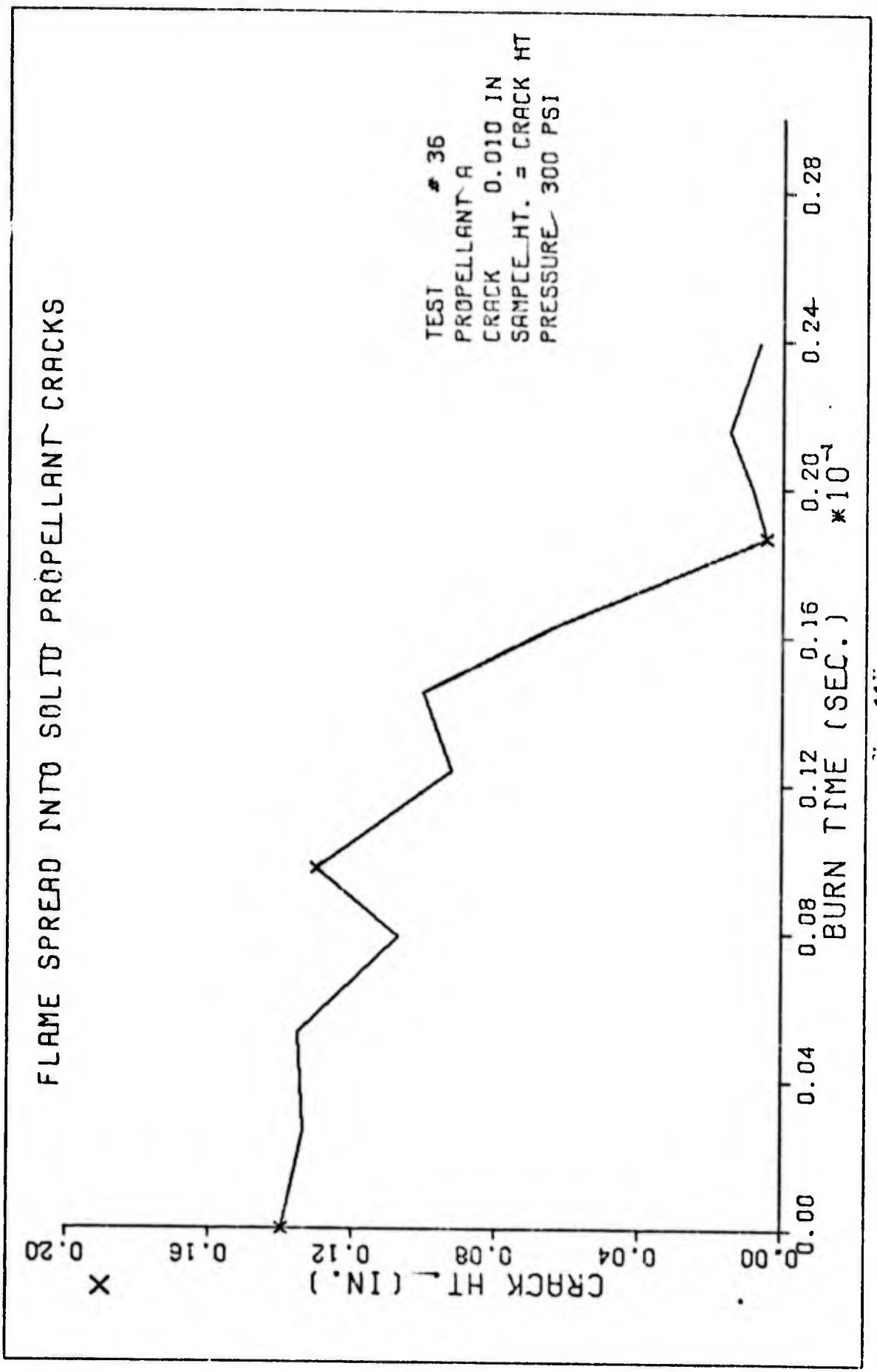
FLAME SPREAD INTO SOLID PROPELLANT CRACKS
TEST # 36
PROPELLANT A
CRACK 0.010 IN
SAMPLE HT. = CRACK HT
PRESSURE 300 PSI
CRACK HT (IN.)
0.00
0.04
0.08
0.12
0.16
0.20
0.24
0.28
BURN TIME (SEC.)
*10⁻¹
X

Fig. 11a.

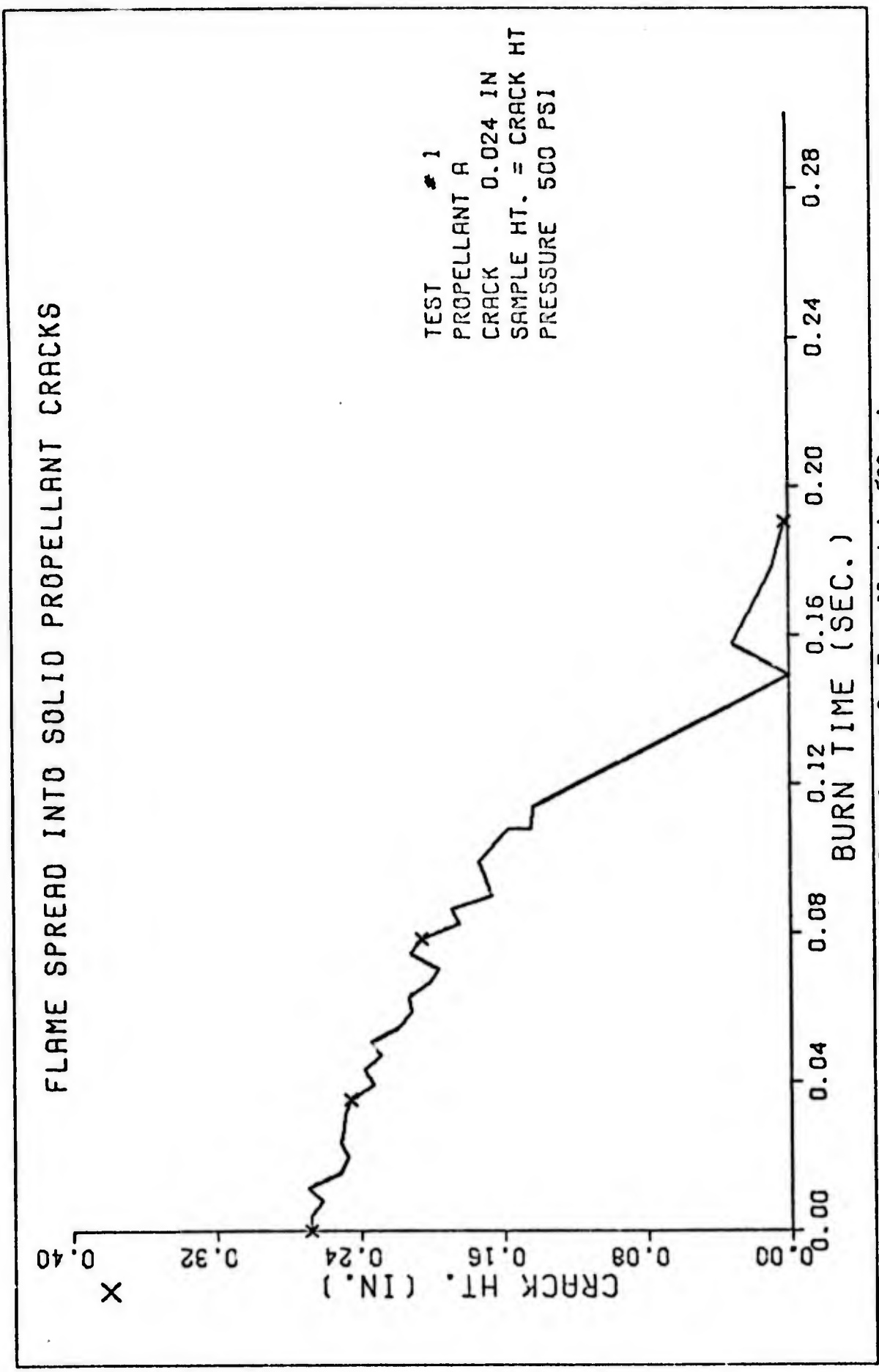

Fig. 12. Data Curves for Propellant A, 500 psi

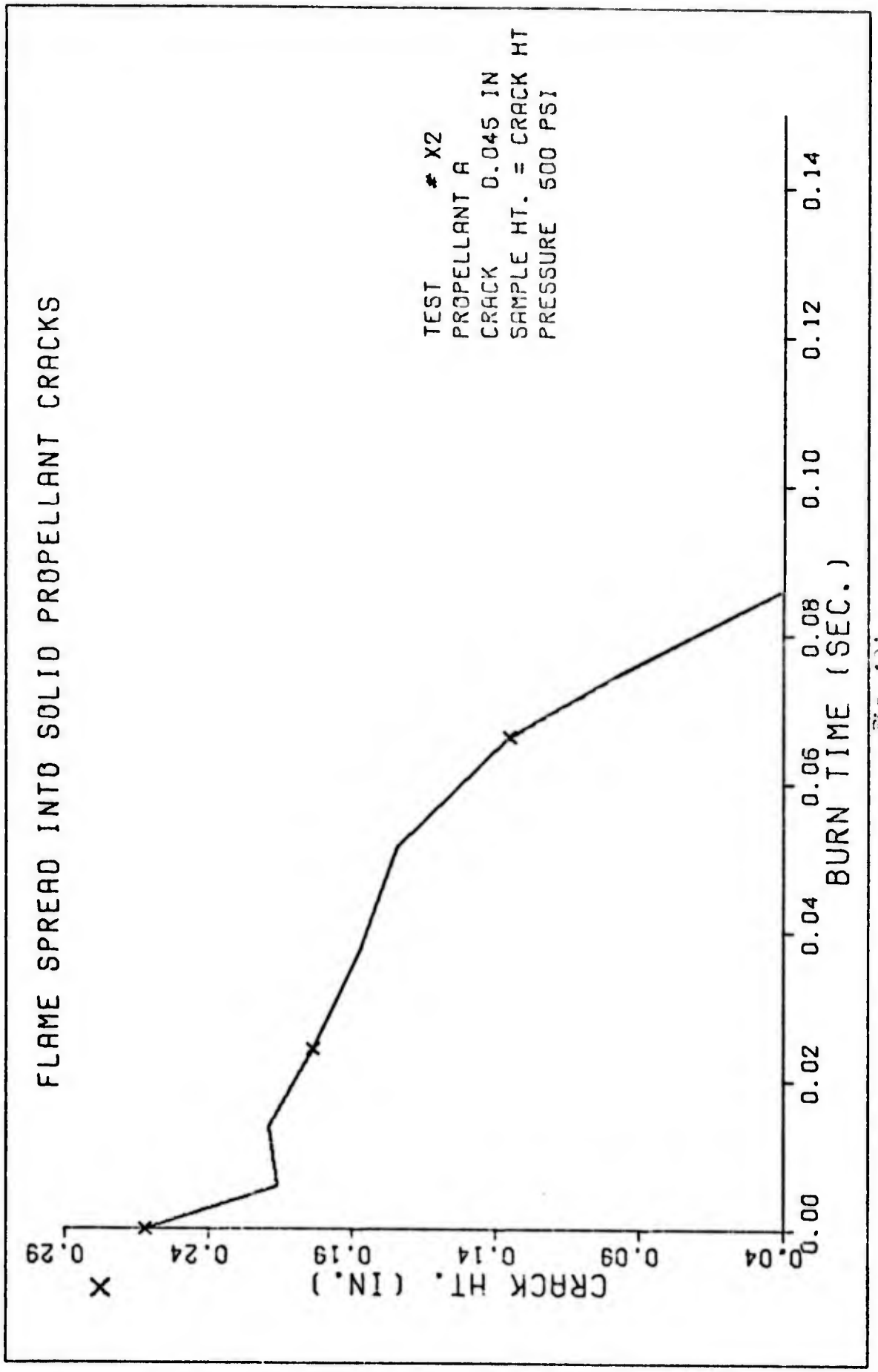
FLAME SPREAD INTO SOLID PROPELLANT CRACKS
TEST # X2
PROPELLANT A
CRACK 0.045 IN
SAMPLE HT. = CRACK HT
PRESSURE 500 PSI
CRACK HT. (IN.)
0.04
0.09
0.14
0.19
0.24
0.29
X
BURN TIME (SEC.)
0.00
0.02
0.04
0.06
0.08
0.10
0.12
0.14

Fig. 12A.

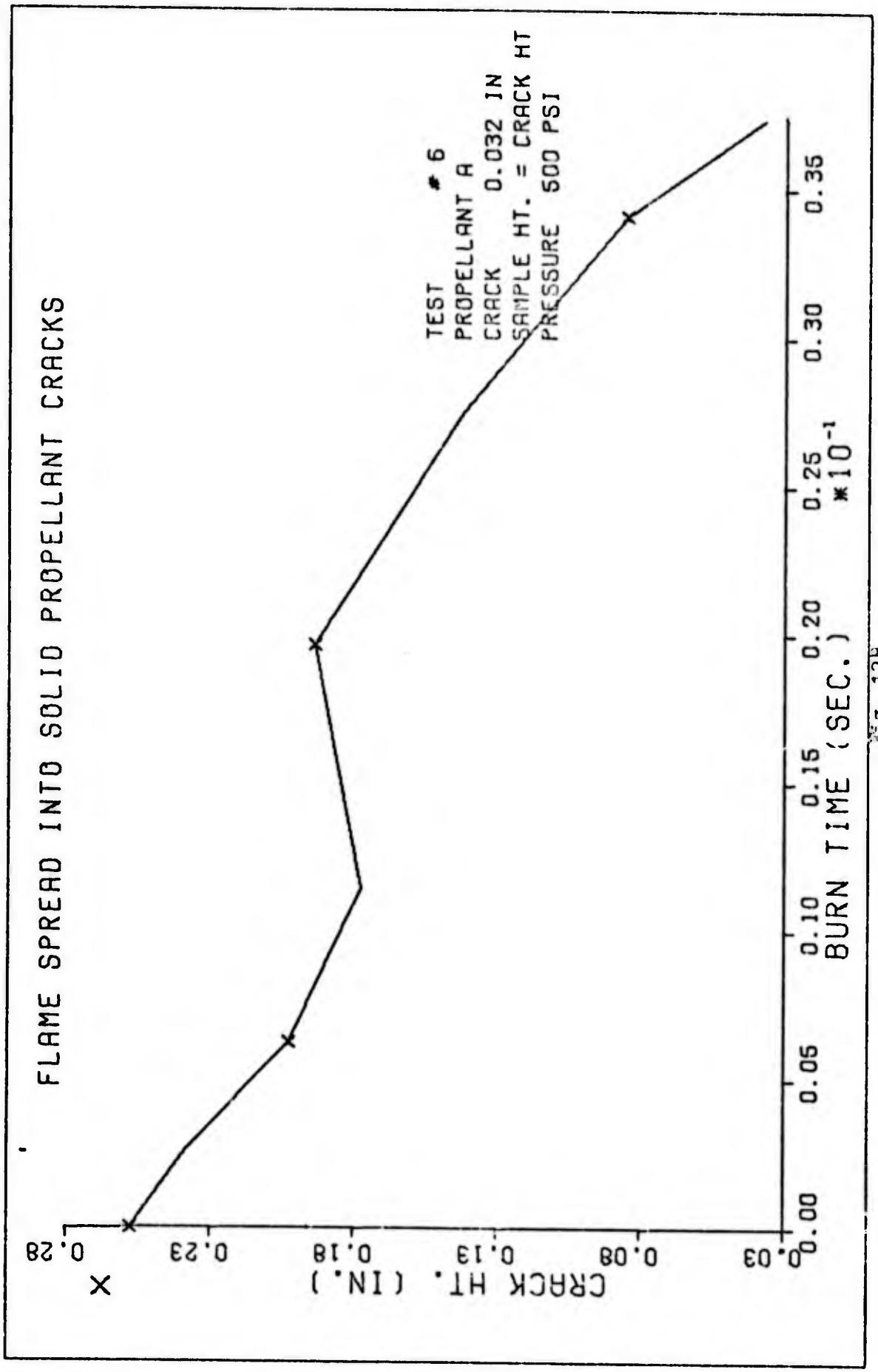
FLAME SPREAD INTO SOLID PROPELLANT CRACKS
TEST # 6
PROPELLANT A
CRACK 0.032 IN
SAMPLE HT. = CRACK HT
PRESSURE 500 PSI
CRACK HT. (IN.)
0.03
0.08
0.13
0.18
0.23
0.28
X
0.00
0.05
0.10
0.15
0.20
0.25
0.30
0.35
BURN TIME (SEC.)
*10⁻¹

Fig. 125.

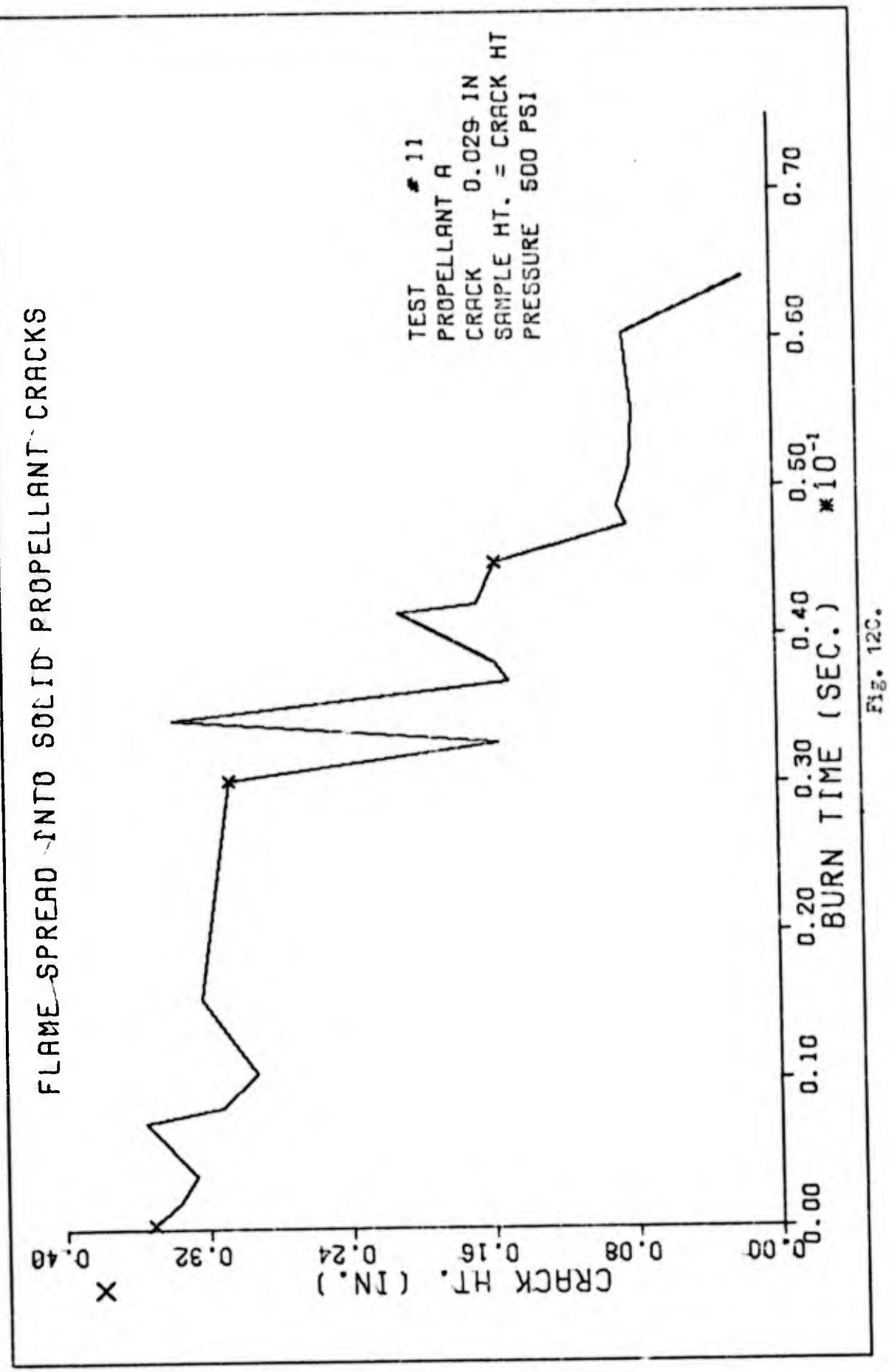
FLAME SPREAD INTO SOLID PROPELLANT CRACKS
TEST # 11
PROPELLANT A
CRACK 0.029 IN
SAMPLE HT. = CRACK HT
PRESSURE 500 PSI
CRACK HT. (IN.)
0.00
0.08
0.16
0.24
0.32
0.40
X
0.00
0.10
0.20
0.30
0.40
0.50
0.60
0.70
BURN TIME (SEC.)
*10⁻¹

Fig. 12C.

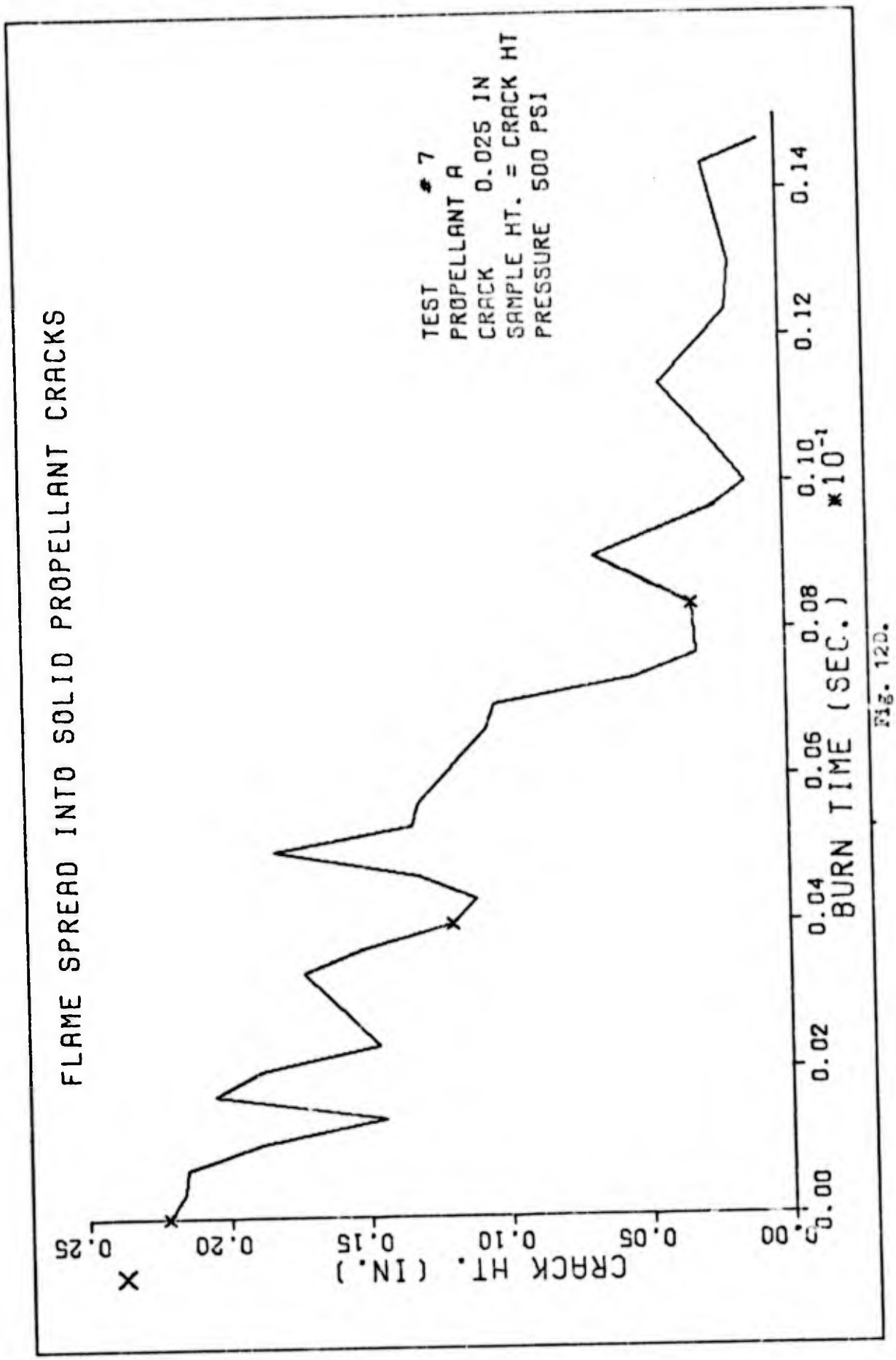
FLAME SPREAD INTO SOLID PROPELLANT CRACKS
TEST # 7
PROPELLANT A
CRACK 0.025 IN
SAMPLE HT. = CRACK HT
PRESSURE 500 PSI
CRACK HT. (IN.)
0.00
0.05
0.10
0.15
0.20
0.25
BURN TIME (SEC.)
0.00
0.02
0.04
0.06
0.08
0.10
0.12
0.14
$\times 10^{-1}$

Fig. 12D.

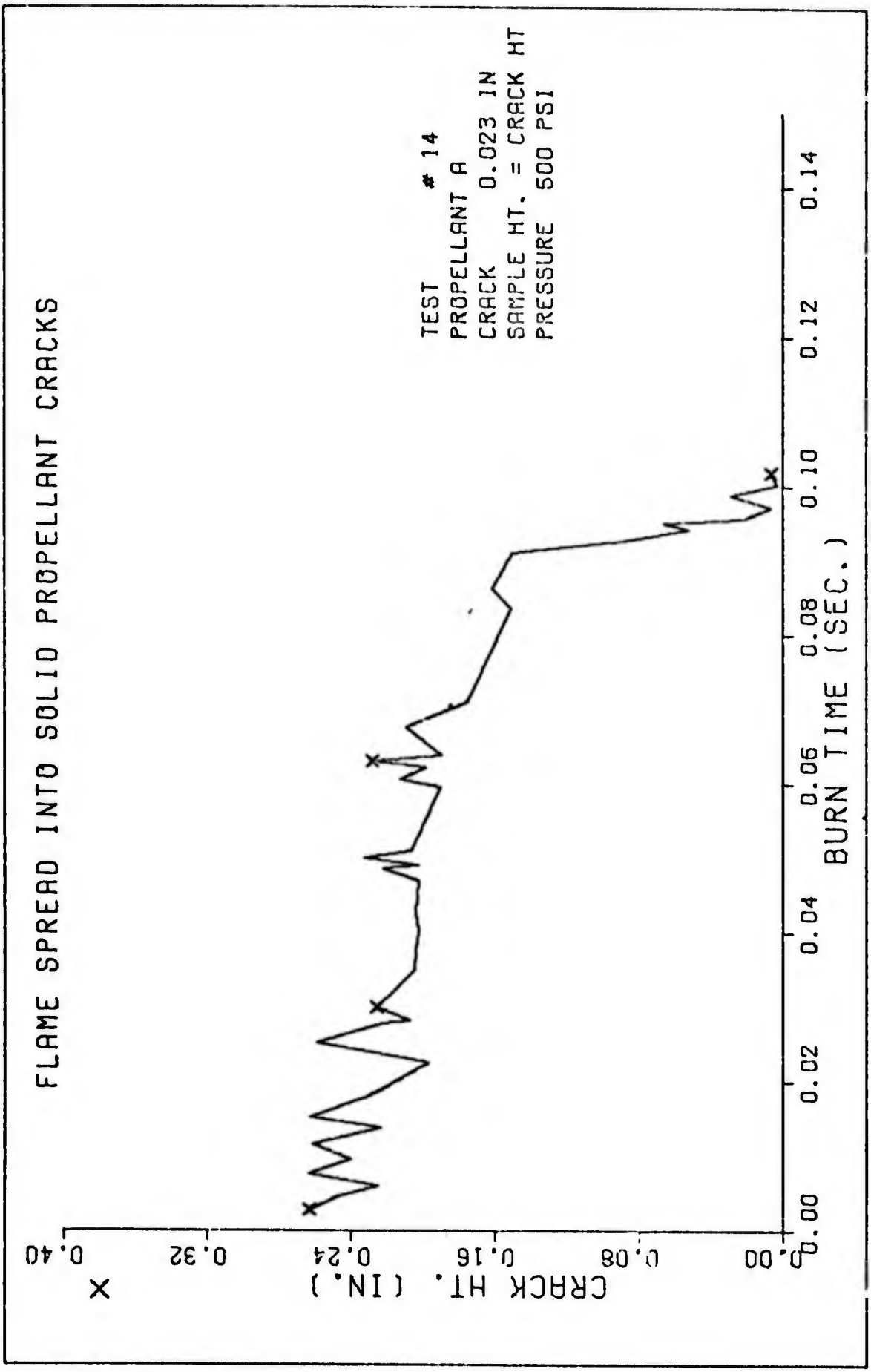
FLAME SPREAD INTO SOLID PROPELLANT CRACKS
TEST # 14
PROPELLANT A
CRACK 0.023 IN
SAMPLE HT. = CRACK HT
PRESSURE 500 PSI
CRACK HT. (IN.)
BURN TIME (SEC.)
0.00
0.02
0.04
0.06
0.08
0.10
0.12
0.14
0.16
0.24
0.32
0.40
X

Fig. 12.

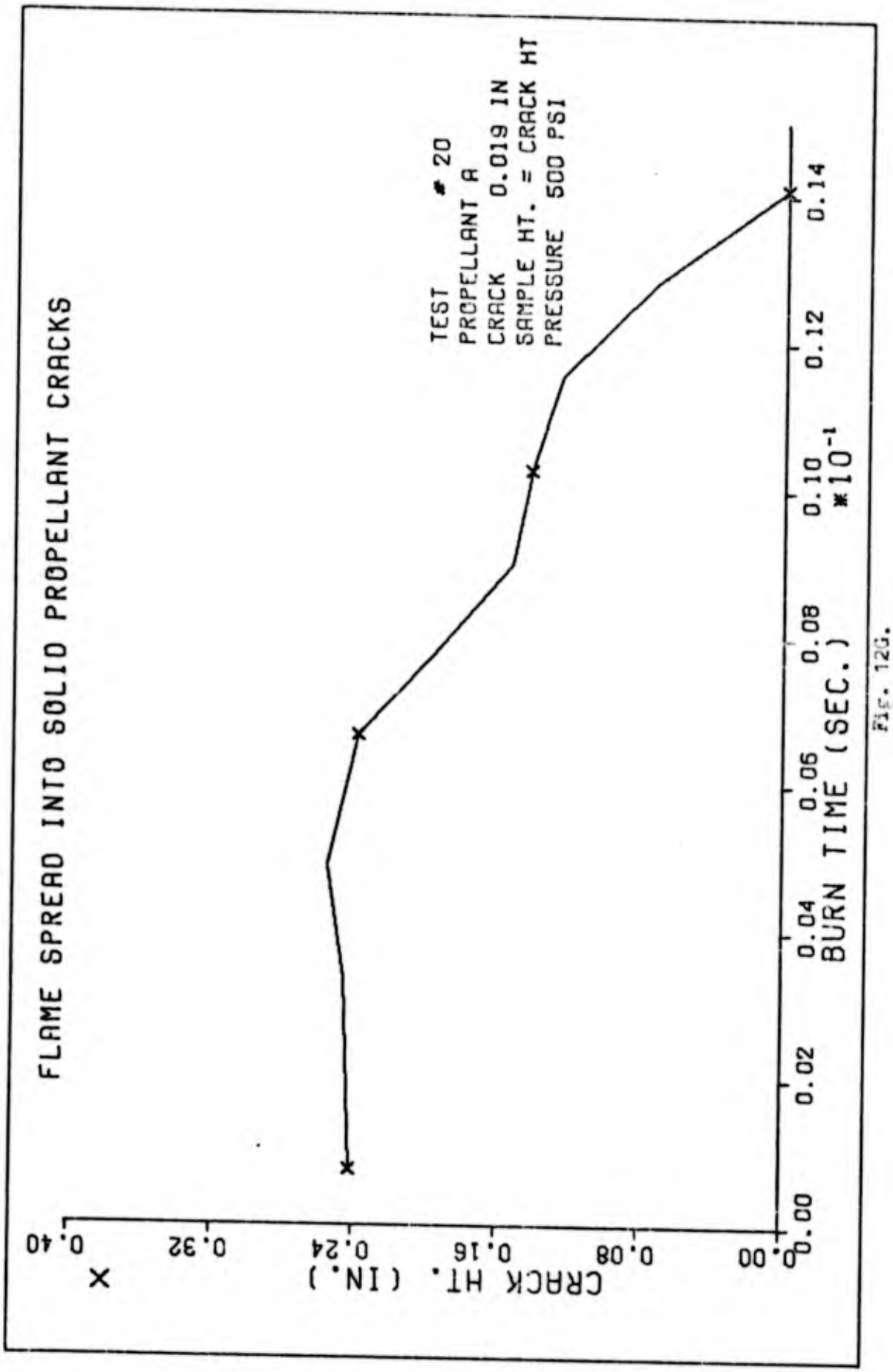
FLAME SPREAD INTO SOLID PROPELLANT CRACKS
TEST # 20
PROPELLANT A
CRACK 0.019 IN
SAMPLE HT. = CRACK HT
PRESSURE 500 PSI
CRACK HT. (IN.)
0.00
0.08
0.16
0.24
0.32
0.40
X
0.00
0.02
0.04
0.06
0.08
0.10
0.12
0.14
BURN TIME (SEC.)
*10⁻¹

Fig. 12G.

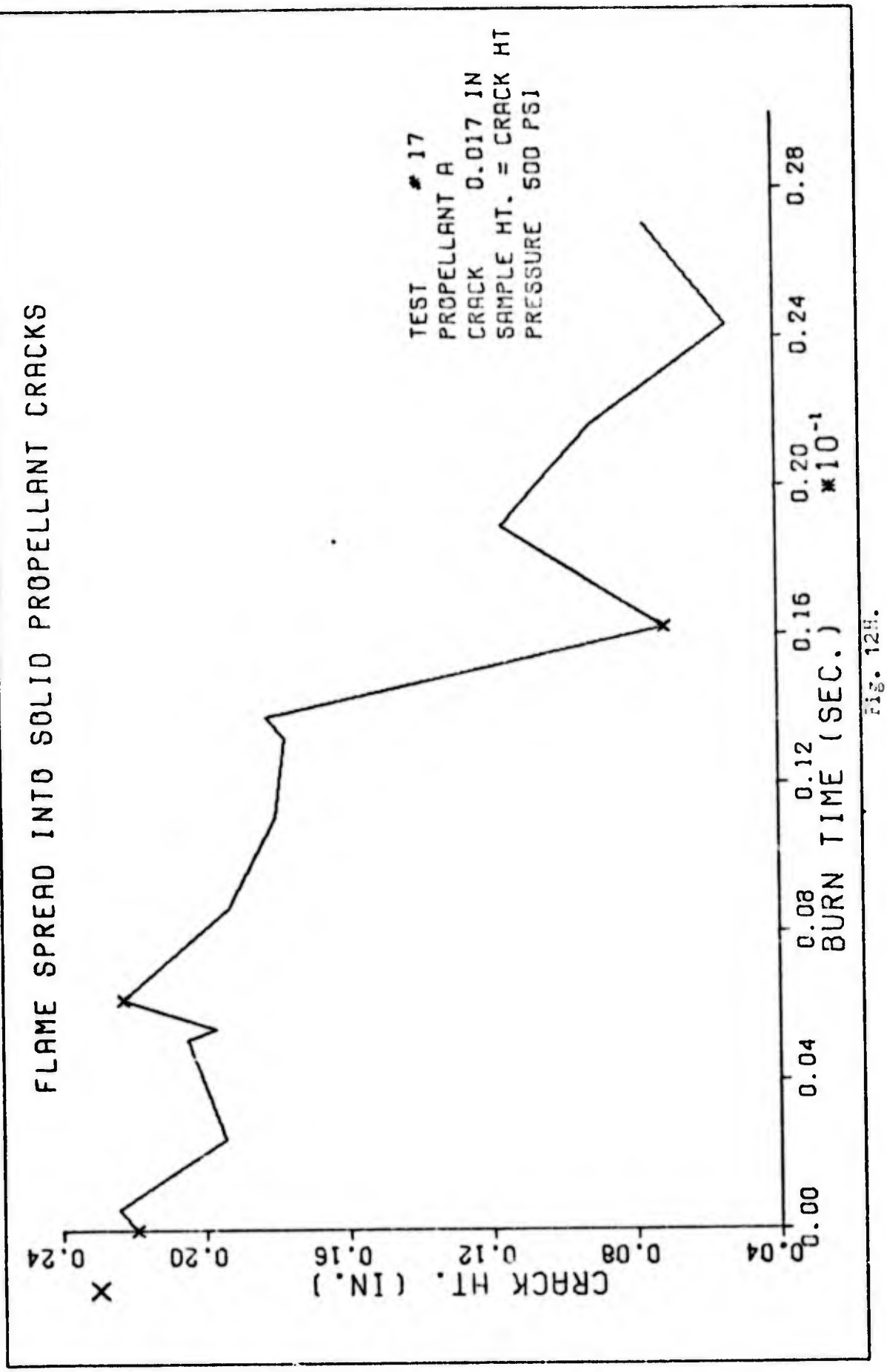
FLAME SPREAD INTO SOLID PROPELLANT CRACKS
TEST # 17
PROPELLANT A
CRACK 0.017 IN
SAMPLE HT. = CRACK HT
PRESSURE 500 PSI
CRACK HT. (IN.)
0.04
0.08
0.12
0.16
0.20
0.24
X
0.00
0.04
0.08
0.12
0.16
0.20
0.24
0.28
BURN TIME (SEC.)
*10⁻¹

Fig. 12H.

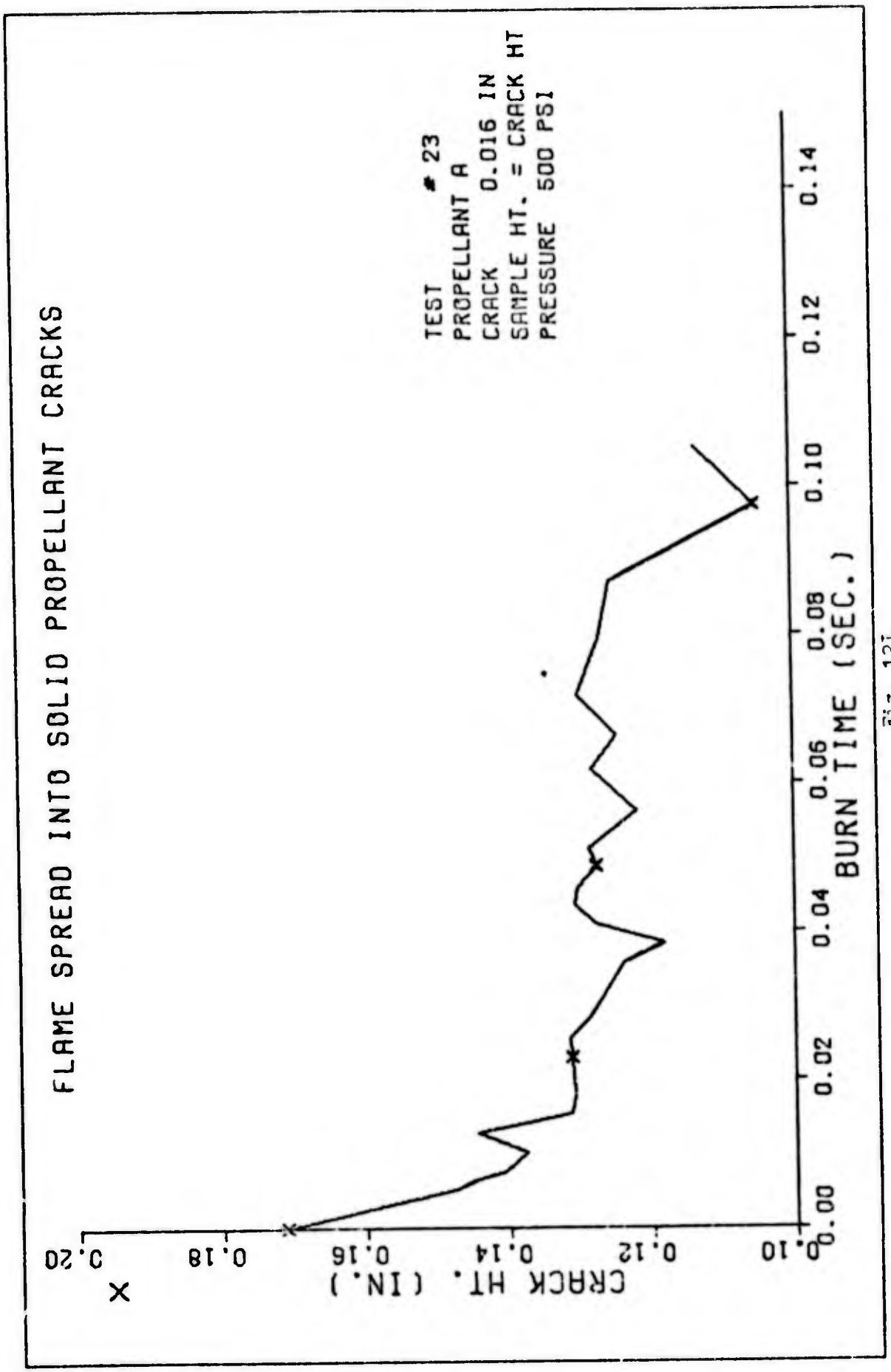
FLAME SPREAD INTO SOLID PROPELLANT CRACKS
TEST # 23
PROPELLANT A
CRACK 0.016 IN
SAMPLE HT. = CRACK HT
PRESSURE 500 PSI
CRACK HT. (IN.)
BURN TIME (SEC.)
0.00
0.02
0.04
0.06
0.08
0.10
0.12
0.14
0.10
0.12
0.14
0.16
0.18
0.20
X

Fig. 12i.

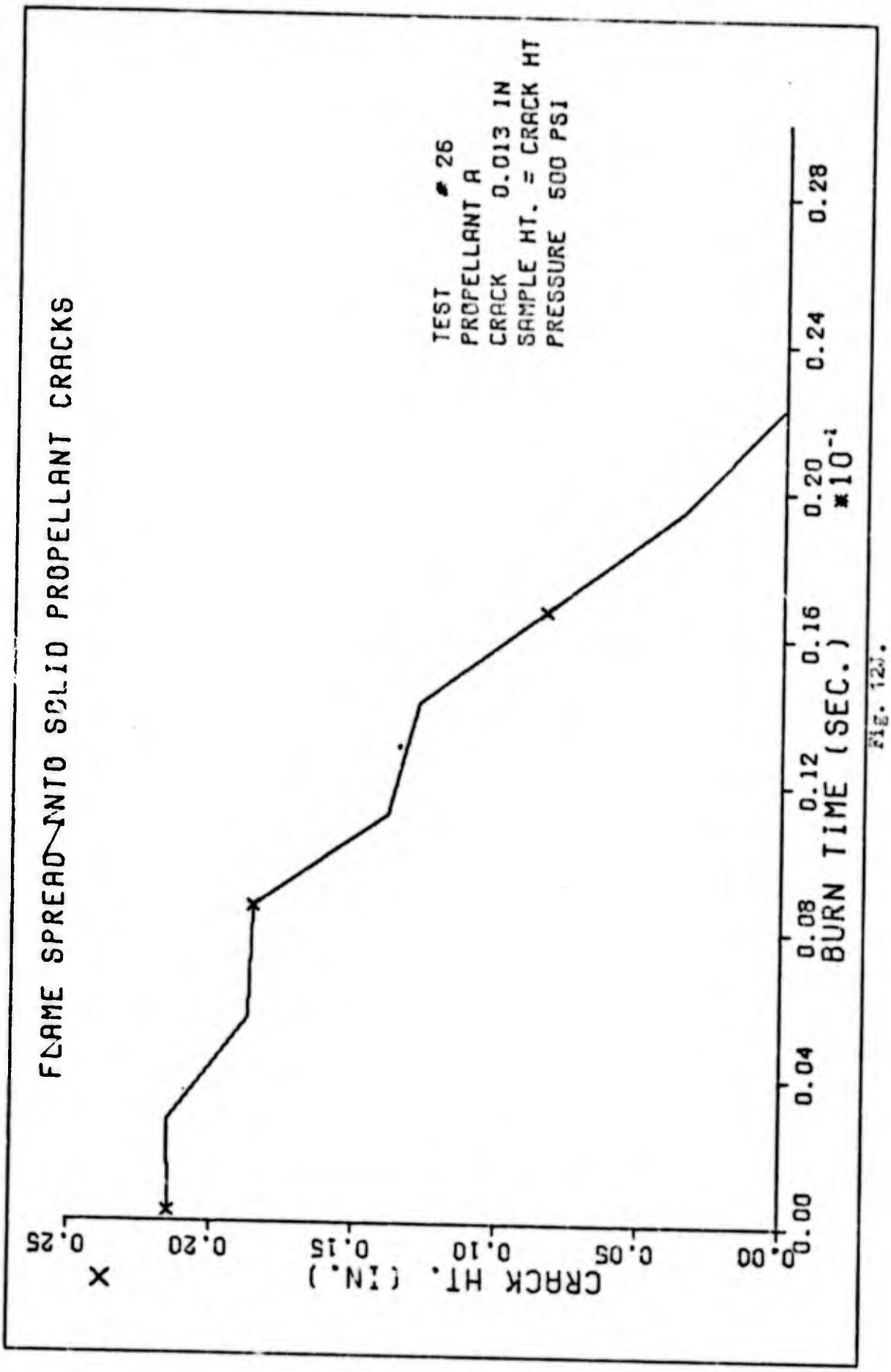
FLAME SPREAD INTO SOLID PROPELLANT CRACKS
TEST # 26
PROPELLANT A
CRACK 0.013 IN
SAMPLE HT. = CRACK HT
PRESSURE 500 PSI
CRACK HT. (IN.)
0.00
0.05
0.10
0.15
0.20
0.25
X
0.00
0.04
0.08
0.12
0.16
0.20
0.24
0.28
BURN TIME (SEC.)
*10-1

Fig. 12.

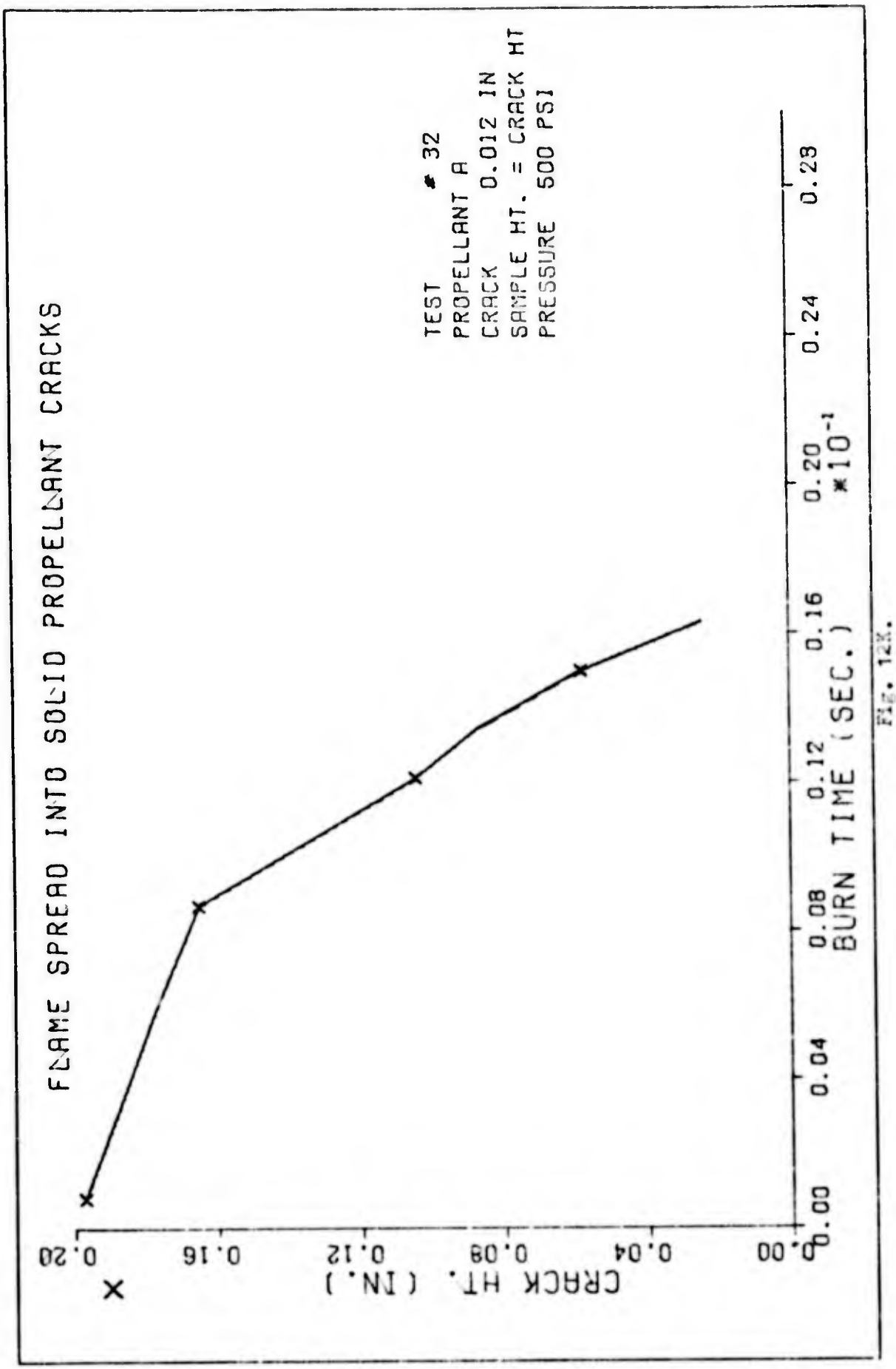
FLAME SPREAD INTO SOLID PROPELLANT CRACKS
TEST # 32
PROPELLANT A
CRACK 0.012 IN
SAMPLE HT. = CRACK HT
PRESSURE 500 PSI
CRACK HT. (IN.)
0.00
0.04
0.08
0.12
0.16
0.20
BURN TIME (SEC.)
0.00
0.04
0.08
0.12
0.16
0.20
0.24
0.28
*10⁻¹

Fig. 12K.

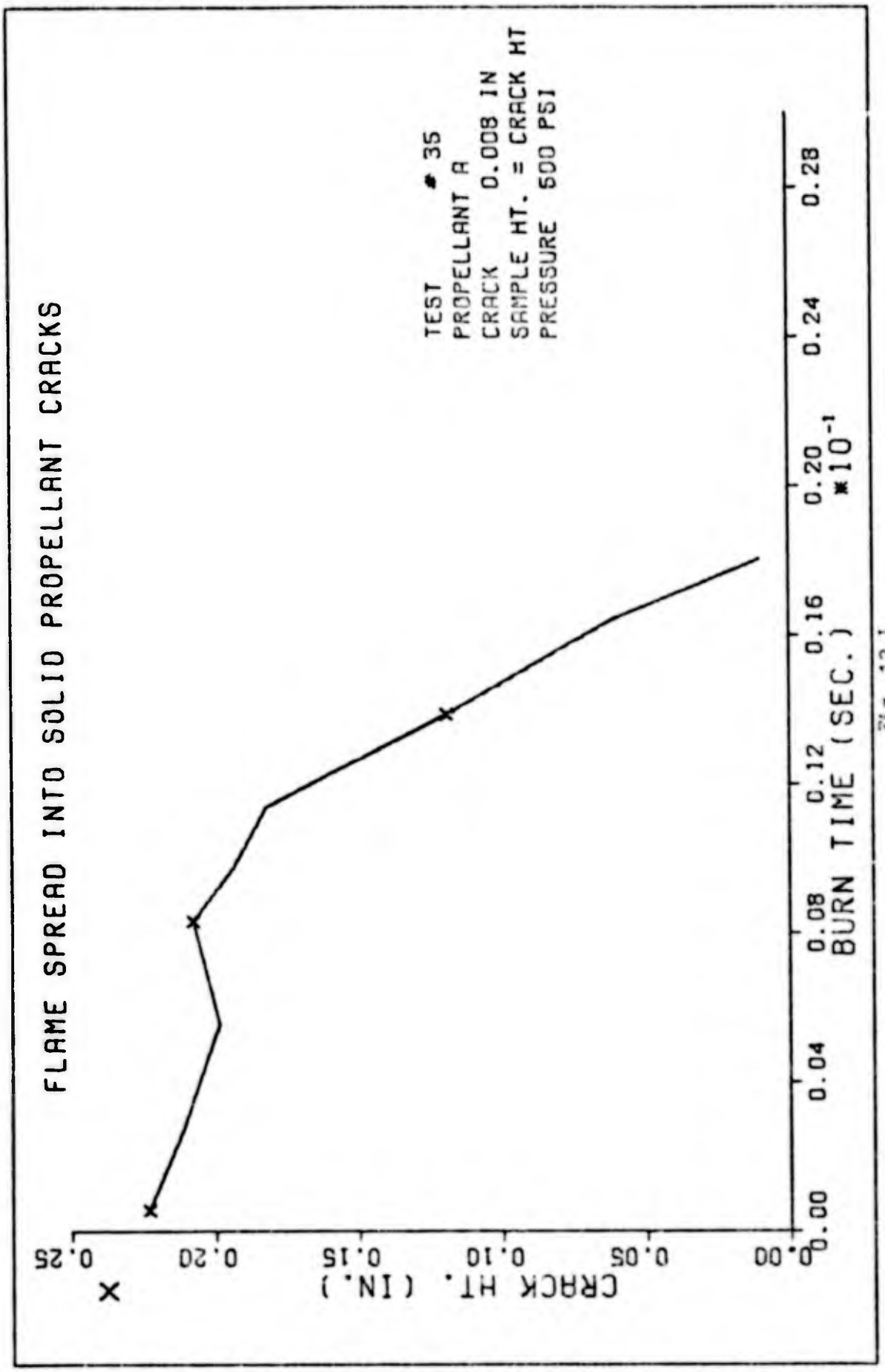
FLAME SPREAD INTO SOLID PROPELLANT CRACKS
TEST # 35
PROPELLANT A
CRACK 0.008 IN
SAMPLE HT. = CRACK HT
PRESSURE 500 PSI
CRACK HT. (IN.)
0.00
0.05
0.10
0.15
0.20
0.25
X
0.00
0.04
0.08
0.12
0.16
0.20
0.24
0.28
BURN TIME (SEC.)
*10⁻¹

Fig. 12 L.

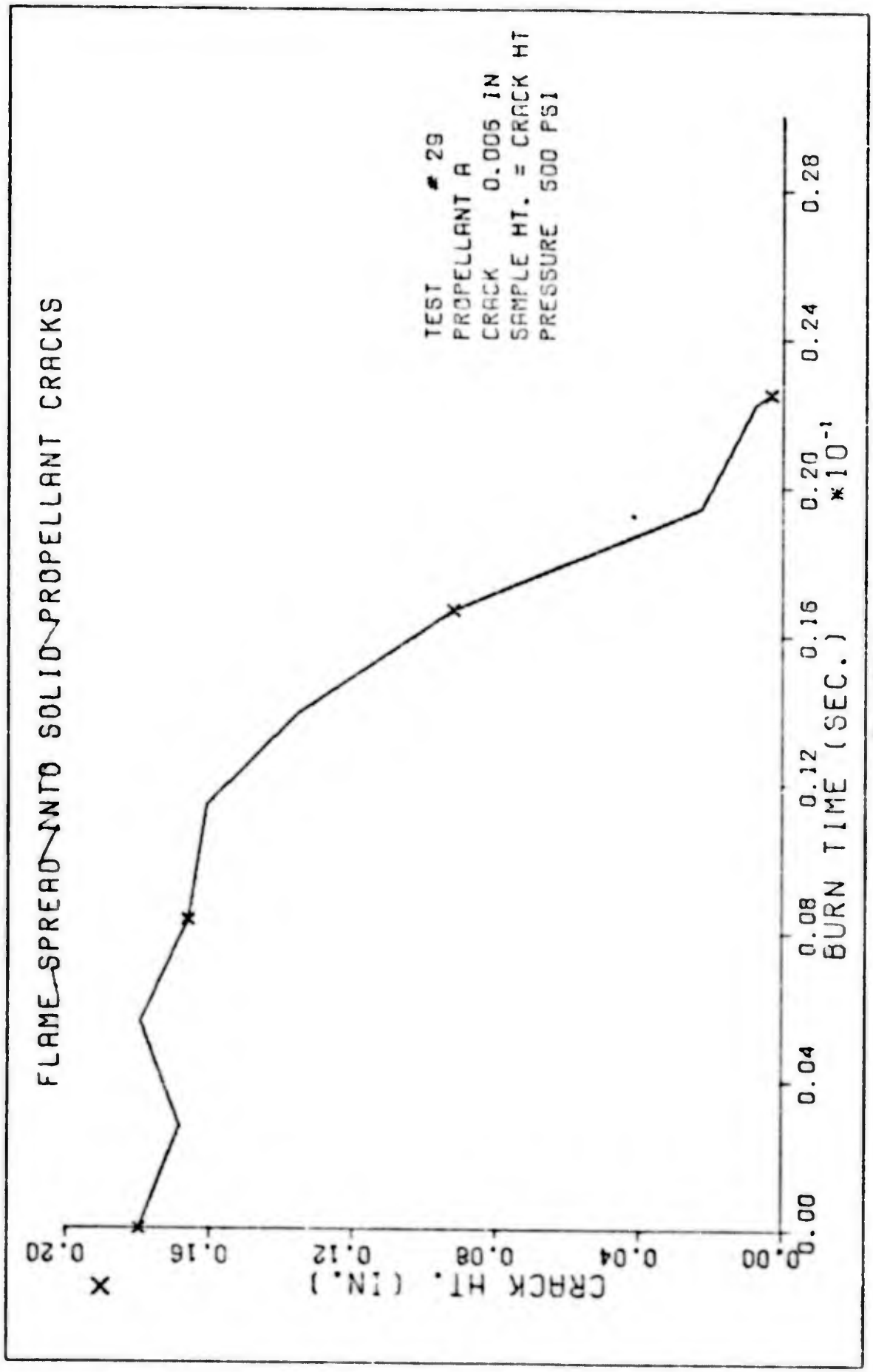
FLAME SPREAD INTO SOLID PROPELLANT CRACKS
TEST # 29
PROPELLANT A
CRACK 0.005 IN
SAMPLE HT. = CRACK HT
PRESSURE 500 PSI
CRACK HT. (IN.)
0.00
0.04
0.08
0.12
0.16
0.20
BURN TIME (SEC.)
0.00
0.04
0.08
0.12
0.16
0.20
0.24
0.28
*10⁻¹

Fig. 12 A.

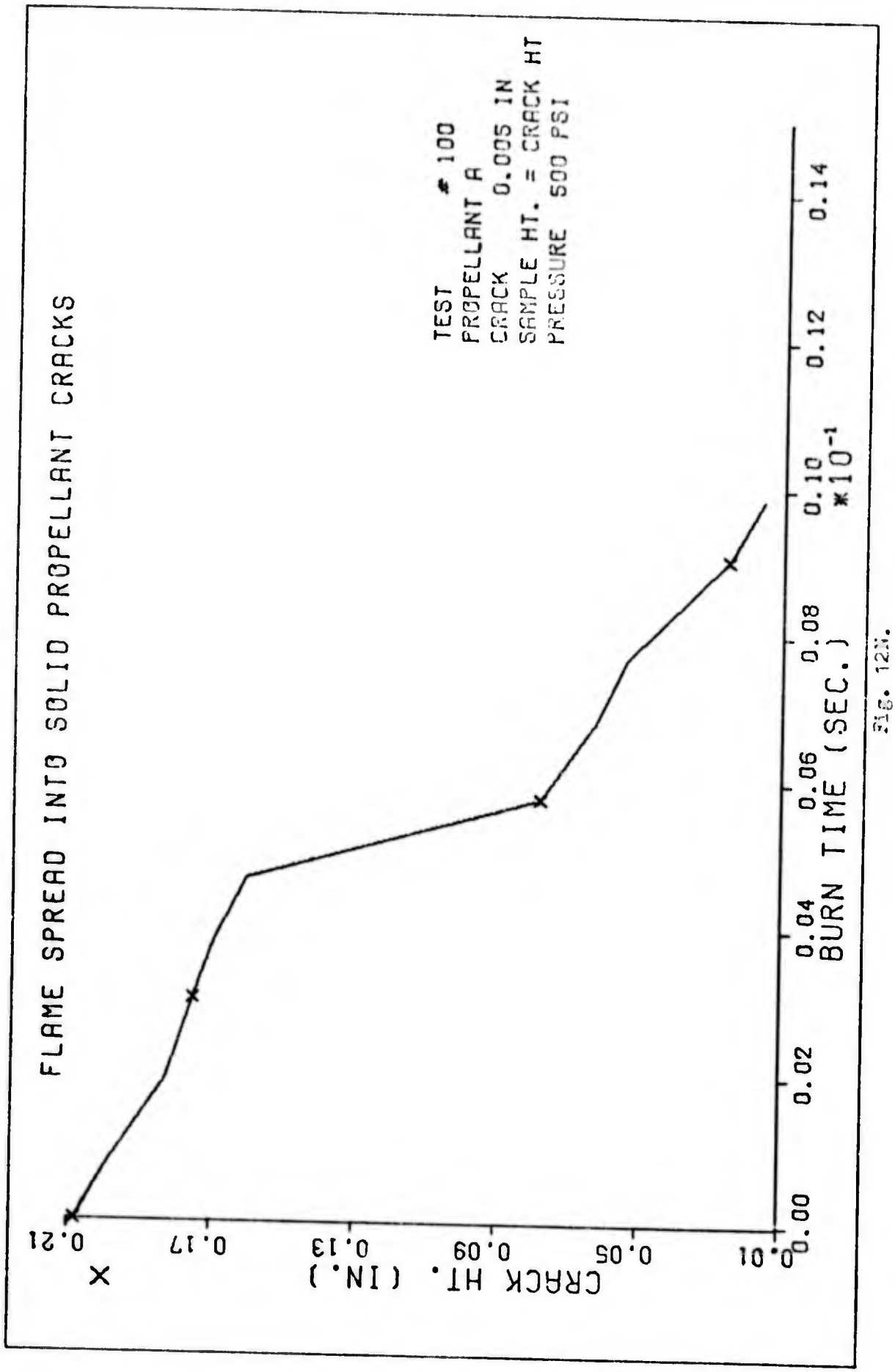
FLAME SPREAD INTO SOLID PROPELLANT CRACKS
TEST # 100
PROPELLANT A
CRACK 0.005 IN
SAMPLE HT. = CRACK HT
PRESSURE 500 PSI
CRACK HT. (IN.)
0.00
0.01
0.05
0.09
0.13
0.17
0.21
X
0.00
0.02
0.04
0.06
0.08
0.10
0.12
0.14
BURN TIME (SEC.)
*10⁻¹

Fig. 12A.

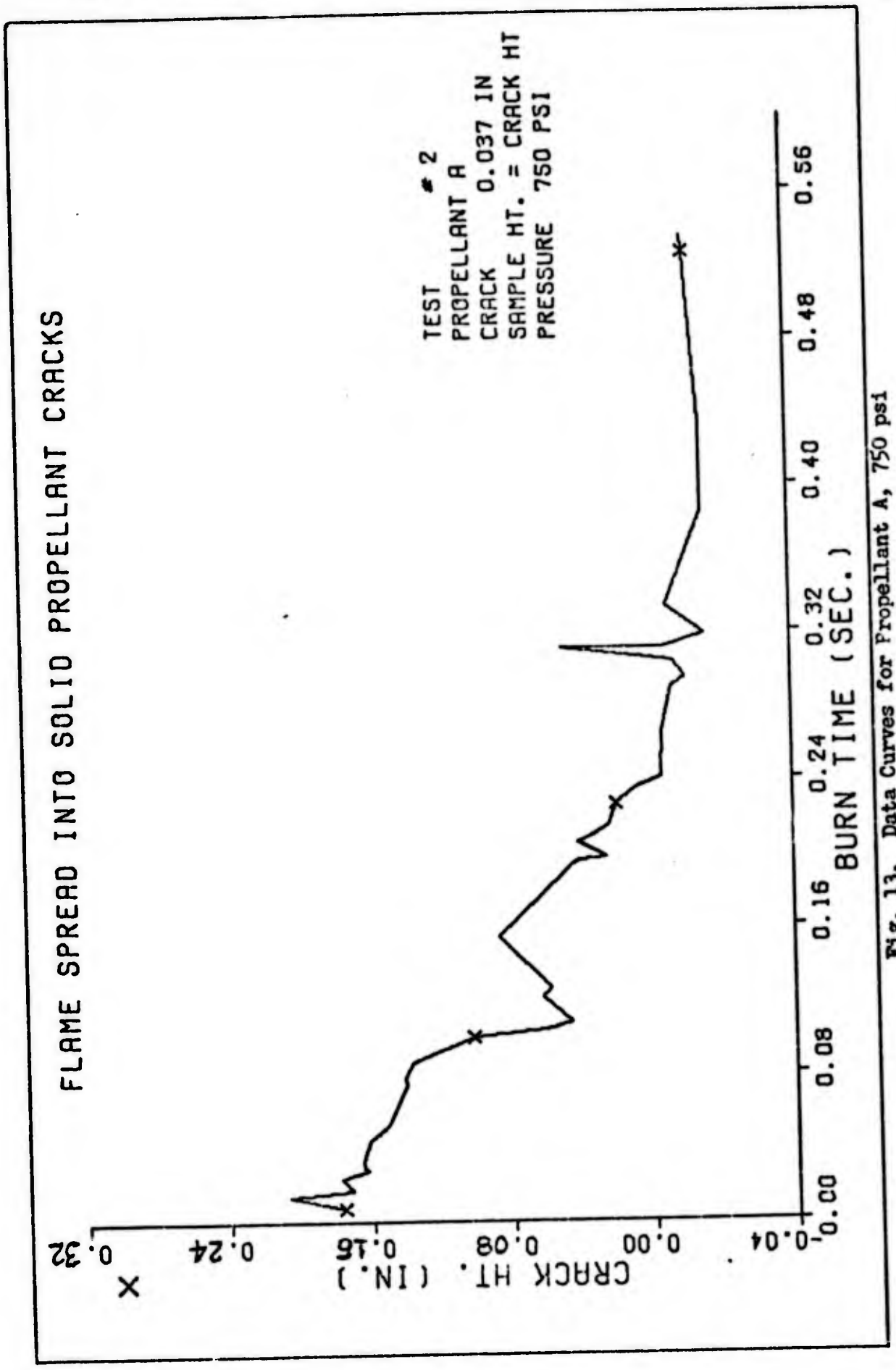

Fig. 13. Data Curves for Propellant A, 750 psi

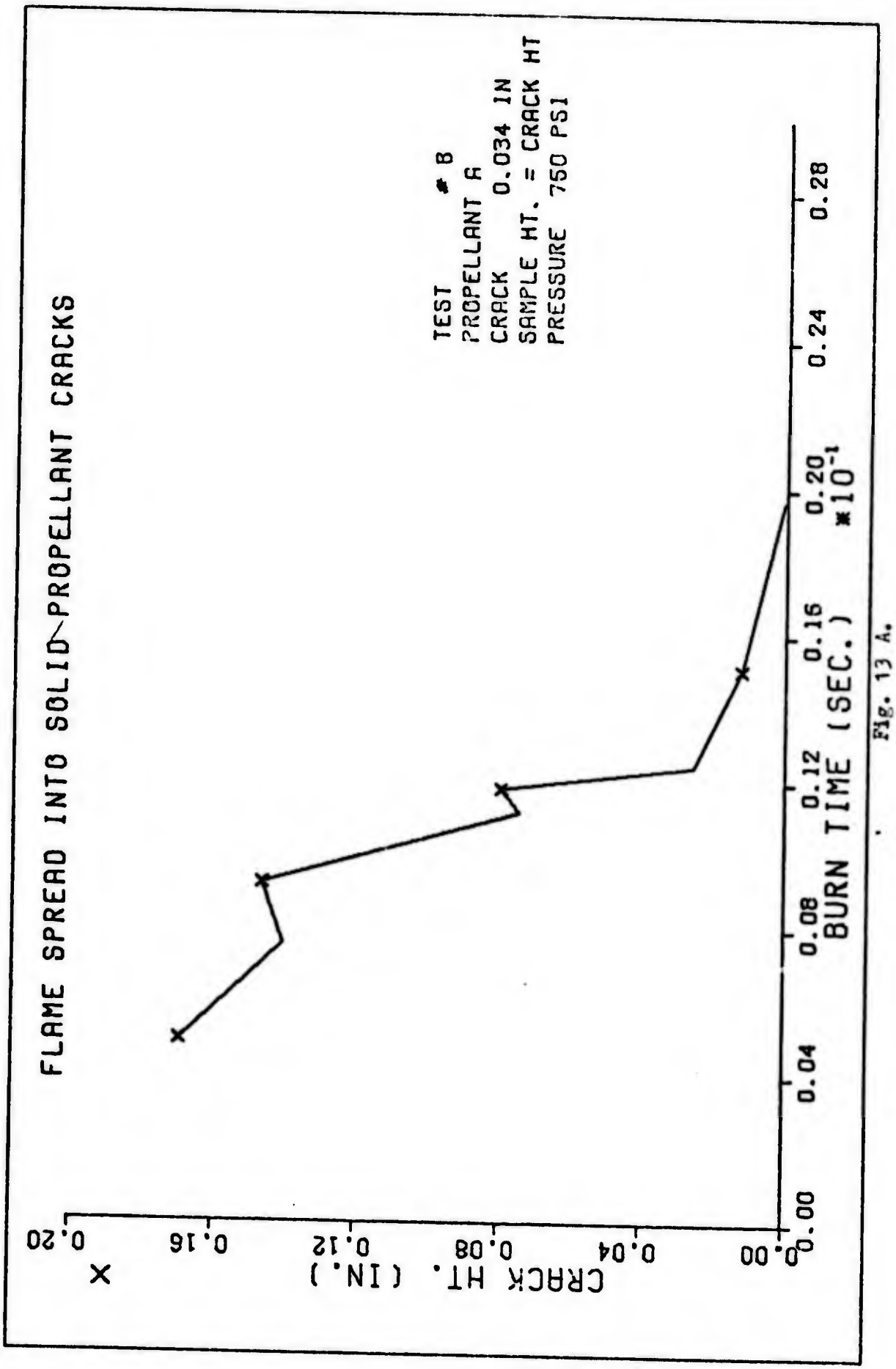
FLAME SPREAD INTO SOLID PROPELLANT CRACKS
TEST # B
PROPELLANT A
CRACK 0.034 IN
SAMPLE HT. = CRACK HT
PRESSURE 750 PSI
CRACK HT. (IN.)
0.00
0.04
0.08
0.12
0.16
0.20
X
BURN TIME (SEC.)
0.00
0.04
0.08
0.12
0.16
0.20
0.24
0.28
*10⁻¹

Fig. 13 A.

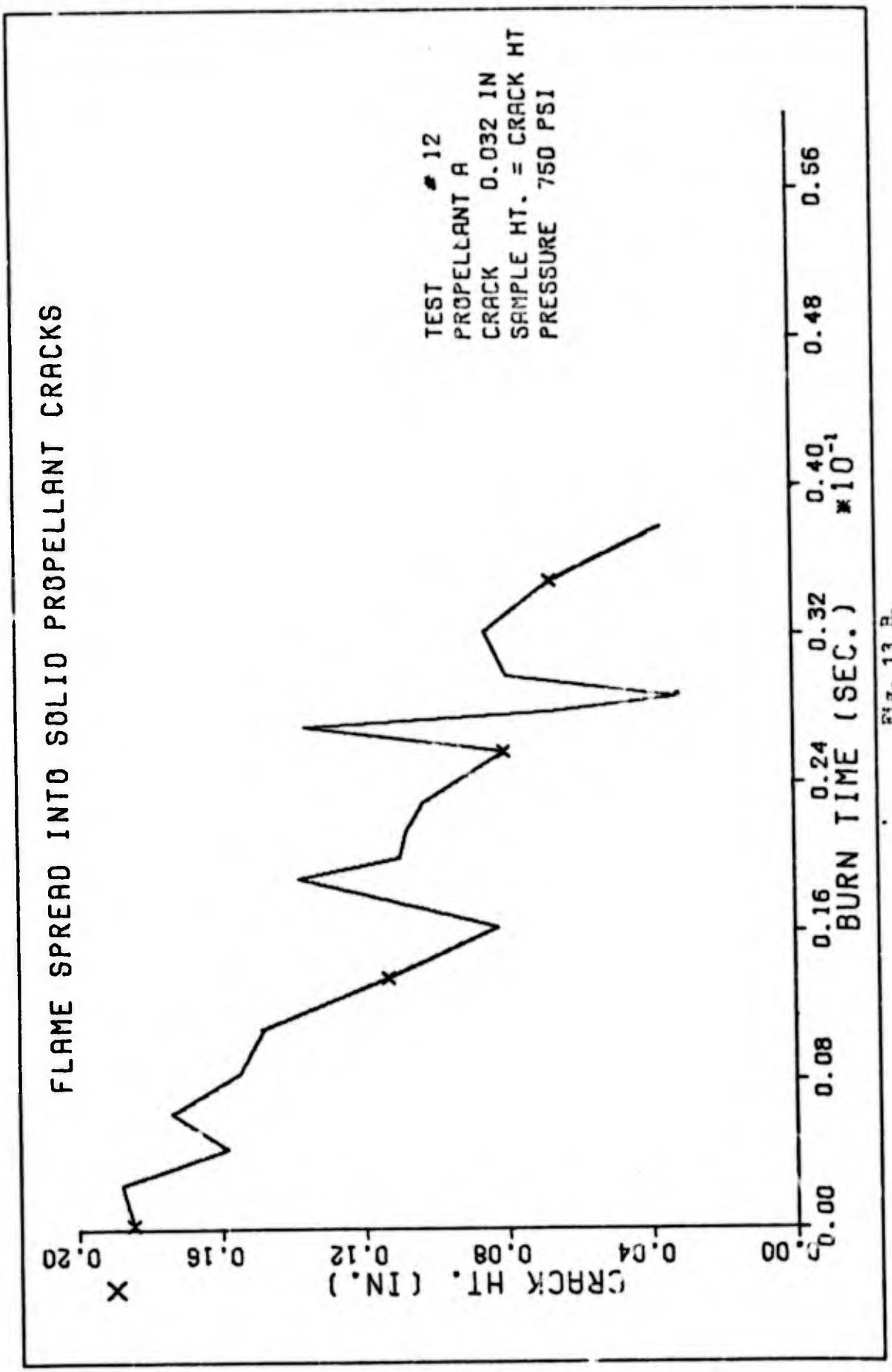
FLAME SPREAD INTO SOLID PROPELLANT CRACKS
TEST # 12
PROPELLANT A
CRACK 0.032 IN
SAMPLE HT. = CRACK HT
PRESSURE 750 PSI
CRACK HT. (IN.)
0.00
0.04
0.08
0.12
0.16
0.20
X
0.00
0.08
0.16
0.24
0.32
0.40
0.48
0.56
BURN TIME (SEC.)
*10^-1

Fig. 13 B.

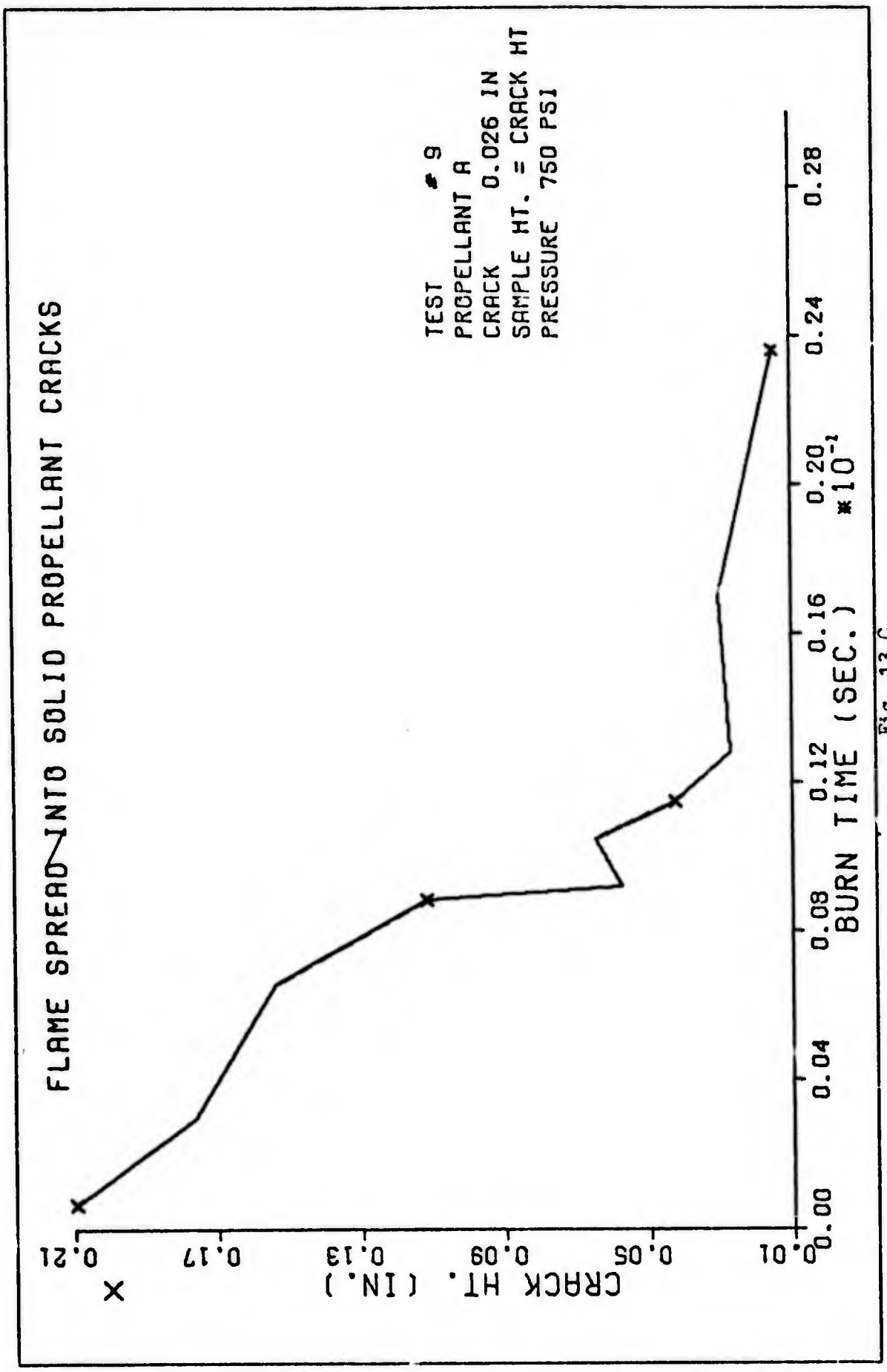
FLAME SPREAD INTO SOLID PROPELLANT CRACKS
TEST # 9
PROPELLANT A
CRACK 0.026 IN
SAMPLE HT. = CRACK HT
PRESSURE 750 PSI
CRACK HT. (IN.)
0.01
0.05
0.09
0.13
0.17
0.21
X
0.00
0.04
0.08
0.12
0.16
0.20
0.24
0.28
BURN TIME (SEC.)
*10⁻¹

Fig. 13 c.

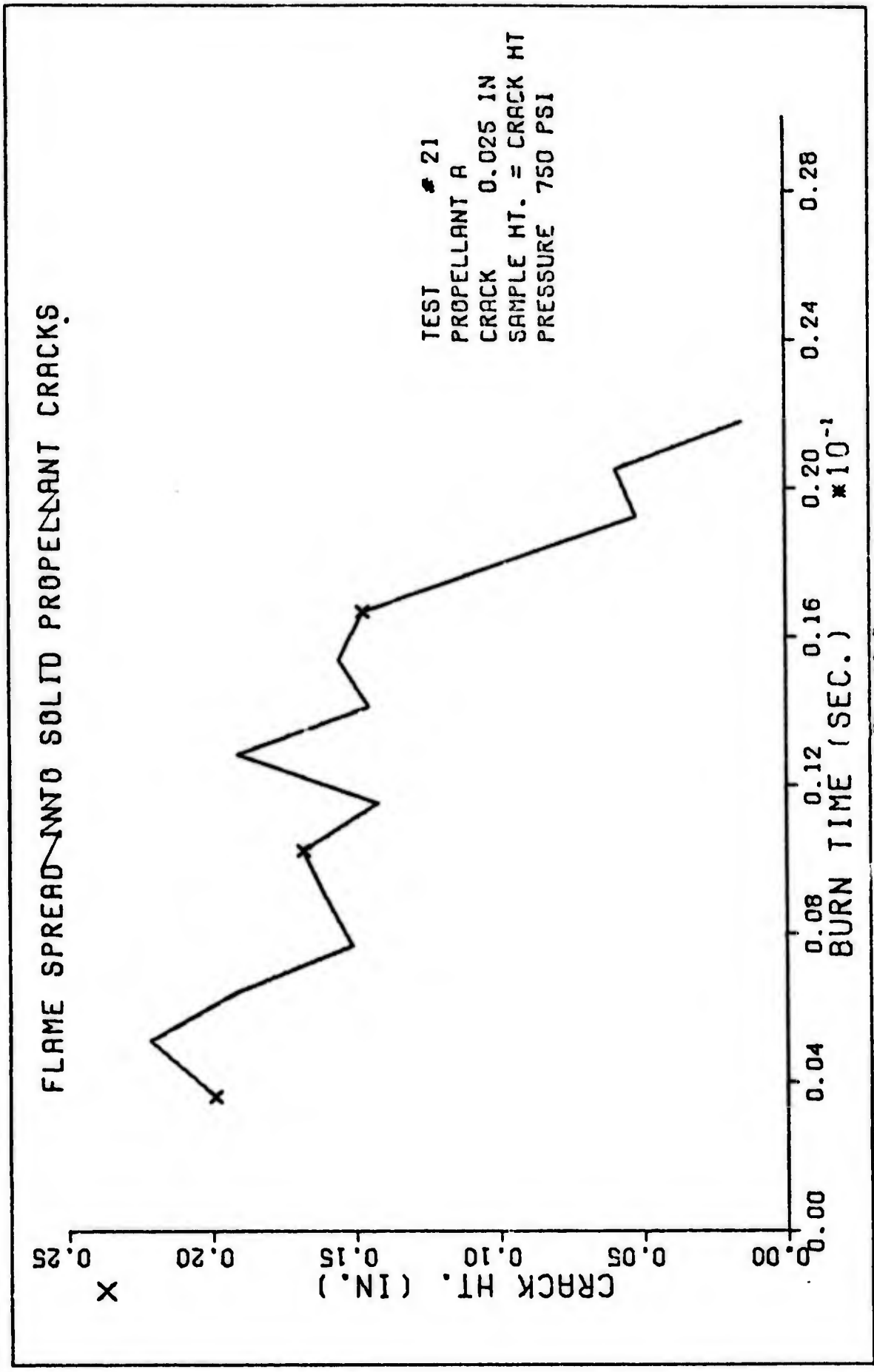
FLAME SPREAD INTO SOLID PROPELLANT CRACKS
TEST # 21
PROPELLANT A
CRACK 0.025 IN
SAMPLE HT. = CRACK HT
PRESSURE 750 PSI
CRACK HT. (IN.)
0.00
0.05
0.10
0.15
0.20
0.25
X
0.00
0.04
0.08
0.12
0.16
0.20
0.24
0.28
BURN TIME (SEC.)
*10⁻¹

Fig. 13 b.

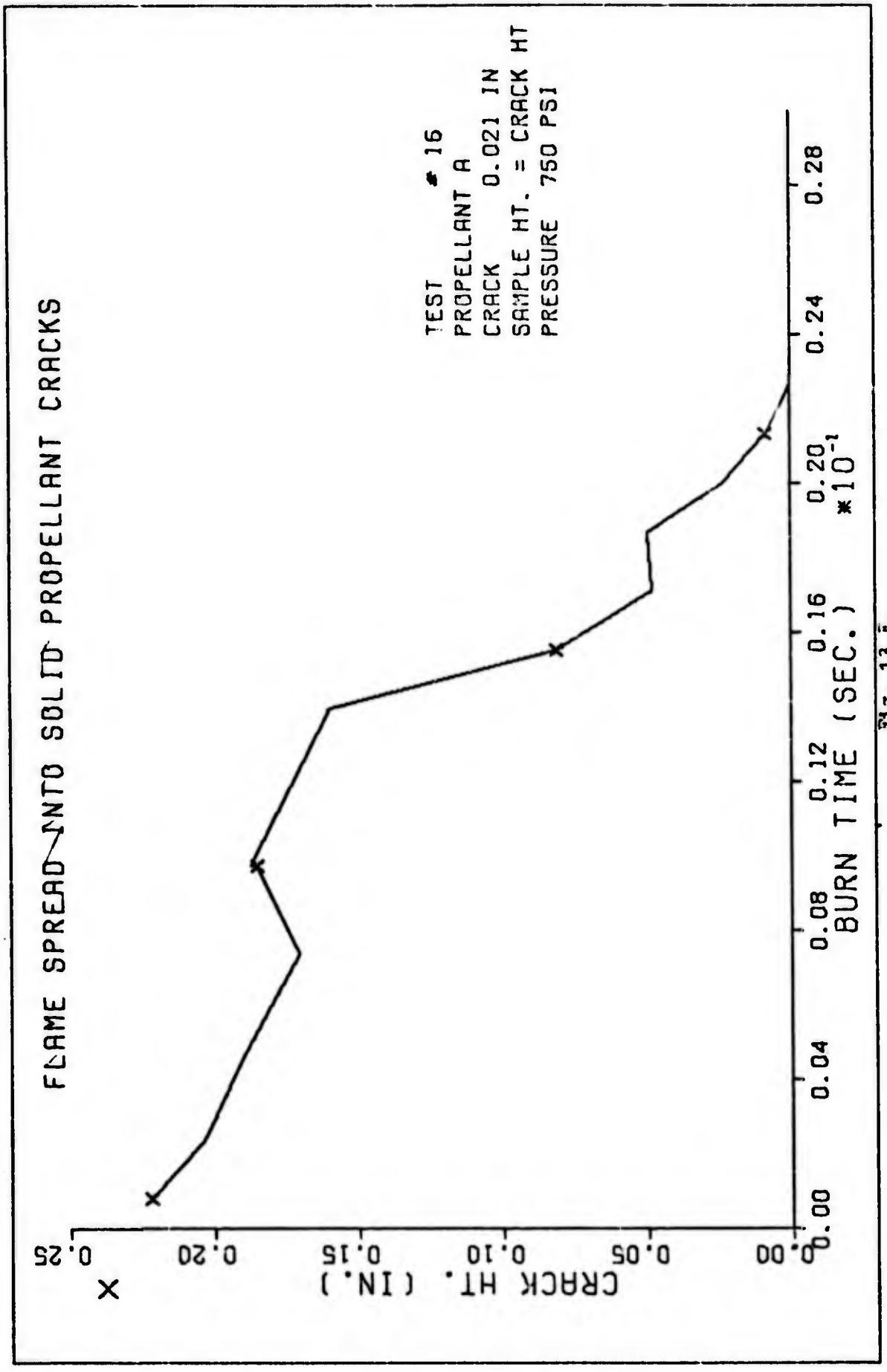
FLAME SPREAD INTO SOLID PROPELLANT CRACKS
TEST # 16
PROPELLANT A
CRACK 0.021 IN
SAMPLE HT. = CRACK HT
PRESSURE 750 PSI
CRACK HT. (IN.)
0.00
0.05
0.10
0.15
0.20
0.25
X
0.00
0.04
0.08
0.12
0.16
0.20
0.24
0.28
BURN TIME (SEC.)
*10⁻¹

Fig. 13 E.

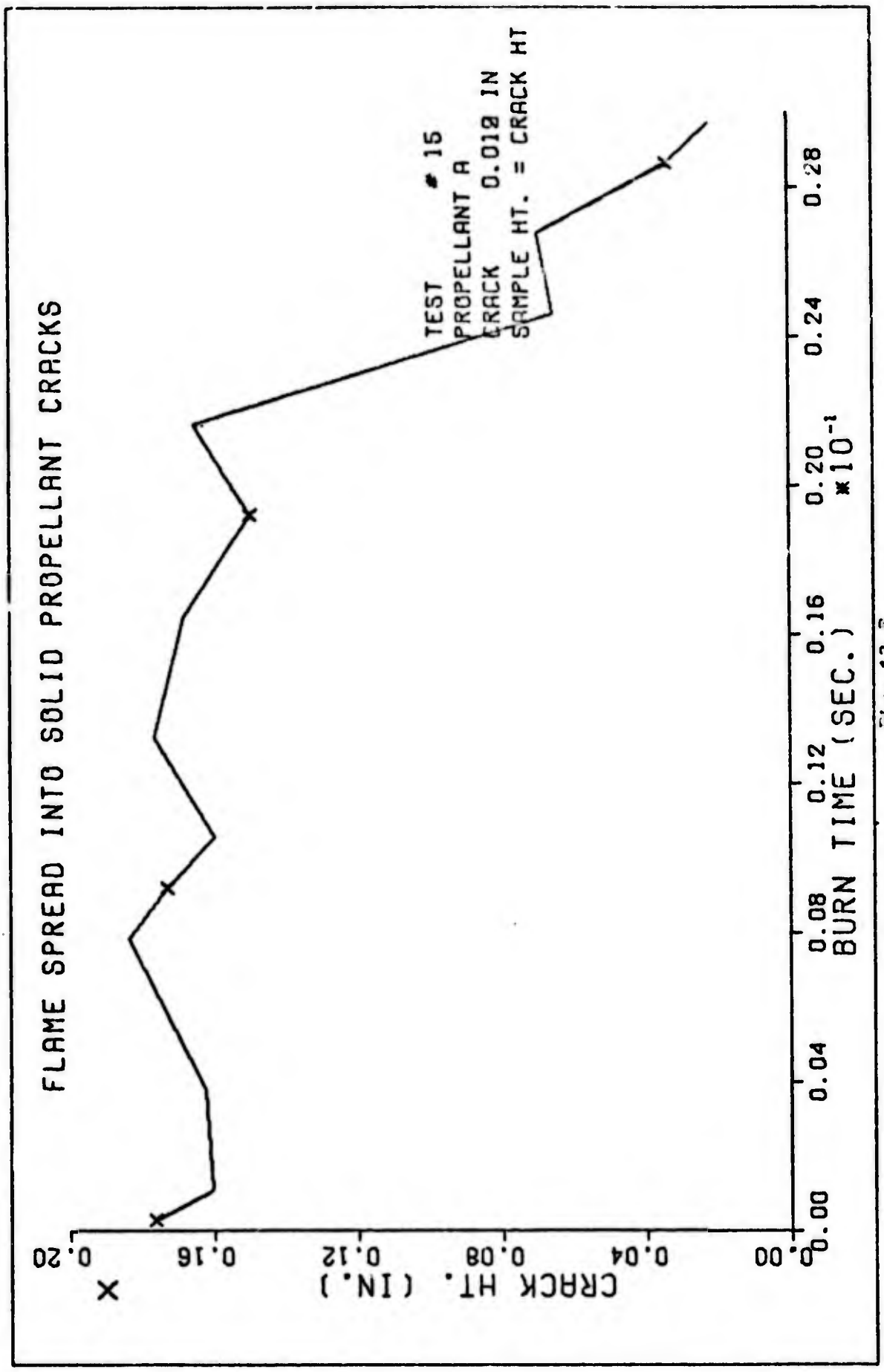
FLAME SPREAD INTO SOLID PROPELLANT CRACKS
TEST # 15
PROPELLANT A
CRACK 0.012 IN
SAMPLE HT. = CRACK HT
CRACK HT. (IN.)
0.00
0.04
0.08
0.12
0.16
0.20
0.24
0.28
BURN TIME (SEC.)
*10⁻¹

Fig. 13 F.

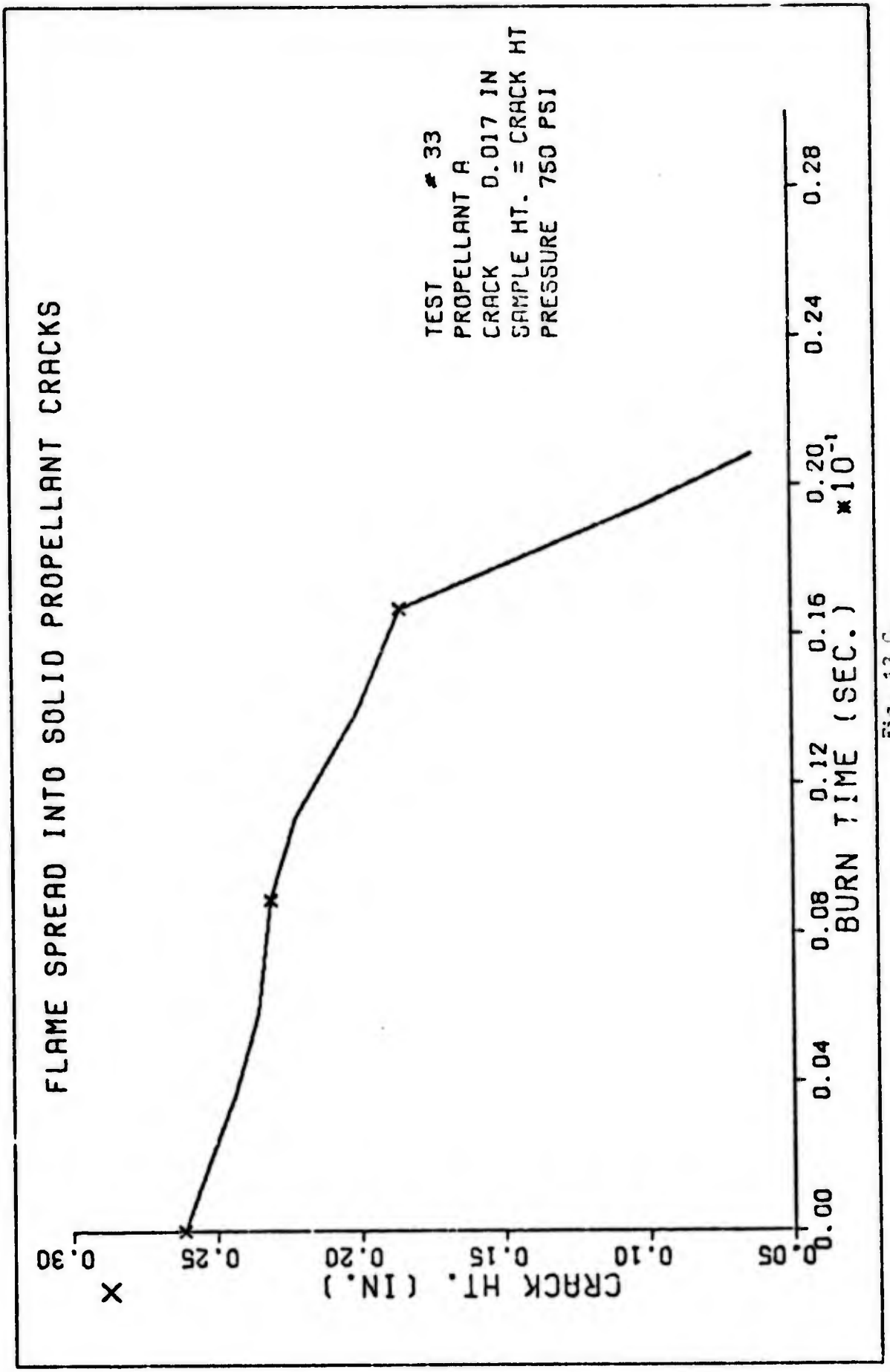
FLAME SPREAD INTO SOLID PROPELLANT CRACKS
TEST # 33
PROPELLANT A
CRACK 0.017 IN
SAMPLE HT. = CRACK HT
PRESSURE 750 PSI
CRACK HT. (IN.)
0.00
0.05
0.10
0.15
0.20
0.25
0.30
BURN TIME (SEC.)
0.00
0.04
0.08
0.12
0.16
0.20
0.24
0.28
*10⁻¹

Fig. 13 c.

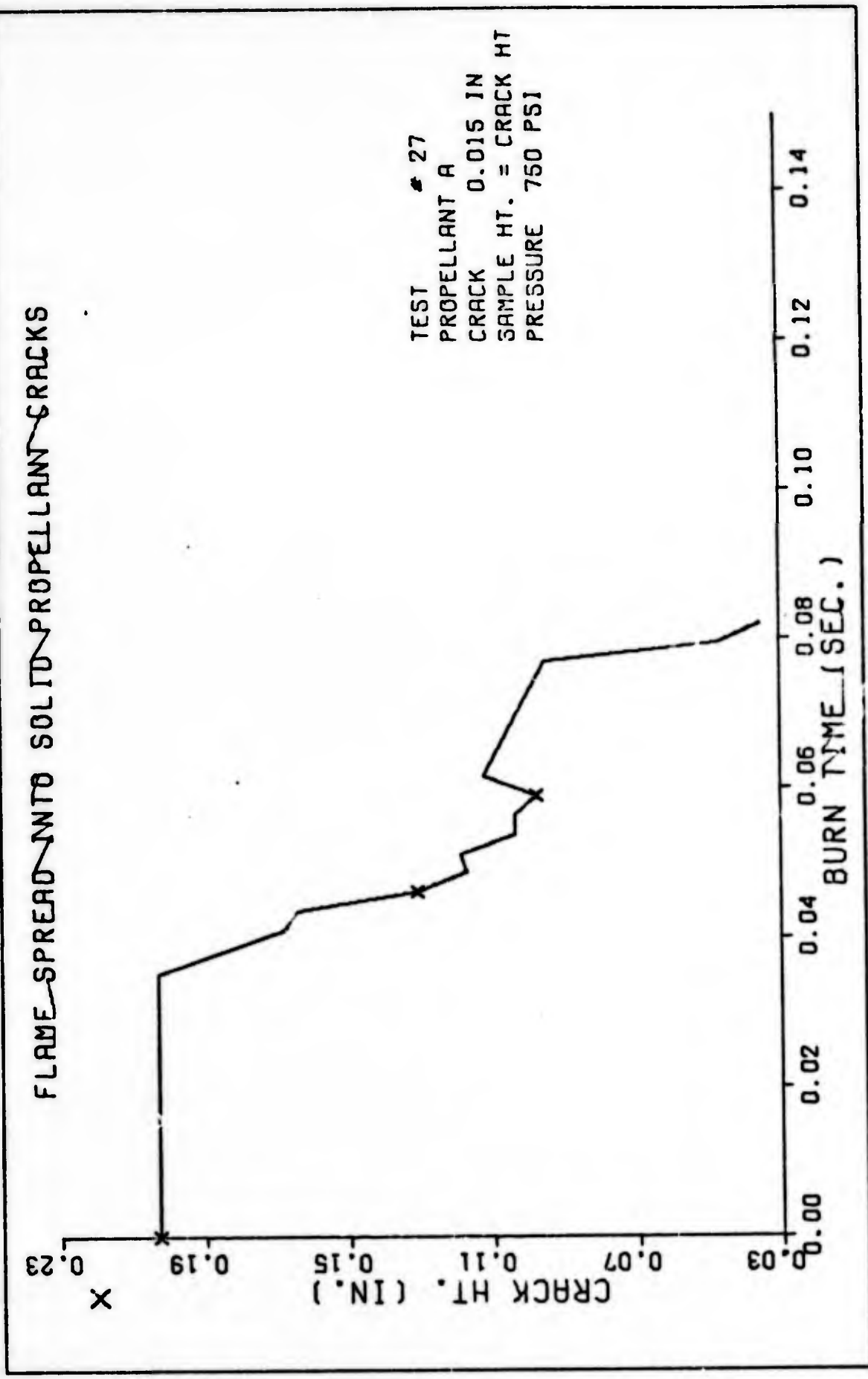
FLAME SPREAD INTO SOLID PROPELLANT CRACKS
TEST # 27
PROPELLANT A
CRACK 0.015 IN
SAMPLE HT. = CRACK HT
PRESSURE 750 PSI
CRACK HT. (IN.)
BURN TIME (SEC.)
0.00
0.02
0.04
0.06
0.08
0.10
0.12
0.14
0.03
0.07
0.11
0.15
0.19
0.23
X

Fig. 13 H.

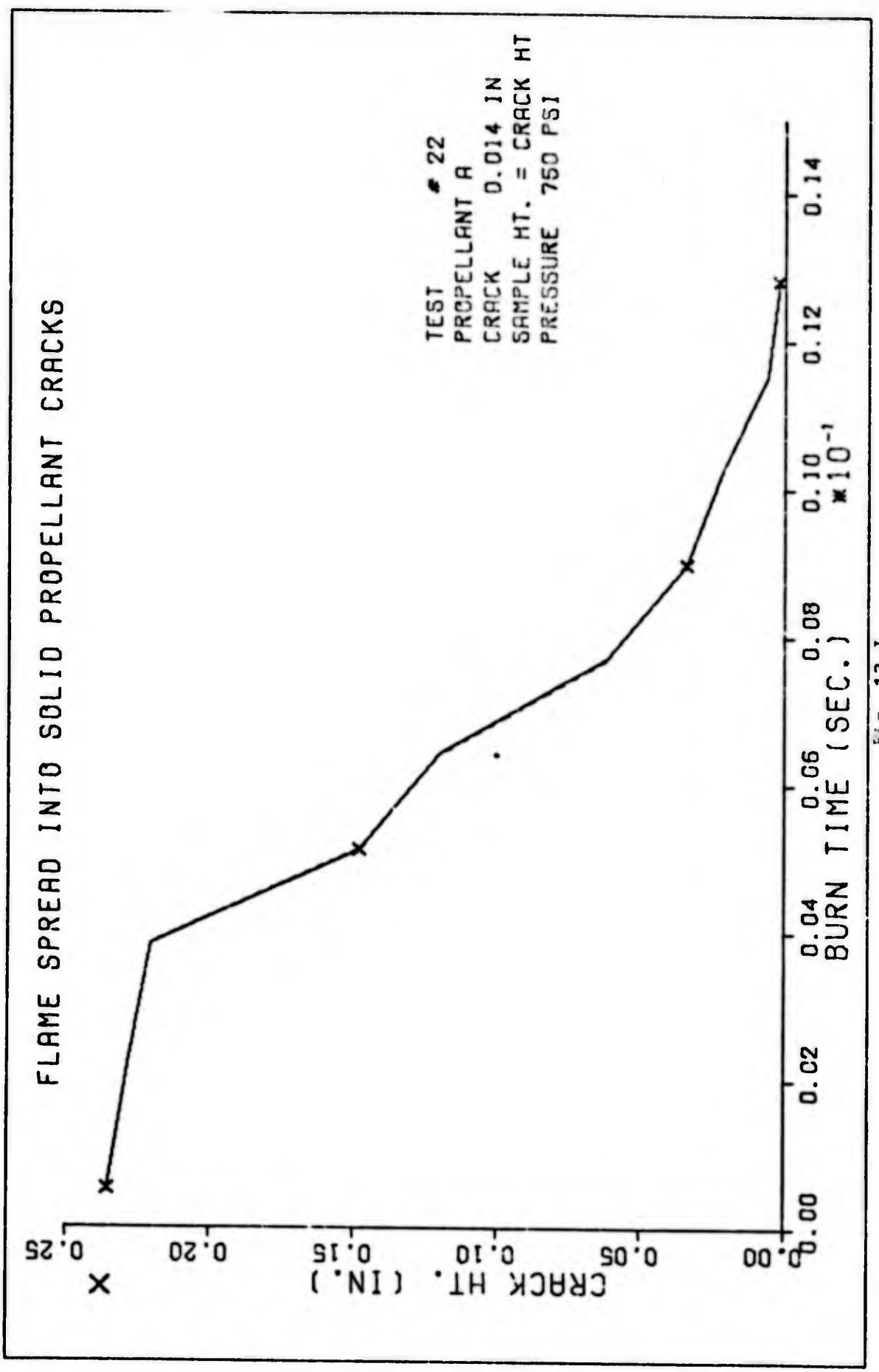
FLAME SPREAD INTO SOLID PROPELLANT CRACKS
TEST # 22
PROPELLANT A
CRACK 0.014 IN
SAMPLE HT. = CRACK HT
PRESSURE 750 PSI
CRACK HT. (IN.)
0.00
0.05
0.10
0.15
0.20
0.25
BURN TIME (SEC.)
0.00
0.02
0.04
0.06
0.08
0.10
0.12
0.14
*10⁻¹

Fig. 13 I.

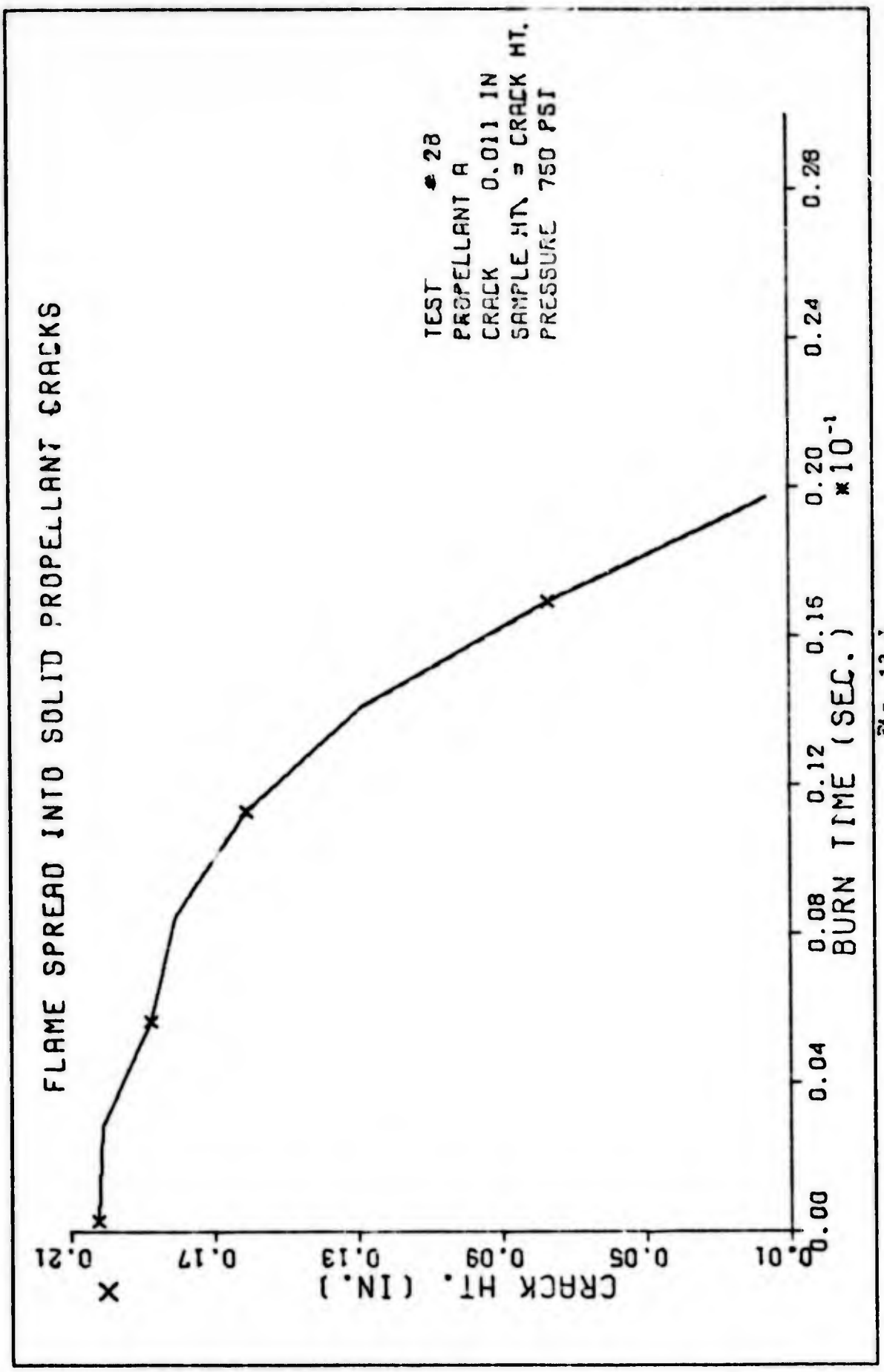
FLAME SPREAD INTO SOLID PROPELLANT CRACKS
TEST # 28
PROPELLANT A
CRACK 0.011 IN
SAMPLE HT = CRACK HT.
PRESSURE 750 PSI
CRACK HT. (IN.)
0.01
0.05
0.09
0.13
0.17
0.21
0.00
0.04
0.08
0.12
0.15
0.20
0.24
0.28
BURN TIME (SEC.)
*10⁻¹

Fig. 13 J.

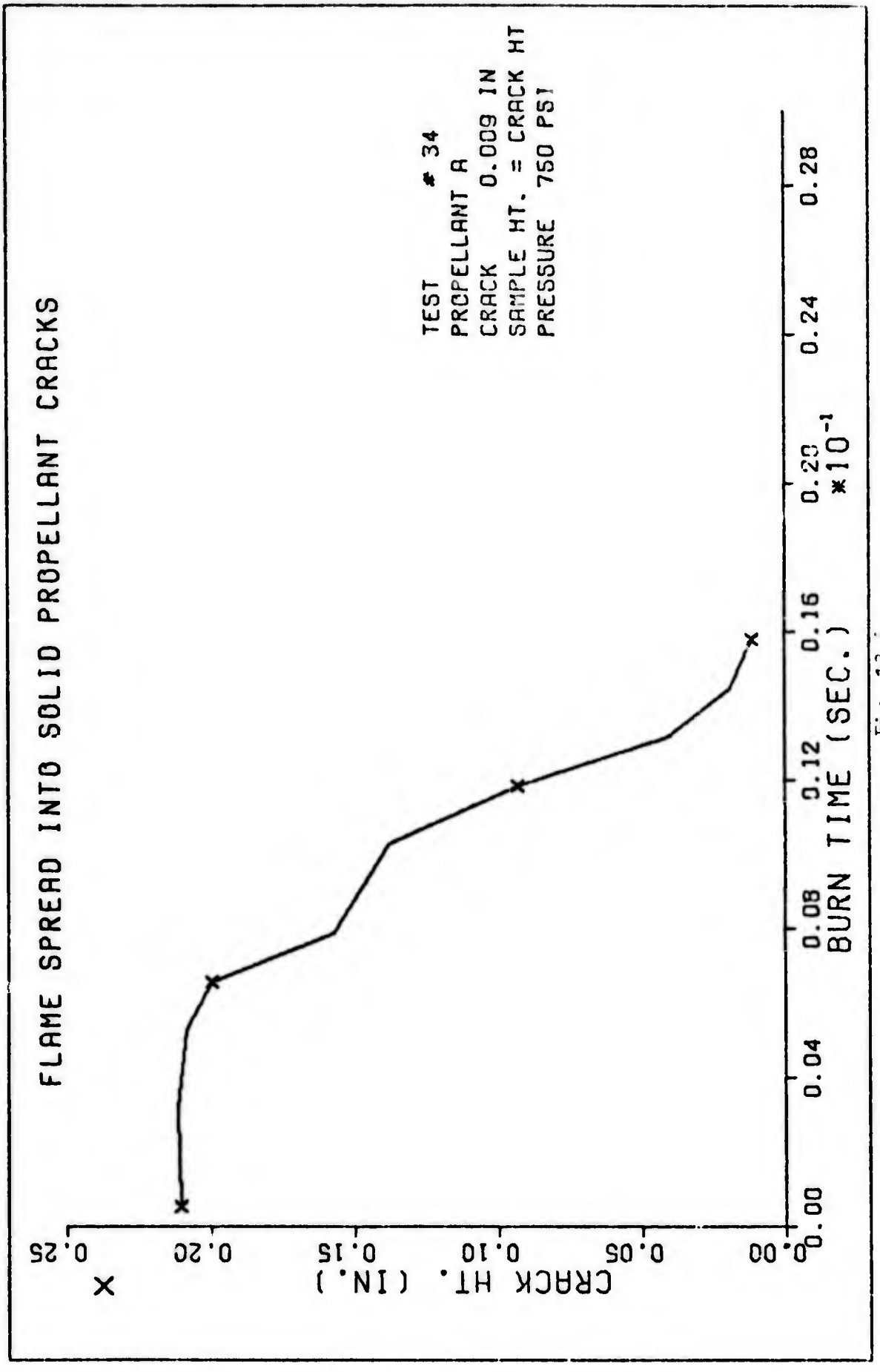
FLAME SPREAD INTO SOLID PROPELLANT CRACKS
TEST # 34
PROPELLANT A
CRACK 0.009 IN
SAMPLE HT. = CRACK HT
PRESSURE 750 PSI
CRACK HT. (IN.)
0.00
0.05
0.10
0.15
0.20
0.25
BURN TIME (SEC.)
0.00
0.04
0.08
0.12
0.16
0.20
0.24
0.28
*10⁻¹

Fig. 13 L.

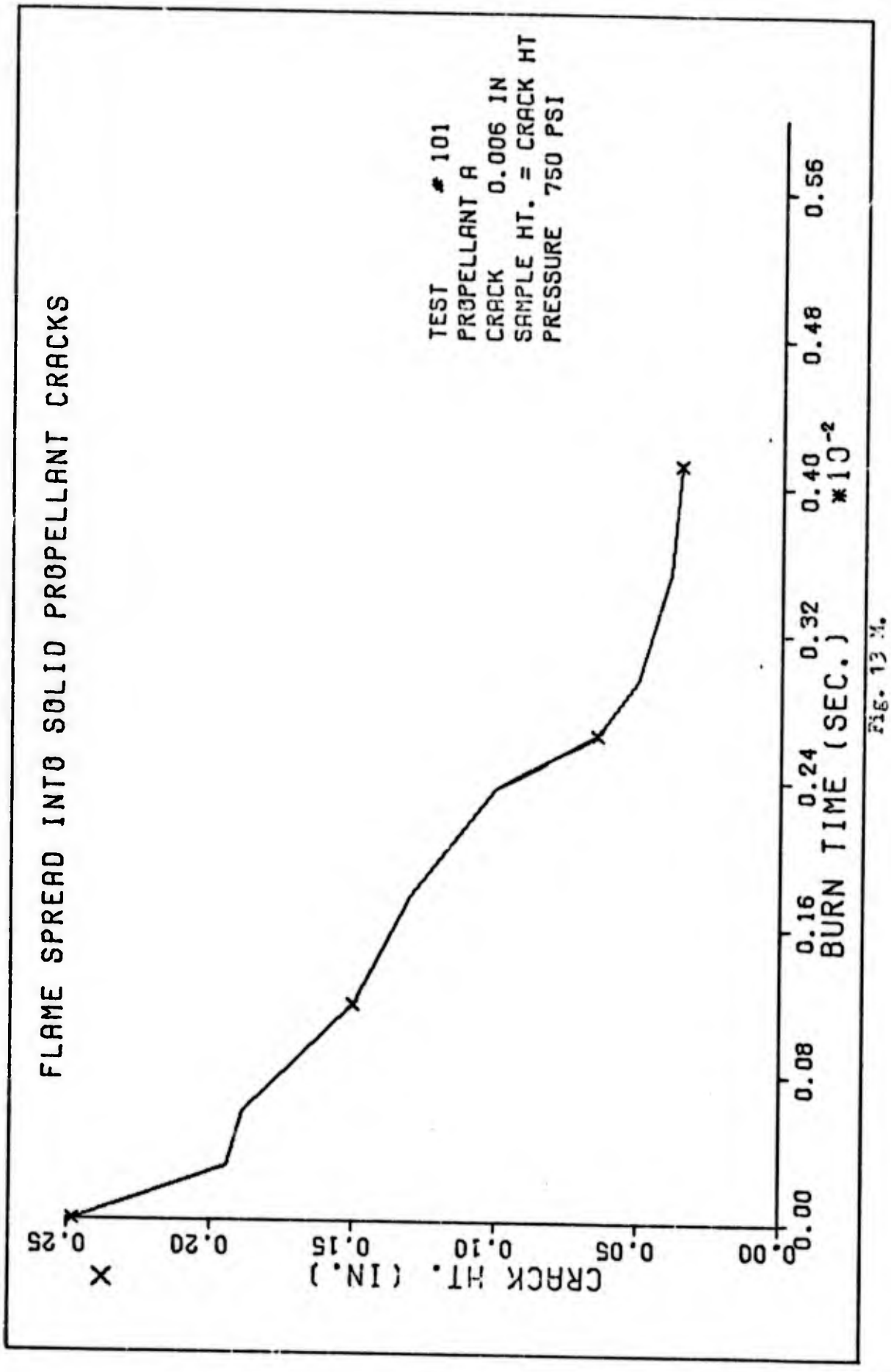
FLAME SPREAD INTO SOLID PROPELLANT CRACKS
TEST # 101
PROPELLANT A
CRACK 0.006 IN
SAMPLE HT. = CRACK HT
PRESSURE 750 PSI
CRACK HT. (IN.)
0.00
0.05
0.10
0.15
0.20
0.25
BURN TIME (SEC.)
0.00
0.08
0.16
0.24
0.32
0.40
0.48
0.56
*10^-2

Fig. 13 a.

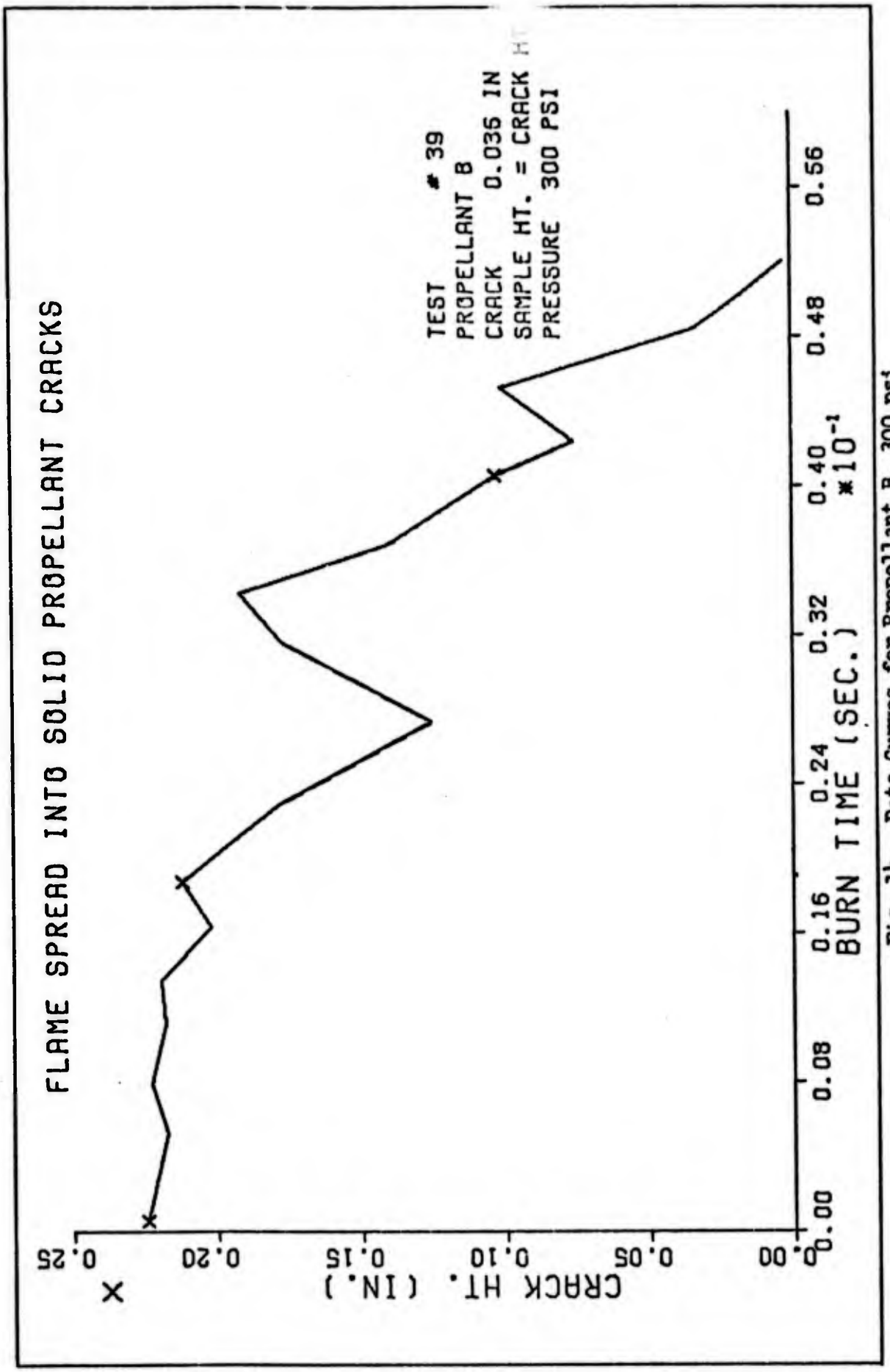

Fig. 14. Data Curves for Propellant B, 300 psi

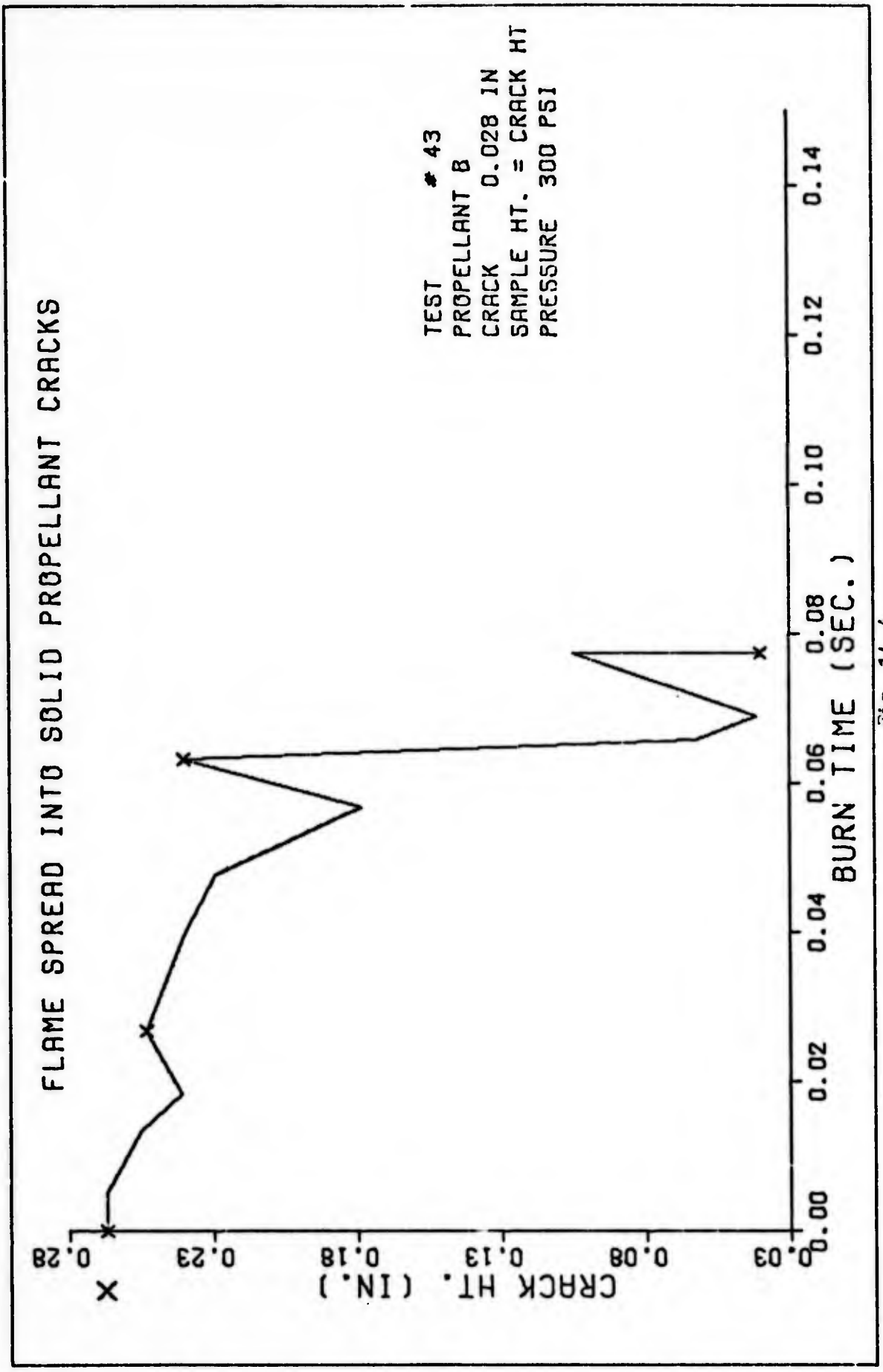
FLAME SPREAD INTO SOLID PROPELLANT CRACKS
TEST # 43
PROPELLANT B
CRACK 0.028 IN
SAMPLE HT. = CRACK HT
PRESSURE 300 PSI
CRACK HT. (IN.)
0.03
0.08
0.13
0.18
0.23
0.28
BURN TIME (SEC.)
0.00
0.02
0.04
0.06
0.08
0.10
0.12
0.14

Fig. 14 A.

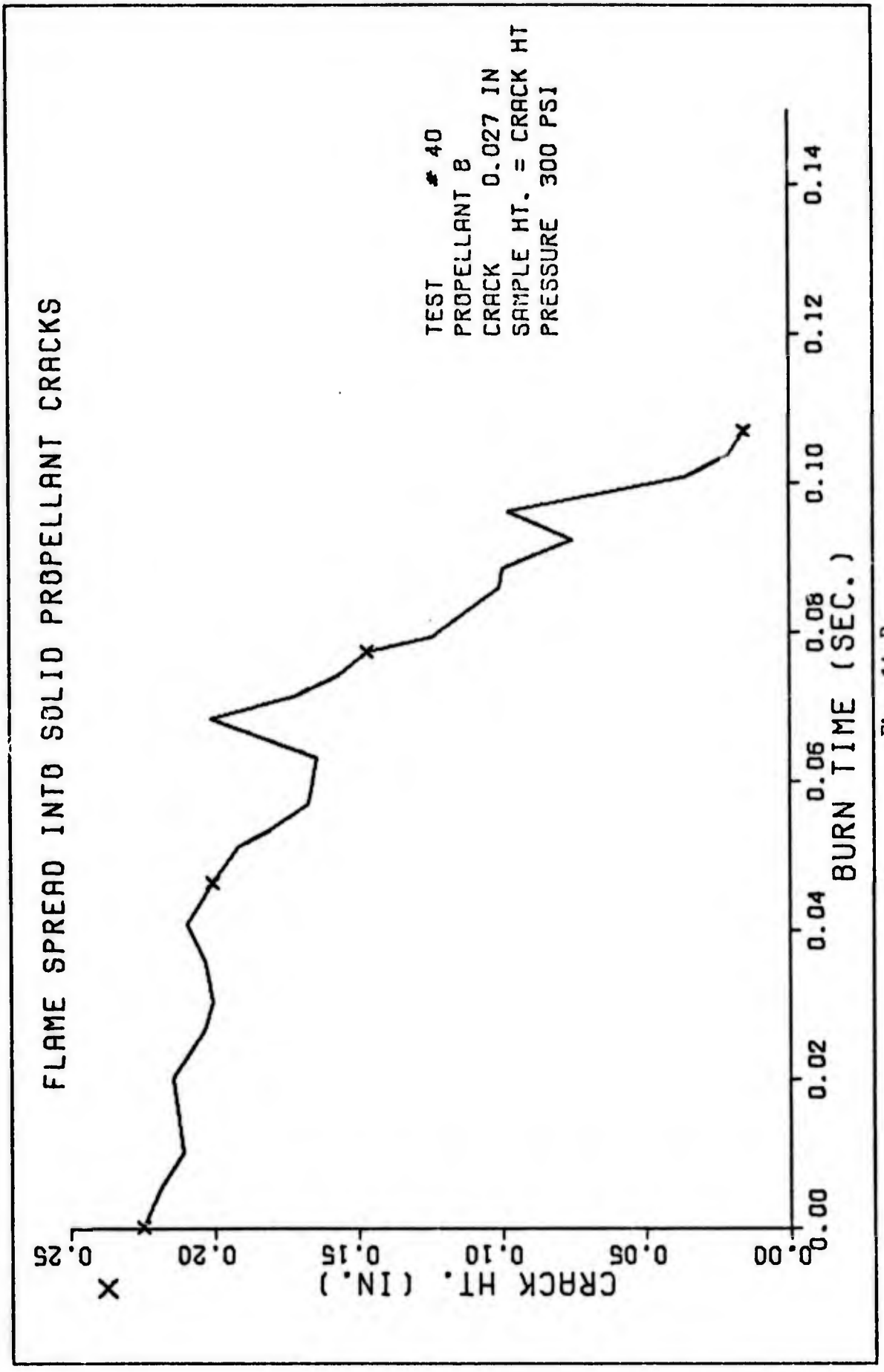
FLAME SPREAD INTO SOLID PROPELLANT CRACKS
TEST # 40
PROPELLANT B
CRACK 0.027 IN
SAMPLE HT. = CRACK HT
PRESSURE 300 PSI
CRACK HT. (IN.)
0.00
0.05
0.10
0.15
0.20
0.25
BURN TIME (SEC.)
0.00
0.02
0.04
0.06
0.08
0.10
0.12
0.14

Fig. 14 B.

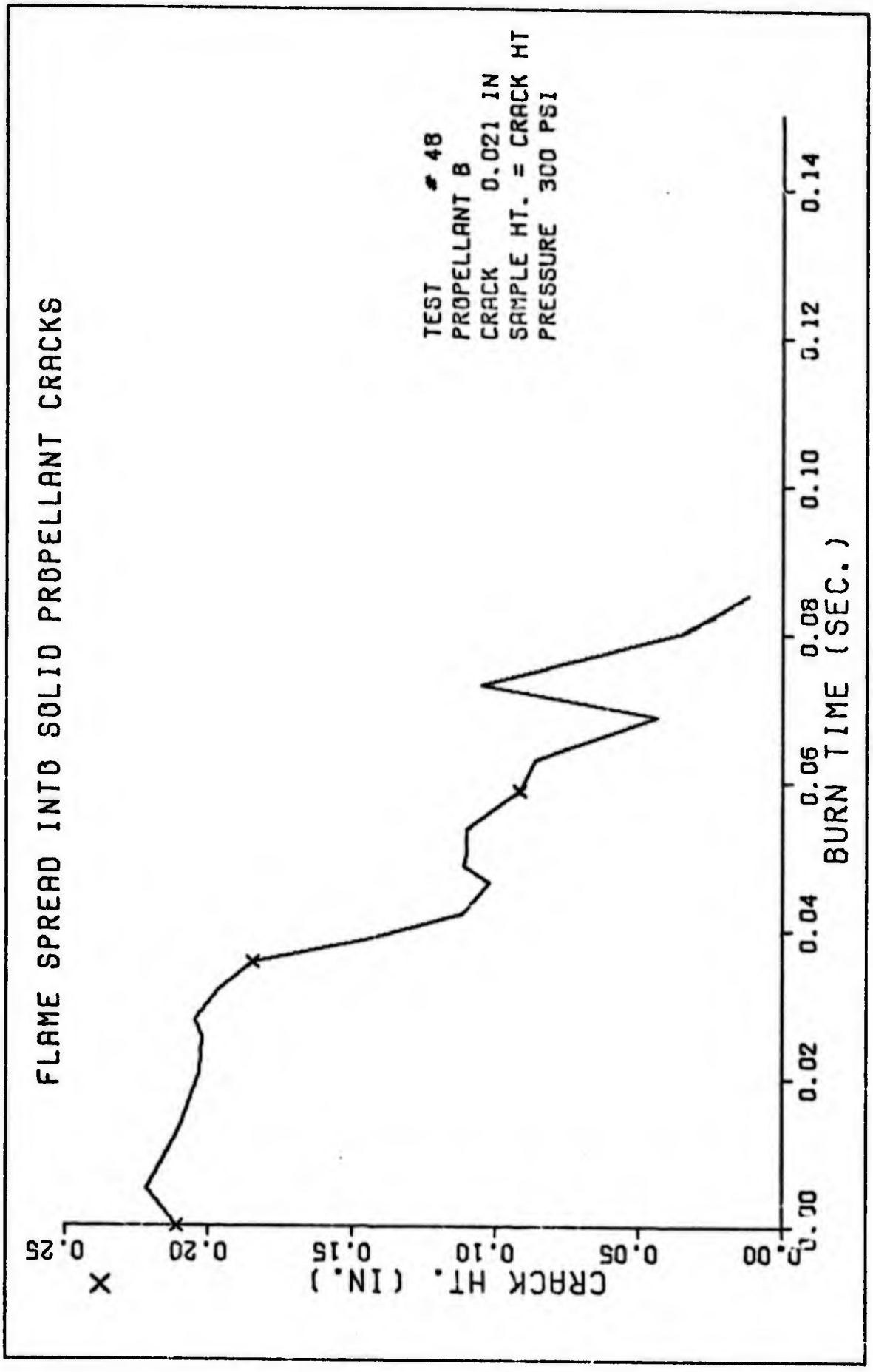
FLAME SPREAD INTO SOLID PROPELLANT CRACKS
TEST # 48
PROPELLANT B
CRACK 0.021 IN
SAMPLE HT. = CRACK HT
PRESSURE 300 PSI
CRACK HT. (IN.)
0.00
0.05
0.10
0.15
0.20
0.25
BURN TIME (SEC.)
0.00
0.02
0.04
0.06
0.08
0.10
0.12
0.14

Fig. 14 c.

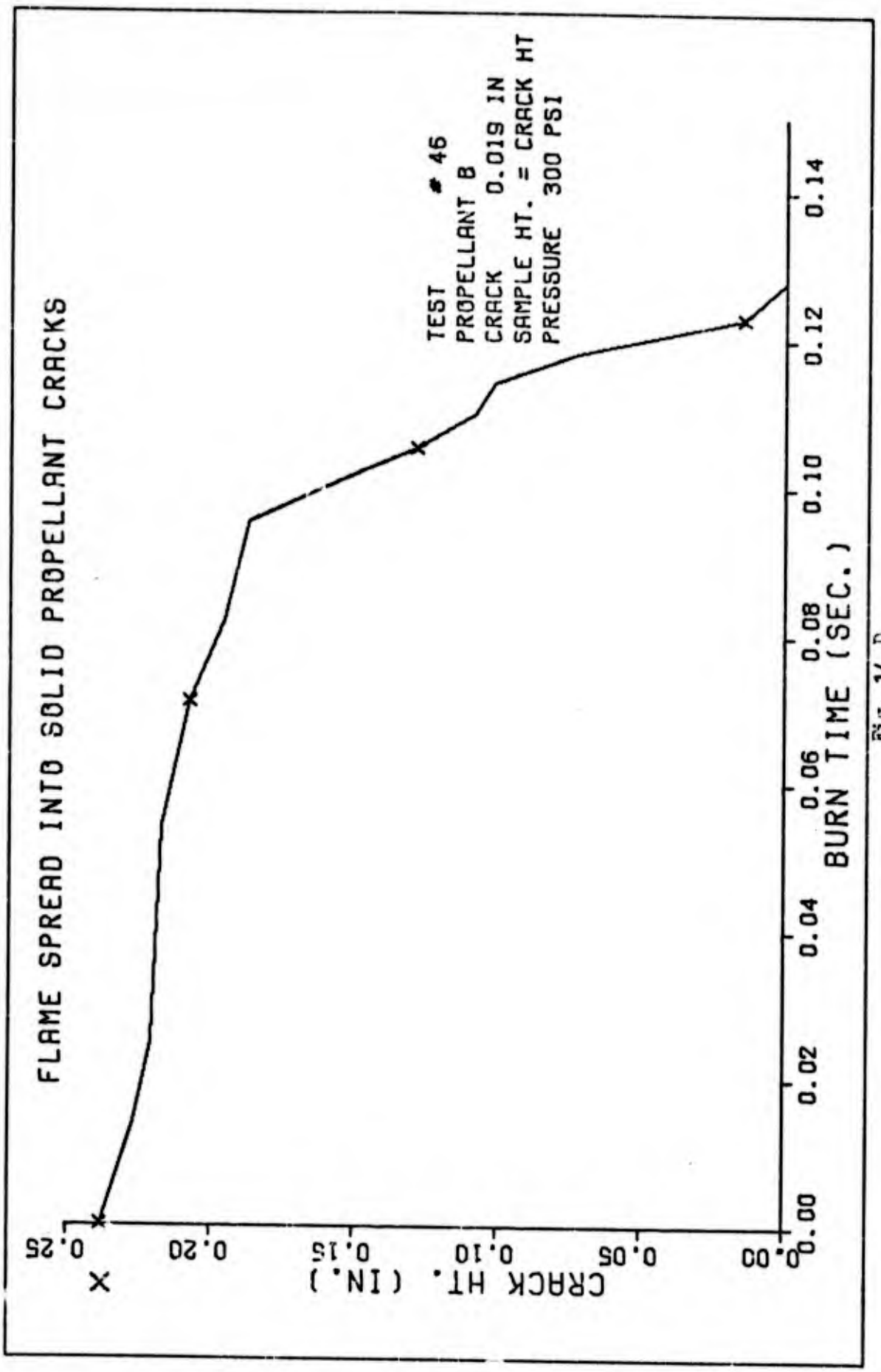
FLAME SPREAD INTO SOLID PROPELLANT CRACKS
TEST # 46
PROPELLANT B
CRACK 0.019 IN
SAMPLE HT. = CRACK HT
PRESSURE 300 PSI
CRACK HT. (IN.)
0.00
0.05
0.10
0.15
0.20
0.25
X
BURN TIME (SEC.)
0.00
0.02
0.04
0.06
0.08
0.10
0.12
0.14

Fig. 14 D.

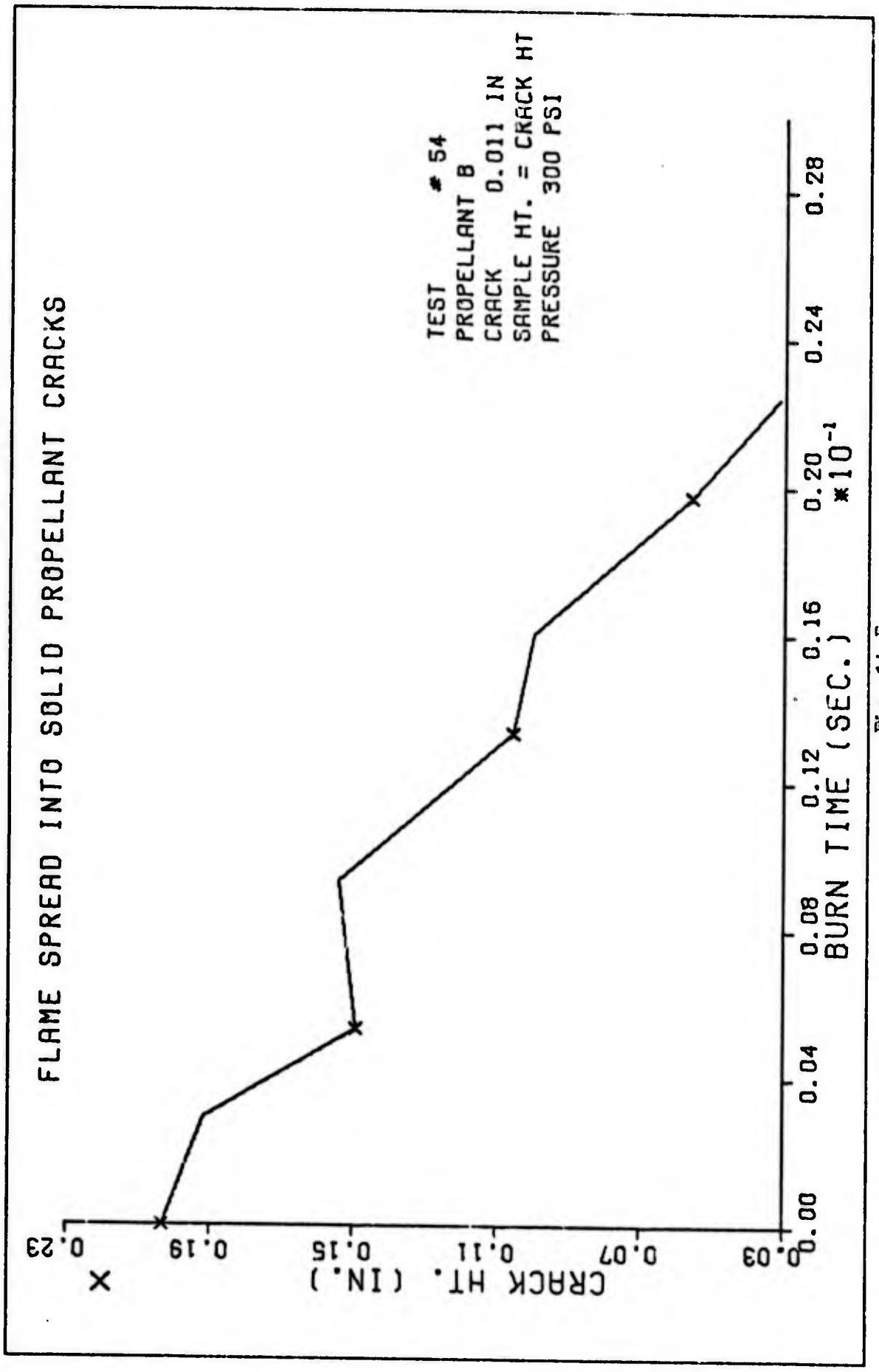
FLAME SPREAD INTO SOLID PROPELLANT CRACKS
TEST # 54
PROPELLANT B
CRACK 0.011 IN
SAMPLE HT. = CRACK HT
PRESSURE 300 PSI
CRACK HT. (IN.)
0.03
0.07
0.11
0.15
0.19
0.23
X
0.00
0.04
0.08
0.12
0.16
0.20
0.24
0.28
BURN TIME (SEC.)
*10⁻¹

Fig. 14 E.

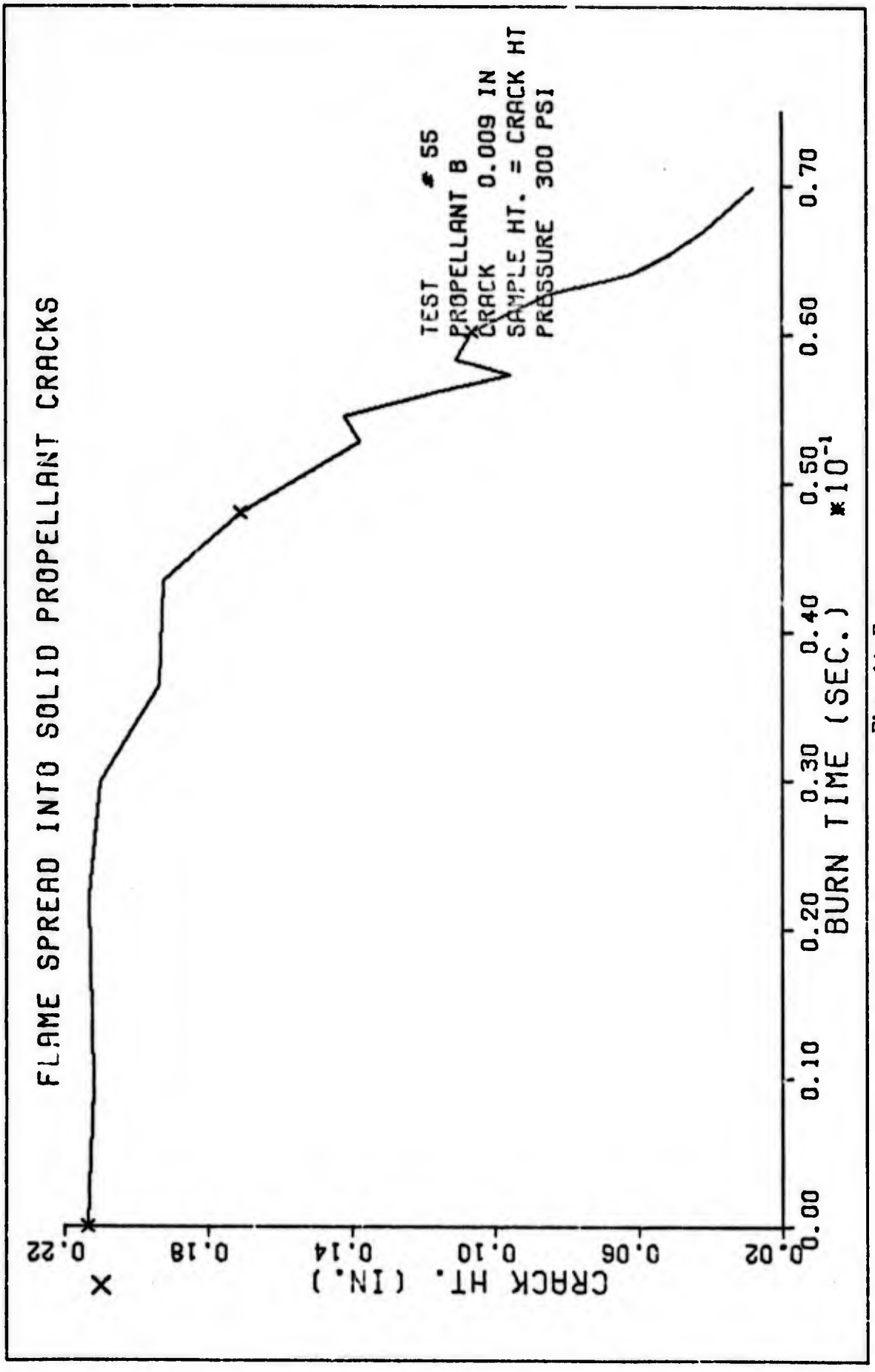
FLAME SPREAD INTO SOLID PROPELLANT CRACKS
TEST # 55
PROPELLANT B
CRACK 0.009 IN
SAMPLE HT. = CRACK HT
PRESSURE 300 PSI
CRACK HT. (IN.)
0.00
0.02
0.06
0.10
0.14
0.18
0.22
X
0.00
0.10
0.20
0.30
0.40
0.50
0.60
0.70
BURN TIME (SEC.)
*10^-1

Fig. 14 F.

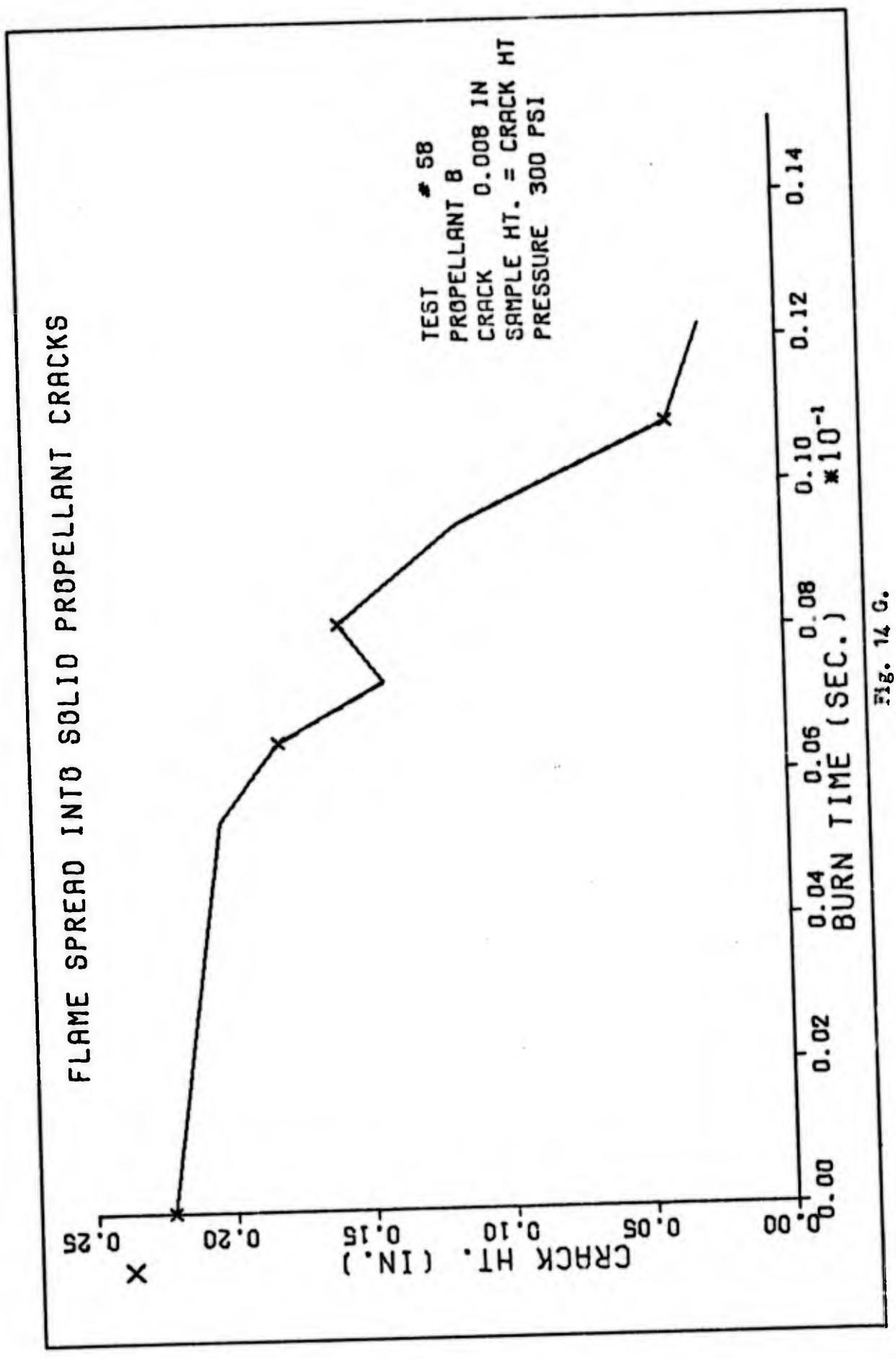
FLAME SPREAD INTO SOLID PROPELLANT CRACKS
TEST # 58
PROPELLANT B
CRACK 0.008 IN
SAMPLE HT. = CRACK HT
PRESSURE 300 PSI
CRACK HT. (IN.)
0.00
0.05
0.10
0.15
0.20
0.25
X
0.00
0.02
0.04
0.06
0.08
0.10
0.12
0.14
BURN TIME (SEC.)
*10^-1

Fig. 14 c.

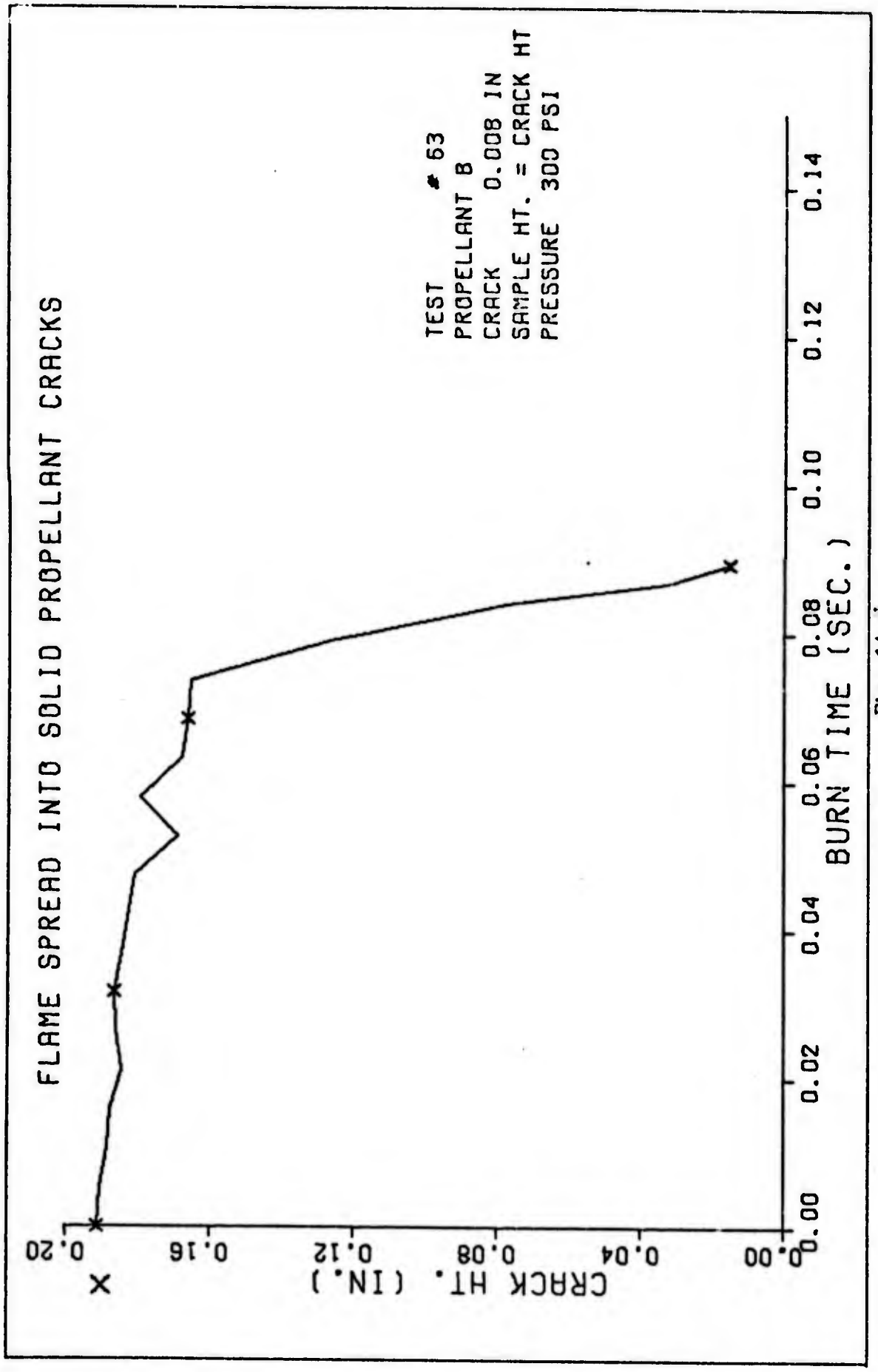
FLAME SPREAD INTO SOLID PROPELLANT CRACKS
TEST # 63
PROPELLANT B
CRACK 0.008 IN
SAMPLE HT. = CRACK HT
PRESSURE 300 PSI
CRACK HT. (IN.)
0.00
0.04
0.08
0.12
0.16
0.20
BURN TIME (SEC.)
0.00
0.02
0.04
0.06
0.08
0.10
0.12
0.14

Fig. 14 f.

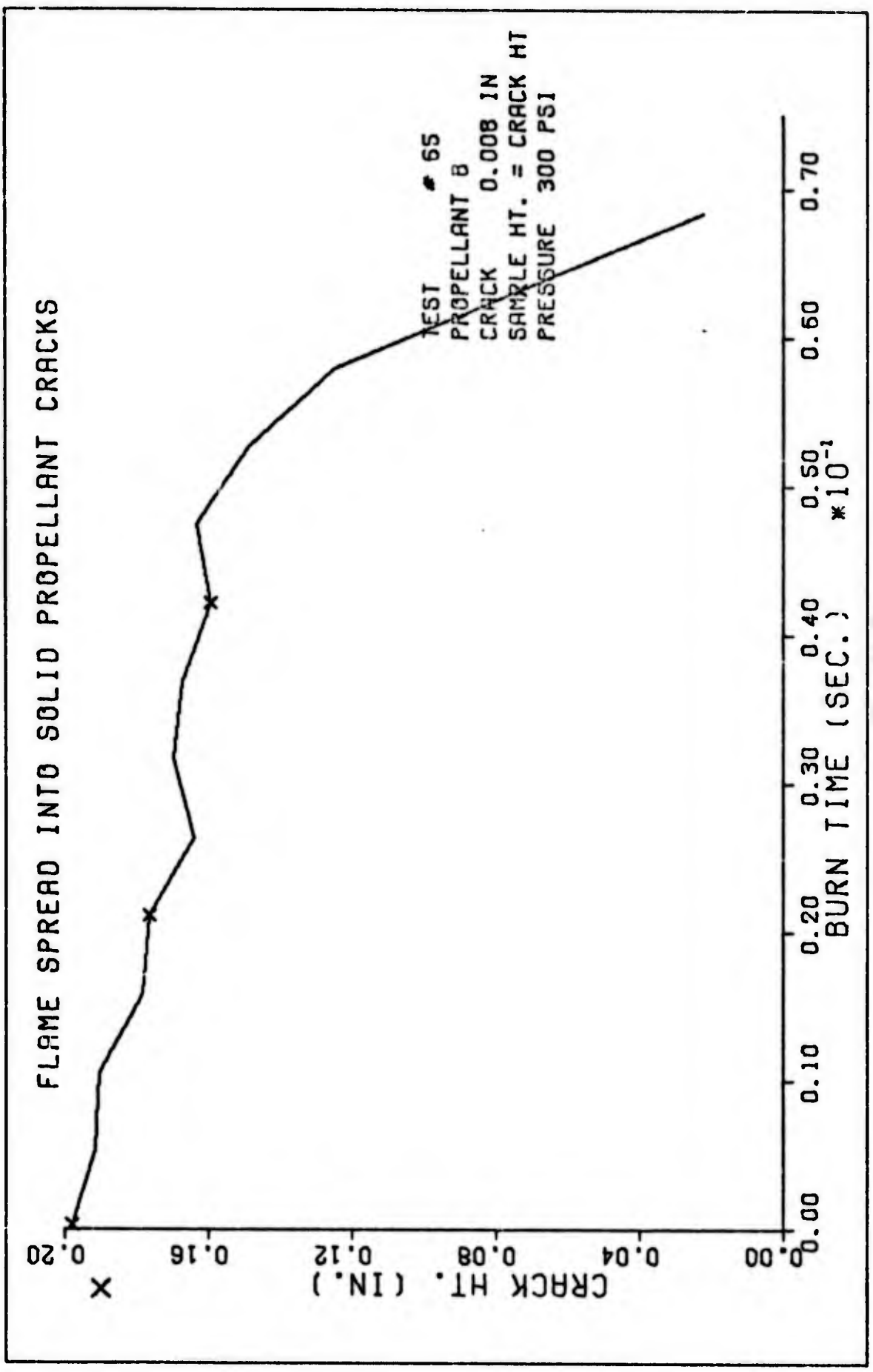
FLAME SPREAD INTO SOLID PROPELLANT CRACKS
TEST # 65
PROPELLANT B
CRACK 0.008 IN
SAMPLE HT. = CRACK HT
PRESSURE 300 PSI
CRACK HT. (IN.)
0.00
0.04
0.08
0.12
0.16
0.20
BURN TIME (SEC.)
0.00
0.10
0.20
0.30
0.40
0.50
0.60
0.70
*10⁻¹

Fig. 14 I.

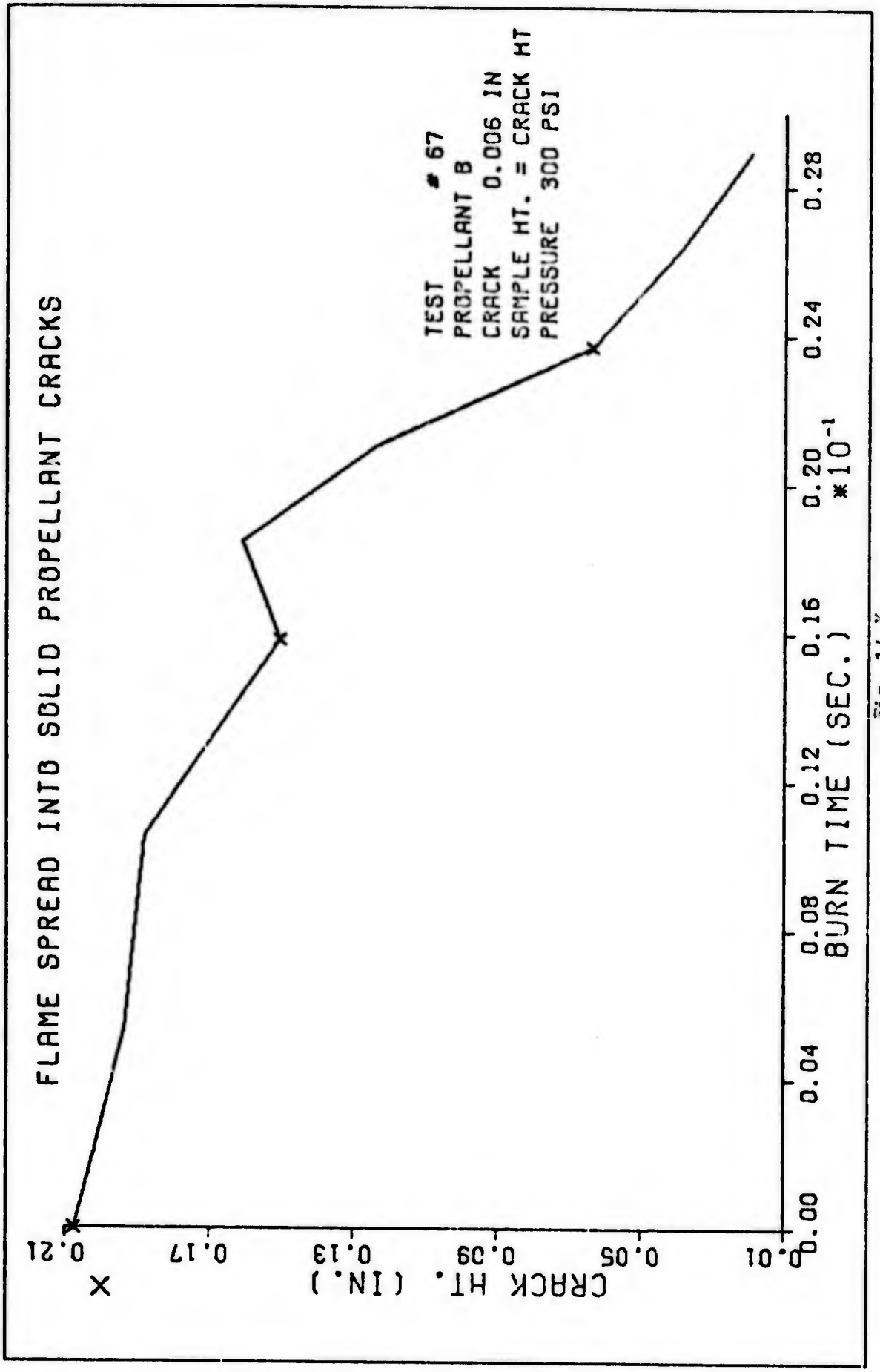
FLAME SPREAD INTO SOLID PROPELLANT CRACKS
TEST # 67
PROPELLANT B
CRACK 0.006 IN
SAMPLE HT. = CRACK HT
PRESSURE 300 PSI
CRACK HT. (IN.)
0.01
0.05
0.09
0.13
0.17
0.21
X
0.00
0.04
0.08
0.12
0.16
0.20
0.24
0.28
BURN TIME (SEC.)
*10⁻¹

Fig. 14 X.

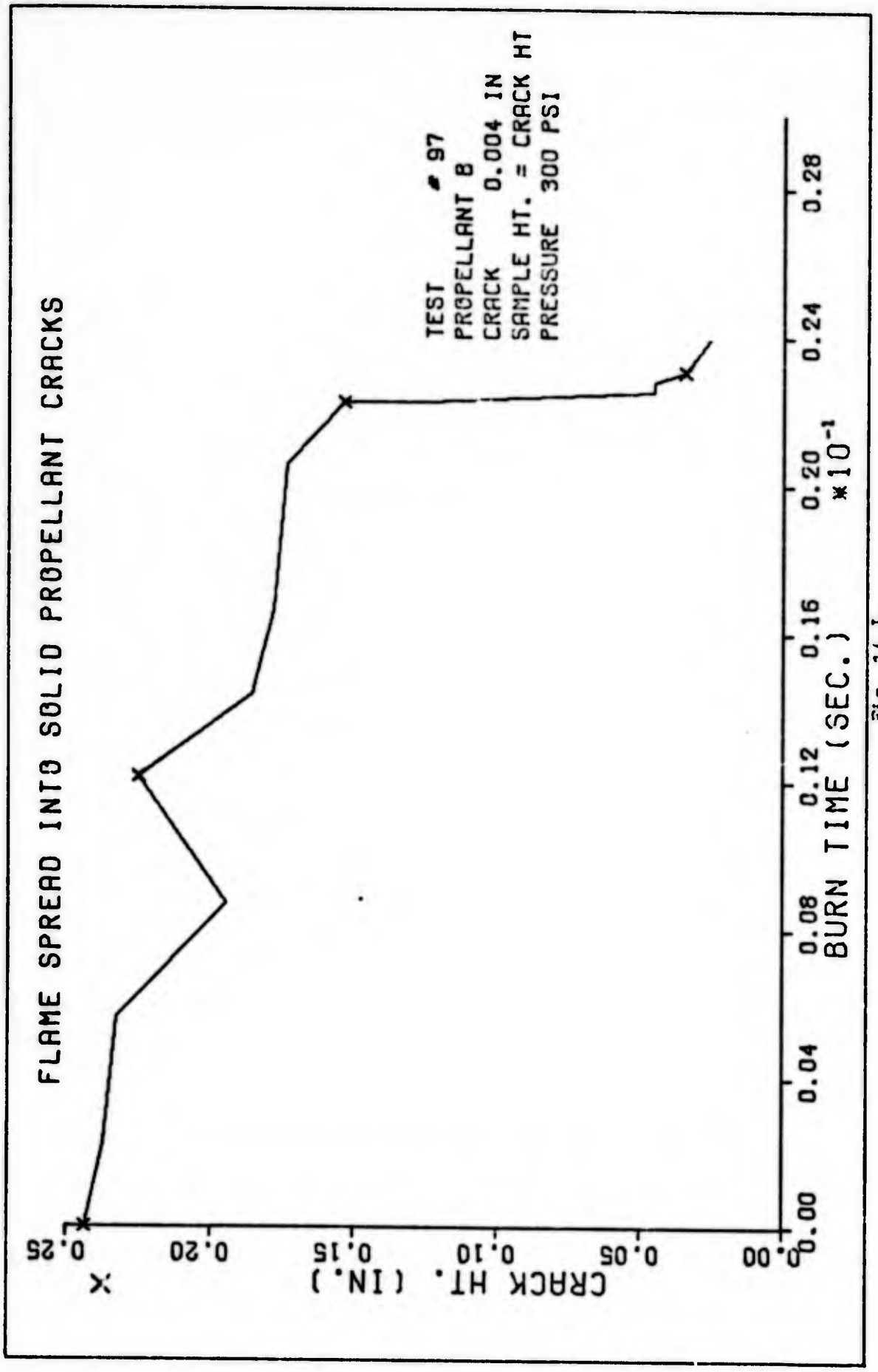
FLAME SPREAD INTO SOLID PROPELLANT CRACKS
TEST # 97
PROPELLANT B
CRACK 0.004 IN
SAMPLE HT. = CRACK HT
PRESSURE 300 PSI
CRACK HT. (IN.)
0.00
0.05
0.10
0.15
0.20
0.25
X
0.00
0.04
0.08
0.12
0.16
0.20
0.24
0.28
BURN TIME (SEC.)
*10⁻¹

Fig. 14 L.

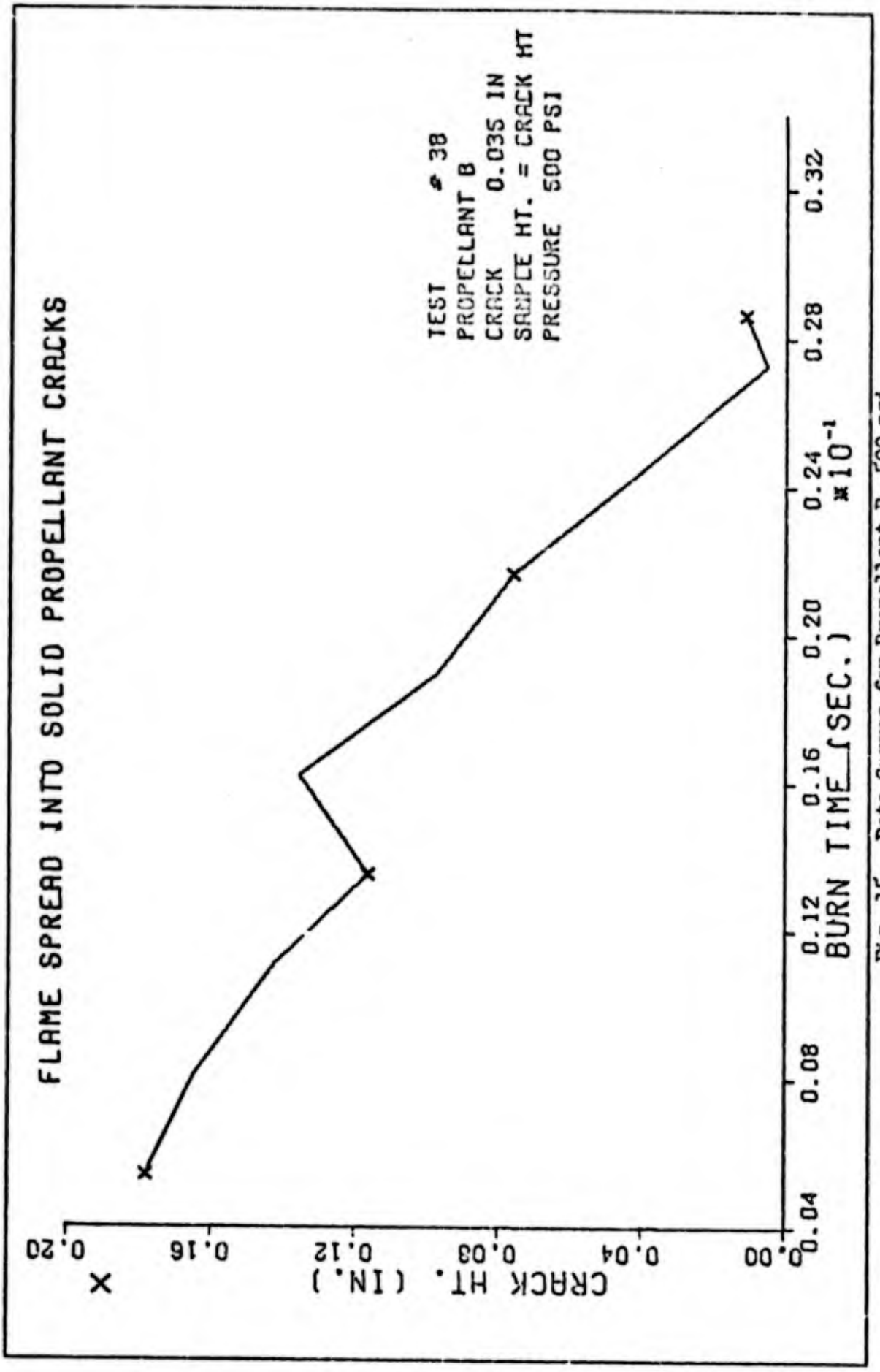

Fig. 15. Data Curves for Propellant B, 500 psi

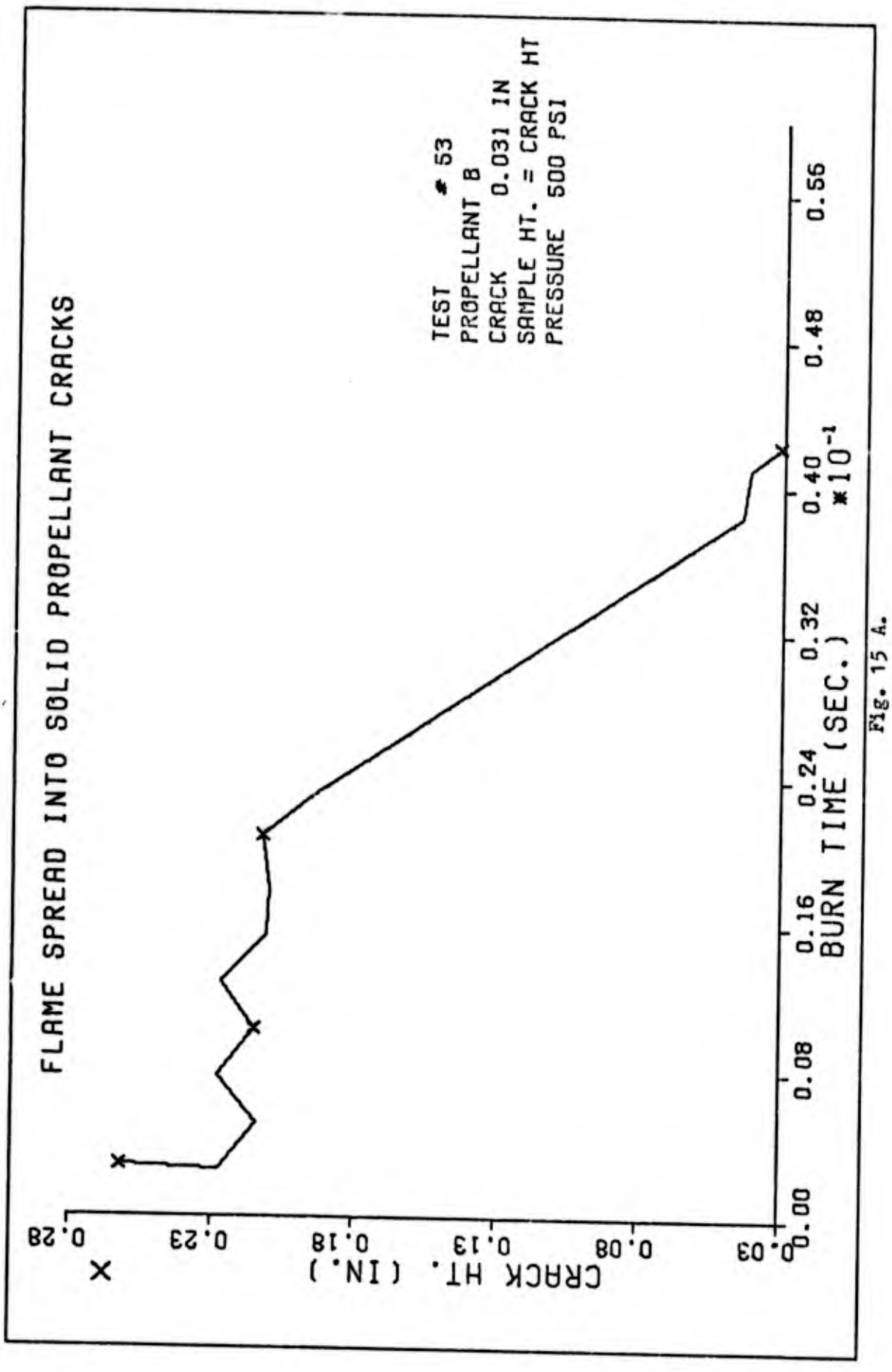
FLAME SPREAD INTO SOLID PROPELLANT CRACKS
TEST # 53
PROPELLANT B
CRACK 0.031 IN
SAMPLE HT. = CRACK HT
PRESSURE 500 PSI
CRACK HT. (IN.)
0.03
0.08
0.13
0.18
0.23
0.28
0.00
0.08
0.16
0.24
0.32
0.40
0.48
0.56
BURN TIME (SEC.)
*10⁻¹

Fig. 15 A.

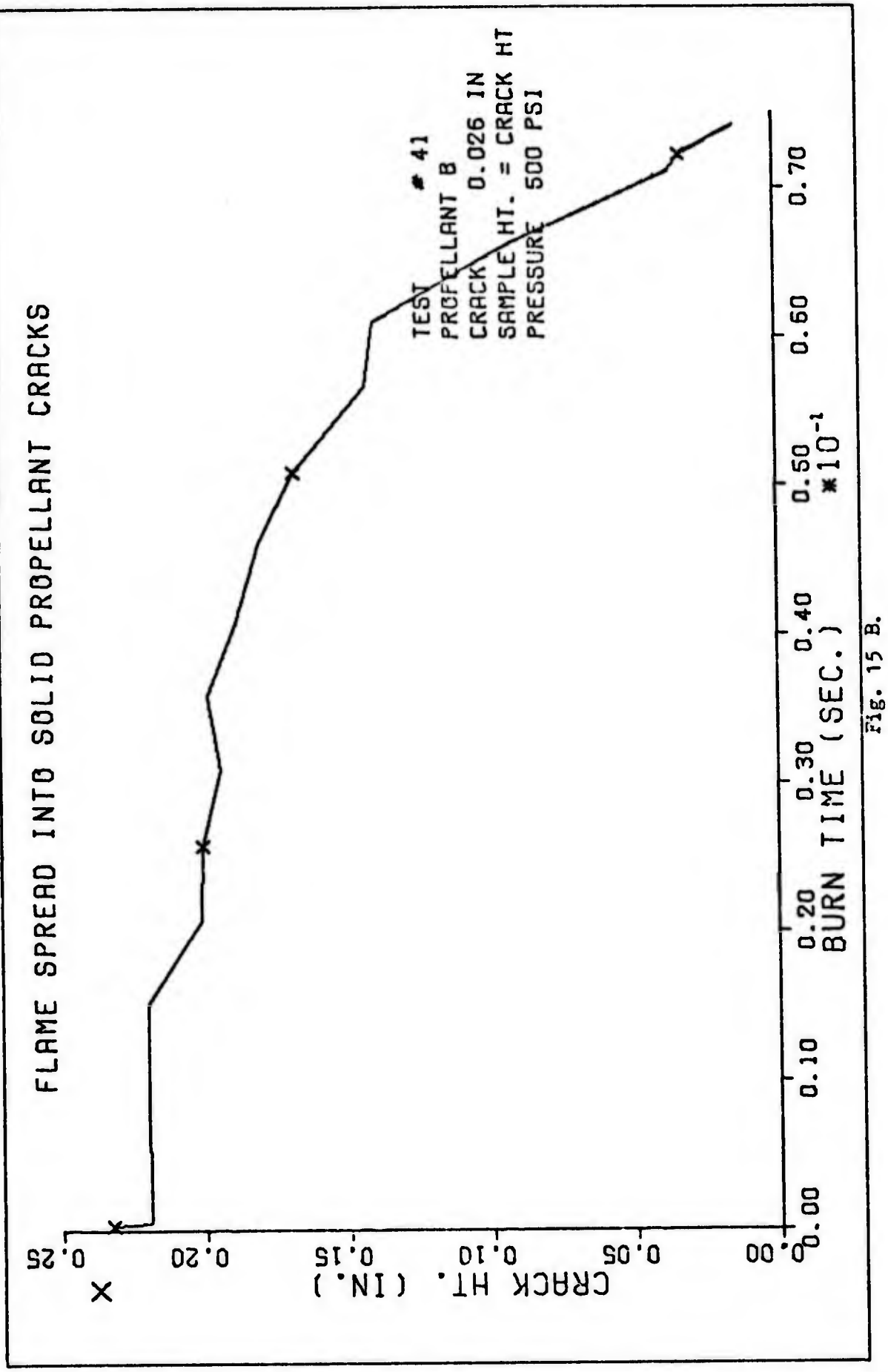
FLAME SPREAD INTO SOLID PROPELLANT CRACKS
TEST # 41
PROPELLANT B
CRACK 0.026 IN
SAMPLE HT. = CRACK HT
PRESSURE 500 PSI
CRACK HT. (IN.)
0.00
0.05
0.10
0.15
0.20
0.25
X
0.00
0.10
0.20
0.30
0.40
0.50
0.60
0.70
BURN TIME (SEC.)
*10⁻¹

Fig. 15 B.

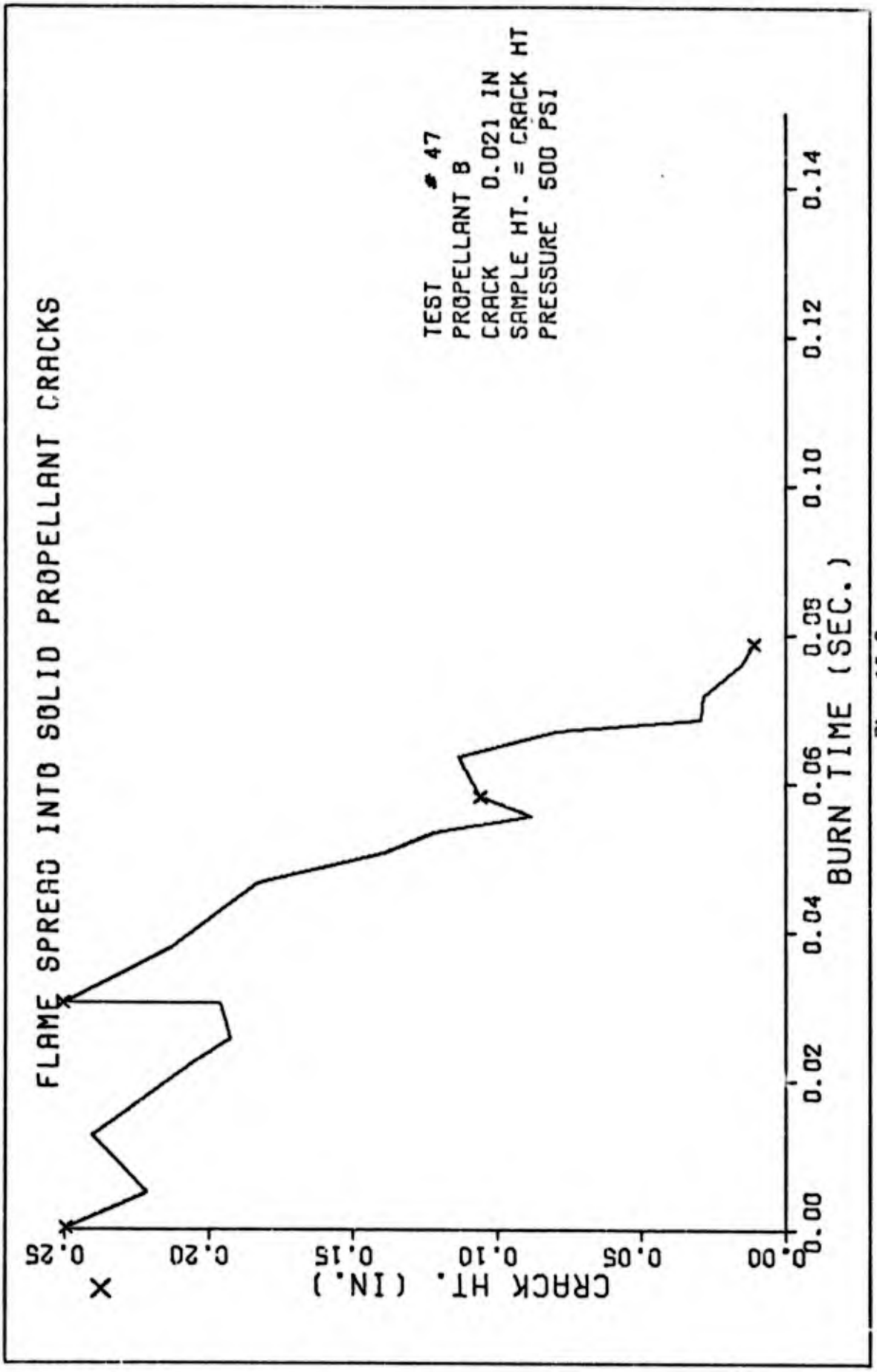
FLAME SPREAD INTO SOLID PROPELLANT CRACKS
TEST # 47
PROPELLANT B
CRACK 0.021 IN
SAMPLE HT. = CRACK HT
PRESSURE 500 PSI
CRACK HT. (IN.)
0.00
0.05
0.10
0.15
0.20
0.25
BURN TIME (SEC.)
0.00
0.02
0.04
0.06
0.08
0.10
0.12
0.14

Fig. 15 c.

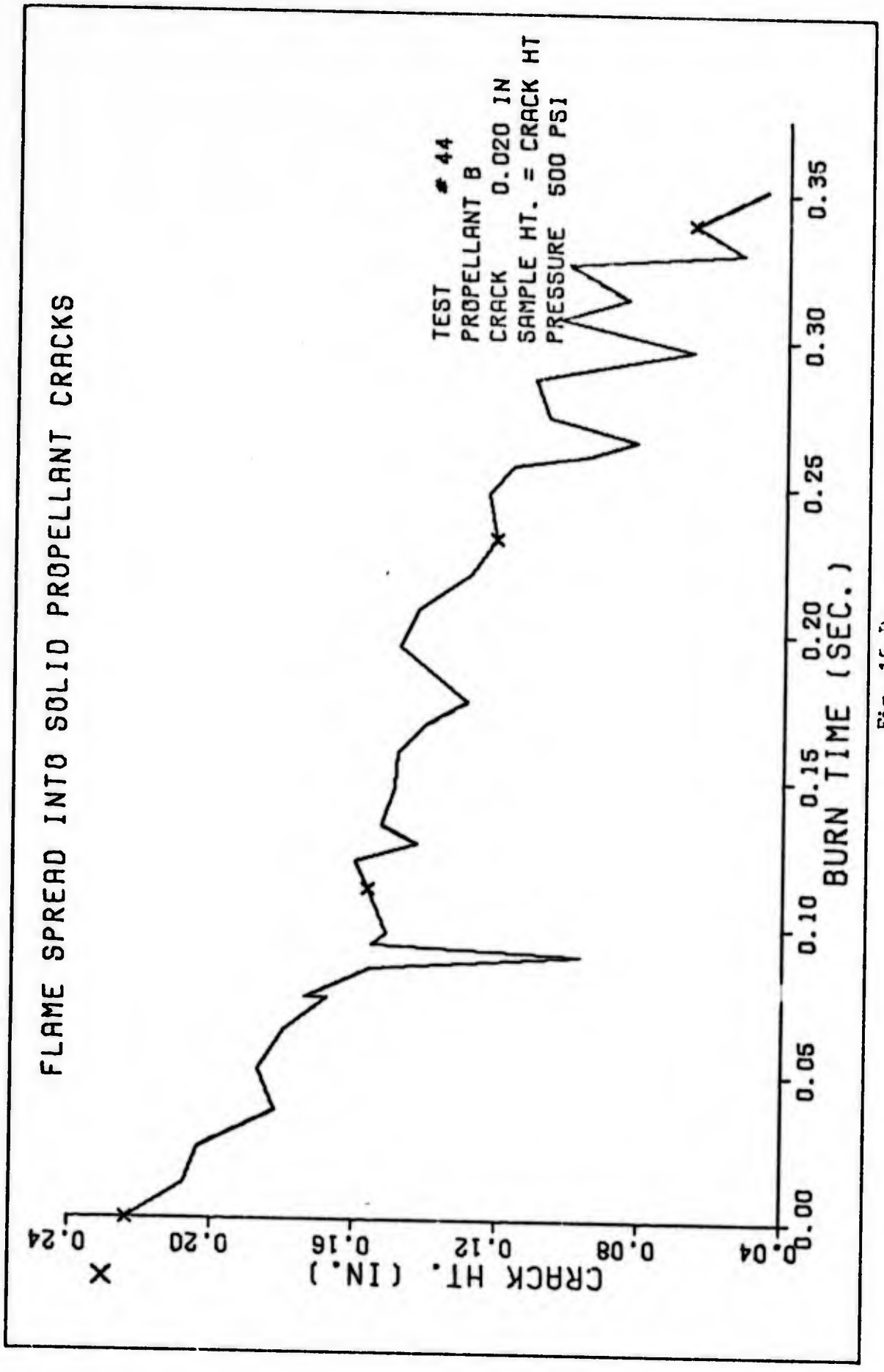
FLAME SPREAD INTO SOLID PROPELLANT CRACKS
TEST # 44
PROPELLANT B
CRACK 0.020 IN
SAMPLE HT. = CRACK HT
PRESSURE 500 PSI
CRACK HT. (IN.)
BURN TIME (SEC.)
0.00
0.05
0.10
0.15
0.20
0.25
0.30
0.35
0.04
0.08
0.12
0.16
0.20
0.24

Fig. 15 b.

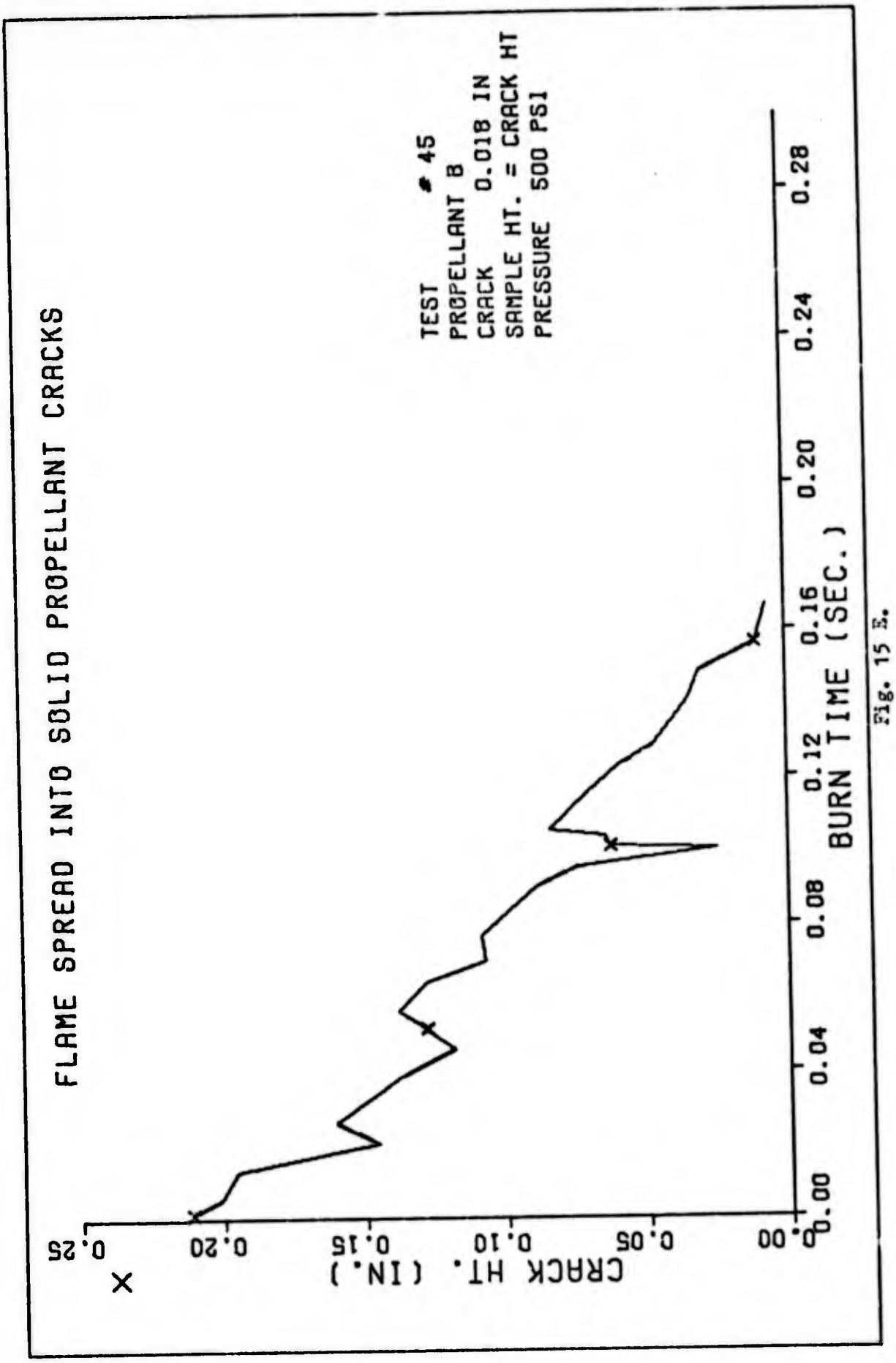
FLAME SPREAD INTO SOLID PROPELLANT CRACKS
TEST # 45
PROPELLANT B
CRACK 0.018 IN
SAMPLE HT. = CRACK HT
PRESSURE 500 PSI
CRACK HT. (IN.)
BURN TIME (SEC.)
0.00
0.04
0.08
0.12
0.16
0.20
0.24
0.28
0.00
0.05
0.10
0.15
0.20
0.25
X

Fig. 15 E.

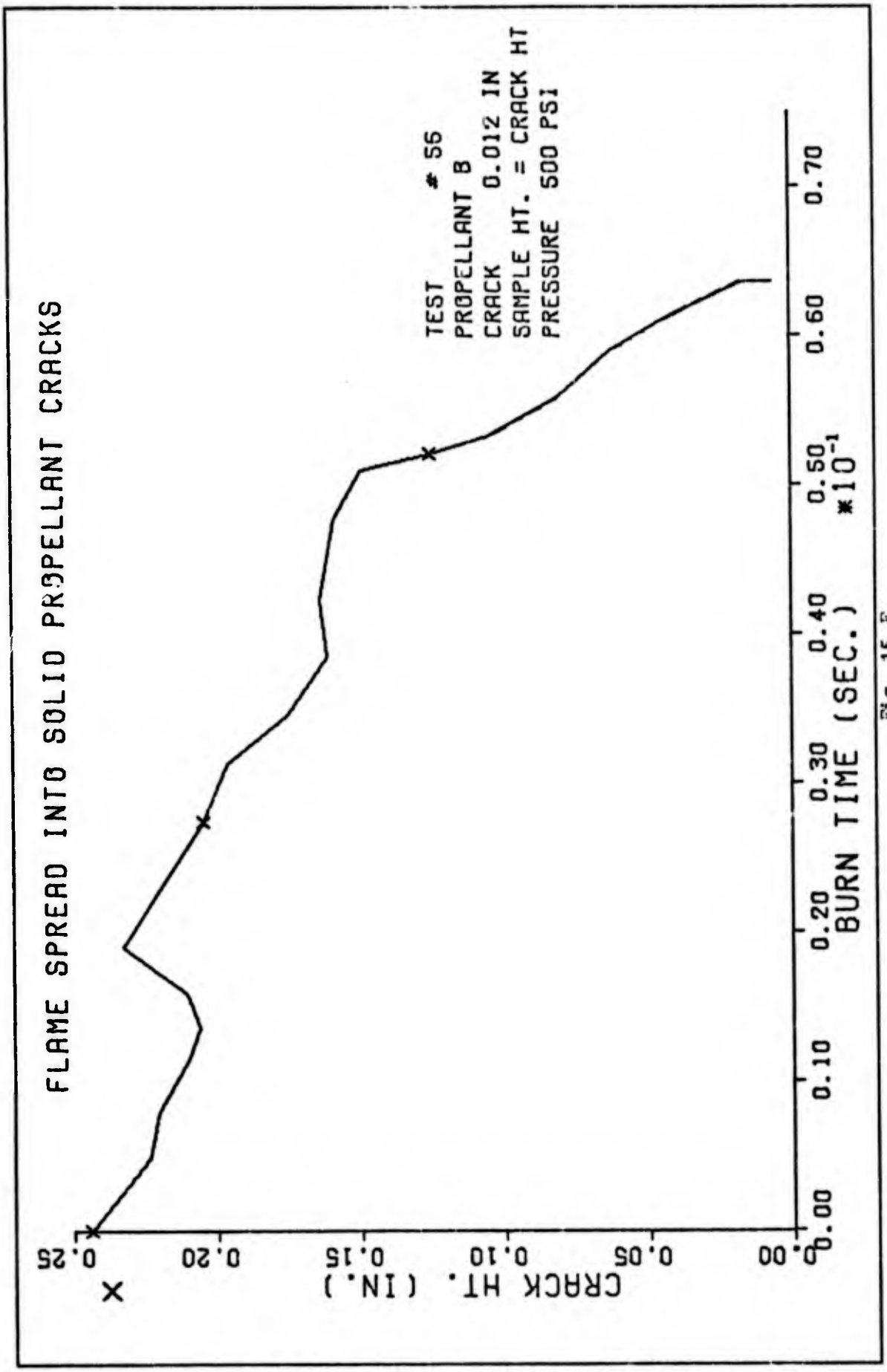
FLAME SPREAD INTO SOLID PROPELLANT CRACKS
TEST # S6
PROPELLANT B
CRACK 0.012 IN
SAMPLE HT. = CRACK HT
PRESSURE 500 PSI
CRACK HT. (IN.)
0.00
0.05
0.10
0.15
0.20
0.25
BURN TIME (SEC.)
0.00
0.10
0.20
0.30
0.40
0.50
0.60
0.70
*10⁻¹

Fig. 15 F.

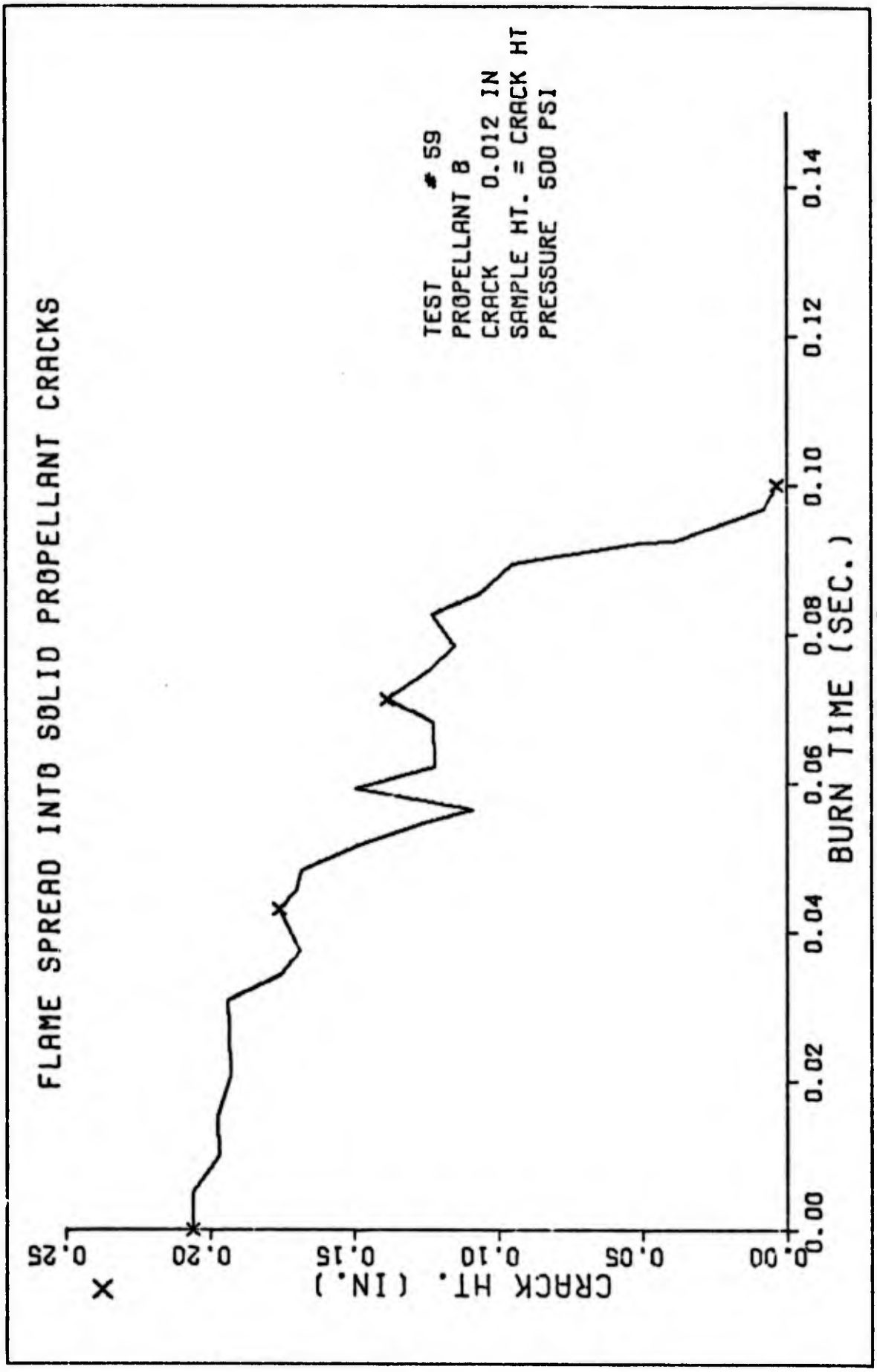
FLAME SPREAD INTO SOLID PROPELLANT CRACKS
TEST # 59
PROPELLANT B
CRACK 0.012 IN
SAMPLE HT. = CRACK HT
PRESSURE 500 PSI
CRACK HT. (IN.)
0.00
0.05
0.10
0.15
0.20
0.25
BURN TIME (SEC.)
0.00
0.02
0.04
0.06
0.08
0.10
0.12
0.14

Fig. 15 c.

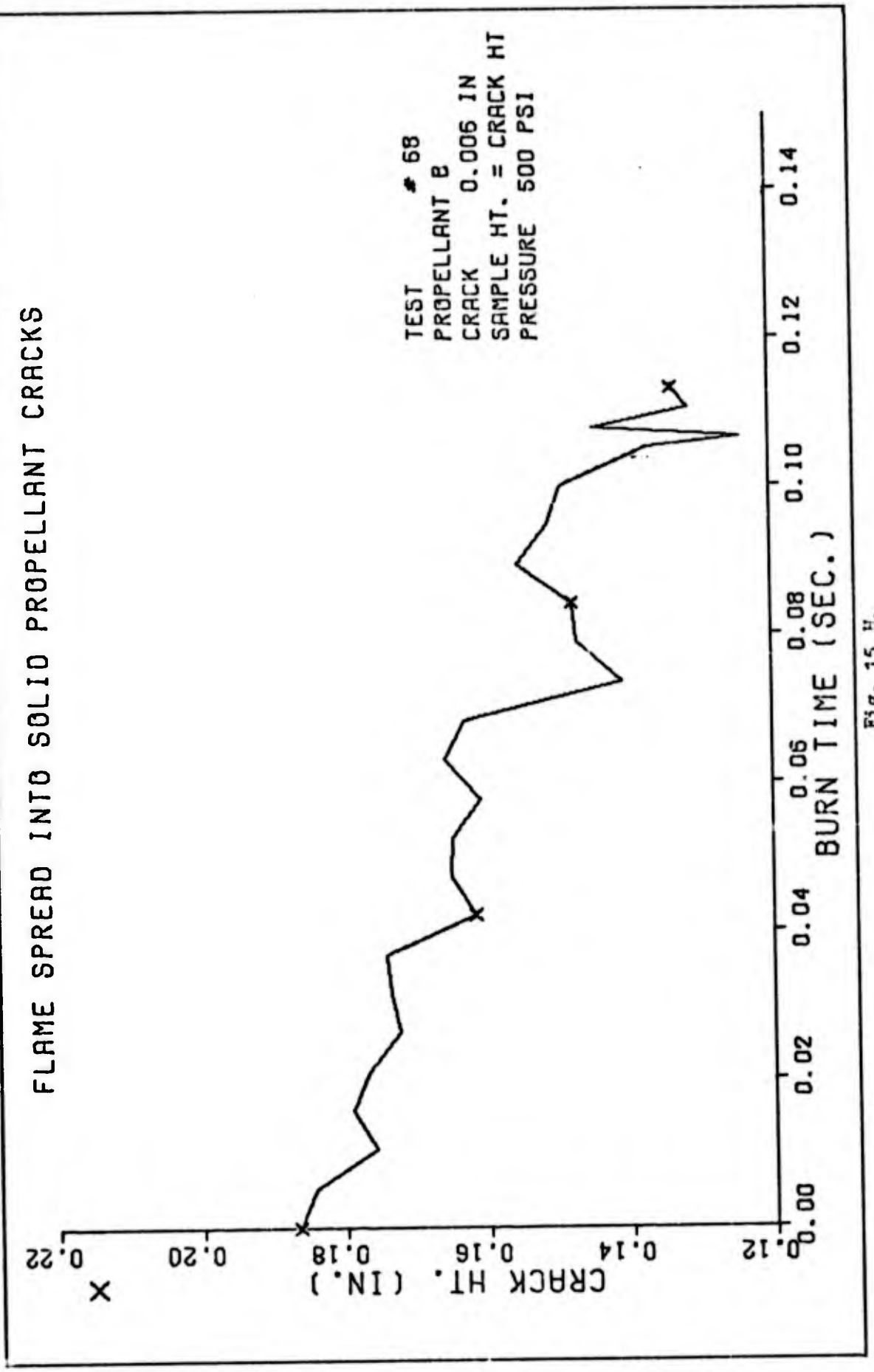
FLAME SPREAD INTO SOLID PROPELLANT CRACKS
TEST # 68
PROPELLANT B
CRACK 0.006 IN
SAMPLE HT. = CRACK HT
PRESSURE 500 PSI
CRACK HT. (IN.)
0.12
0.14
0.16
0.18
0.20
0.22
X
0.00
0.02
0.04
0.06
0.08
0.10
0.12
0.14
BURN TIME (SEC.)

Fig. 15 H.

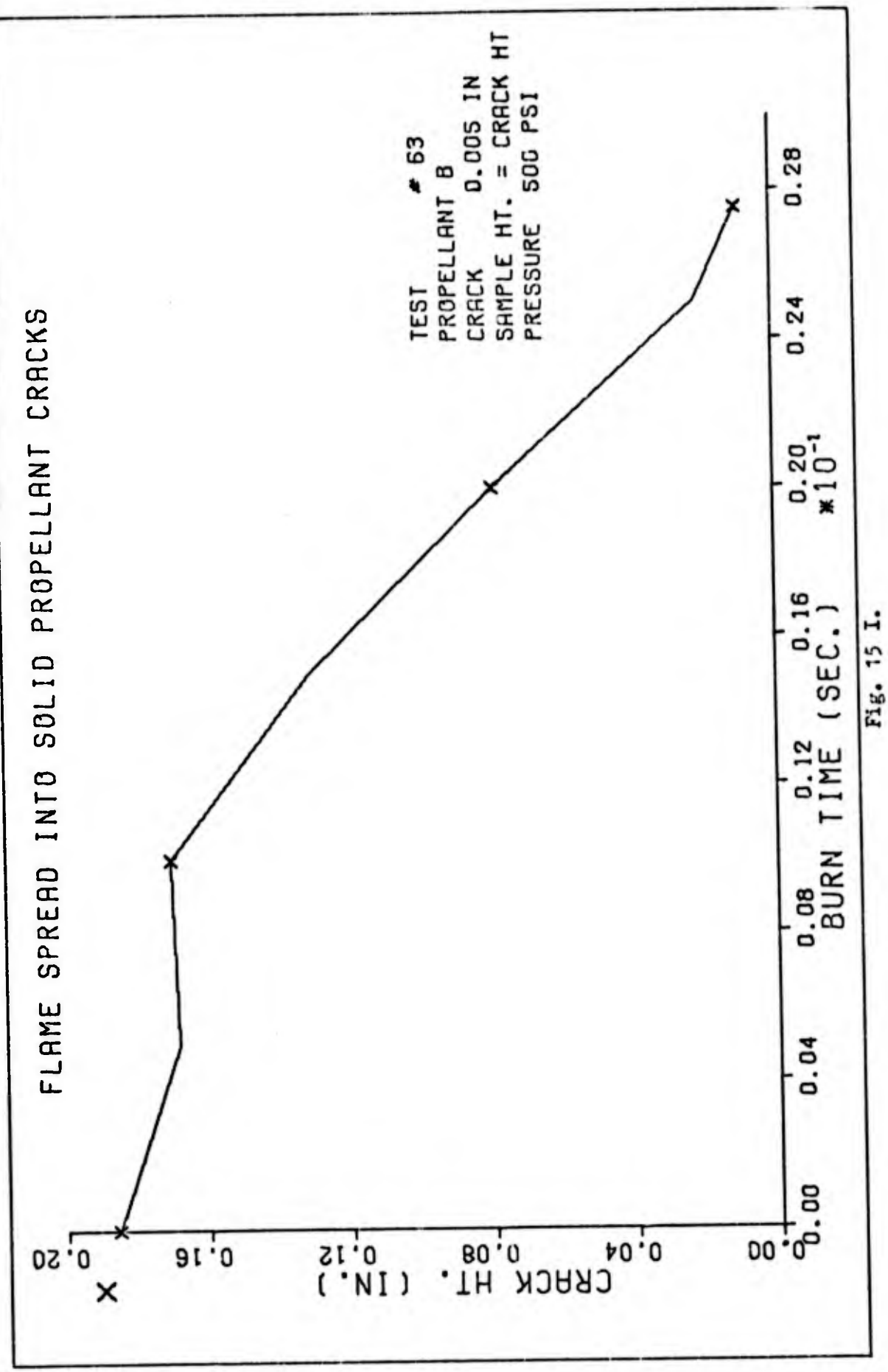
FLAME SPREAD INTO SOLID PROPELLANT CRACKS
TEST # 63
PROPELLANT B
CRACK 0.005 IN
SAMPLE HT. = CRACK HT
PRESSURE 500 PSI
CRACK HT. (IN.)
0.00
0.04
0.08
0.12
0.16
0.20
BURN TIME (SEC.)
0.00
0.04
0.08
0.12
0.16
0.20
0.24
0.28
*10^-1

Fig. 15 I.

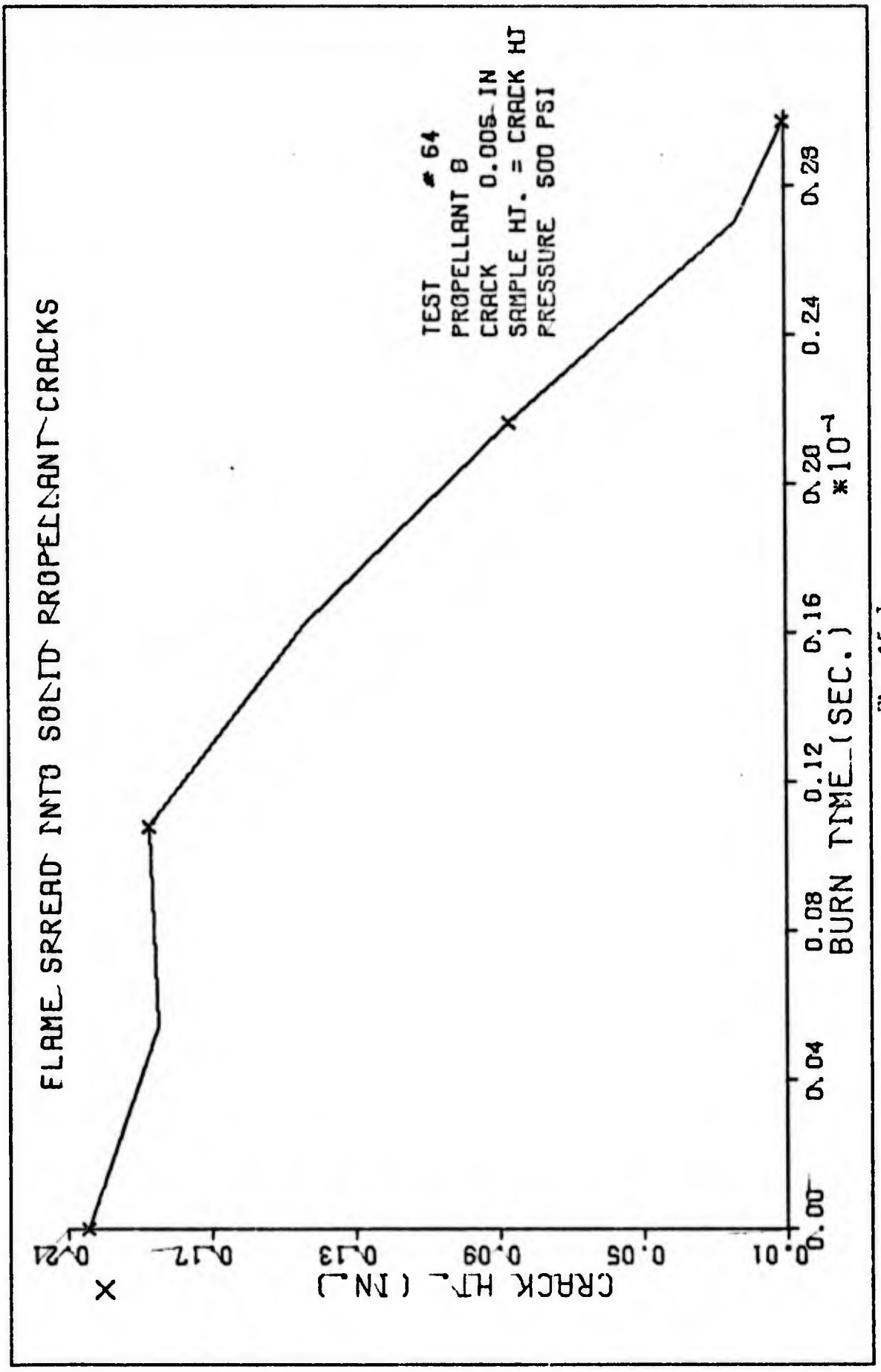
FLAME SPREAD INTO SOLID PROPELLANT CRACKS
TEST # 64
PROPELLANT B
CRACK 0.005 IN
SAMPLE HT. = CRACK HT
PRESSURE 500 PSI
CRACK HT. (IN.)
BURN TIME (SEC.)
*10⁻¹
0.00
0.04
0.08
0.12
0.16
0.20
0.24
0.28
0.01
0.05
0.09
0.13
0.17
0.21

Fig. 15 J.

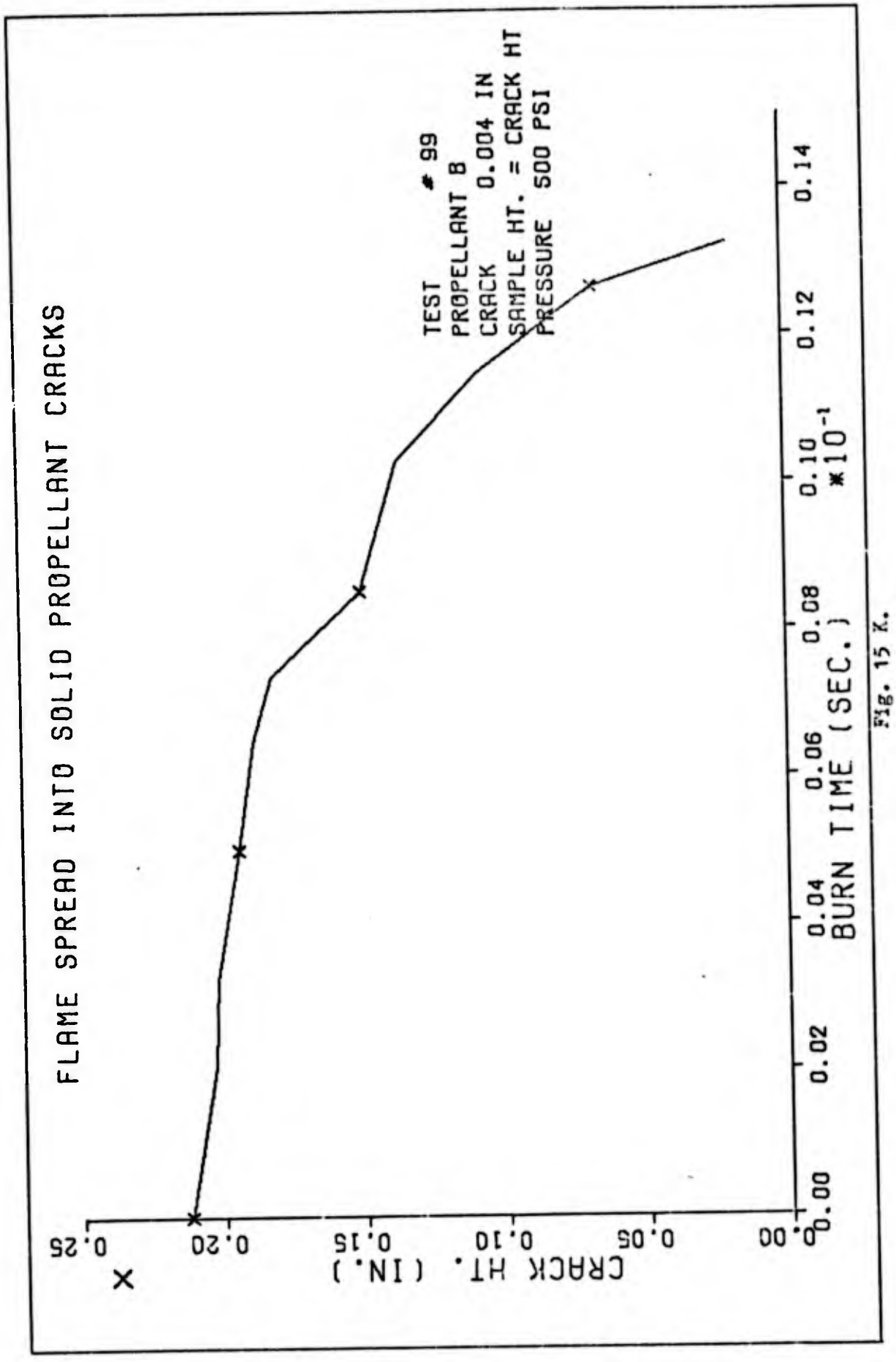
FLAME SPREAD INTO SOLID PROPELLANT CRACKS
TEST # 99
PROPELLANT B
CRACK 0.004 IN
SAMPLE HT. = CRACK HT
PRESSURE 500 PSI
CRACK HT. (IN.)
0.00
0.05
0.10
0.15
0.20
0.25
BURN TIME (SEC.)
0.00
0.02
0.04
0.06
0.08
0.10
0.12
0.14
*10⁻¹

Fig. 15 K.

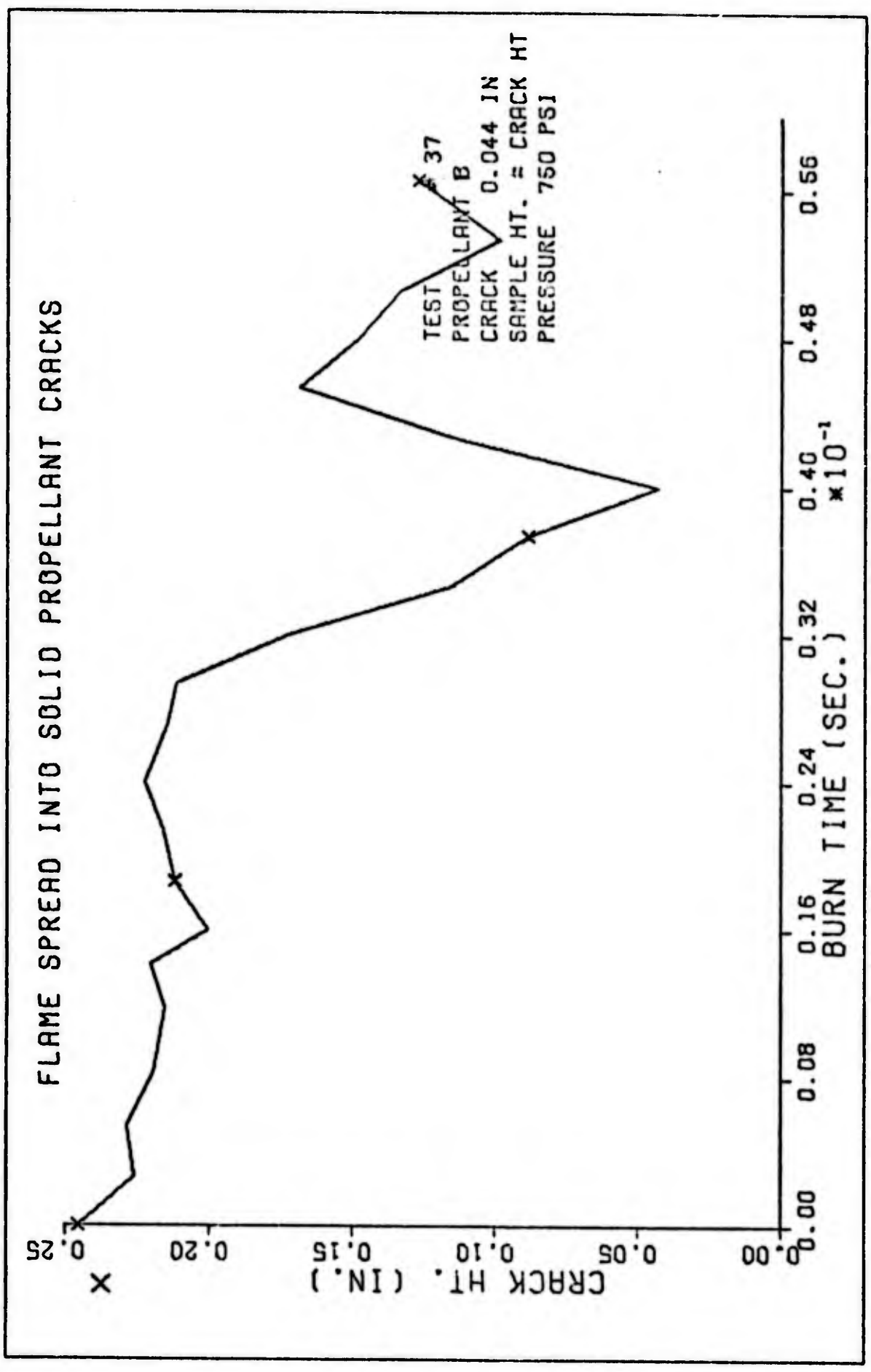

Fig. 16. Data Curves for Propellant B, 750 psi

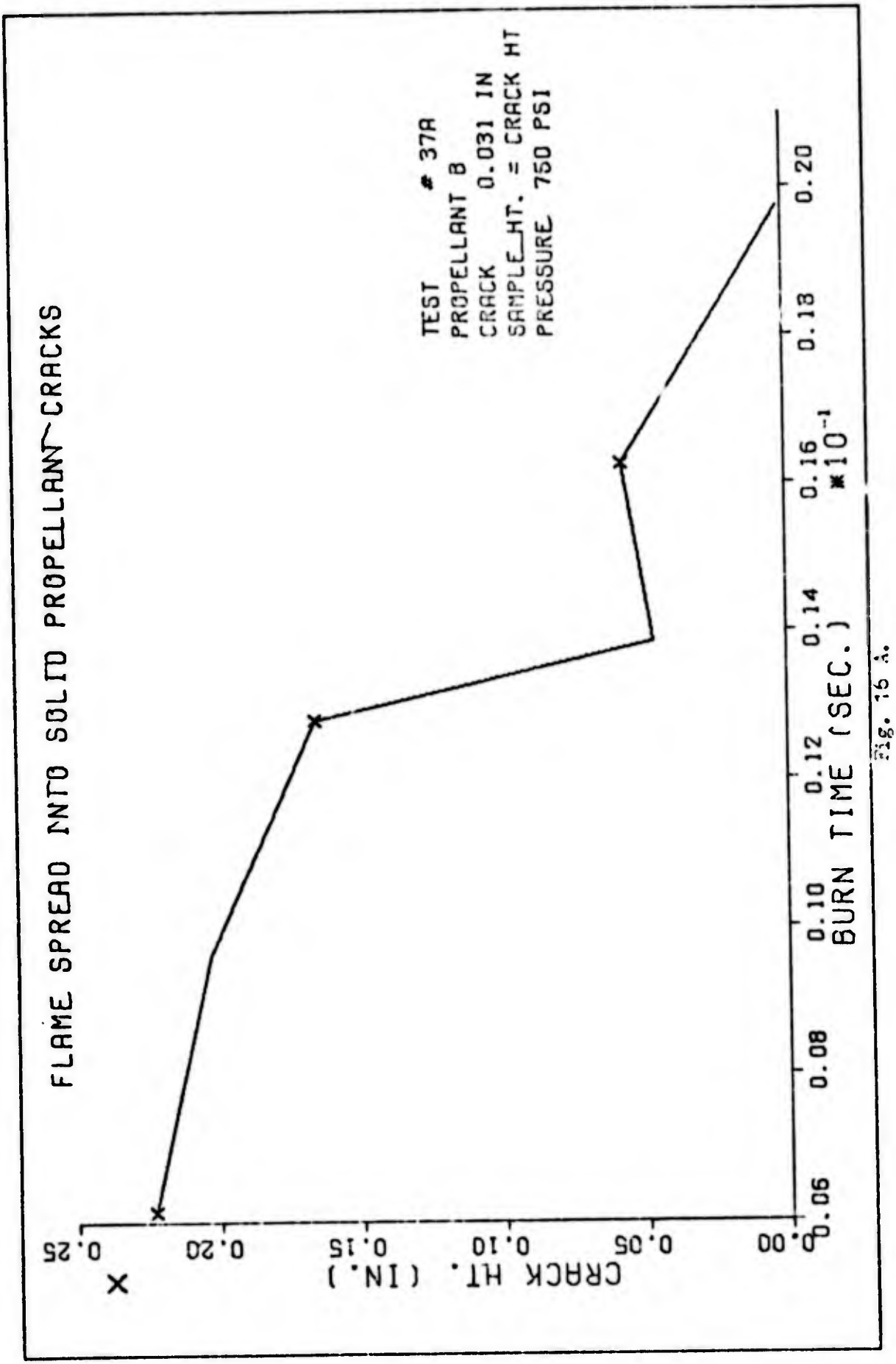
FLAME SPREAD INTO SOLID PROPELLANT CRACKS
TEST # 37A
PROPELLANT B
CRACK 0.031 IN
SAMPLE_HT. = CRACK HT
PRESSURE 750 PSI
CRACK HT. (IN.)
0.00
0.05
0.10
0.15
0.20
0.25
X
0.06
0.08
0.10
0.12
0.14
0.16
0.18
0.20
BURN TIME (SEC.)
*10⁻¹

Fig. 15 a.

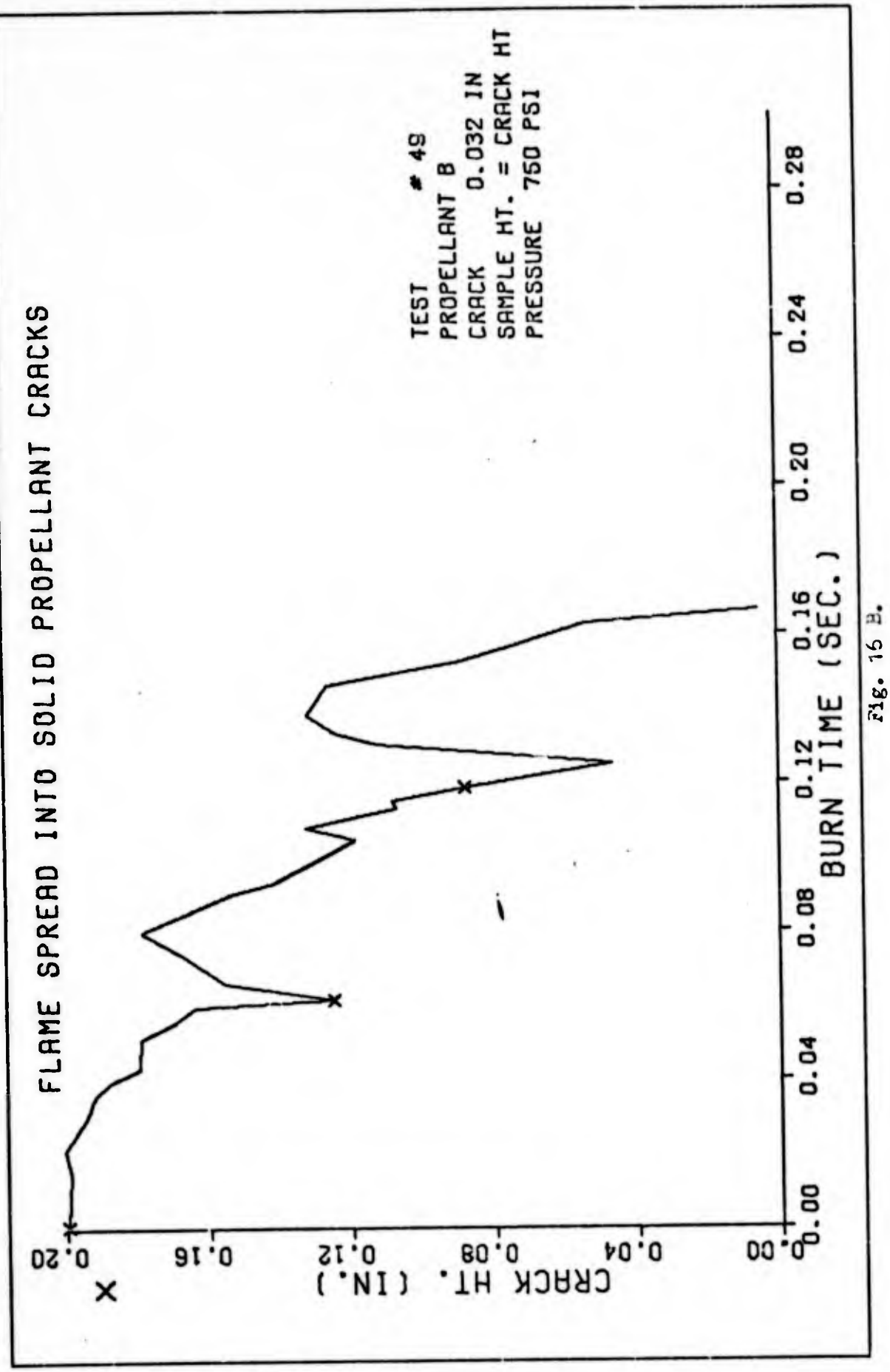
FLAME SPREAD INTO SOLID PROPELLANT CRACKS
TEST # 49
PROPELLANT B
CRACK 0.032 IN
SAMPLE HT. = CRACK HT
PRESSURE 750 PSI
CRACK HT. (IN.)
0.00
0.04
0.08
0.12
0.16
0.20
BURN TIME (SEC.)
0.00
0.04
0.08
0.12
0.16
0.20
0.24
0.28

Fig. 16 B.

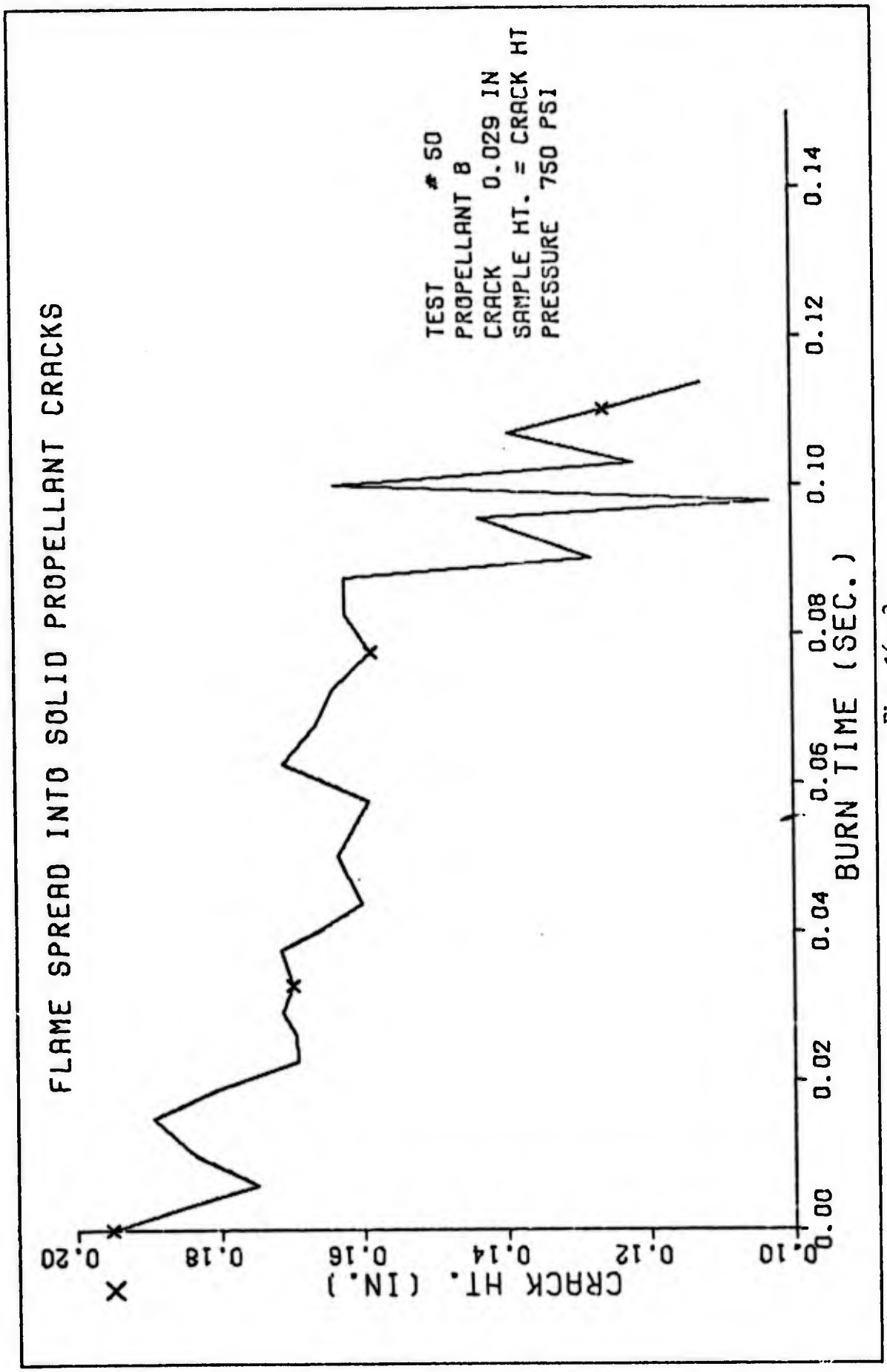
FLAME SPREAD INTO SOLID PROPELLANT CRACKS
TEST # 50
PROPELLANT B
CRACK 0.029 IN
SAMPLE HT. = CRACK HT
PRESSURE 750 PSI
CRACK HT. (IN.)
0.10
0.12
0.14
0.16
0.18
0.20
BURN TIME (SEC.)
0.00
0.02
0.04
0.06
0.08
0.10
0.12
0.14

Fig. 16 c.

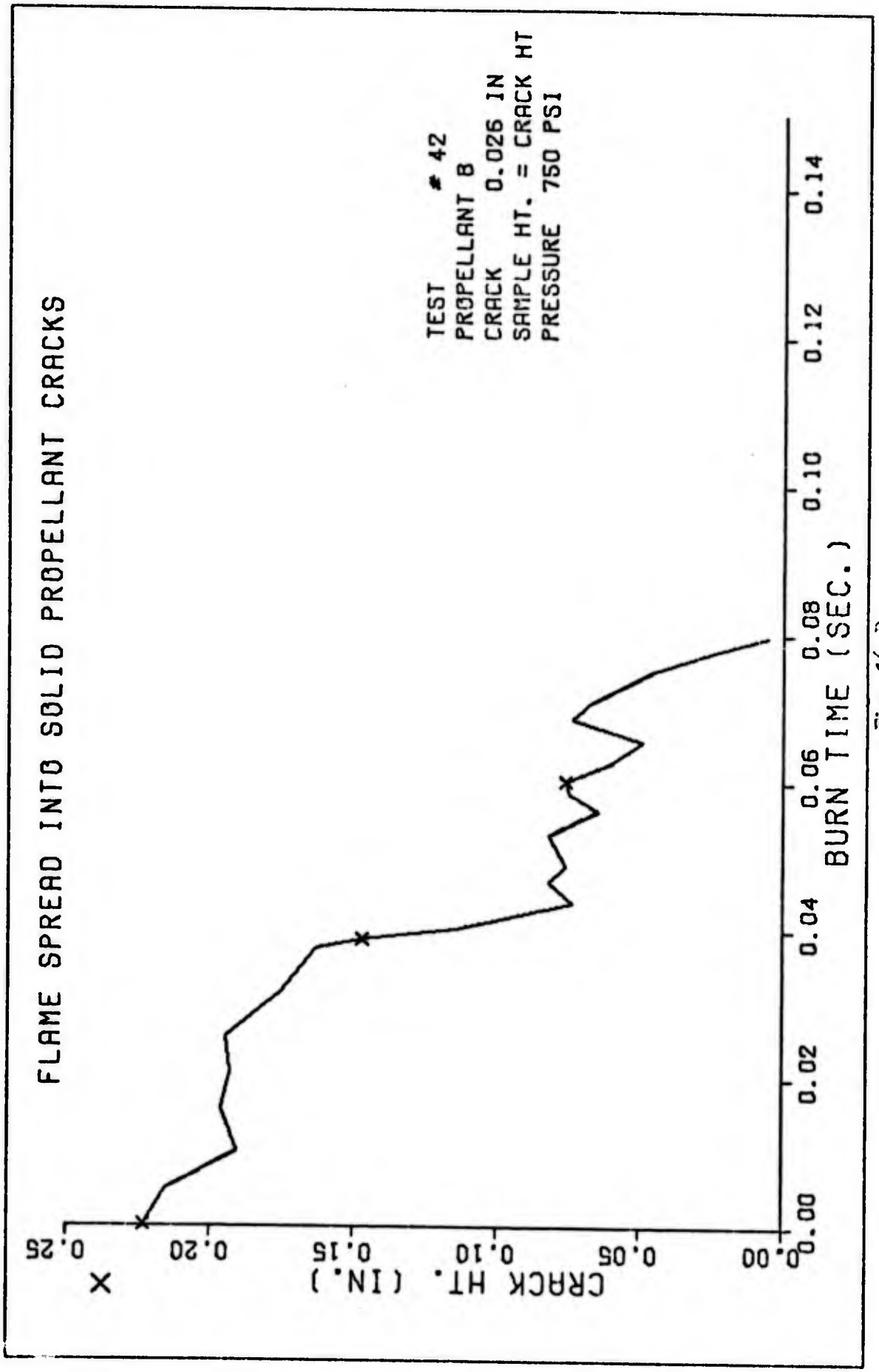
FLAME SPREAD INTO SOLID PROPELLANT CRACKS
TEST # 42
PROPELLANT B
CRACK 0.026 IN
SAMPLE HT. = CRACK HT
PRESSURE 750 PSI
CRACK HT. (IN.)
0.00
0.05
0.10
0.15
0.20
0.25
BURN TIME (SEC.)
0.00
0.02
0.04
0.06
0.08
0.10
0.12
0.14

Fig. 15 D.

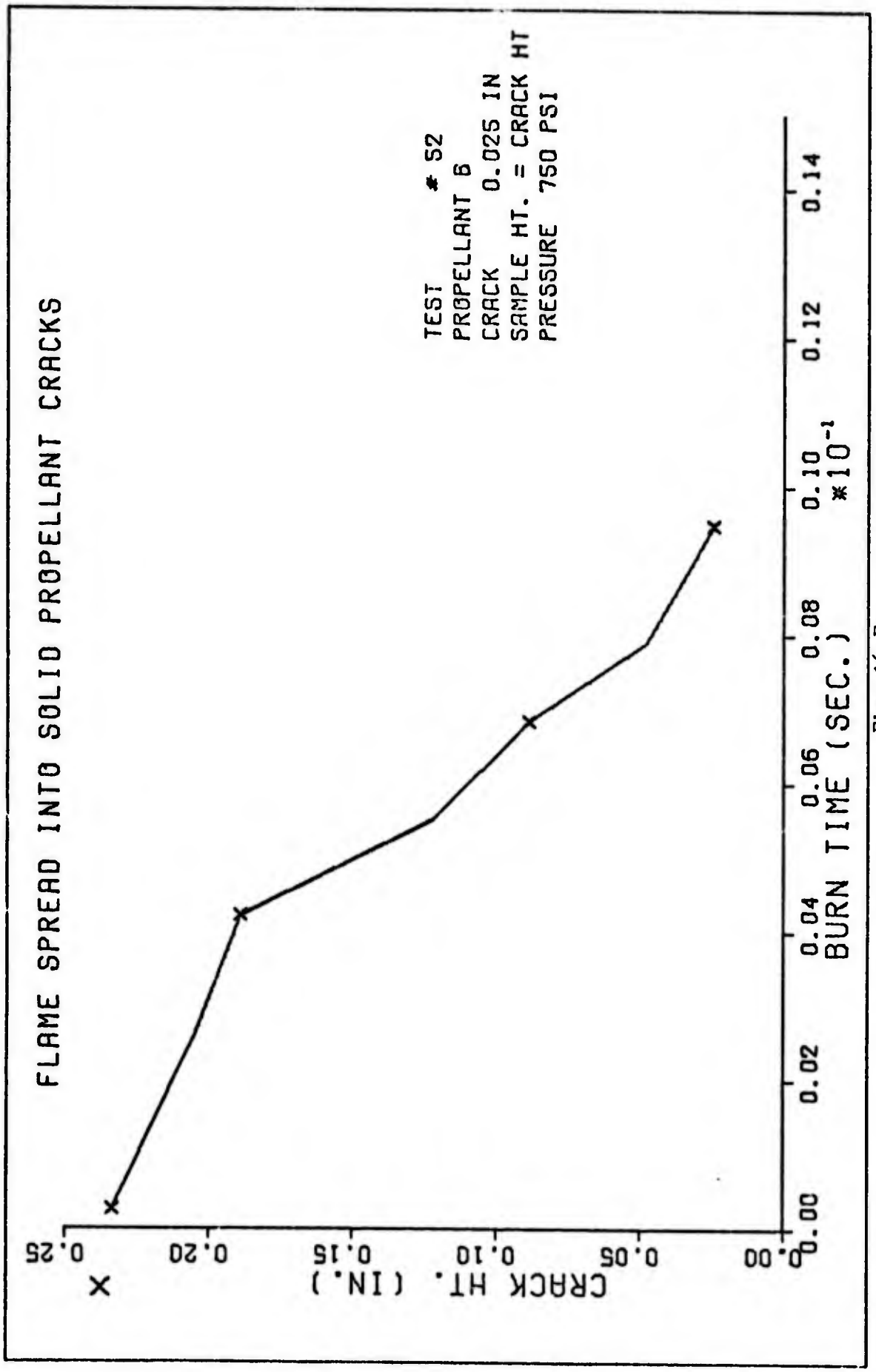
FLAME SPREAD INTO SOLID PROPELLANT CRACKS
TEST # S2
PROPELLANT B
CRACK 0.025 IN
SAMPLE HT. = CRACK HT
PRESSURE 750 PSI
CRACK HT. (IN.)
0.00
0.05
0.10
0.15
0.20
0.25
BURN TIME (SEC.)
0.00
0.02
0.04
0.06
0.08
0.10
0.12
0.14
*10⁻¹

Fig. 16 E.

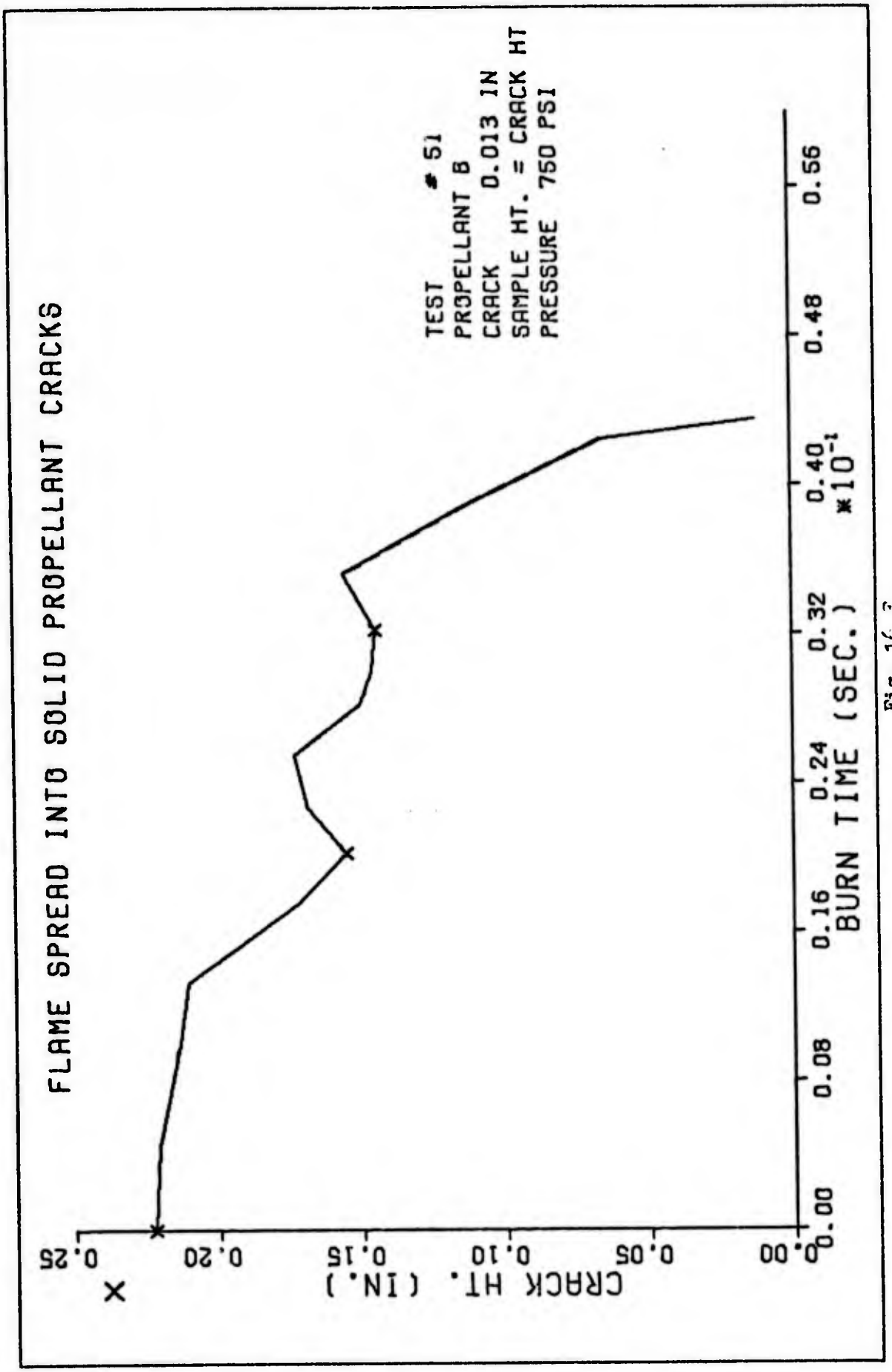
FLAME SPREAD INTO SOLID PROPELLANT CRACKS
TEST # 51
PROPELLANT B
CRACK 0.013 IN
SAMPLE HT. = CRACK HT
PRESSURE 750 PSI
CRACK HT. (IN.)
0.00
0.05
0.10
0.15
0.20
0.25
X
0.00
0.08
0.16
0.24
0.32
0.40
0.48
0.56
BURN TIME (SEC.)
*10⁻¹

Fig. 16 a.

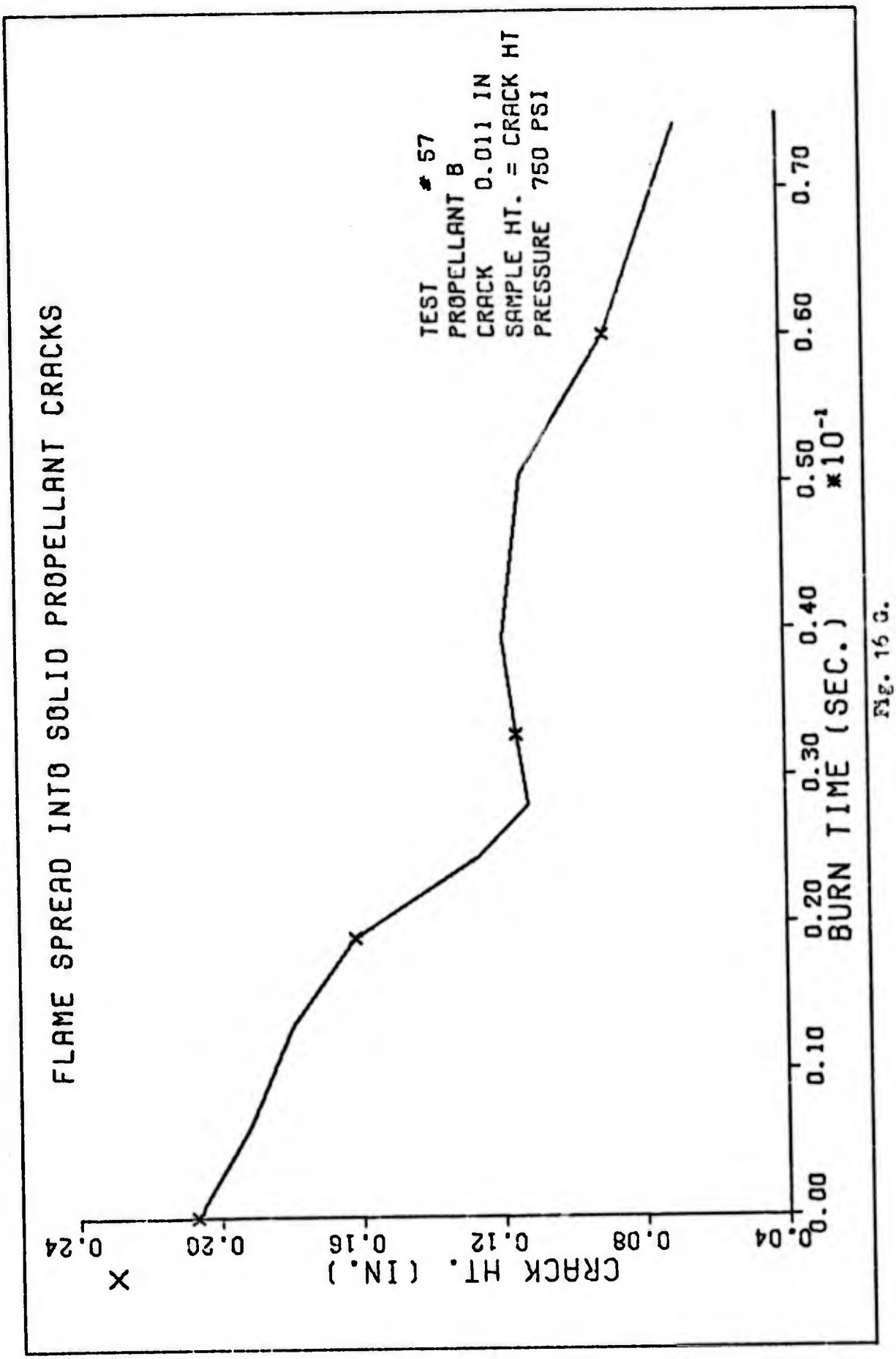
FLAME SPREAD INTO SOLID PROPELLANT CRACKS
TEST # 57
PROPELLANT B
CRACK 0.011 IN
SAMPLE HT. = CRACK HT
PRESSURE 750 PSI
CRACK HT. (IN.)
0.04
0.08
0.12
0.16
0.20
0.24
X
0.00
0.10
0.20
0.30
0.40
0.50
0.60
0.70
BURN TIME (SEC.)
*10⁻¹

Fig. 15 a.

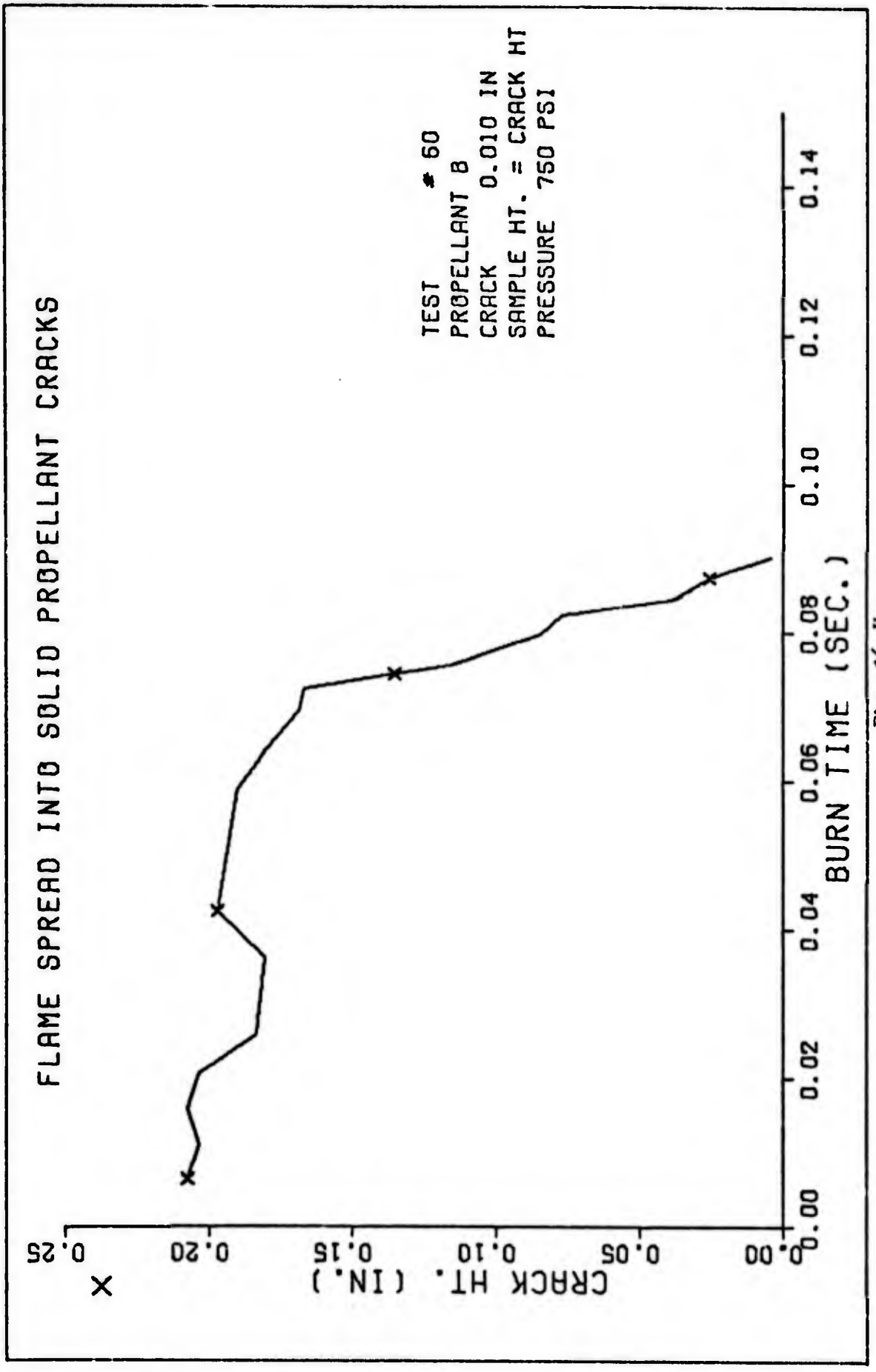
FLAME SPREAD INTO SOLID PROPELLANT CRACKS
TEST # 60
PROPELLANT B
CRACK 0.010 IN
SAMPLE HT. = CRACK HT
PRESSURE 750 PSI
CRACK HT. (IN.)
0.00
0.05
0.10
0.15
0.20
0.25
BURN TIME (SEC.)
0.00
0.02
0.04
0.06
0.08
0.10
0.12
0.14

Fig. 16 H.

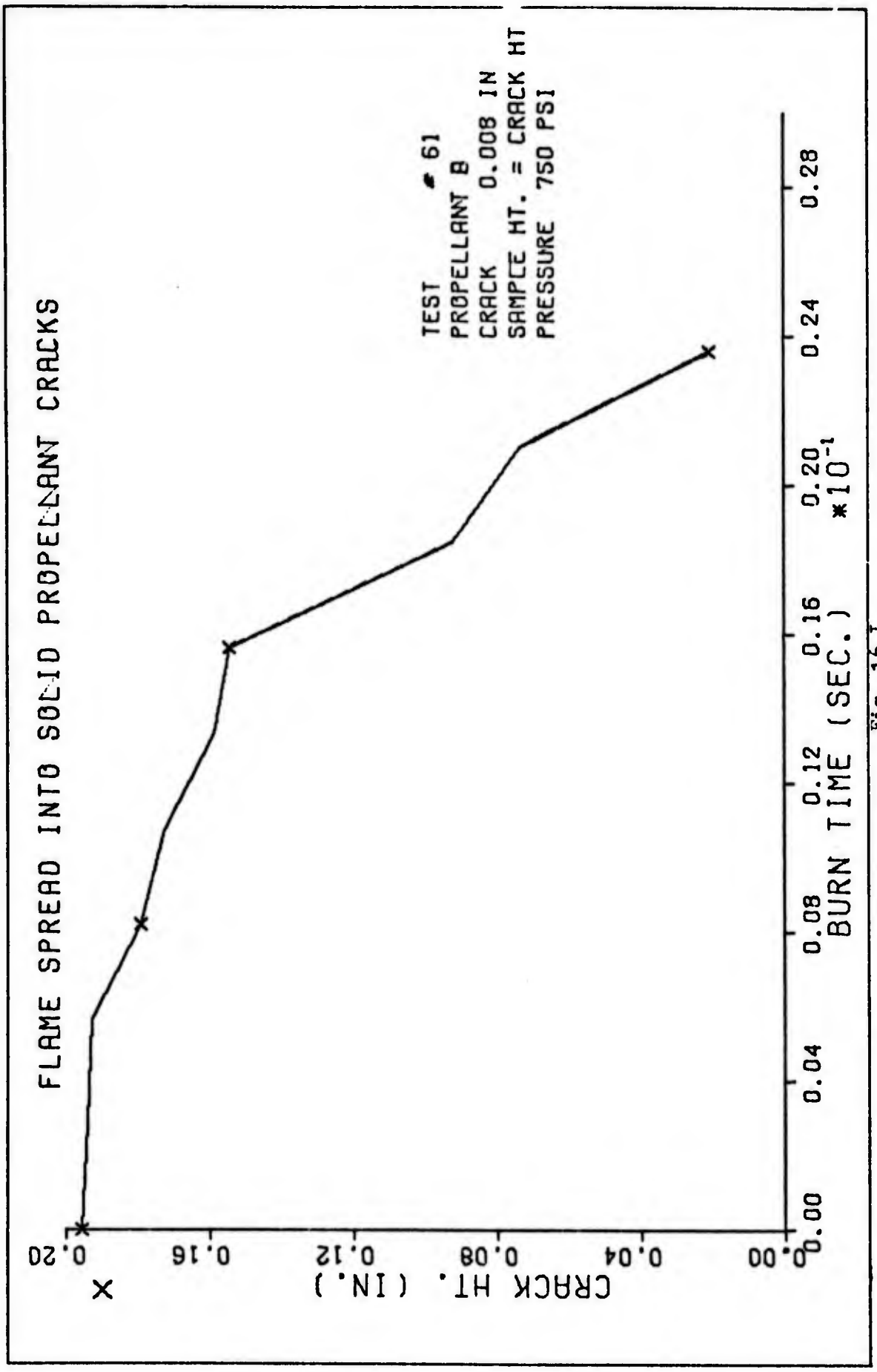
FLAME SPREAD INTO SOLID PROPELLANT CRACKS
TEST # 61
PROPELLANT B
CRACK 0.008 IN
SAMPLE HT. = CRACK HT
PRESSURE 750 PSI
CRACK HT. (IN.)
0.00
0.04
0.08
0.12
0.16
0.20
0.24
0.28
BURN TIME (SEC.)
*10^-1

Fig. 16 I.

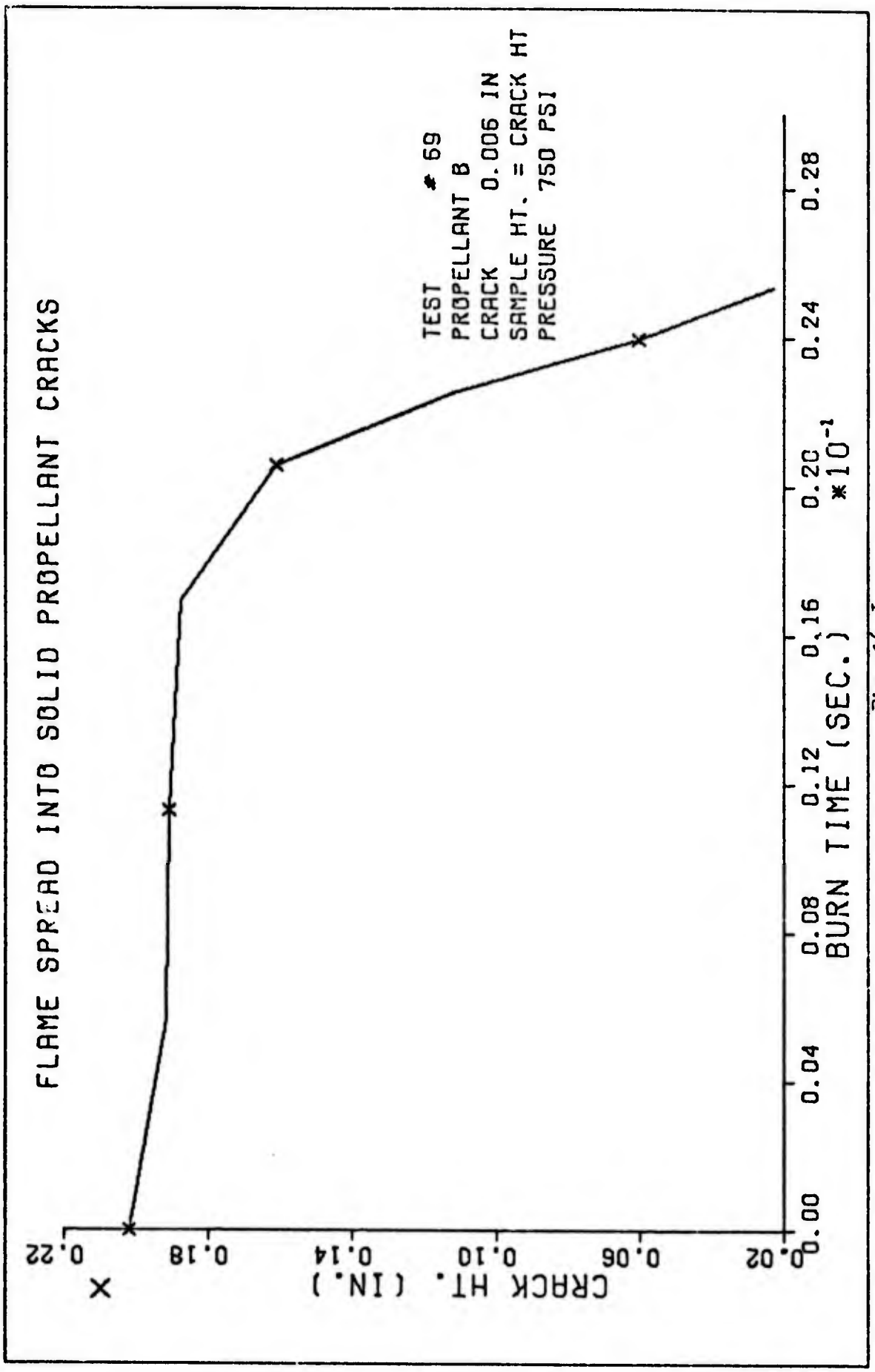
FLAME SPREAD INTO SOLID PROPELLANT CRACKS
TEST # 69
PROPELLANT B
CRACK 0.006 IN
SAMPLE HT. = CRACK HT
PRESSURE 750 PSI
CRACK HT. (IN.)
0.00
0.02
0.06
0.10
0.14
0.18
0.22
BURN TIME (SEC.)
0.00
0.04
0.08
0.12
0.16
0.20
0.24
0.28
*10⁻¹

Fig. 16 J.

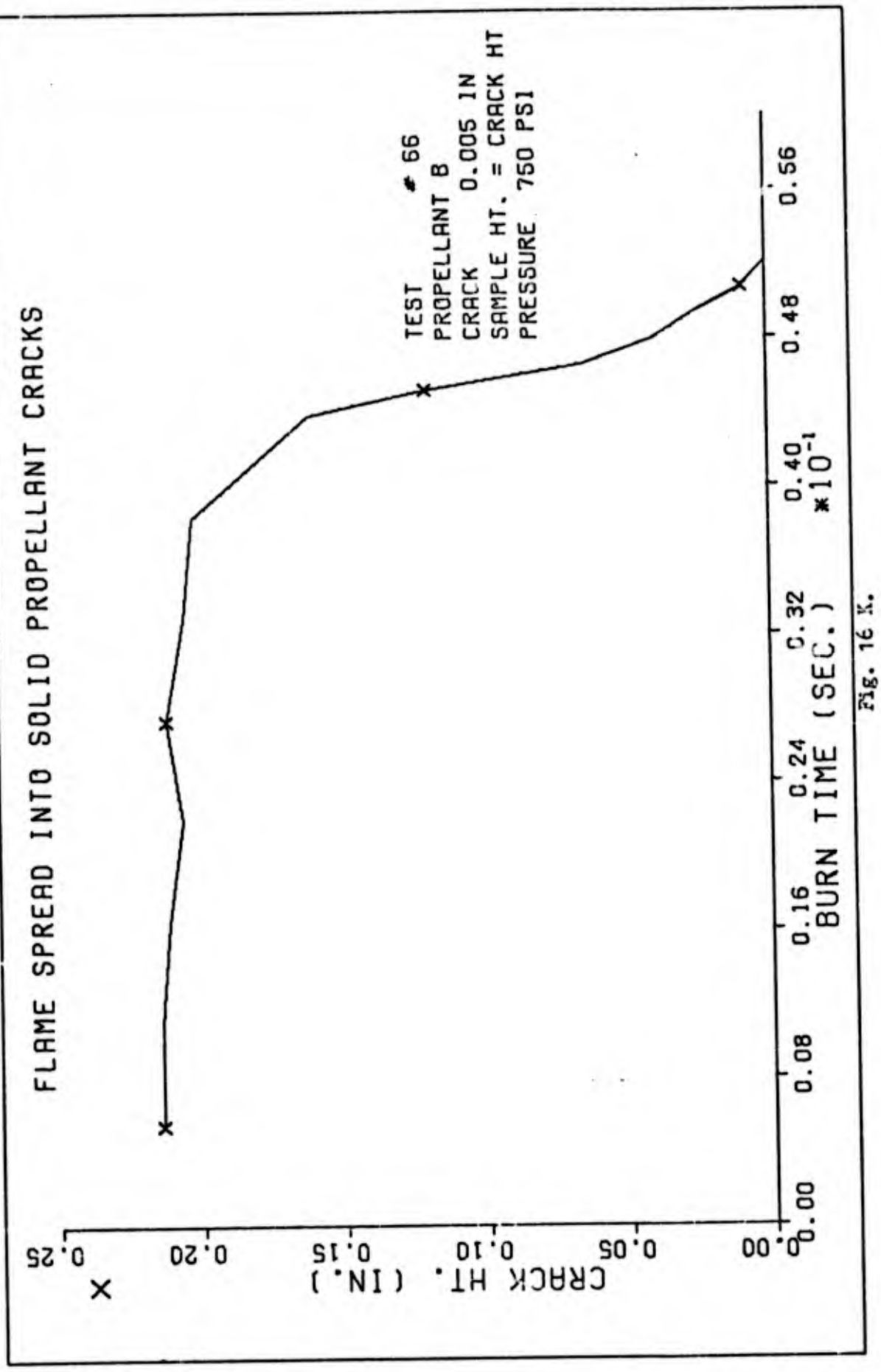
FLAME SPREAD INTO SOLID PROPELLANT CRACKS
TEST # 66
PROPELLANT B
CRACK 0.005 IN
SAMPLE HT. = CRACK HT
PRESSURE 750 PSI
CRACK HT. (IN.)
0.00
0.05
0.10
0.15
0.20
0.25
0.00
0.08
0.16
0.24
0.32
0.40
0.48
0.56
BURN TIME (SEC.)
*10^-1

Fig. 16 K.

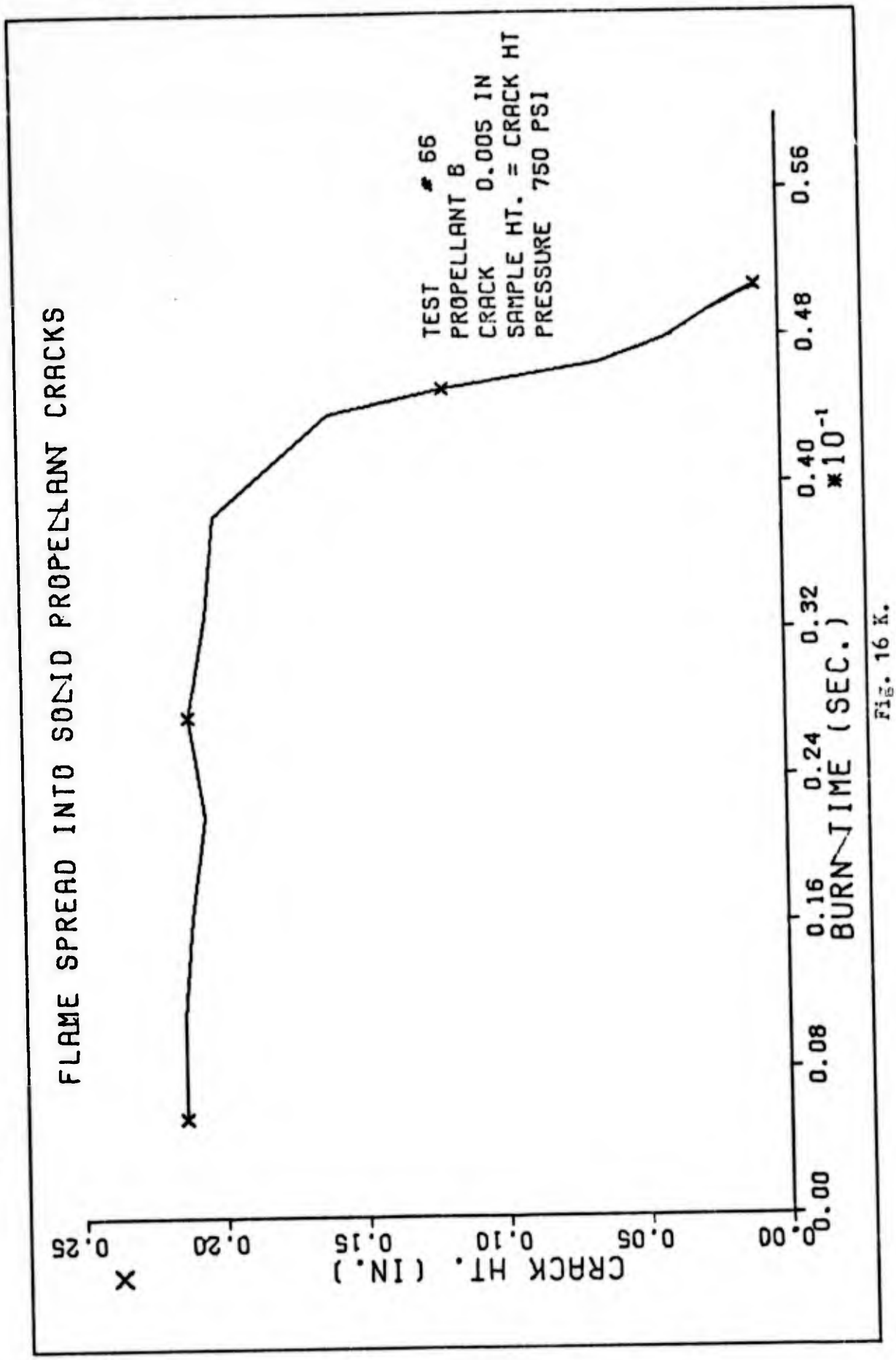
FLAME SPREAD INTO SOLID PROPELLANT CRACKS
TEST # 66
PROPELLANT B
CRACK 0.005 IN
SAMPLE HT. = CRACK HT
PRESSURE 750 PSI
CRACK HT. (IN.)
0.00
0.05
0.10
0.15
0.20
0.25
0.00
0.08
0.16
0.24
0.32
0.40
0.48
0.56
BURN TIME (SEC.)
*10⁻¹

Fig. 16 K.

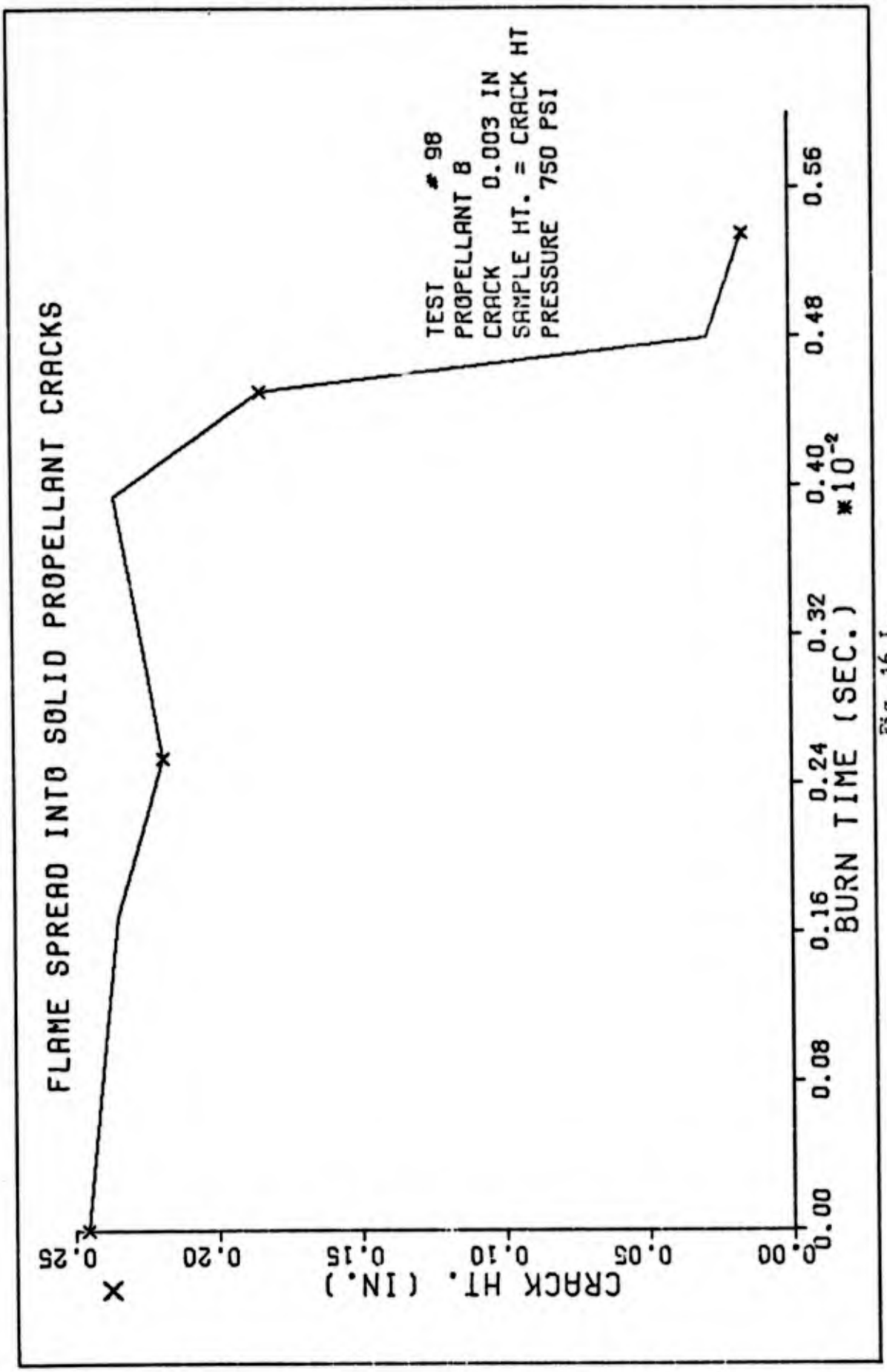
FLAME SPREAD INTO SOLID PROPELLANT CRACKS
TEST # 98
PROPELLANT B
CRACK 0.003 IN
SAMPLE HT. = CRACK HT
PRESSURE 750 PSI
CRACK HT. (IN.)
0.00
0.05
0.10
0.15
0.20
0.25
BURN TIME (SEC.)
0.00
0.08
0.16
0.24
0.32
0.40
0.48
0.56
*10^-2

Fig. 16 L.

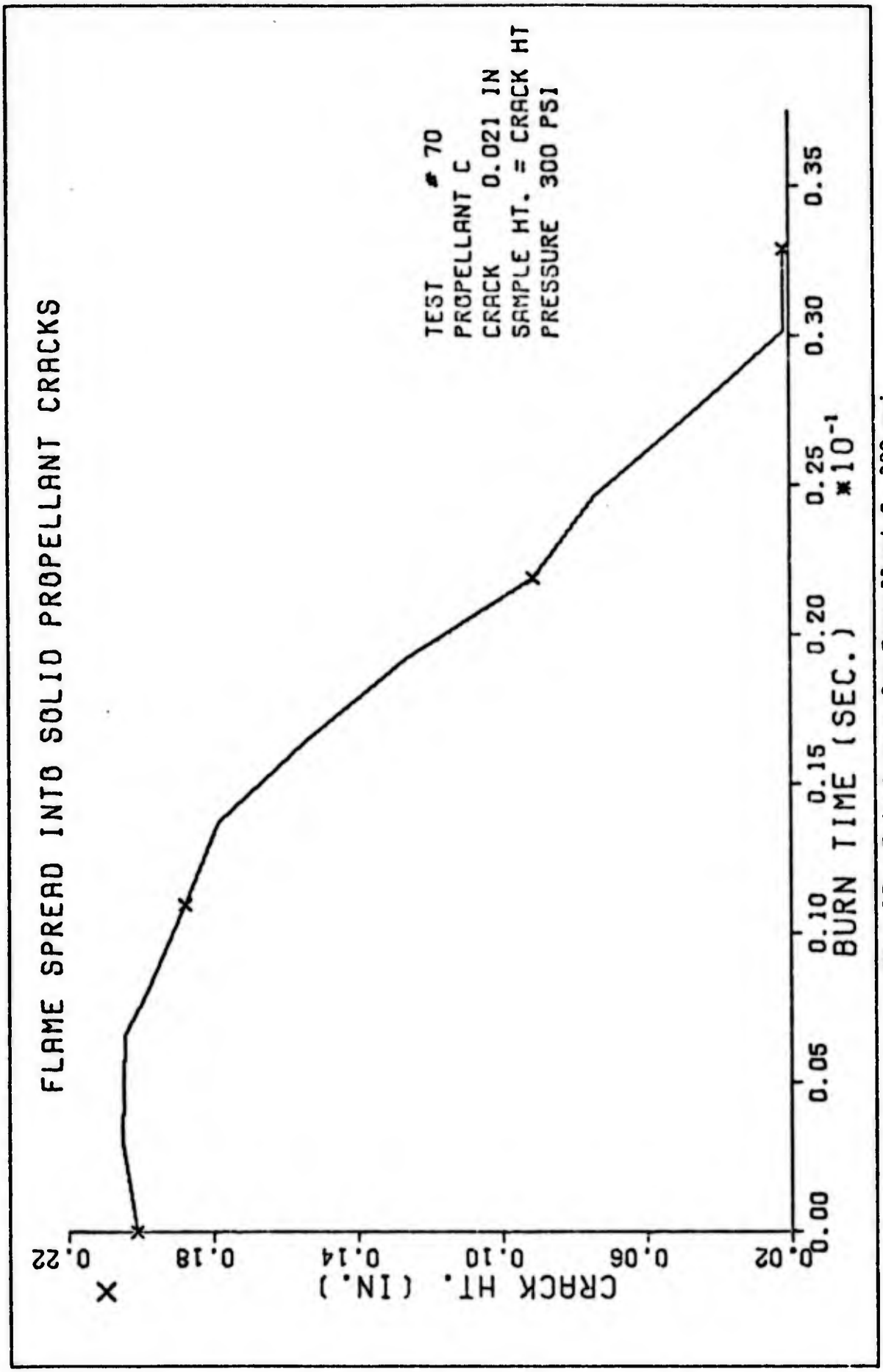

Fig. 17. Data Curves for Propellant C, 300 psi

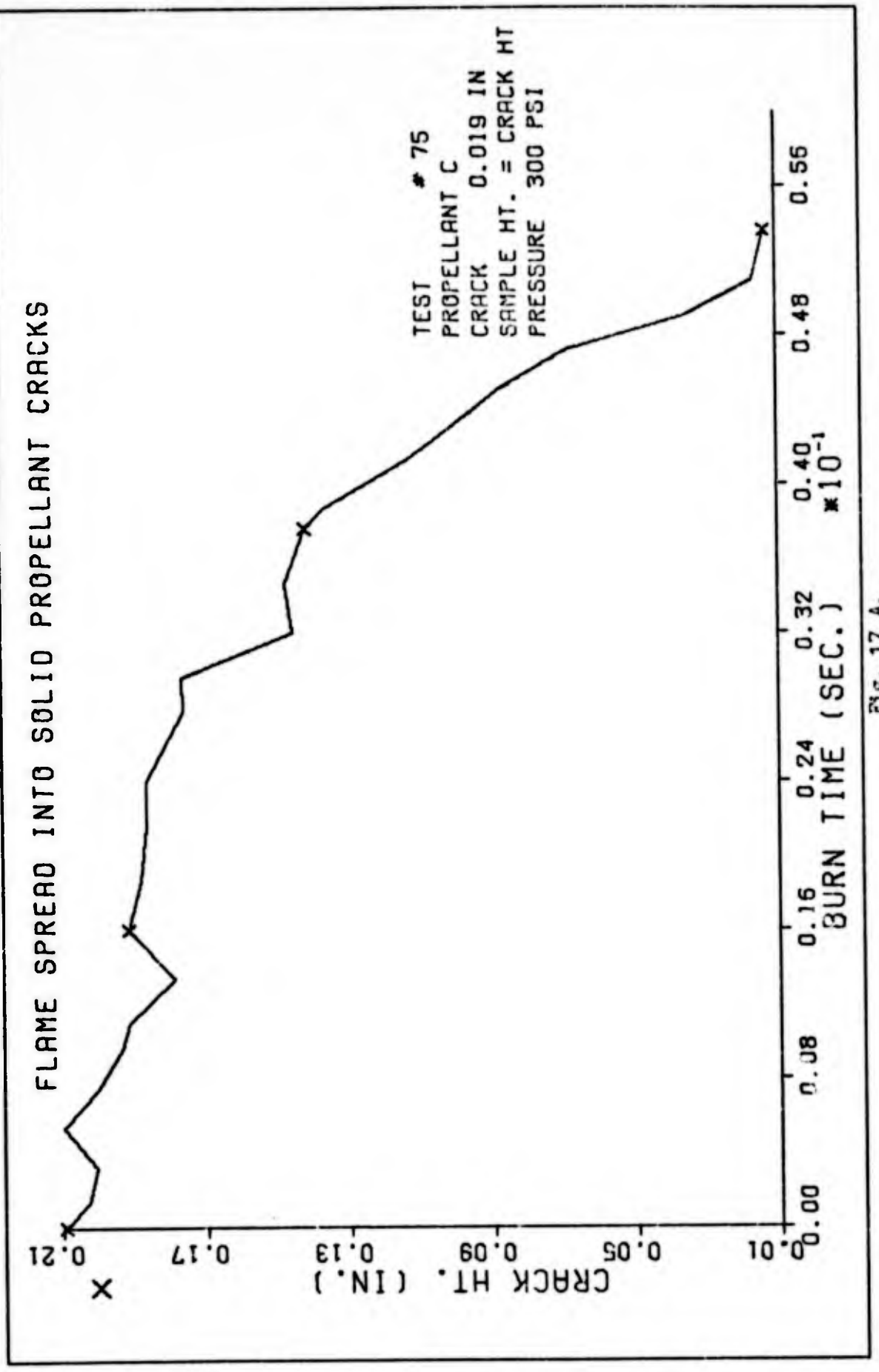
FLAME SPREAD INTO SOLID PROPELLANT CRACKS
TEST # 75
PROPELLANT C
CRACK 0.019 IN
SAMPLE HT. = CRACK HT
PRESSURE 300 PSI
CRACK HT. (IN.)
0.00
0.05
0.09
0.13
0.17
0.21
BURN TIME (SEC.)
0.00
0.08
0.16
0.24
0.32
0.40
0.48
0.56
*10^-1

Fig. 17 A.

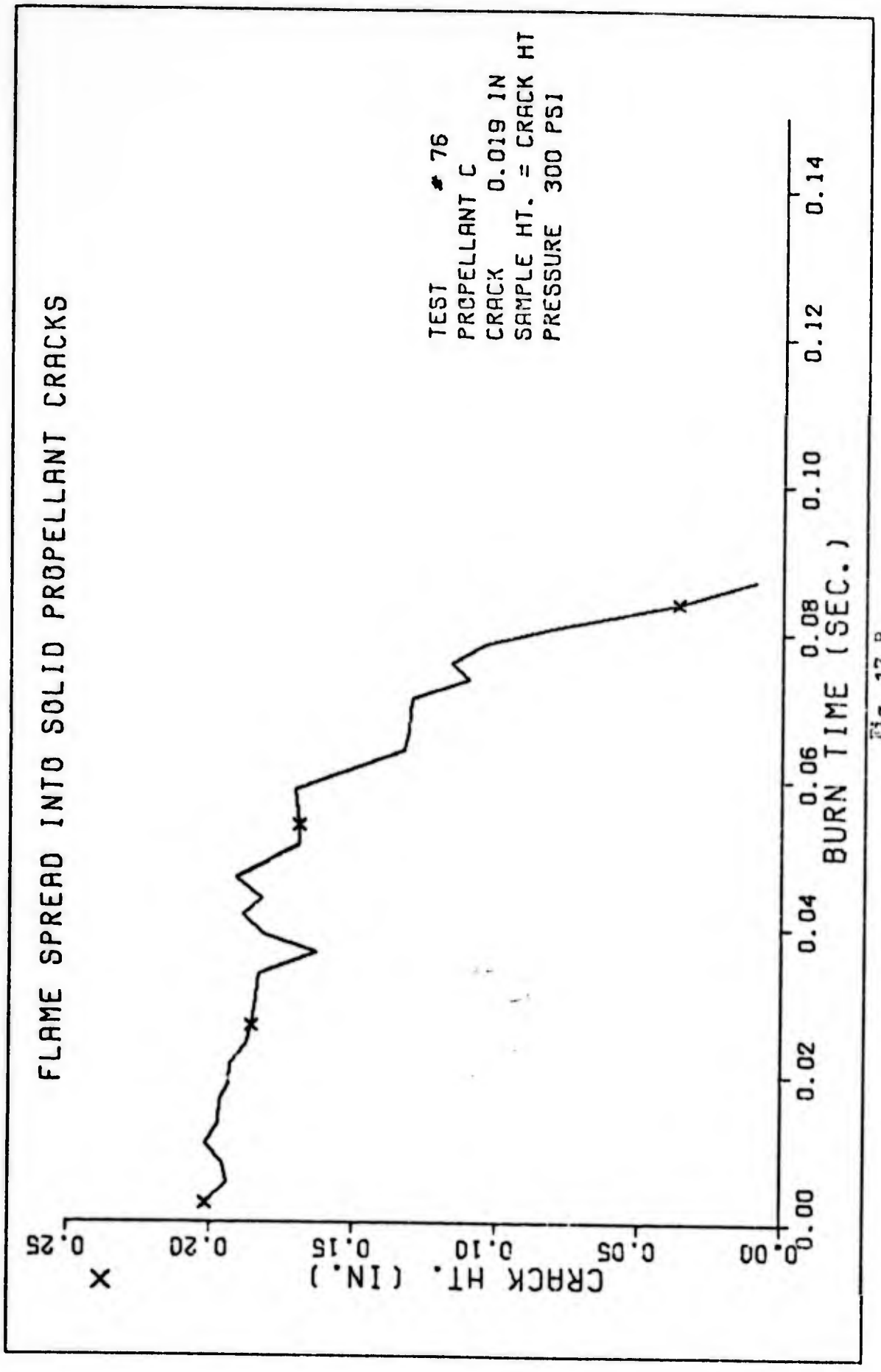
FLAME SPREAD INTO SOLID PROPELLANT CRACKS
TEST # 76
PROPELLANT C
CRACK 0.019 IN
SAMPLE HT. = CRACK HT
PRESSURE 300 PSI
CRACK HT. (IN.)
0.00
0.05
0.10
0.15
0.20
0.25
BURN TIME (SEC.)
0.00
0.02
0.04
0.06
0.08
0.10
0.12
0.14

Fig. 17 B.

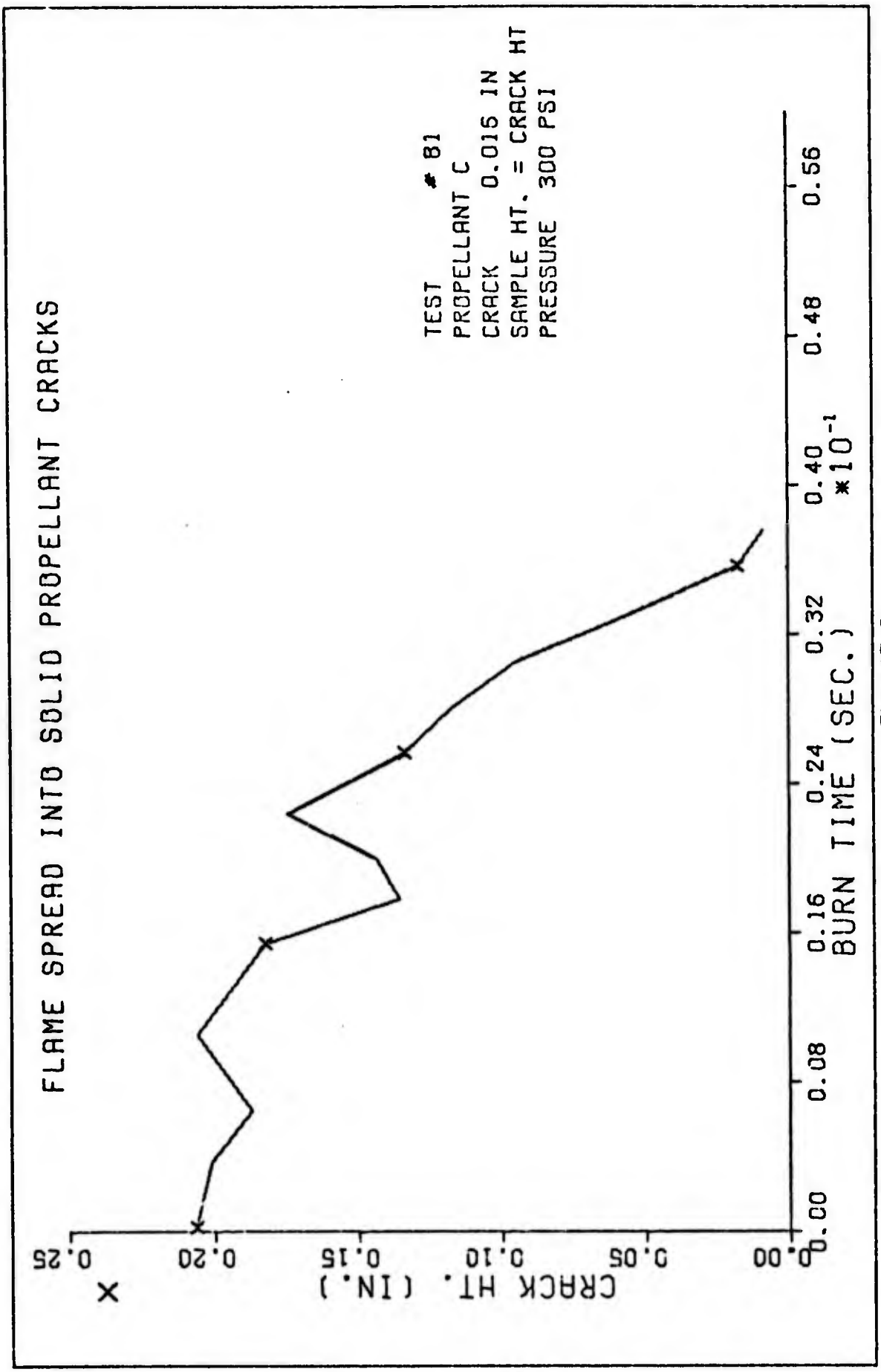
FLAME SPREAD INTO SOLID PROPELLANT CRACKS
TEST # 81
PROPELLANT C
CRACK 0.016 IN
SAMPLE HT. = CRACK HT
PRESSURE 300 PSI
CRACK HT. (IN.)
0.00
0.05
0.10
0.15
0.20
0.25
X
0.00
0.08
0.16
0.24
0.32
0.40
0.48
0.56
BURN TIME (SEC.)
*10⁻¹

Fig. 17 C.

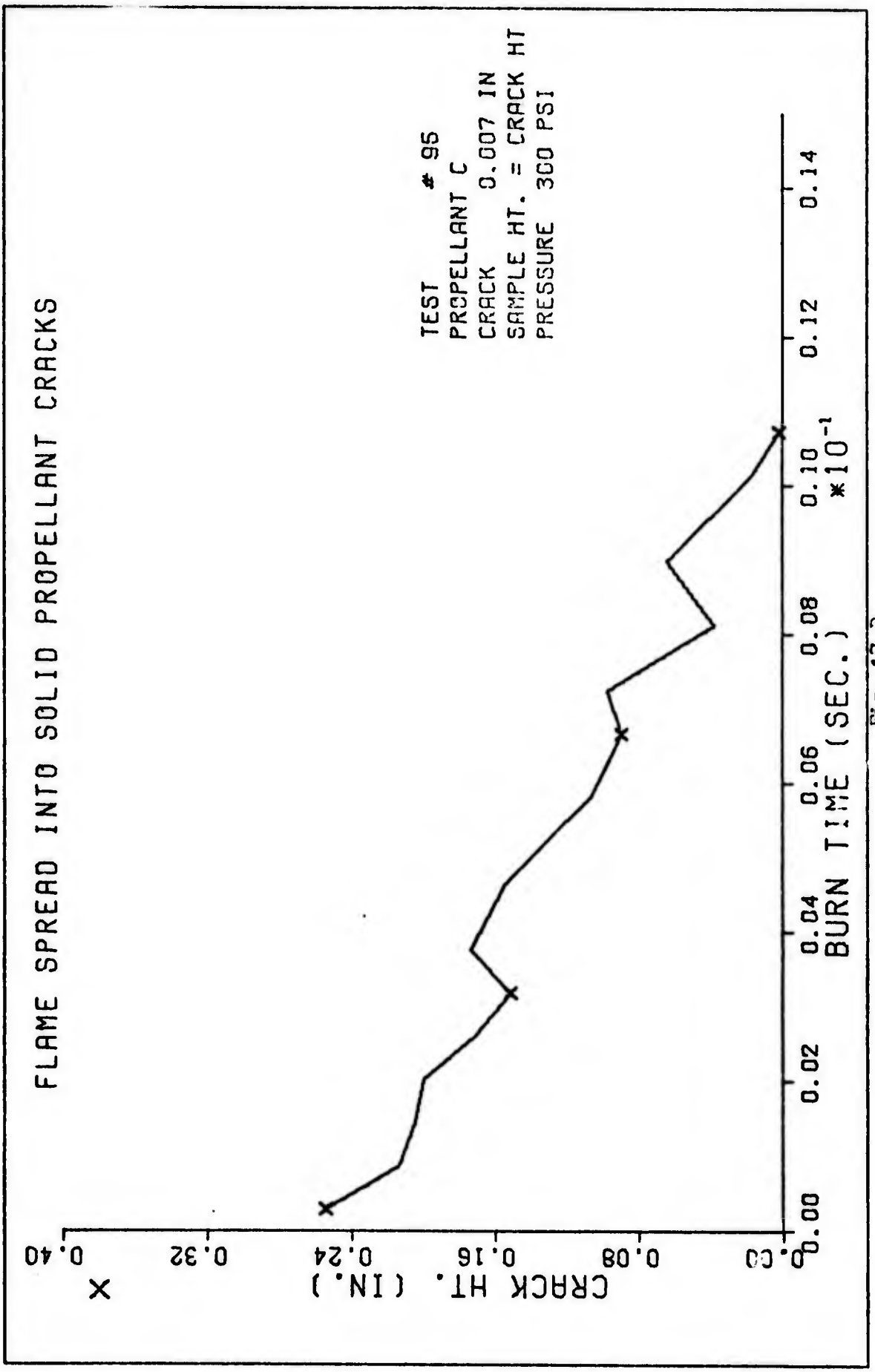
FLAME SPREAD INTO SOLID PROPELLANT CRACKS
TEST # 95
PROPELLANT C
CRACK 0.007 IN
SAMPLE HT. = CRACK HT
PRESSURE 300 PSI
CRACK HT. (IN.)
0.00
0.08
0.16
0.24
0.32
0.40
X
0.00
0.02
0.04
0.06
0.08
0.10
0.12
0.14
BURN TIME (SEC.)
*10⁻¹

Fig. 17 b.

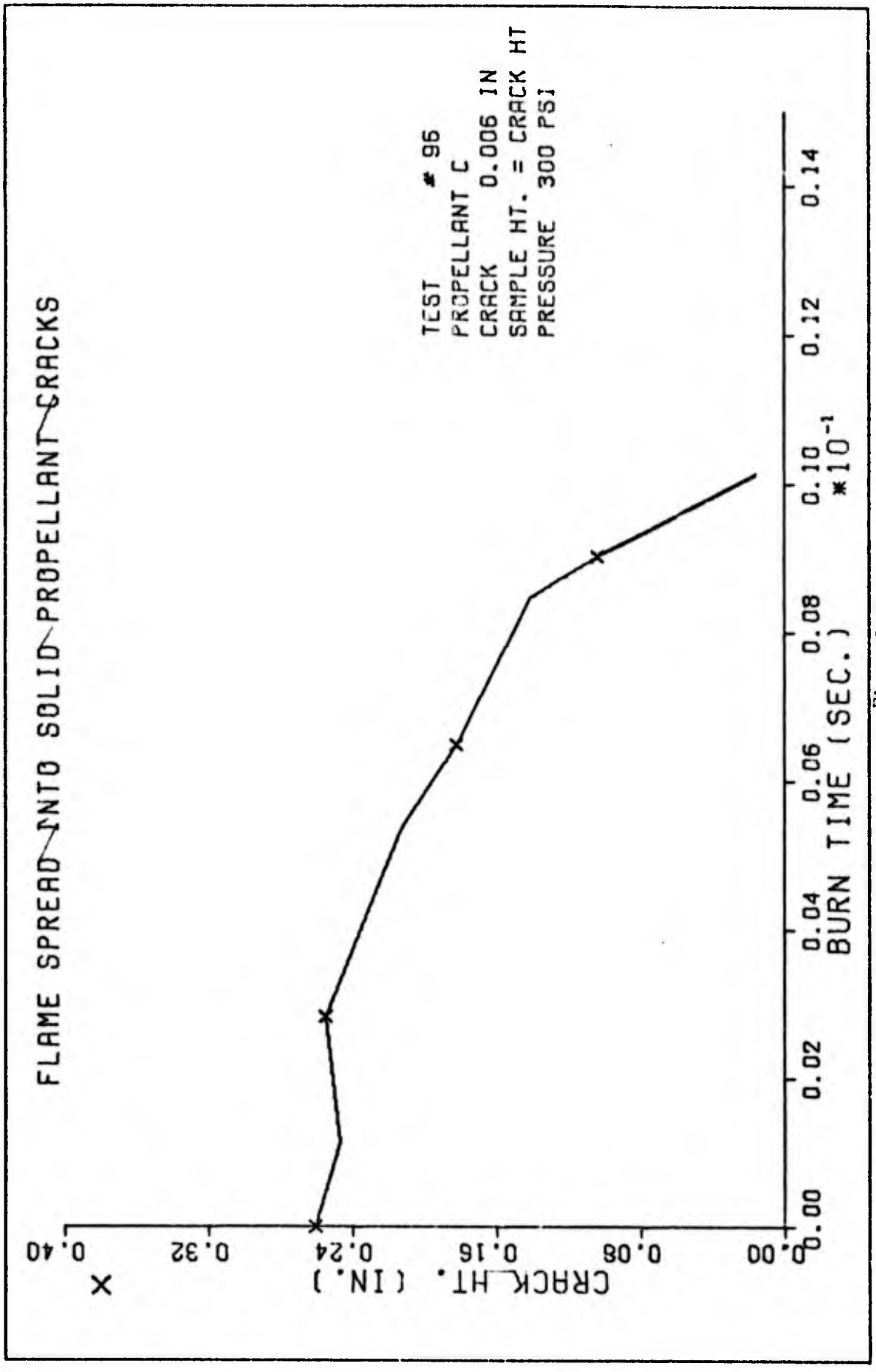
FLAME SPREAD INTO SOLID PROPELLANT CRACKS
TEST # 96
PROPELLANT C
CRACK 0.006 IN
SAMPLE HT. = CRACK HT
PRESSURE 300 PSI
CRACK HT. (IN.)
0.00
0.08
0.16
0.24
0.32
0.40
0.00
0.02
0.04
0.06
0.08
0.10
0.12
0.14
BURN TIME (SEC.)
*10⁻¹

Fig. 17 E.

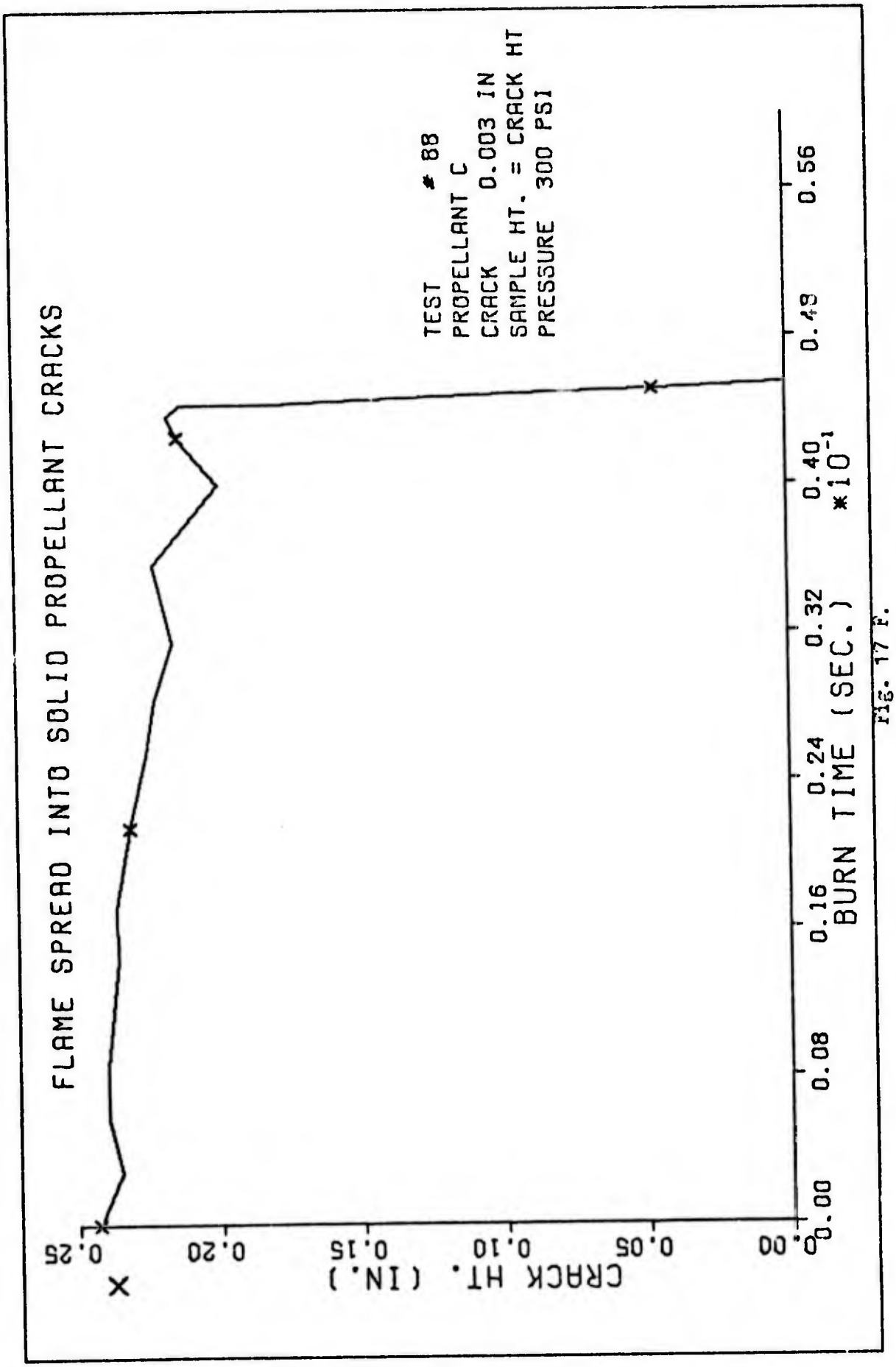
FLAME SPREAD INTO SOLID PROPELLANT CRACKS
TEST # 88
PROPELLANT C
CRACK 0.003 IN
SAMPLE HT. = CRACK HT
PRESSURE 300 PSI
CRACK HT. (IN.)
0.00
0.05
0.10
0.15
0.20
0.25
BURN TIME (SEC.)
0.00
0.08
0.16
0.24
0.32
0.40
0.48
0.56
*10^-1

Fig. 17 F.

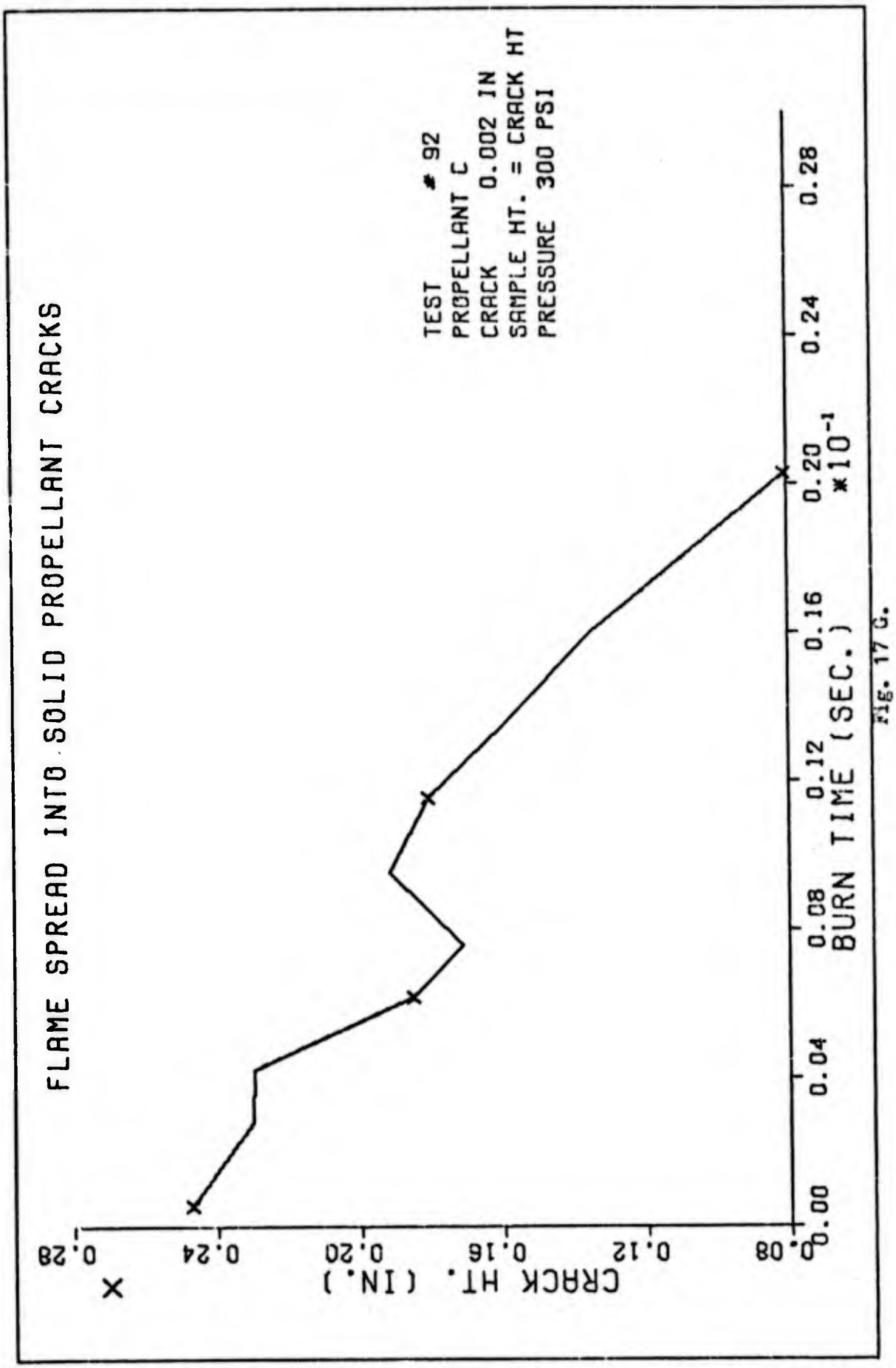
FLAME SPREAD INTO SOLID PROPELLANT CRACKS
TEST # 92
PROPELLANT C
CRACK 0.002 IN
SAMPLE HT. = CRACK HT
PRESSURE 300 PSI
CRACK HT. (IN.)
0.00
0.04
0.08
0.12
0.16
0.20
0.24
0.28
BURN TIME (SEC.)
*10⁻¹

Fig. 17 c.

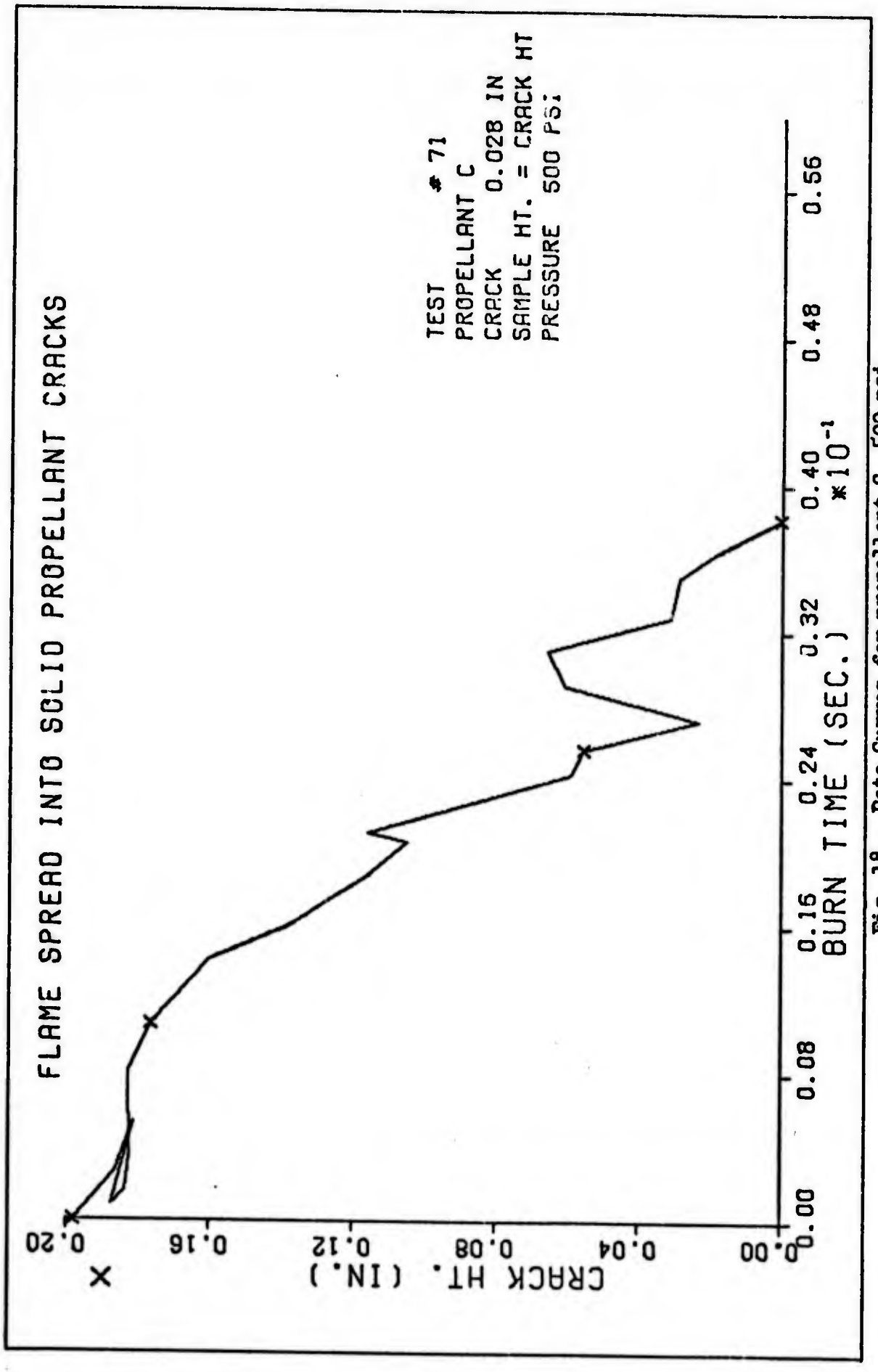

Fig. 18. Data Curves for propellant C, 500 psi

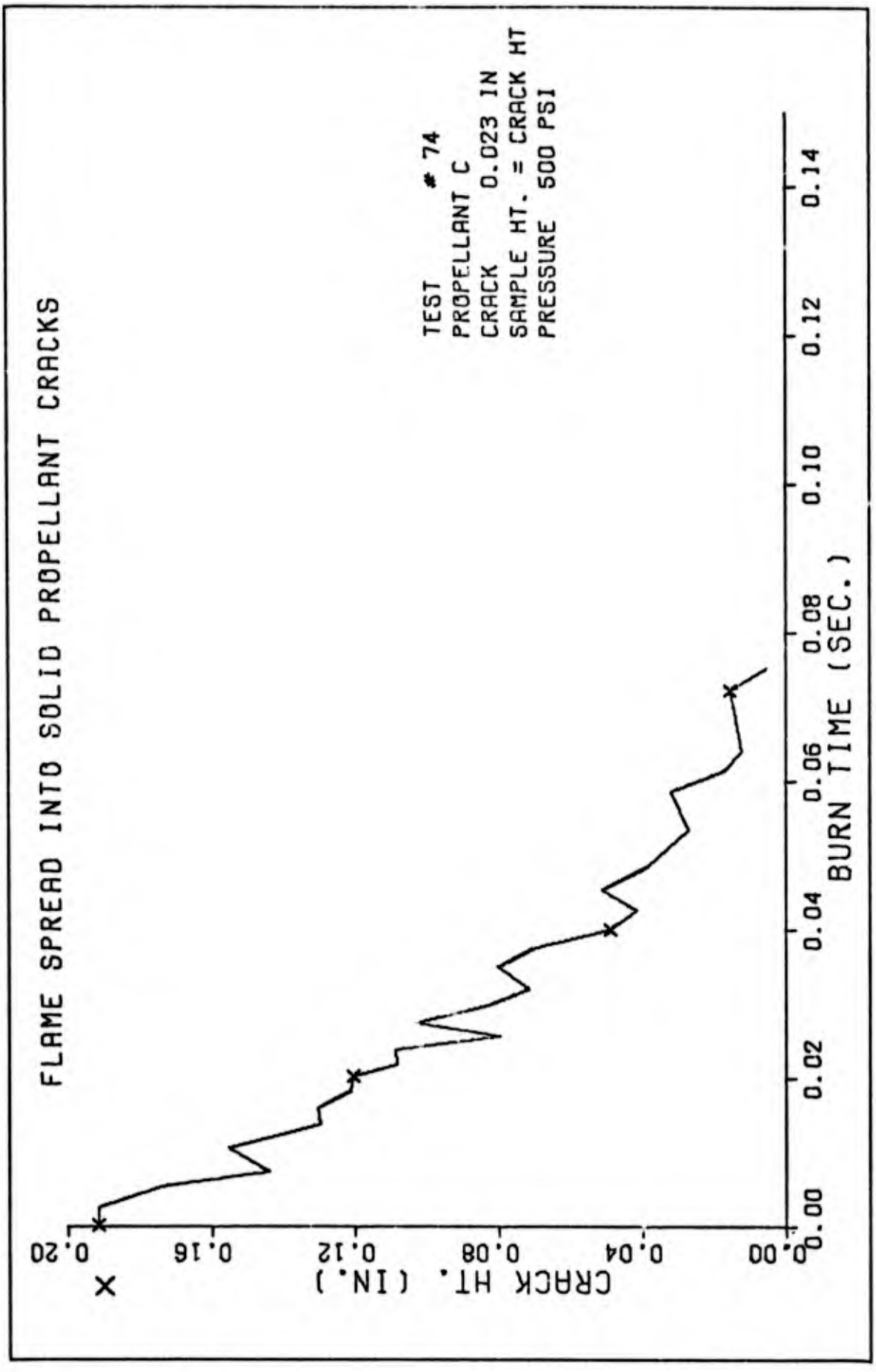
FLAME SPREAD INTO SOLID PROPELLANT CRACKS
TEST # 74
PROPELLANT C
CRACK 0.023 IN
SAMPLE HT. = CRACK HT
PRESSURE 500 PSI
CRACK HT. (IN.)
0.00
0.04
0.08
0.12
0.16
0.20
BURN TIME (SEC.)
0.00
0.02
0.04
0.06
0.08
0.10
0.12
0.14

Fig. 18 A.

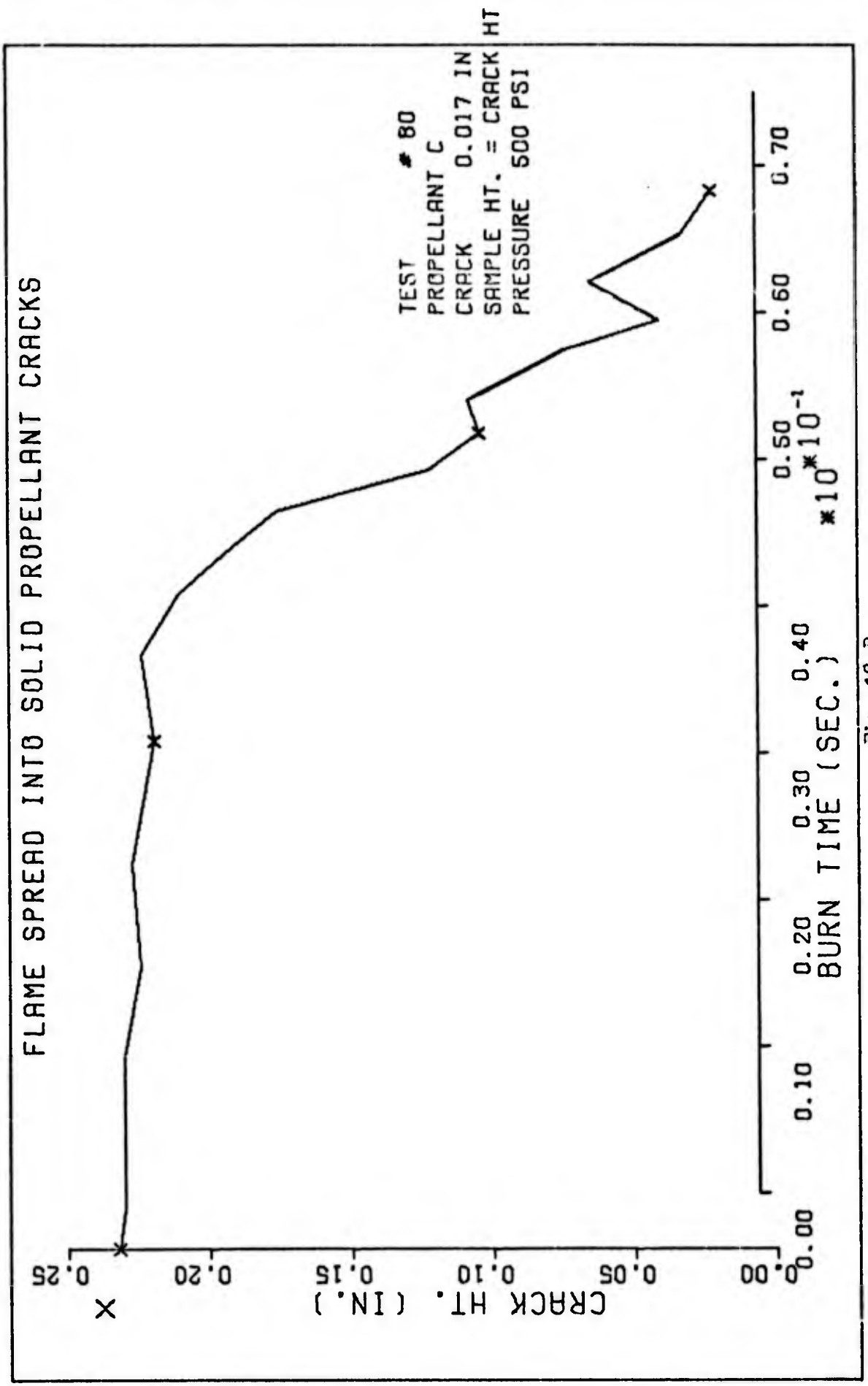
FLAME SPREAD INTO SOLID PROPELLANT CRACKS
TEST # 80
PROPELLANT C
CRACK 0.017 IN
SAMPLE HT. = CRACK HT
PRESSURE 500 PSI
CRACK HT. (IN.)
0.00
0.05
0.10
0.15
0.20
0.25
BURN TIME (SEC.)
0.00
0.10
0.20
0.30
0.40
0.50
0.60
0.70
*10*10⁻¹

Fig. 18 B.

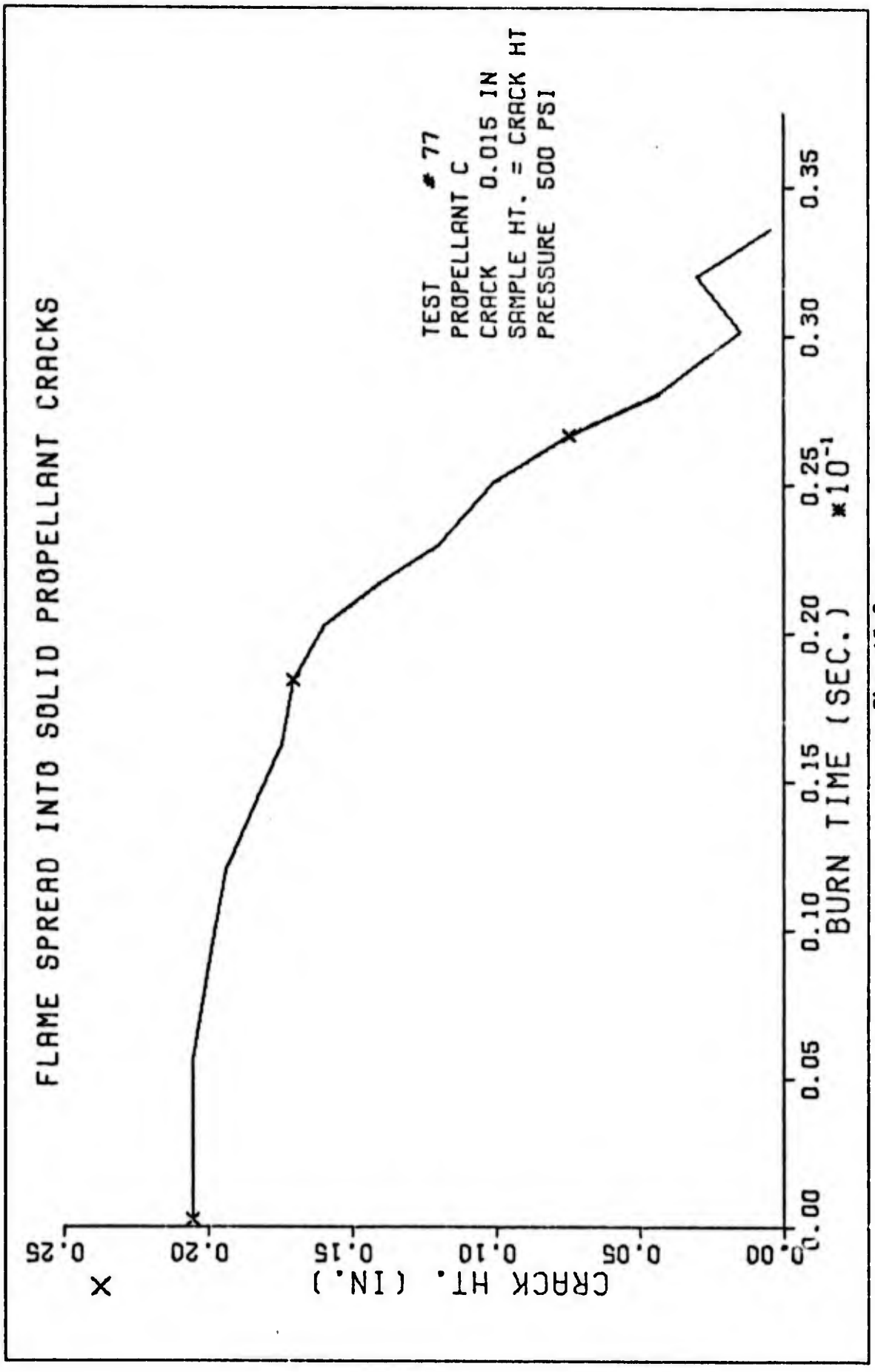
FLAME SPREAD INTO SOLID PROPELLANT CRACKS
TEST # 77
PROPELLANT C
CRACK 0.015 IN
SAMPLE HT. = CRACK HT
PRESSURE 500 PSI
CRACK HT. (IN.)
0.00
0.05
0.10
0.15
0.20
0.25
BURN TIME (SEC.)
0.00
0.05
0.10
0.15
0.20
0.25
0.30
0.35
*10⁻¹

Fig. 18 C.

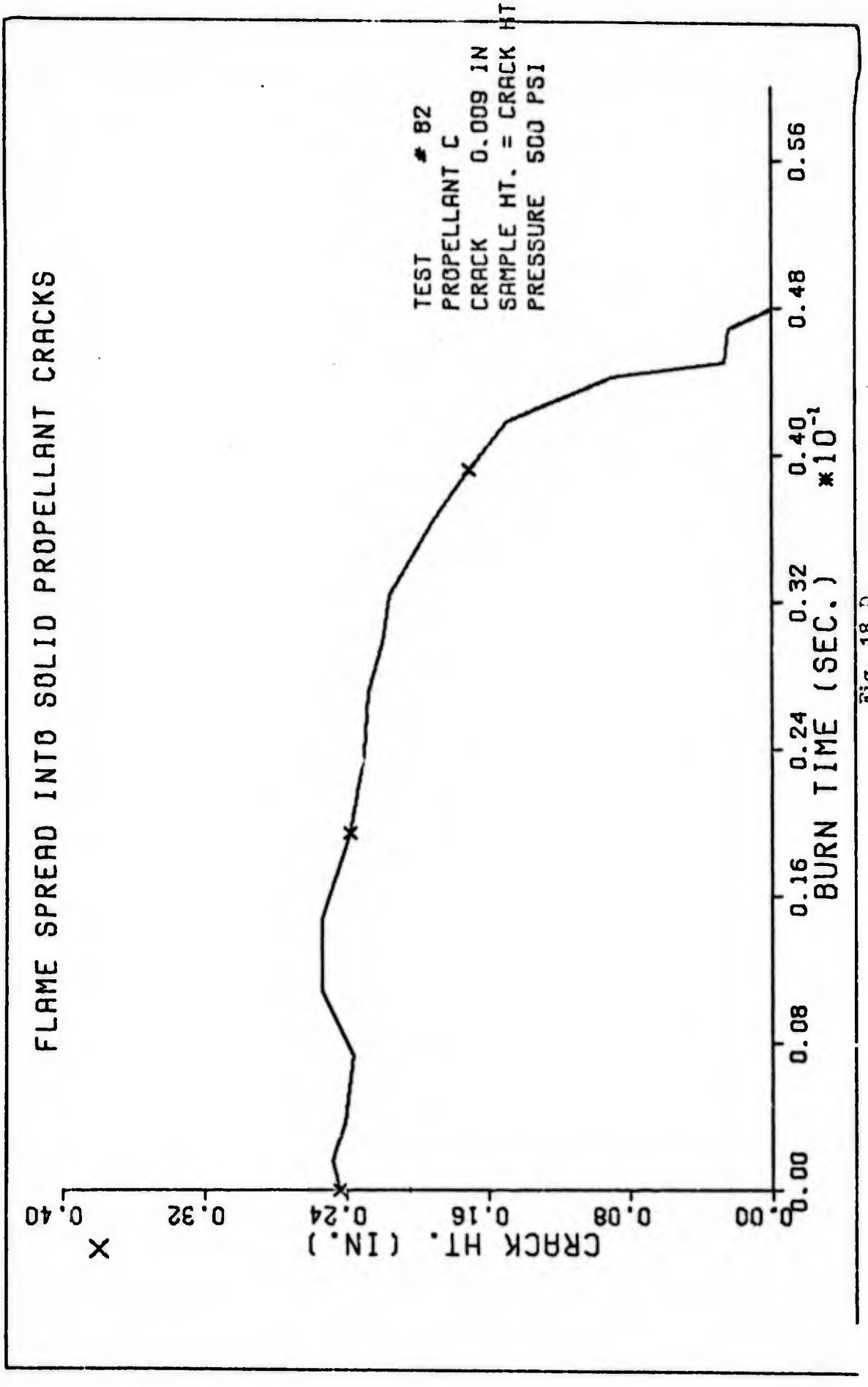
FLAME SPREAD INTO SOLID PROPELLANT CRACKS
TEST # 82
PROPELLANT C
CRACK 0.009 IN
SAMPLE HT. = CRACK HT
PRESSURE 500 PSI
CRACK HT. (IN.)
0.00
0.08
0.16
0.24
0.32
0.40
X
BURN TIME (SEC.)
0.00
0.08
0.16
0.24
0.32
0.40
0.48
0.56
*10⁻¹

Fig. 18 D.

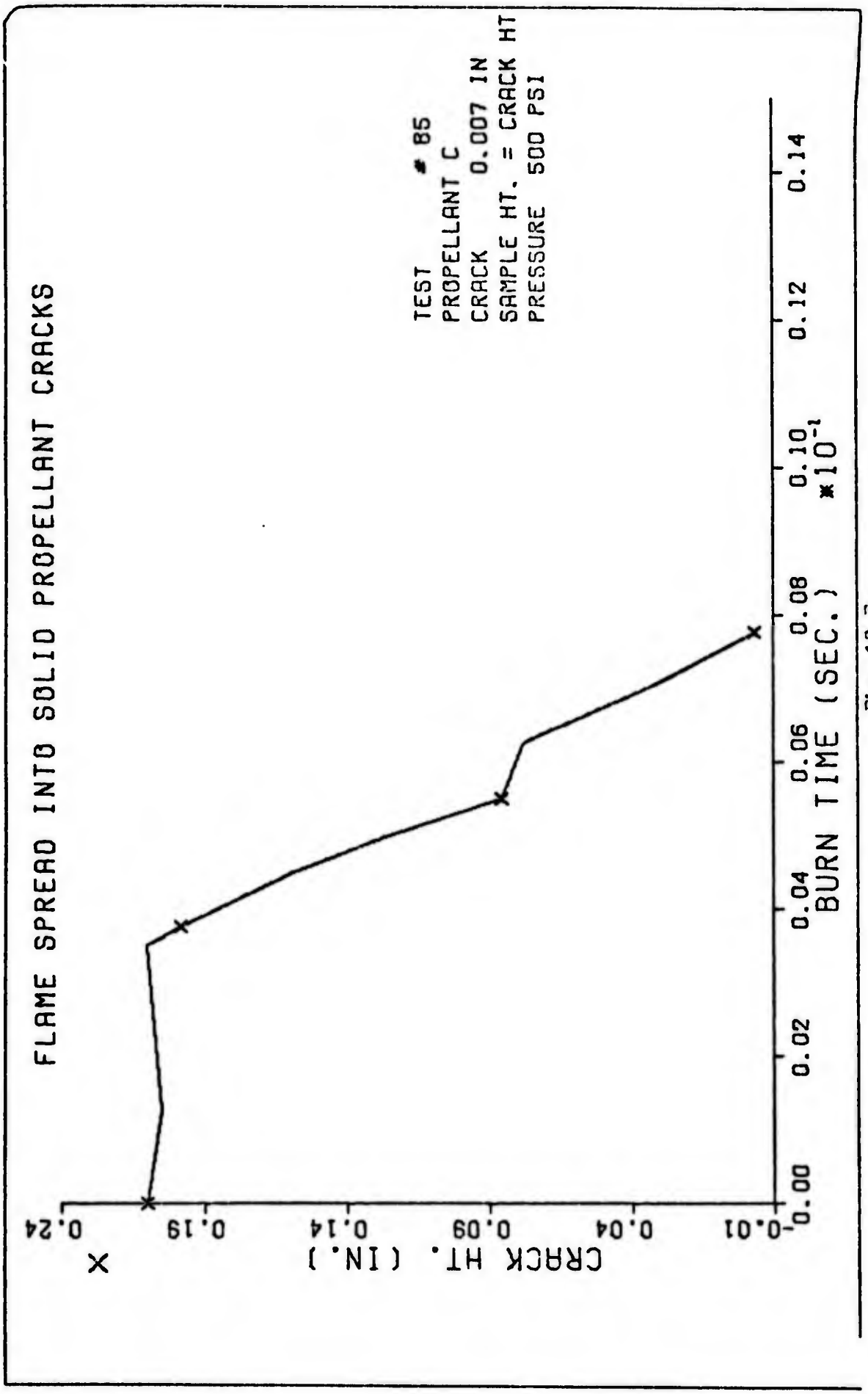
FLAME SPREAD INTO SOLID PROPELLANT CRACKS
TEST # 85
PROPELLANT C
CRACK 0.007 IN
SAMPLE HT. = CRACK HT
PRESSURE 500 PSI
CRACK HT. (IN.)
0.24
0.19
0.14
0.09
0.04
-0.01
0.00
0.02
0.04
0.06
0.08
0.10
0.12
0.14
BURN TIME (SEC.)
*10^-1

Fig. 18 3.

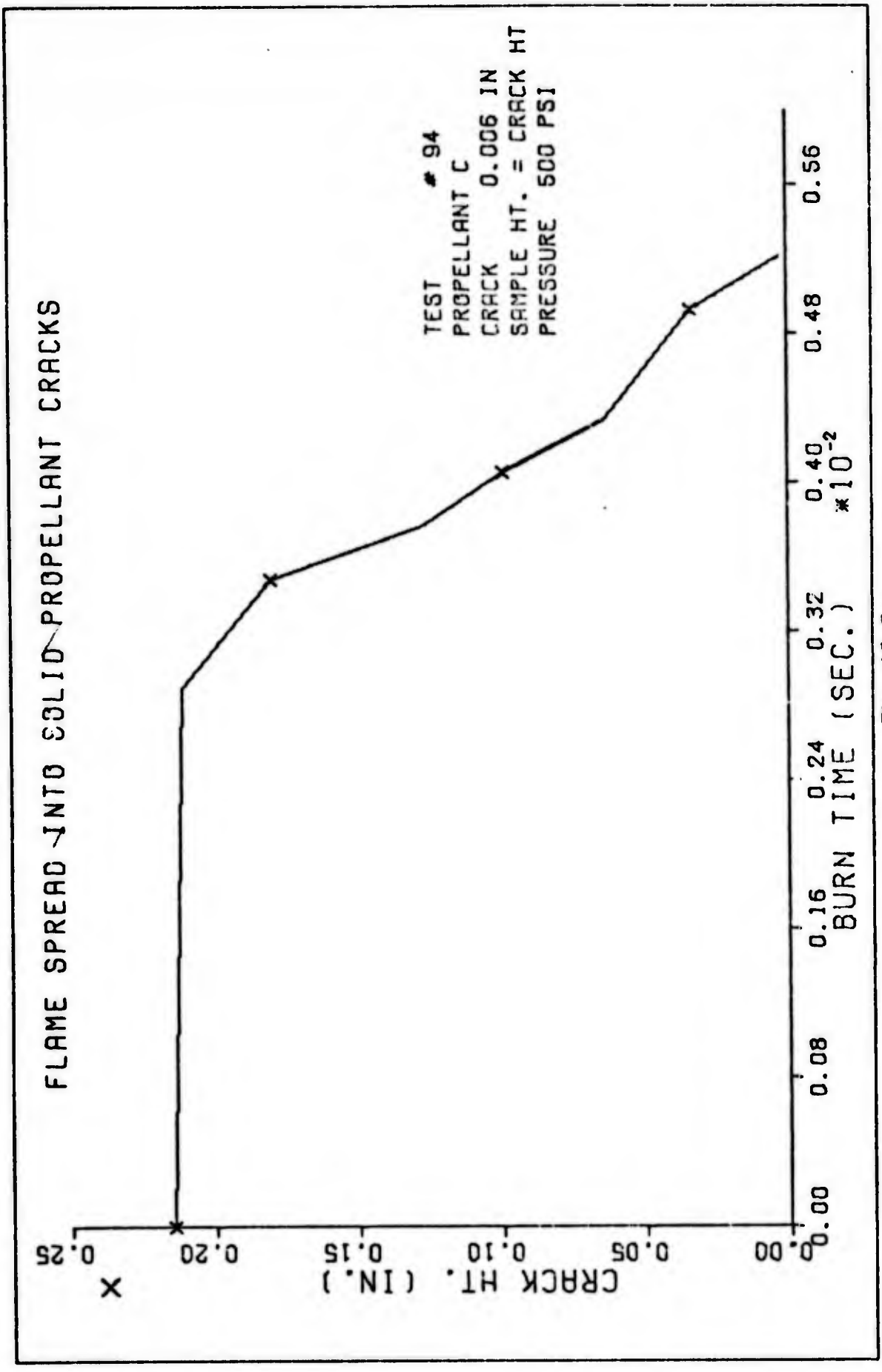
FLAME SPREAD INTO SOLID PROPELLANT CRACKS
TEST # 94
PROPELLANT C
CRACK 0.006 IN
SAMPLE HT. = CRACK HT
PRESSURE 500 PSI
CRACK HT. (IN.)
0.00
0.05
0.10
0.15
0.20
0.25
BURN TIME (SEC.)
0.00
0.08
0.16
0.24
0.32
0.40
0.48
0.56
*10^-2

Fig. 18 F.

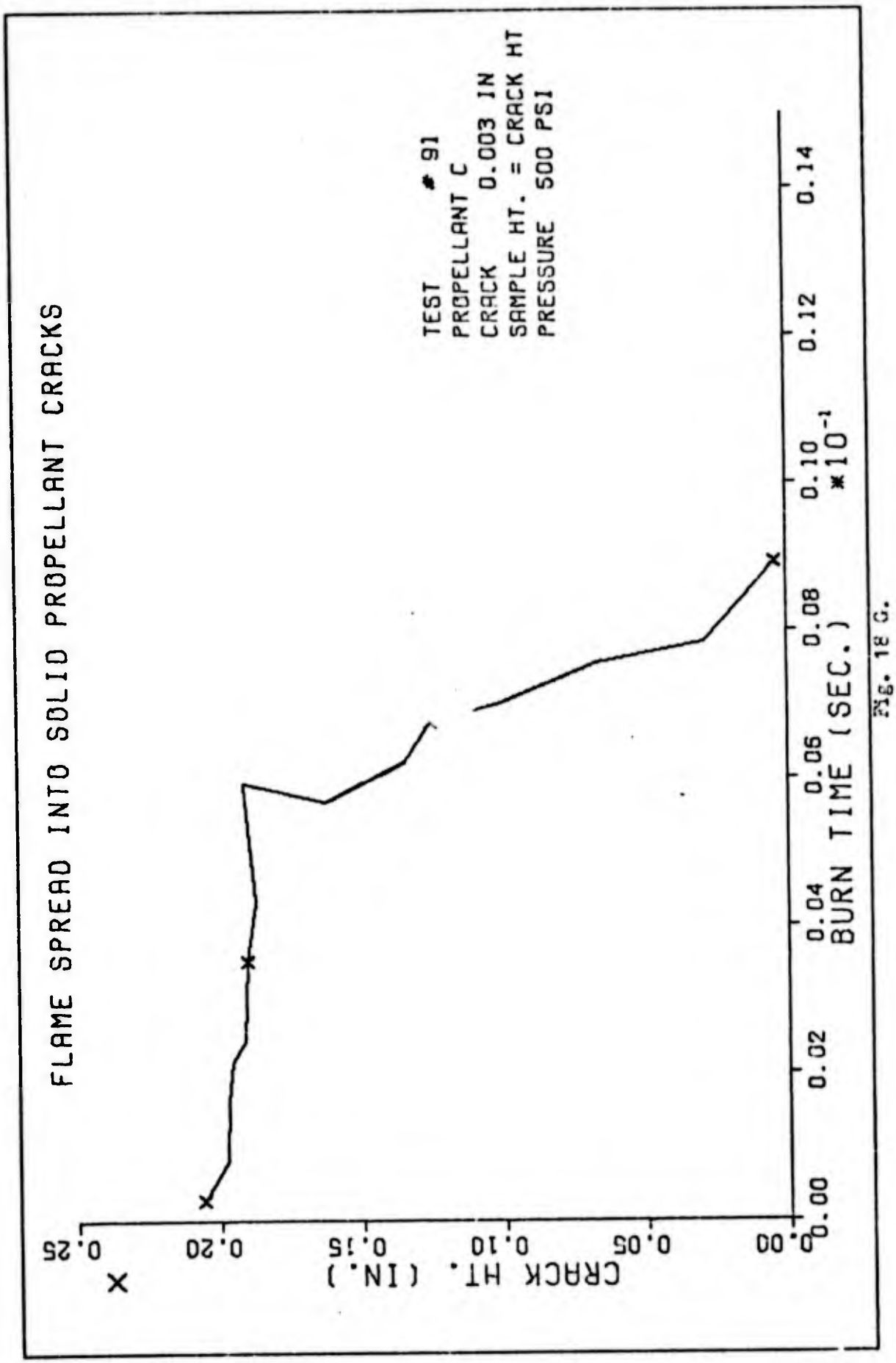
FLAME SPREAD INTO SOLID PROPELLANT CRACKS
TEST # 91
PROPELLANT C
CRACK 0.003 IN
SAMPLE HT. = CRACK HT
PRESSURE 500 PSI
CRACK HT. (IN.)
0.00
0.05
0.10
0.15
0.20
0.25
X
0.00
0.02
0.04
0.06
0.08
0.10
0.12
0.14
BURN TIME (SEC.)
*10⁻¹

Fig. 18 c.

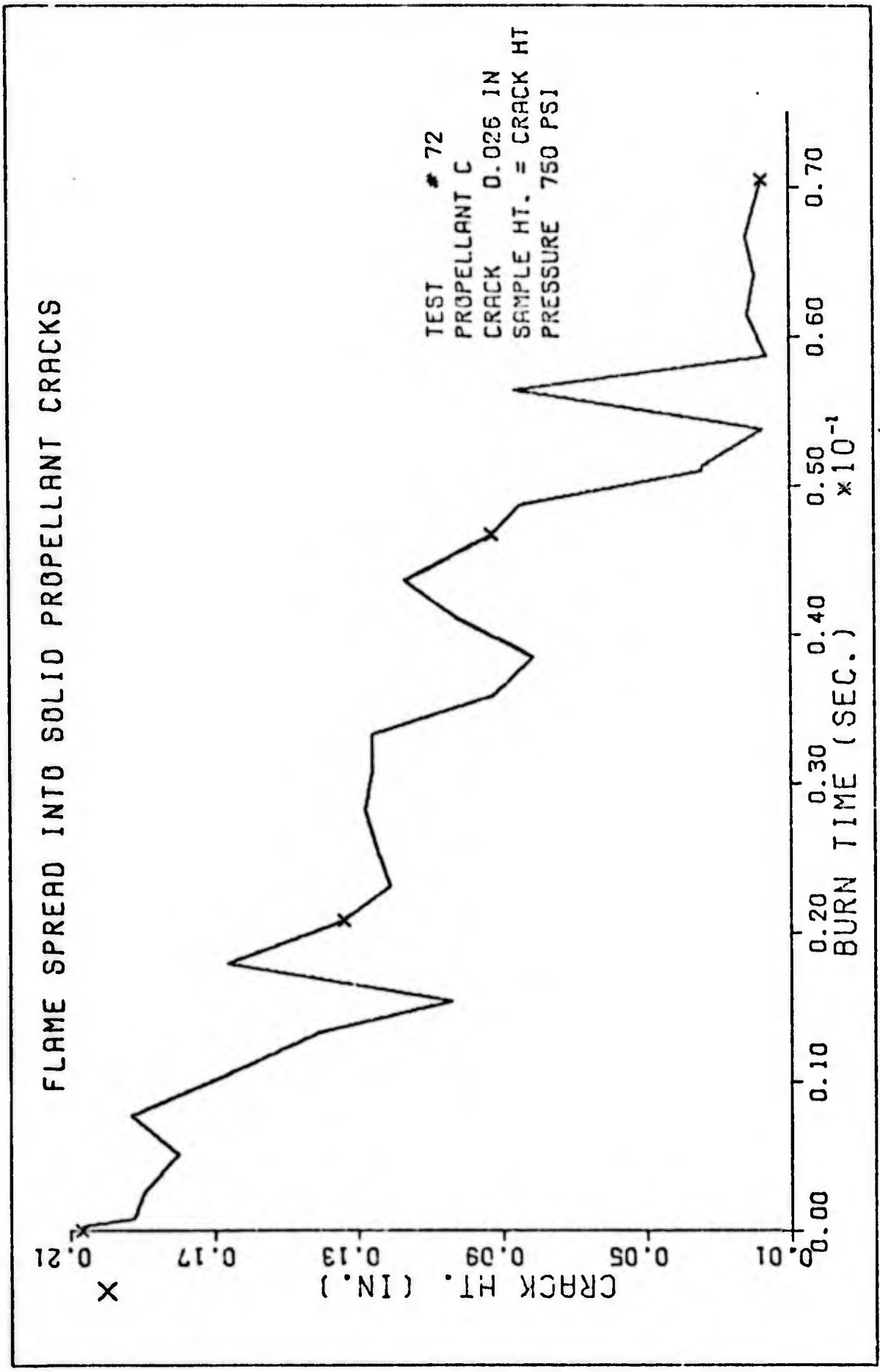

Fig. 19. Data Curves for Propellant C, 750 psi

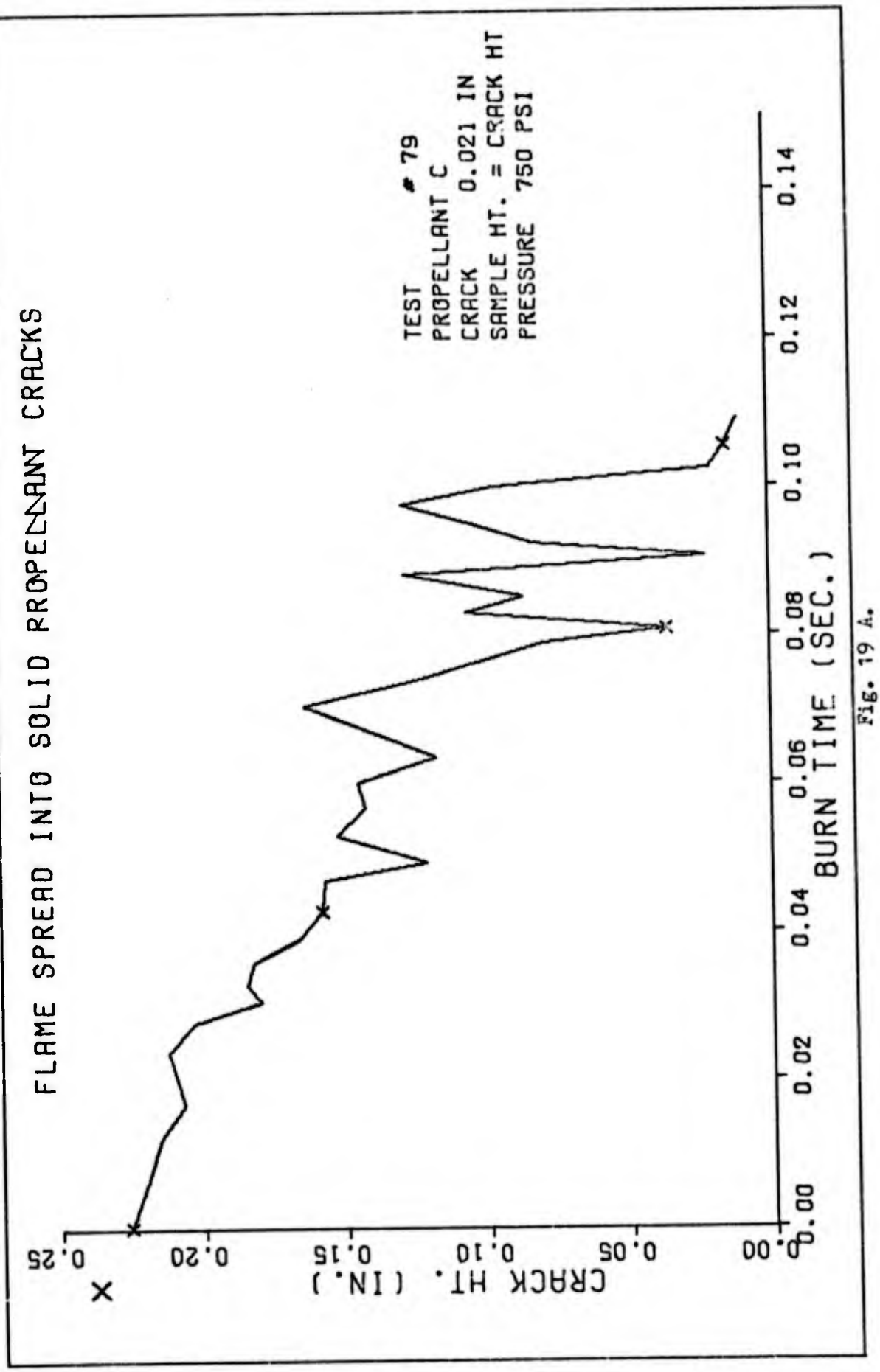
FLAME SPREAD INTO SOLID PROPELLANT CRACKS
TEST # 79
PROPELLANT C
CRACK 0.021 IN
SAMPLE HT. = CRACK HT
PRESSURE 750 PSI
CRACK HT. (IN.)
0.00
0.05
0.10
0.15
0.20
0.25
BURN TIME (SEC.)
0.00
0.02
0.04
0.06
0.08
0.10
0.12
0.14

Fig. 19 A.

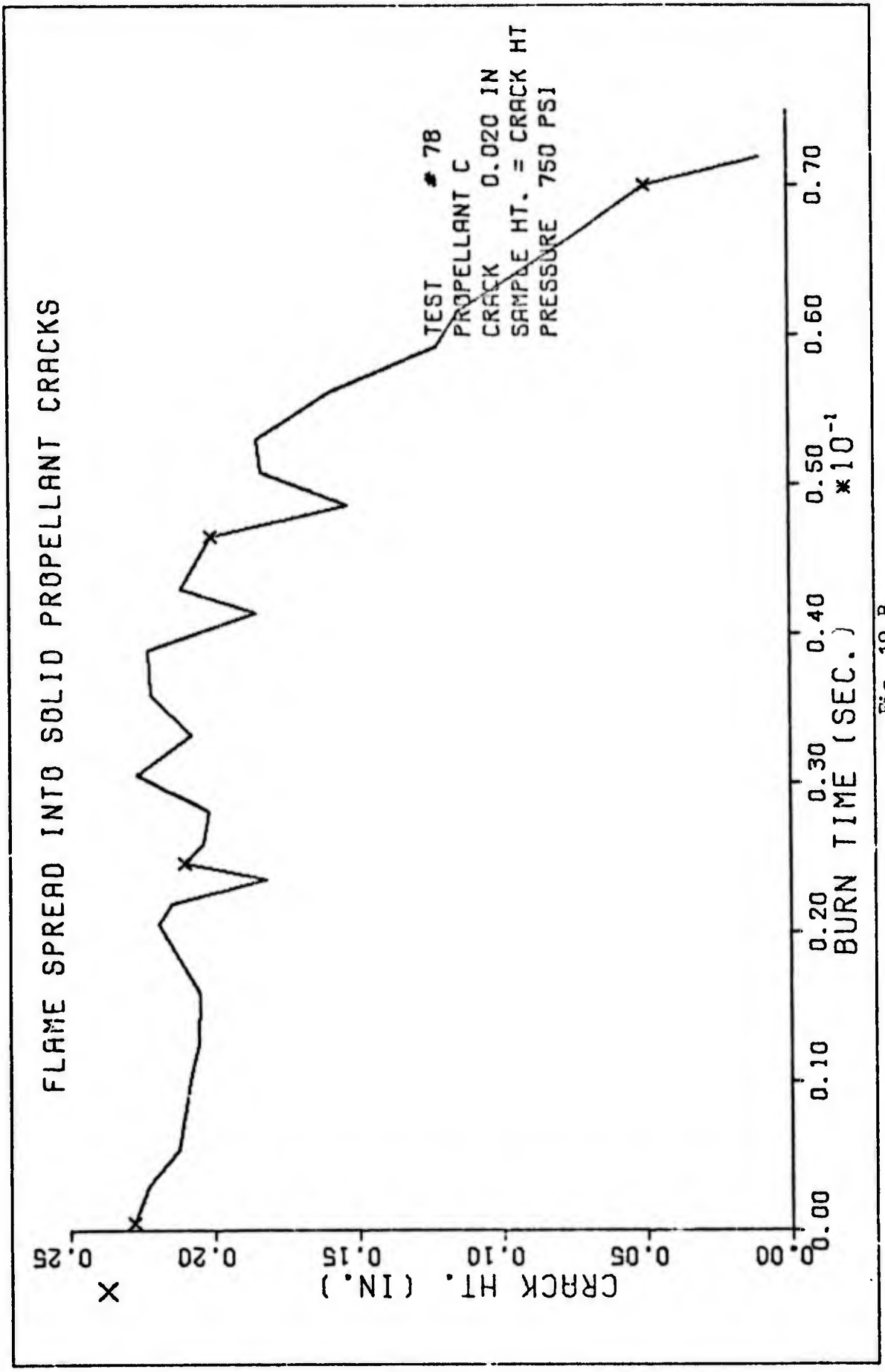
FLAME SPREAD INTO SOLID PROPELLANT CRACKS
TEST # 78
PROPELLANT C
CRACK 0.020 IN
SAMPLE HT. = CRACK HT
PRESSURE 750 PSI
CRACK HT. (IN.)
0.00
0.05
0.10
0.15
0.20
0.25
BURN TIME (SEC.)
0.00
0.10
0.20
0.30
0.40
0.50
0.60
0.70
*10⁻¹

Fig. 19 B.

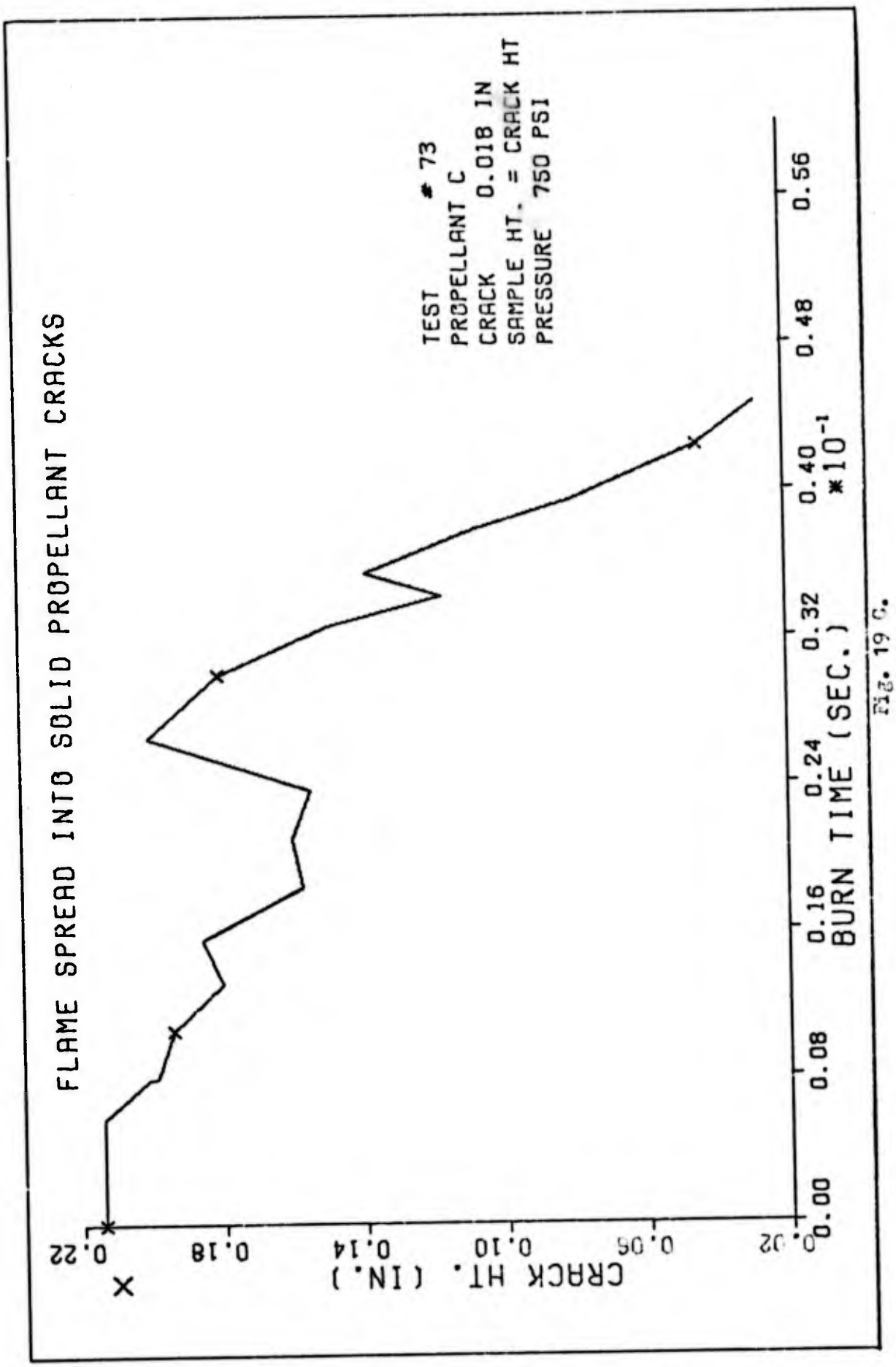
FLAME SPREAD INTO SOLID PROPELLANT CRACKS
TEST # 73
PROPELLANT C
CRACK 0.018 IN
SAMPLE HT. = CRACK HT
PRESSURE 750 PSI
CRACK HT. (IN.)
0.00
0.02
0.05
0.10
0.14
0.18
0.22
0.00
0.08
0.16
0.24
0.32
0.40
0.48
0.56
BURN TIME (SEC.)
*10⁻¹

Fig. 19 c.

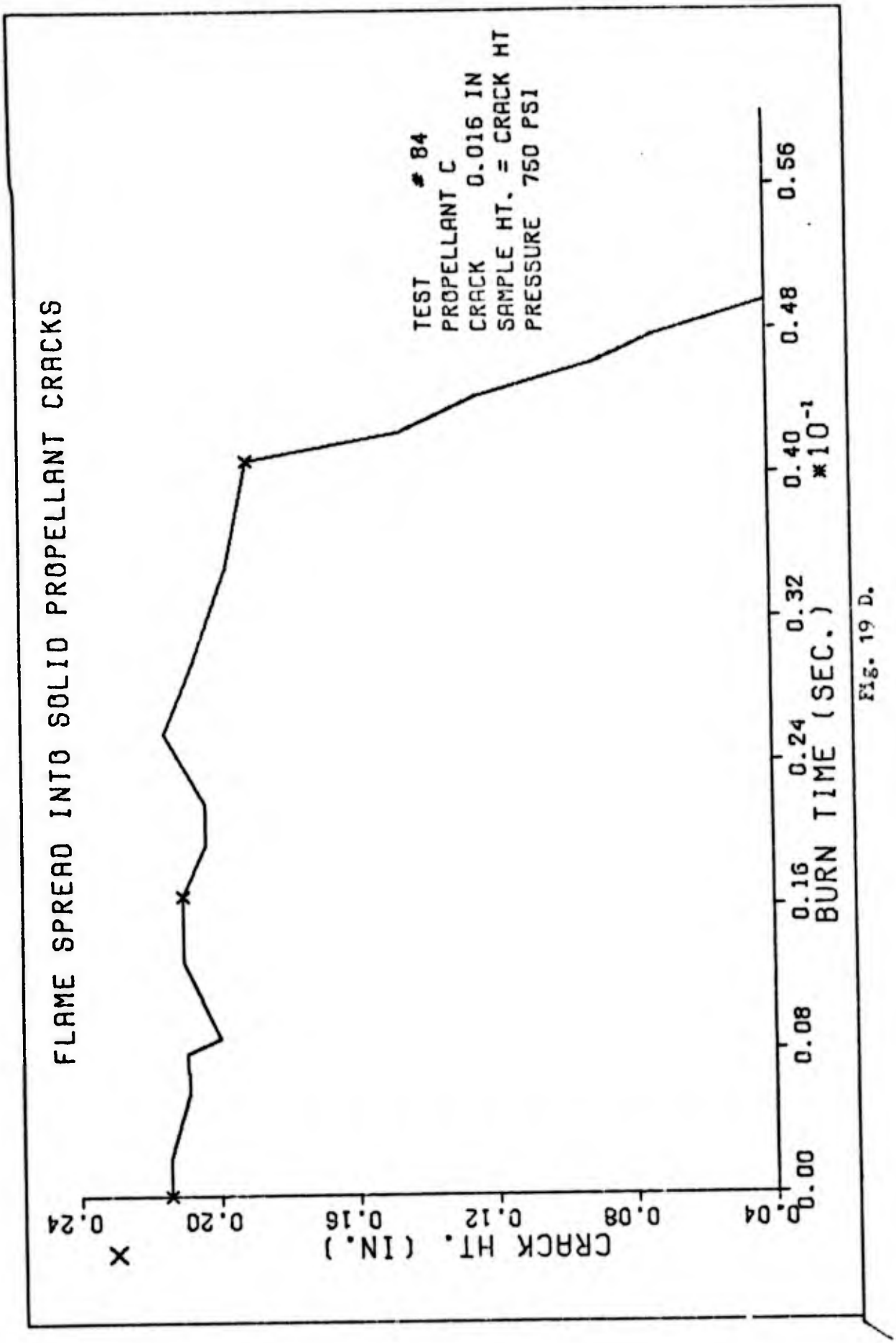
FLAME SPREAD INTO SOLID PROPELLANT CRACKS
TEST # 84
PROPELLANT C
CRACK 0.016 IN
SAMPLE HT. = CRACK HT
PRESSURE 750 PSI
CRACK HT. (IN.)
0.04
0.08
0.12
0.16
0.20
0.24
X
0.00
0.08
0.16
0.24
0.32
0.40
0.48
0.56
BURN TIME (SEC.)
*10⁻¹

Fig. 19 D.

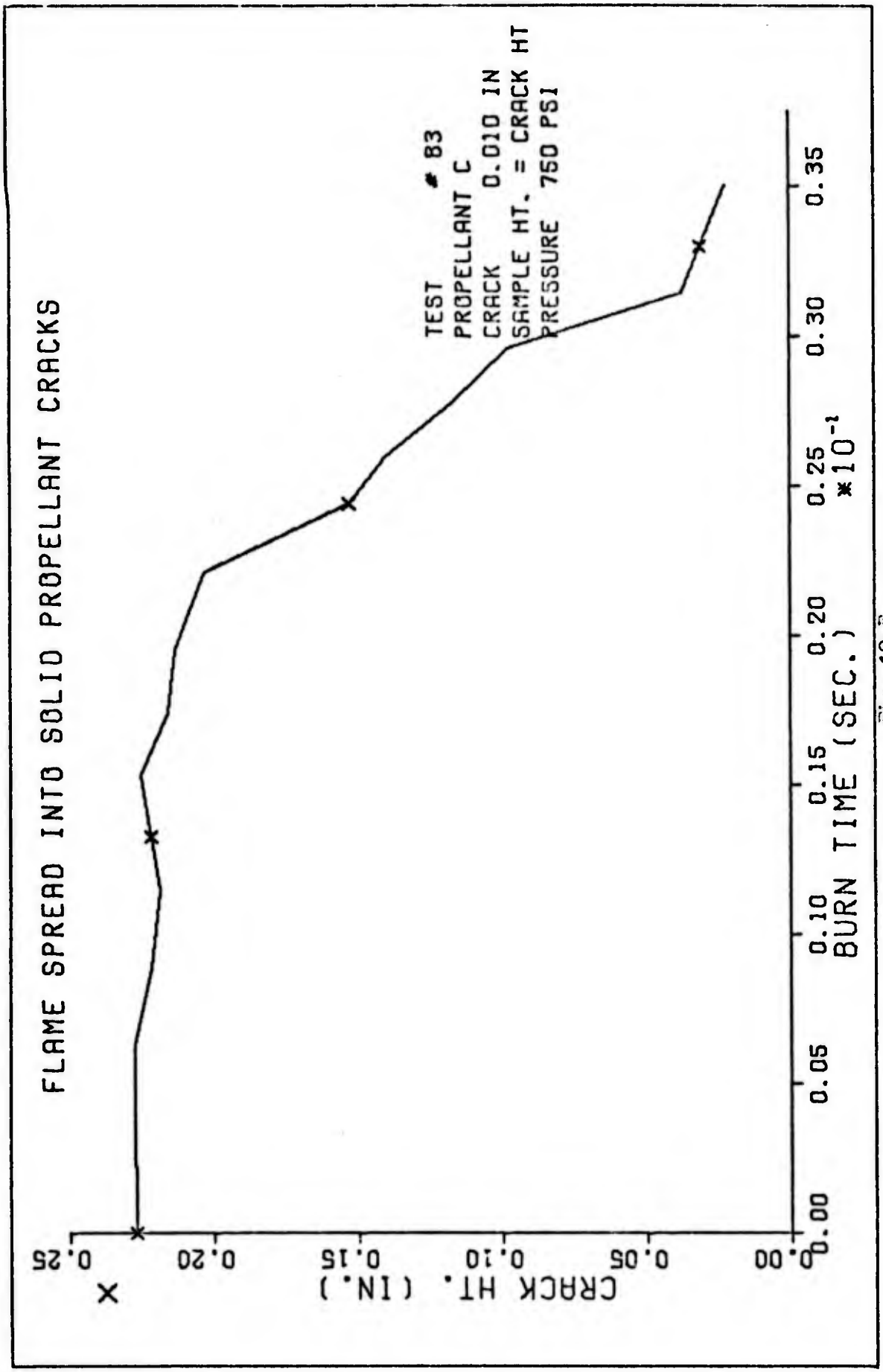
FLAME SPREAD INTO SOLID PROPELLANT CRACKS
TEST # 83
PROPELLANT C
CRACK 0.010 IN
SAMPLE HT. = CRACK HT
PRESSURE 750 PSI
CRACK HT. (IN.)
0.00
0.05
0.10
0.15
0.20
0.25
BURN TIME (SEC.)
*10⁻¹
0.00
0.05
0.10
0.15
0.20
0.25
0.30
0.35

Fig. 19 E.

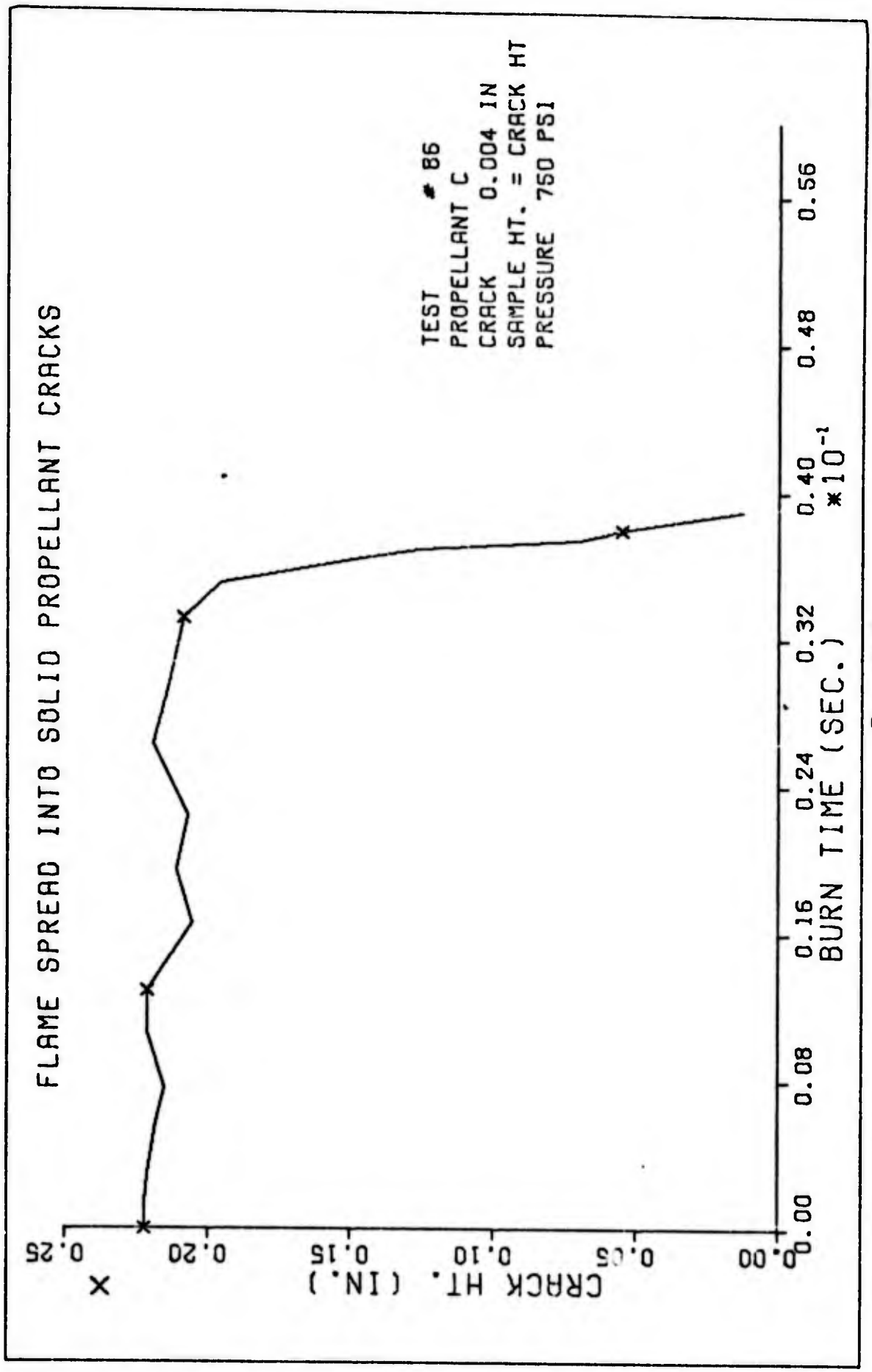
FLAME SPREAD INTO SOLID PROPELLANT CRACKS
TEST # 86
PROPELLANT C
CRACK 0.004 IN
SAMPLE HT. = CRACK HT
PRESSURE 750 PSI
CRACK HT. (IN.)
0.00
0.05
0.10
0.15
0.20
0.25
BURN TIME (SEC.)
0.00
0.08
0.16
0.24
0.32
0.40
0.48
0.56
*10⁻¹

Fig. 19 F.

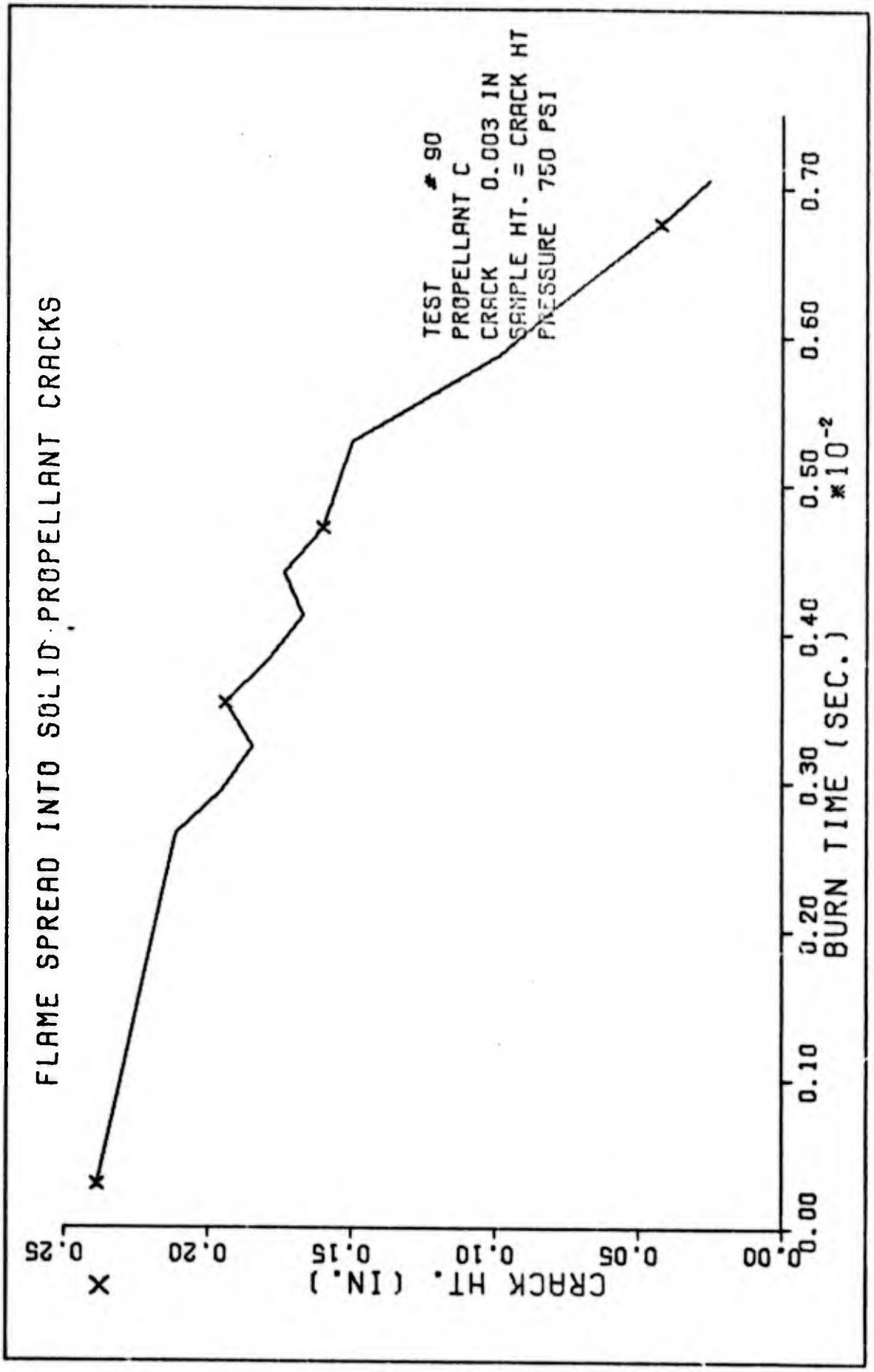
FLAME SPREAD INTO SOLID PROPELLANT CRACKS
TEST # 90
PROPELLANT C
CRACK 0.003 IN
SAMPLE HT. = CRACK HT
PRESSURE 750 PSI
CRACK HT. (IN.)
0.00
0.05
0.10
0.15
0.20
0.25
BURN TIME (SEC.)
0.00
0.10
0.20
0.30
0.40
0.50
0.60
0.70
*10^-2

Fig. 19 G.

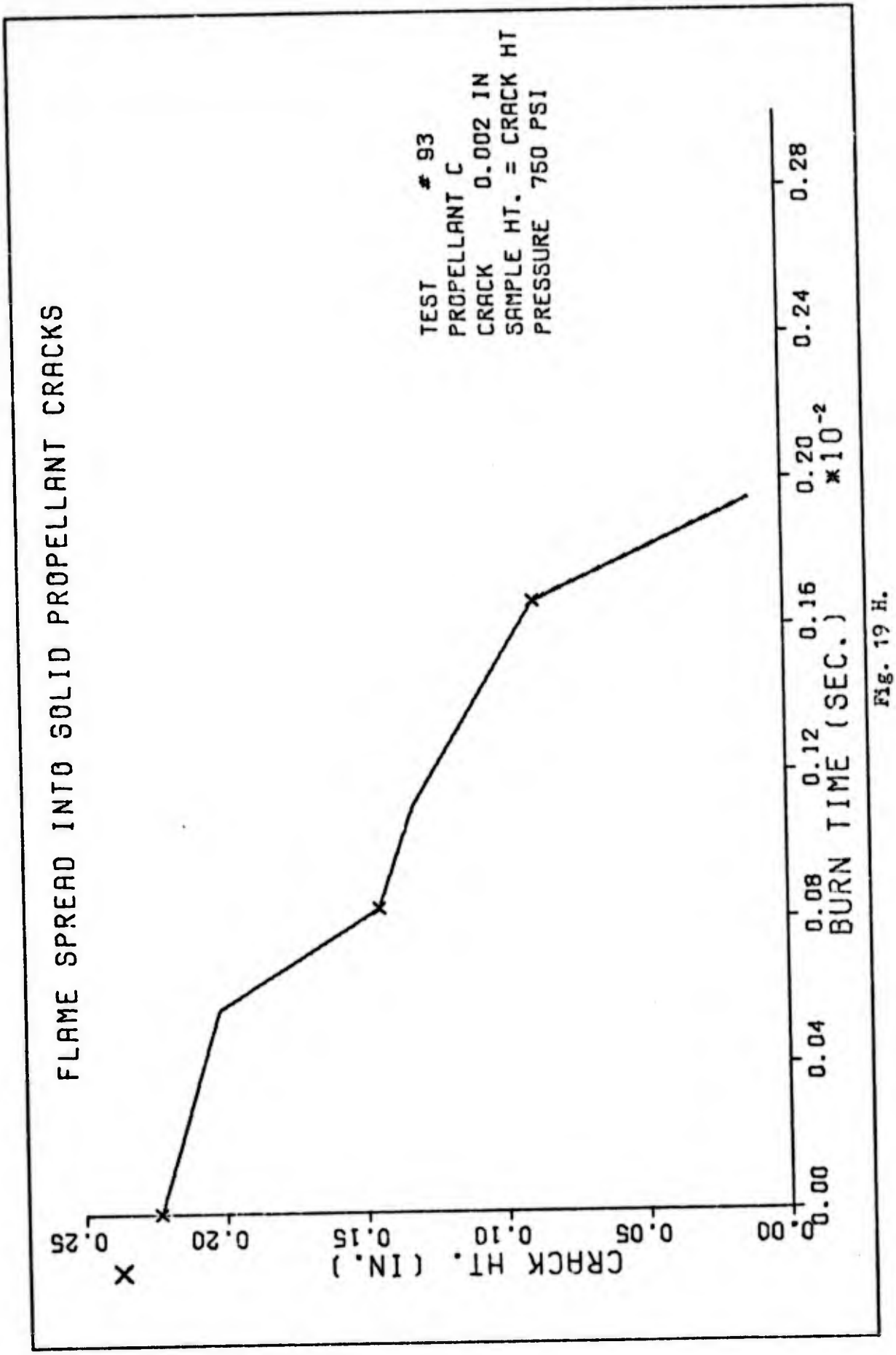
FLAME SPREAD INTO SOLID PROPELLANT CRACKS
TEST # 93
PROPELLANT C
CRACK 0.002 IN
SAMPLE HT. = CRACK HT
PRESSURE 750 PSI
CRACK HT. (IN.)
0.00
0.05
0.10
0.15
0.20
0.25
BURN TIME (SEC.)
0.00
0.04
0.08
0.12
0.16
0.20
0.24
0.28
*10^-2

Fig. 19 H.

Vita

Jerald Lane Cunningham was born on [redacted]. He attended Western Michigan University, then the University of Michigan from which he received the Degree of Bachelor of Science in Aeronautical and Astronautical Engineering and a commission in the USAF in 1966. After Navigator Training, he served as a B-52 Navigator-bombadier with the Strategic Air Command and then as an F-4 Weapons System Officer with the Tactical Air Command. He entered the Graduate Aeronautical Engineering Program at the Air Force Institute of Technology in June 1973.

[redacted]